# FOREST DYNAMICS ACROSS TEMPORAL AND SPATIAL SCALES

A DISSERTATION
SUBMITTED TO THE DEPARTMENT OF BIOLOGY
AND THE COMMITTEE ON GRADUATE STUDIES
OF STANFORD UNIVERSITY
IN PARTIAL FULFILLMENT OF THE REQUIREMENTS
FOR THE DEGREE OF
DOCTOR OF PHILOSOPHY

Eben North Broadbent

May 2012



This dissertation is online at: http://purl.stanford.edu/hs625bt1189

I certify that I have read this dissertation and that, in my opinion, it is fully adequate in scope and quality as a dissertation for the degree of Doctor of Philosophy.

**Christopher Field, Primary Adviser**

I certify that I have read this dissertation and that, in my opinion, it is fully adequate in scope and quality as a dissertation for the degree of Doctor of Philosophy.

**Gregory Asner, Co-Adviser**

I certify that I have read this dissertation and that, in my opinion, it is fully adequate in scope and quality as a dissertation for the degree of Doctor of Philosophy.

**Rodolfo Dirzo**

I certify that I have read this dissertation and that, in my opinion, it is fully adequate in scope and quality as a dissertation for the degree of Doctor of Philosophy.

**Peter Vitousek**

Approved for the Stanford University Committee on Graduate Studies.

**Patricia J. Gumport, Vice Provost Graduate Education**

*This signature page was generated electronically upon submission of this dissertation in electronic format. An original signed hard copy of the signature page is on file in University Archives.*

## ABSTRACT

The research conducted in this dissertation is focused on understanding different aspects of forest degradation and regeneration in the tropics. Similar to the multiple spatial and temporal scales this topic encompasses, the studies described in this dissertation encompass spatial scales ranging from as large as the Brazilian Amazon to as small as an individual leaf and temporal scales ranging from one-minute micro-climate measurements to multi-decadal remote sensing analyses. The causes and effects of forest degradation are numerous and require methods and concepts crossing traditional disciplinary boundaries. Likewise, this dissertation incorporates varied methods and concepts as required to understand forest dynamics within different study systems. The core of this dissertation is the development and integration of new remote sensing methods. In this theme, I use a variety of remote sensors, including satellite based Landsat and Quickbird sensors and the Carnegie Airborne Observatory (CAO) – which integrates airborne LiDAR with hyperspectral imagery. I also include a study (chapter 5) focusing specifically on issues related to forest dynamics following swidden agricultural abandonment.

## ACKNOWLEDGEMENTS

The work presented in this dissertation was funded by the Department of Biology of Stanford University, a Department of Energy Global Climate Change Education Fellowship (DOE GCEP), a National Science Foundation Doctoral Dissertation Improvement Grant (NSF DDIG), the Department of Global Ecology of the Carnegie Institution for Science, a NASA LBA-ECO grant (NNG06GE32A), the Sustainability Science Program (SSP) at Harvard University with support from Italy's Ministry for Environment, Land and Sea, the Center for Responsible Travel (CREST), and the Woods Institute for the Environment at Stanford University.

Logistical support crucial to the success of this dissertation was provided by the Instituto Boliviano de Investigation Forestal (IBIF), the Institute of Pacific Islands Forestry (IPIF), the University of Hawaii at Hilo, La Chonta Ltda., the Hilo office of the Department of Forestry and Wildlife (DOFAW), and the *Sí Cómo No* and *El Parador* hotels in Manuel Antonio, Costa Rica. Additional vital logistic support was generously provided by communities located throughout Madre de Dios in Peru, Acre in Brazil, Pando in Bolivia – especially the community of Molienda, in the Manuel Antonio region of Costa Rica, and in Laupahoehoe, Hawaii.

I cannot sufficiently thank my committee who has helped in every step along the way: Chris Field, Greg Asner, Rodolfo Dirzo, Peter Vitousek, and William Durham. Missy Holbrook, William Clark, and Nancy Dickson also served important roles in the final writing and analysis component during my time in the Sustainability Science Program at Harvard. I give thanks to the members of the Asner, Field and Dirzo labs who were wonderful colleagues, with whom I had many adventures, and who – in addition to academic support, made graduate school such a fun experience. I give my great thanks to my wife Angélica M. Almeyda Zambrano, who has collaborated with me on every part of this process, who has been patient and supportive without fail, and whose dedication and perseverance inspire me each and every day.

I am deeply indebted to the support of my immediate family: Jeff Broadbent, Taihaku (Gretchen) Priest, Jeylan Mortimer, Leafye Pante, and Marcus Pante, as well

as to my extended family in Peru, Lucero-, Carmen-, Sandra- and Coco- Almeyda Zambrano; Georget Almeyda and, Elena Zambrano. I would like to give special thanks to Kai Turbo who keeps me laughing even in the heaviest tropical rainstorms. I give great thanks to Valerie Kiszka, Dan King and Linda Longoria who helped me in many ways over the years, including navigating the logistics of the PhD process.

In addition to the collaborators listed on each chapter, many people helped me complete these projects, individually, and the dissertation as a whole. I give sincere thanks, in alphabetical order, to: Berry J, Bingham J, Brauman K, Busby P, Clark W, Curran L, Dahlin K, Davidson E, Dickson N, Epps K, Farrington H, Fortini L, Freyberg D, Funk Jason, Funk Jen, Gelber D, Gilbert M, Honey M, Hughes F, Hwang B, Inman-Narahari F, Johnson J, Kellner J, Laurance W, Leopold D, Lunch C, Mendez R, Naesborg R, Ostertag B, Paritosh B, Price J, Pringle E, Pringle R, Raybin R, Rosenthal A,Tidwell H, Tobeck T, Tweiten M, Uowolo A, Vargas E, Williams C, Wolf A, and Woods G. To those whose names I have forgotten to include, please forgive the oversight and accept my gratitude.

## TABLE OF CONTENTS

ABSTRACT ..... iv
ACKNOWLEDGEMENTS ..... v
TABLE OF CONTENTS ..... vii
LIST OF TABLES ..... xii
LIST OF ILLUSTRATIONS ..... xv
LIST OF SUPPLEMENTARY MATERIALS ..... xx

CHAPTER 1: INTRODUCTION ..... 1
1.1 Author Contributions ..... 5
1.2 References ..... 7
1.3 Figures ..... 16

CHAPTER 2: FOREST FRAGMENTATION AND EDGE EFFECTS FROM DEFORESTATION AND SELECTIVE LOGGING IN THE BRAZILIAN AMAZON ..... 20
2.1 Abstract ..... 20
2.2 Introduction ..... 21
2.3 Materials and Methods ..... 24
2.3.1 Study region ..... 24
2.3.2 Deforestation and logging maps ..... 24
2.3.3 Forest fragmentation and structure ..... 25
2.3.4 Forest edge effects ..... 27
2.3.5 Literature review ..... 27
2.4 Results ..... 27
2.4.1 Forest fragmentation ..... 27
2.4.2 Forest edge effects ..... 28
2.4.3 Literature review ..... 29
2.5 Discussion ..... 31
2.6 Conclusions ..... 35

2.7 Acknowledgements ..... 36
2.8 References ..... 36
2.9 Tables ..... 45
2.10 Figures ..... 47
2.11 Supplementary Materials ..... 55

CHAPTER 3: SPATIAL PARTITIONING OF BIOMASS AND DIVERSITY IN A LOWLAND BOLIVIAN FOREST: LINKING FIELD AND REMOTE SENSING MEASUREMENTS ..... 62
3.1 Abstract ..... 62
3.2 Introduction ..... 63
3.3 Methods ..... 64
3.3.1 Study area ..... 64
3.3.2 Forest structure ..... 66
3.3.3 Forest composition ..... 68
3.3.4 Spatial analyses ..... 68
3.4 Results ..... 70
3.4.1 Forest structure ..... 70
3.4.2 Forest composition ..... 72
3.4.3 Spatial analyses ..... 72
3.5 Discussion ..... 75
3.5.1 Spatial distribution of forest biomass ..... 75
3.5.2 Spatial distribution of forest diversity ..... 76
3.5.3 Linking field and remote sensing measurements ..... 77
3.6 Conclusions ..... 79
3.7 Acknowledgements ..... 79
3.8 References ..... 80
3.9 Tables ..... 84
3.10 Figures ..... 91
3.11 Supplementary Materials ..... 98

CHAPTER 4: PREDICTING LEAF TRAIT VARIATION IN A HAWAIIAN RAINFOREST UNDERSTORY: A MICROCLIMATE MODELING APPROACH BASED ON FUSION OF AIRBORNE LIDAR AND HYPERSPECTRAL IMAGERY ..... 101
4.1 Abstract ..... 101
4.2 Introduction ..... 102
4.3 Materials and methods. ..... 106
4.3.1 Study design ..... 106
4.3.2 Study site ..... 106
4.3.3 Study plots ..... 107
4.3.4 Georeferencing. ..... 108
4.3.5 Climate measurements. ..... 109
4.3.6 Leaf traits ..... 110
4.3.7 Airborne remote sensing. ..... 115
4.3.8 Interior forest microclimate modeling. ..... 117
4.3.9 Data integration. ..... 120
4.4 Results ..... 121
4.4.1 Plant diversity and structure ..... 121
4.4.2 Microclimate ..... 122
4.4.3 Leaf trait variation ..... 122
4.4.4 Leaf trait clusters ..... 123
4.5 Discussion ..... 125
4.5.1 Remote sensing ..... 126
4.5.2 Sources of leaf trait variation ..... 128
4.5.3 Species and structure ..... 129
4.5.4 Light and air temperature ..... 130
4.5.5 Stable isotopes ..... 133
4.5.6 Clusters ..... 135
4.6 Conclusions ..... 136
4.7 Acknowledgements ..... 137

4.8 References ..... 137
4.9 Tables ..... 153
4.10 Figures ..... 160
4.11 Supplementary Materials ..... 169

CHAPTER 5: PREDICTORS OF LEAF TRAIT VARIATION IN TREE SPECIES DURING FOREST SUCCESSION IN THE BOLIVIAN AMAZON ..... 177
5.1 Abstract ..... 177
5.2 Introduction ..... 178
5.3 Materials and Methods ..... 181
5.3.1 Study Sites ..... 181
5.3.2 Forest structure and composition ..... 182
5.3.3 Soil properties ..... 184
5.3.4 Foliar properties ..... 185
5.3.5 Statistical analysis ..... 186
5.4 Results ..... 189
5.4.1 Forest structure and composition ..... 189
5.4.2 Soil properties ..... 191
5.4.3 Leaf traits ..... 192
5.5 Discussion ..... 194
5.5.1 Stand structure and composition ..... 194
5.5.2 Soil properties ..... 196
5.5.3 Leaf traits ..... 202
5.6 Integration and conclusion ..... 213
5.7 Acknowledgements ..... 214
5.8 References ..... 215
5.9 Tables ..... 234
5.10 Figures ..... 238
5.11 Supplementary material ..... 246

CHAPTER 6 - APPENDIX: THE EFFECT OF LAND USE CHANGE AND ECOTOURISM ON BIODIVERSITY: A CASE STUDY OF MANUEL ANTONIO, COSTA RICA, FROM 1985-2008 ..... 251
6.1 Abstract ..... 251
6.2 Introduction ..... 252
6.3 Methods ..... 255
6.3.1 Study area ..... 255
6.3.2 Study design ..... 256
6.3.3 Spatial analyses ..... 257
6.3.4 Socioeconomic analyses ..... 259
6.3.5 Wildlife analyses ..... 259
6.4 Results ..... 260
6.4.1 Spatial analyses ..... 260
6.4.2 Socioeconomic analyses ..... 261
6.4.3 Wildlife analyses ..... 262
6.5 Discussion ..... 263
6.6 Conclusions ..... 267
6.7 Acknowledgments ..... 268
6.8 Tables ..... 270
6.9 Figure captions ..... 273
6.10 References ..... 278
6.11 Supplementary material ..... 284

## LIST OF TABLES

**Table 2.1:** Fragmentation statistics for all deforestation and logging combinations within our study region. ..... 45

**Table 2.2:** Descriptive statistics of edge distance (m) into interior forest by disturbance category. ..... 46

**Table 3.1:** Abundance and structural variables (mean (±S.E.) for trees ≥20 cm in DBH in the four 1-ha plots included in this study ..... 84

**Table 3.2:** Abundance, basal area and biomass per DBH classes present throughout the four 1-ha study plots ..... 85

**Table 3.3:** Forest structure and crown characteristics per crown exposure class ..... 86

**Table 3.4:** Allometric relationships between crown width (*W*), length (*L*), and area (*A*) and tree DBH and tree total height (*H*) ..... 87

**Table 3.5:** Sorensen's index of species composition similarity between crown position classes ..... 88

**Table 3.6:** Remote sensing (RS) and field delineated crown area ($m^2$), tree diameter (cm) and individual tree biomass (Mg) statistics ..... 89

**Table 3.7:** Kolmogorov–Smirnov comparison D values between remote sensing (circle and polygon approaches) and field measurement distributions across the four 1-ha study plots ..... 90

**Table 4.1:** Plant diversity transects. Density (# individuals / 1000 $m^2$), volume (basal area * height $cm^3$), frequency (% transects occurring). Species are ranked by their importance value (IV). Sampled (cluster) = whether foliar samples were collected and to which cluster the species was assigned. ..... 153

**Table 4.2:** Mean ± standard deviation daytime (sun elevation > 25° C) climatic conditions at top of canopy tower locations between Dec 17$^{th}$ 2010 and June 19$^{th}$ 2011. Rainfall is the total over this period. ..... 154

**Table 4.3:** General linear model results for leaf traits versus taxonomic, ecological and structural categories (# parameters). Data is the Akaike Information Criteria (AIC) (adj-$R^2$) degrees of freedom and *P*-value. AIC allows intra-row

comparisons and models > 20 above the minimum AIC have been removed. ..... 155

**Table 4.4:** Best subsets models of leaf traits versus structural and modeled mean and standard deviation (SD) photosynthetic photon flux density (PPFD; µmol $m^{-2}$ $s^{-1}$) and air temperature (°C). Data represents the *t*-ratio (*F*-ratio) and *P*-value significance, with increasing *, **, ***, ****, and ϕ representing *P*-values of 0.1, 0.05, 0.01, 0.001, and < 0.0001, respectively. ..... 156

**Table 4.5:** Predictors of Hapu'u (*Cibotium glaucum*) and Ohia (*Metrosideros polymorpha*) leaf traits. Data represents the slope (adj-$R^2$) degrees of freedom and *P*-value of linear regressions. ..... 157

**Table 4.6**: Leaf trait mean ± standard deviation for *K*-means low, medium and high modeled light clusters and results of among cluster one-way ANOVAs sorted by the adjusted $R^2$ value. ..... 158

**Table 4.7**: Forest elevation, structure and micro-climate mean ± standard deviation (SD) for low, medium and high light environment *K*-means clusters and results of among cluster one-way ANOVAs. Categorical classifications are % true and differences among clusters are assessed using the Pearson test. ..... 159

**Table 5.1:** Stand characteristics of all successional and primary (Pr) forest study sites (mean±std. dev.). ..... 234

**Table 5.2:** Soil properties for all successional and primary (Pr) forest study sites. 235

**Table 5.3:** Characteristics of tree species selected for analysis of foliar properties. ..... 236

**Table 5.4:** Best subsets models of leaf traits versus stand age, species successional status, and Principal Component Analysis (PCA) derived gradients in stand biomass and structure, and soil texture and fertility. Data represents the *t*-ratio (*F*-ratio) and *P*-value significance, with increasing * representing *P*-values of 0.1, 0.05, 0.01, and 0.001, respectively, and ϕ < 0.0001. ..... 237

**Table 6.1:** Forest fragmentation and land cover from 1985 to 2008..... 270

**Table 6.2:** Perceived impacts of the Sí Cómo No (SCN) and El Parador (EP) hotels versus tourism in general (T). Ranks range from 1-5; values > 3 indicate a

negative impact and < 3 a positive impact. The matched pairs statistical analysis was used for mean comparisons. ..... 271

**Table 6.3:** Ranked household perceptions of most important reasons to protect forest and for having natural protected areas. ..... 272

## LIST OF ILLUSTRATIONS

**Figure 1.1:** Spatial scale of forest dynamics addressed by each chapter and the appendix in this dissertation. ..... 17

**Figure 1.2:** Interactions among themes related to forest dynamics across spatial and temporal scales addressed in this dissertation. ..... 18

**Figure 1.3:** Spatial and temporal scale and resolution addressed by each chapter and the appendix in this dissertation. ..... 19

**Figure 2.1:** Interior and edge-forest (≤2 km edge) within our study area following deforestation and cumulative logging (2000-2002). White areas represent non-forest areas (i.e., pasture or agriculture) within our study area while grey areas represent those areas not included due to cloud interference or missing imagery. A map of the general study area is presented in Supplementary Materials 2.2. ..... 48

**Figure 2.2:** Example of spatio-temporal dynamics of deforestation and selective logging in the years 1999-2002 (A-D, respectively) in central Mato Grosso. Areas of deforestation and new logging are indicated by yellow and red arrows, respectively. Subdivided forest fragments are visible within logged areas ..... 49

**Figure 2.3:** Total number (left) and cumulative percentage (right) of edge effects documented in our literature review. Arrows indicate the distance under which 99% of documented edge effects occurred. References are provided in Supplementary Materials 2.1. ..... 50

**Figure 2.4:** Cumulative percentage of (A) total non-contiguous forest fragments in our study region versus each fragment's area ($km^2$), (B) total forested area in our study region versus the area of individual non-contiguous forest fragments, (C) cumulative total forested area ($km^2$), and (D) total remaining forest, located within individual 100 m distance increments up to two km from the nearest forest edge. Logging impacts are in addition to those caused by deforestation. ..... 51

**Figure 2.5:** Mean annual change in edge-forest area and the percentage of total remaining forest impacted within individual 100 m distance increments up to two km into the forest interior. New logging and cumulative logging (2000–2002) impacts are in addition to those of deforestation. ..... 52

**Figure 2.6:** Literature review of edge effects divided into: (A) forest structure, (B) tree mortality, (C) forest microclimatic and (D) biodiversity disturbance categories. When multiple sources were identified the minimum (horizontal bar) and maximum (error bar) are provided. These effects are overlaid on area graphs to illustrate the cumulative percentage of remaining forest potentially impacted by each variable following year 2000–2002 deforestation (D012) and combined D012 and year 2000–2002 cumulative logging (CL012). The Y axis refers to the% remaining forest when logged areas are defined as either intact (D012) or degraded forest (D012–CL012). Complete references are provided in the Supplementary Materials ..... 53

**Figure 3.1:** Cumulative percentage of total woody stems ≥20 cm in diameter (DBH) within individual crown exposure classes along a DBH gradient. Crown exposure classes 1–5 are completely shaded to fully exposed tree crowns. .... 91

**Figure 3.2:** Tree stem density by crown exposure class and for all exposure classes combined. Areas having no individuals are represented as a density of zero. Error bars represent standard deviation of the mean among the four one ha study plots. The asterisk represents significant differences among crown positions ($P < 0.05$). ..... 92

**Figure 3.3:** Field geolocated tree crowns (DBH ≥20 cm) in crown exposure classes 1 (shaded understory) through 5 (emergent) for the four study plots. Crown delineations are overlaid on the panchromatic Quickbird satellite image. Areas within each plot but outside delineated tree crowns represent crowns of trees not meeting our DBH ≥20 cm threshold. ..... 93

**Figure 3.4:** Mean number of stems covered by trees belonging to crown exposure class 5, 4 and 3. Error bars represent standard errors of the mean. ..... 94

**Figure 3.5:** Correction factors for obscured understory trees for: tree abundance (A and B), basal area (C and D) and biomass (E and F) for trees with DBH ≥20 cm using crown length and crown area. Equations are provided in Supplementary Materials 3C. STD represents the standard deviation of the six biomass equations used in the analysis and is provided to indicate the potential error in the biomass estimation.....95

**Figure 3.6:** Automated circle and polygon crown delineations in study plots 1–4 (top left corner) overlaid on the panchromatic Quickbird satellite image. .....96

**Figure 3.7:** Abundance of trees by 10 cm DBH classes (a) and biomass (Mg) (b). The x-axis labels represent the lower limit of the size class. Biomass derived using remote sensing circle and polygon approaches is calculated using the corrected biomass equation incorporating obscured tree stems provided in Supplementary Materials 3C. .....97

**Figure 4.1:** Overview of remote sensing and field data integration and analysis. Hyperspectral and waveform light detection and ranging (LiDAR) data were collected simultaneously using the Carnegie Airborne Observatory (CAO) while discrete LiDAR was collected separately. Field data collected for parameterization and validation included: (a) LAI-2000 for leaf area index (LAI; two-dimensional), (b) vertical leaf area density (LAD; three-dimensional) transects, (c) microclimatic data, and (d) leaf trait measurements throughout the study transect. Leaf traits included chemical and gas exchange analyses. Microclimate data included modeled daytime mean and standard deviation photosynthetic photon flux density (PPFD) and modeled mean daytime air temperature. Spatial data included location, elevation and forest structural information. Taxonomic data included species, native vs. exotic status, and life form. Principal component analysis (PCA) axes were input into *k*-means analysis to identify ecophysiological similar clusters that were explained through differences in microclimate, taxonomy and spatial location. .....161

**Figure 4.3:** Tree height (m) and leaf area index (LAI; $m^2$ $m^{-2}$) for 50 m elevation classes. Data derived from airborne hyperspectral imagery (1.25 x 1.25 m resolution) with $N$ > 500,000 pixels per elevation class. ..... 163

**Figure 4.4:** Measured daily average daytime (solar elevation > 25°) photosynthetic photon flux density (PPFD; µmol $m^{-2}$ $s^{-1}$), diffuse PPFD (%), and air temperature (°C) at the mid elevation top-of-canopy climate tower. Julian dates extend from January 1st, 2010 (40179 JD) through June 17th, 2011 (40711 JD). ..... 164

**Figure 4.5:** Measured hourly mean daytime (solar elevation > 25°) photosynthetic photon flux density (PPFD; µmol $m^{-2}$ $s^{-1}$), diffuse PPFD (%), and air temperature (°C) at mid elevation top-of-canopy climate tower. ..... 165

**Figure 4.6:** Principal leaf trait clusters identified through *k*-means analysis. Low, medium and high light clusters are represented by the colors red, blue, and green, respectively. ..... 166

**Figure 4.7:** Relationships (log-log regressions) between $A_{max}$ (maximum µmol $C0_2$ $m^{-2}$ $s^{-1}$) and modeled mean daily PPFD (µmol $m^{-2}$ $s^{-1}$) for the entire community and modeled low, medium and high light leaf trait clusters. Regressions for the community and modeled medium and high light leaf trait clusters are significant ($P$ < 0.05). ..... 167

**Figure 4.8:** Relationship of multiple regression foliar $\delta^{15}N$ residuals versus modeled mean daytime air temperature (°C) and leaf height (m). ..... 168

**Figure 5.1:** Linear relationship between stand age (years) and species successional status mean (years; left), standard error (SE; middle) and annual change (years; right). Stand values are calculated using all tree stems within each secondary forest stand. ..... 239

**Figure 5.2:** Percentage total living trees in understory and overstory crown exposure (CE) positions; 1-3, and 4-5, respectively. Stand development phases (top) correspond to those described by Waring & Running (2007). ..... 240

**Figure 5.3:** Stand structural and species characteristics for successional forest study sites. Species diversity is calculated using the Shannon-Weiner metric and

species similarity is calculated using a Chao-Jaccard index versus primary forest composition. Michaelis-Menten relationship is shown between biomass and stand age, while quadratic are shown between tree height and diameter at breast height (DBH) and stand age. ..... 241

**Figure 5.4:** Selected soil properties for successional forest study sites. Significant linear regressions are shown in grey ($N = 13$). Linear regressions for soil $\delta^{15}N$ were significant using separate depth points ($N = 39$) and for soil $\delta^{13}C$ following exclusion of the 7 year old stand outlier ($N = 12$). ..... 242

**Figure 5.5:** Soil $\delta^{15}N$ values versus stand age by soil depth. A significant relationship exists between stand age and $\delta^{15}N$ for all samples ($R^2 = 0.26$, $P = 0.0881$, $N = 12$) and a trend at 5 cm depth ($R^2 = 0.26$, $P = 0.0881$, $N = 12$). . 243

**Figure 5.6:** Foliar $\delta^{15}N$ and $\delta^{13}C$ values versus stand age and species successional status. Significant linear regressions are shown in grey. ..... 244

**Figure 5.7:** Foliar-minus-soil $\delta^{15}N$ and $\delta^{13}C$ values versus stand age and species successional status. Significant linear regressions are shown in grey. ..... 245

**Figure 6.1:** Detailed forest classification map of the study area in the year 2008. Insets show: (A) a close up of the park (MANP) and hotel nature preserves; and (B) the general location of study area in Costa Rica. The scale bar applies to the overview map only. ..... 274

**Figure 6.2:** Land cover change (% area) from 1985 through 2008 within the Manuel Antonio National Park (MANP), its buffer (1.5 km), and across the entire study area.. ..... 275

**Figure 6.3:** Land cover classes (% area) in the year 2008 within selected study sites, including the Manuel Antonio National Park (MA), and their adjacent buffer areas (1.5 km). ..... 276

**Figure 6.4:** Least cost paths between all study sites (SS), including the Manuel Antonio National Park (MA) and core primary forest (CPF). The proposed biological corridor (800 m width) location is provided in the right inset. ..... 277

## LIST OF SUPPLEMENTARY MATERIALS

**SM 2.1:** Tropical and temperate forest edge effects and sources for four disturbance categories. Data used for Fig. 6 of the main text. ..... 55

**SM 2.2:** General study area and logging data used in this study as described in Asner et al. (2005). ..... 61

**SM 3.1:** Above ground biomass equations found in the literature (kg). $\rho$ = wood density (g/cm$^3$), DBH = Bole diameter at breast height (1.3 m; cm), H = Total tree height (m). ..... 98

**SM 3.2:** Bivariate power regressions between all forest structural variables. R values are presented in parentheses and P value significance is provided as:* = $p <$ 0.05, ** = $p < 0.01$, *** = $p < 0.001$, NS = non-significant, following each equation. ..... 99

**SM 3.3:** Correction equations for converting nadir top-of-canopy estimations based on the single visible tree crown (RS) to corrected forest biomass incorporating obscured tree stems ≥ 20 cm DBH (FB). *P*-values are provided following each equation and $R^2$ values are provided in parentheses. * = $P < 0.05$, ** = $P <$ 0.01, *** = $P < 0.001$. NS = non-significant. $N \geq 314$. ..... 100

**SM 4.1:** Pearson correlations between elevation and forest structure variables and modeled mean and standard deviation (SD) photosynthetic photon flux density (µmol m$^{-2}$ s$^{-1}$) and air temperature (°C). *P*-value significance increases from white (<0.05), light grey (< 0.01) to dark grey (< 0.001). Row numbers refer to numbered column variables. ..... 170

**SM 4.2:** Pearson correlations between foliar variables. *P*-values < 0.05, 0.01, 0.001 and 0.0001 are represented by increasing shades of grey. Row numbers refer to numbered column variables. ..... 171

**SM 4.3:** Leaf trait principal component analysis (PCA) eigenvectors. PCA 1 and 2 have significant positive relationships with modeled mean photosynthetic photon flux density (µmol m$^{-2}$ s$^{-1}$) and modeled mean air temperature (°C), respectively. ..... 172

**SM 4.4:** Relationships between multiple regression residuals of axis one and two of principal component analysis (PCA) of foliar ecophysiological variables versus box-cox transformed modeled mean photosynthetic photon flux density (µmol $m^{-2}$ $s^{-1}$) and modeled mean air temperature (°C). ..... 173

**SM 4.5:** Clear sky top-of-canopy photosynthetic active radiation (PAR) model coded in R language. This model was used to validate calibration of top-of-canopy PAR sensors at each climate tower. ..... 174

**SM 5.1:** Ultrametric tree of species used for leaf trait phylogenetic signal analyses. Foliar %C is provided after the species name as it was the only trait identified as having significant phylogenetic signal. The scale bar (lower left corner) represents 10 million years. ..... 246

**SM 5.2:** Eigenvectors of stand and soil Principal Components Analysis (PCA) axes. Stand and soil property variables are explained and units provided in Table 5.1 and 5.2 of the main text. ..... 247

**SM 5.3:** Pearson correlations among leaf trait variables. Data is the correlation value (N) and P-value expressed as + < 0.1, * < 0.05, ** < 0.01, and *** < 0.001. ..... 248

**SM 5.4:** Pearson correlations among the predictor variables stand age (years), species successional status (status), and the PCA derived axes of stand biomass and structure and soil texture and fertility. Data is the correlation value (N) and P-value expressed as + < 0.1, * < 0.05, ** < 0.01, and *** < 0.001. ..... 249

**SM 5.5:** Regressions of foliar variables versus stand age (years) / species successional status (years). Statistics provided are Adj-$R^2$ (F) *df* and *P*-value. Model comparisons are conducted using the F-test in R and P values are presented as: blank < 0.1, * < 0.05, ** < 0.01, *** < 0.001, **** < 0.0001. 250

**SM 6.1:** Landsat satellite imagery. ..... 284

**SM 6.2:** Land cover change from 1985 to 2008. ..... 285

**SM 6.3:** Comparison between Sí Cómo No (SCN) and El Parador (EP) hotels employees and their neighbors (C) on average values of background variables. ..... 286

**SM 6.4:** Comparison between Sí Cómo No (SCN) and El Parador (EP) hotels employees and their neighbors (NE) on average monthly household expenditures (US $) for the month of June, 2009. ..... 287

# CHAPTER 1

## INTRODUCTION

Global biodiversity comprises some 100 phyla of living organisms (Margulis and Schwartz 1998), with eukaryotic organisms having between five and 15 million species (May 2000). While biodiversity is distributed throughout the world, a strong latitudinal gradient exists with higher species richness being found in tropical areas (Gaston 2000). The Neotropics are, in particular, epicenters of both richness within a habitat (alpha) and turnover among habitats (beta) diversity (Willing et al. 2003). In addition, island ecosystems are often, sometimes contrary to their latitude, exceptionally high in endemic biodiversity due to their isolation (Olson 1998; Paulay 1994). Global net primary productivity (NPP) also follows similar latitudinal trends, being highest in tropical areas (Field et al. 1998), as well as other ecosystem properties (Chapin et al. 2002; Bond et al. 2005).

Of all ecosystems within the Neotropics, tropical forests represent those harboring the greatest richness of biodiversity (Dirzo and Raven 2003), containing approximately 50% of described and up to 50% of undescribed species. For example, a classic study by Gentry (1988) showed the forests of upper Amazonia, in particular within Peru, to have the highest tree species richness of any plots reported in the world – approximately 300 species > 10 cm diameter per hectare. Erwin (1982) fogged tree canopies in Panama and calculated there were over 41,000 species of arthropods per hectare, raising the global species estimate from 1.5 million at the time to as high as 30 million. In addition, tropical forests play a significant role in modulating global carbon and energy cycles (IPCC 2002). Melillo et al. (1993) used a process-based model to show that while over half of annual global NPP occurred in the tropics, a disproportionate amount of the global production was due to tropical evergreen forests [32-36%, see Field et al. 1998].

Without anthropogenic disturbance, forests in general are estimated to have had an original extent of between 55.3 (Ramankutty and Foley 1999) and 58.6

(Goldewijk 2001) million $km^2$. Tropical forests specifically are estimated to have originally covered between 14.4 to 21.5 million $km^2$ (Simberloff 1986; Reid 1992; Myers 2000; Wright 2005; Asner et al. 2009) [see Grainger 2008 for a discussion of this variance in estimated area]. In the 1970s, deforestation in the humid tropics was converting approximately 75,000 $km^2$/yr (Houghton et al. 1985), resulting in an annual loss of carbon to the atmosphere of 0.51-1.55 Pg/yr (DeFries et al. 2002) or up to 2.2 Pg C yr-1 in the 1990s (Houghton et al. 1985; Houghton 2003; Ramankutty et al. 2007). Between 1990-1997, 58,000 $km^2$ (0.56%) of remaining forests were converted annually, and during the five years period from 2000 and 2005 alone, 274,615 $km^2$ (1.4%) were deforested (Asner et al. 2009). As a result, more than half of the original potential extent of tropical forest area has been lost through conversion for human activities (Wright 2005), and Cramer et al. (2004) project that only 15-40% of potential forested habitat, down from 92% in 1900 (Klein Goldewijk 2001), will remain forested in 2100. The resultant loss of global biodiversity is occurring at an unprecedented rate (NRC 1988), with the conversion of tropical forests described as one of the greatest threats (Dirzo and Raven 2003). Dirzo (2001) extrapolates current patterns of tropical forest conversion to estimate that up to 19% of species living in these areas could be driven to extinction by the year 2040.

Degradation of tropical forest habitat and ecosystem function differs from deforestation in that complete conversion does not occur. Forest degradation takes place because of, among other drivers [i.e., wildfires (Nepstad et al. 1999)], selective logging and climate change. The forested area impacted by selective logging encompasses up to 20.3% globally of all remaining tropical forests in 2000 (Asner et al. 2009), and in the Brazilian Amazon alone affects an area equivalent to 60-123% of the area deforested – resulting in a gross carbon flux of 0.1 Pg/yr (Asner et al. 2005). Although selectively logged areas are often preferentially deforested in the years following harvest (Asner et al. 2006) – and especially proximate to roads, many logged areas and their access roads remain which extend deep into intact contiguous forested areas resulting in the generation of up to 20,000 km of forest edge annually (Broadbent et al. 2008a). The effects of selective logging and deforestation in the

Brazilian Amazon on forest fragmentation and edge effects are the subject of Chapter 2 of this dissertation (Broadbent et al. 2008a). Chapter 2 represents the study in this dissertation having the largest spatial extent and coarsest spatial resolution (Figure 1.1).

Regeneration of secondary forests occurs following abandonment of infertile areas (Rey Benayas et al. 2007), shifting cultivation strategies (Uhl 1987) or logging activities (Asner et al. 2006), and is occurring at a scale relevant globally (Corlett 1995). For example, DeFries et al. (2002) estimated that the mean annual carbon loss from Pantropical deforestation of 0.97 Pg yr-1 was partially offset by regrowth that created a mean annual carbon gain of 0.05 Pg/yr (or 5.2%). Achard et al. (2002) estimate that there are 10,000 $km^2$ of new secondary forests generated each year in the regions supporting tropical forests. Asner et al. (2009) estimate that there are now 235,209 $km^2$ (or 1.2%) of tropical forests globally now undergoing secondary regrowth. Secondary forests have considerable biodiversity value (Barlow et al. 2007) and are now being integrated into conservation strategies within human dominated landscapes (Daily 1997).

Secondary stand regeneration dynamics are determined by many factors, including edaphic conditions (Moran et al. 2000; Zarin et al. 2001), fire history (Zarin et al. 2005) and historical land use type or intensity (Fearnside and Guimarães 1996). Research on secondary forest dynamics, and in particular interactions between above- and below-ground components (Binkley and Giardina 1998), remains an active research topic (Guariguata and Ostertag 2001; Chazdon et al. 2010). Developing a more detailed understanding of secondary forest dynamics is the focus of chapter five of this dissertation (Figure 1.1, 1.2; Broadbent et al. 2012b).

Forest conversion, degradation and regeneration result from complex interactions among socio-economic and biophysical variables across spatial and temporal scales (Figure 1.2). Increasing awareness of the human influence on natural ecosystems (Vitousek et al. 1986; 1997) and that forests, likewise, are becoming human dominated landscapes (Noble and Dirzo 1997) has prompted research into: (a) the drivers of human-environment interactions (Rudel et al. 1997; Almeyda Zambrano

et al. 2010), and (b) the impacts of such interactions on, among many topics, biodiversity (Sala et al. 2000), and ecosystem services (Foley et al. 2005; 2007). This complexity has resulted in the emergence of a new interdisciplinary field of research termed land change science (Turner et al. 2007). Efforts have been made to identify hotspots in areas of high biodiversity and human land use pressure (Myers et al. 2000), and when possible to create protected areas to maximize biodiversity conservation (Rodrigues et al. 2004), which have resulted in reduced land conversion in these areas (Brooks et al. 2009).

In spite of these efforts, protected areas fail to adequately represent global diversity (Rodrigues et al. 2004) and are rapidly becoming isolated from other forested areas (DeFries et al. 2005), although less speciose wilderness areas do remain (Mittermeier et al. 2003). Land use science urgently needs to understand the implications of land use choices to maximize both ecological and human well-being (DeFries et al. 2004; Broadbent et al. 2012c), to generate effective 'win-win' sustainable development strategies (Lélé 1991). Understanding human-environment interactions, in particular defaunation (Wright et al. 2007), and land use dynamics around a high biodiversity protected area is the focus of the appendix (Figure 1.1, 1.3; Broadbent et al. 2012c).

New efforts to promote sustainable use of ecosystems are designed to pay landholders, or nations, for the conservation of their natural resources. One of such efforts, broadly defined as reduced emissions from deforestation and forest degradation (REDD), has received considerable attention (Karsenty 2008). While the REDD approach has been shown to have great possibility (Stickler et al. 2009), its effectiveness is less understood (Brooks et al. 2009), and efficient approaches to monitor emissions are only now being developed (Gibbs et al. 2007; Asner 2011). Although new approaches are having success integrating satellite and airborne techniques (Asner 2009), further research is required. In chapter three, I couple extensive three-dimensional maps of forest structure and tree diversity to parameterize and validate a new tree crown-mapping algorithm (Broadbent et al. 2008b). Using this

information, I develop allometric correction equations to facilitate biomass and diversity assessments from high-resolution space-borne sensors (Figure 1.1, 1.3).

Climate change integrates human impacts with ecological systems (Vitousek 1994; Chapin III et al. 2008), and requires new approaches to forest conservation (Hannah et al. 2002). In spite of their global relevance, it remains unclear if forests in general (Dixon et al. 1994), or tropical forests specifically (Clark 2004a; 2004b), will be sources or sinks of carbon given future climatic changes. Cramer et al. (2004) used multiple dynamic global vegetation models to show that large increases in carbon loss from tropical forests could occur due to drought stress from increasing temperature and reduced rainfall. Such changes could result in potential tipping point beyond which large areas of tropical forest (i.e., the Amazon) could, through feedbacks with increased wildfire, transition to a savanna-like state (Nepstad et al. 2008). Large changes in the structure and dynamics of old growth forests throughout the tropics have already been documented (Lewis et al. 2004; Malhi 2004; Wright 2005).

Elevation gradients are one of the most convenient methods to understand the effects of change in climate on ecosystems (Körner 2007), and in particular on forests which are difficult to manipulate experimentally. In chapter four, I use an elevation gradient along the flank of the Mauna Kea volcano on the Big Island of Hawaii to assess interactions between climatic differences and forest structure (Broadbent et al. 2012a). Although much of this study is conducted at the leaf scale (Figure 1.3), integration with the Carnegie Airborne Observatory allows extrapolation of results to stand scales and provides insight into ecosystem function in a native Hawaiian forest undergoing simultaneous climate change and exotic species invasion.

## 1.1 Author Contributions

Although I am the lead author of the research presented in this dissertation, none of these studies would have been possible without the help and support of numerous individuals and institutions. I describe below the principal contributors and

co-authors critical to each study. Chapters two, three, and the appendix have already been published, as described below, and chapters four and five are written in a format suitable for submission to a peer-reviewed journal.

*Chapter 2: Forest fragmentation and edge effects from deforestation and selective logging in the Brazilian Amazon.* Gregory P. Asner, David E. Knapp and Paulo J. C. Oliveira contributed to study design. All co-authors contributed to interpretation of the data and manuscript preparation. This chapter has been published in the peer-reviewed journal Biological Conservation (Broadbent et al. 2008a). Elsevier has highlighted this chapter as one of the top 50 most cited articles in the journal from 2008 through 2011.

*Chapter 3: Spatial partitioning of biomass and diversity in a lowland Bolivian forest: linking field and remote sensing measurements.* Gregory P. Asner contributed to study design. Marlene Soriano helped with collection of field data. Marielos Peña-Claros helped with field logistics and manuscript preparation. Michael Palace helped with data analysis. This chapter has been published in the peer-reviewed journal Forest Ecology and Management (Broadbent et al. 2008b).

*Chapter 4: Predicting leaf trait variation in a Hawaiian rainforest understory: a microclimate modeling approach based on fusion of airborne LiDAR and hyperspectral imagery.* Angelica M. Almeyda Zambrano, Gregory P. Asner, Christopher B. Field contributed to study design and manuscript preparation. Angelica M. Almeyda, Brad E. Rosenheim, Ty Kennedy-Bowdoin, Aravindh Balaji, and David Knapp helped with data analysis and laboratory work. Angelica M. Almeyda and David Burke assisted with field data collection. Christian Giardina and Susan Cordell assisted with logistical issues and data interpretation.

*Chapter 5: Predictors of leaf trait variation in tree species during forest succession in the Bolivian Amazon.* Angélica M. Almeyda Zambrano and Marlene Soriano

contributed to study design. Angelica M. Almeyda, Gregory P. Asner, Christopher B. Field and Marielos Peña-Claros contributed to logistical assistance, data analysis and manuscript preparation. Angelica M. Almeyda, Marlene Soriano, and Harrison Ramos de Souza assisted with field data collection. Rachel Adams contributed to data analysis. Larry Giles assisted with lab analyses.

*Chapter 6 (Appendix): The effect of land use change and ecotourism on biodiversity: A case study of Manuel Antonio, Costa Rica, from 1985-2008.* Angélica M. Almeyda Zambrano, Rodolfo Dirzo, William H. Durham, Laura Driscoll, Patrick Gallagher, Rosalyn Salters, Jared Schultz, Angélica Colmenares assisted with logistics, study design, and field data collection. Angelica M. Almeyda assisted with data analysis, interpretation, and manuscript preparation. Shannon G. Randolph assisted with manuscript preparation. This work has been published in the journal Landscape Ecology (Broadbent et al. 2011c).

## 1.2 References

Achard F, Eva HD, Stibig H-J, Mayaux P, Gallego J, Richards T, Malingreau J-P. 2002. Determination of deforestation rates of the world's humid tropical forests. Science 297:999-1002

Almeyda Zambrano AM, Broadbent EN, Schmink M, Perz SG, Asner GP. 2010. Deforestation drivers in Southwest Amazonia: Comparing smallholder farmers in Iñapari, Peru, and Assis Brasil, Brazil. Conservation and Society 8:157-170

Asner GP, Knapp DE, Broadbent EN, Oliveira PJC, Keller M, Silva JN. 2005. Selective logging in the Brazilian Amazon. Science 310:480-482

Asner GP, Broadbent EN, Oliveira PJC, Keller M, Knapp DE, Silva JNM. 2006. Condition and fate of logged forests in the Brazilian Amazon. PNAS 103:12947-12950

Asner GP. 2009. Tropical forest carbon assessment: integrating satellite and airborne mapping approaches. Environmental Research Letters 4:034009

Asner GP. 2011. Painting the world REDD: addressing scientific barriers to monitoring emissions from tropical forests. Environmental Research Letters 6:021002

Barlow J, Gardner TA, Araujo IS, Avila-Pires TC, Bonaldo AB, Costa JE, Esposito MC, Ferreira LV, Hawes J, Hernandez MIM, Hoogmoed MS, Leite RN, Lo-Man-Hung NF, Malcolm JR, Martins MB, Mestre LAM, Miranda-Santos R, Nunes-Gutjahr AL, Overal WL, Parry L, Peters SL, Ribeiro-Junior MA, da Silva MNF, da Silva Motta C, Peres CA. 2007. Quantifying the biodiversity value of tropical primary, secondary, and plantation forests. PNAS 104:18555-18560

Binkley D, Giardina C. 1998. Why do tree species affect soils? The warp and woof of tree-soil interactions. Biogeochemistry 42:89-106

Bond WJ, Woodward FI, Midgley GF. 2005. The global distribution of ecosystems in a world without fire. The New Phytologist 165:525-537

Broadbent EN, Asner GP, Keller M, Knapp DE, Oliveira PJC, Silva JN. 2008a. Forest fragmentation and edge effects from deforestation and selective logging in the Brazilian Amazon. Biological Conservation 141:1745-1757

Broadbent EN, Asner GP, Peña-Claros M, Palace M, Soriano M. 2008b. Spatial partitioning of biomass and diversity in a lowland Bolivian forest: Linking field and remote sensing measurements. Forest Ecology and Management 255:2602-2616

Broadbent EN, Almeyda Zambrano AM, Asner GP, Field CB, Rosenheim BE, Kennedy-Bowdoin T, Balaji A, Knapp D, Burke D, Giardina C, Cordell S. 2012a. Predicting leaf trait variation in a Hawaiian rainforest: a microclimate modeling approach using airborne LiDAR - hyperspectral fusion. In preparation.

Broadbent EN, Almeyda Zambrano AM., Asner GP, Soriano M, Field CB., Ramos de Souza H, Peña-Claros M, Adams R, Giles L. 2012b. Predictors of leaf trait variation in tree species during forest succession in the Bolivian Amazon. In preparation.

Broadbent EN, Almeyda Zambrano AM., Dirzo R, Durham WH, Driscoll L, Gallagher P, Salters R, Schultz J, Colmenares A, Randolph SG. 2012c. The effect of land use change and ecotourism on biodiversity: A case study of Manuel Antonio, Costa Rica, from 1985-2008. Landscape Ecology 27:731-744

Brooks TM, Wright SJ, Sheil D. 2009. Evaluating the success of conservation actions in safeguarding tropical forest biodiversity. Conservation Biology 23:1448-1457

Chapin III FS, Matson PA, Mooney HA. 2002. Principles of Terrestrial Ecosystem Ecology. New York, USA: Springer.

Chapin III FS, Randerson JT, McGuire AD, Foley JA, Field CB. 2008. Changing feedbacks in the climate-biosphere system. Frontiers in Ecology and the Environment. 6:313-320

Chazdon RL, Finegan B, Capers RS, Salgado-Negret B, Casanoves F, Boukili V, Norden N. 2010. Composition and dynamics of functional groups of trees during tropical forest succession in northeastern Costa Rica. Biotropica 42:31-40

Clark DA. 2004a. Tropical forests and global warming: slowing it down or speeding it up? Frontiers in Ecology and the Environment 2:73-80

Clark DA. 2004b. Sources or sinks? The responses of tropical forests to current and future climate and atmospheric composition. 359:477-491

Corlett RT. 1995. Tropical secondary forests. Progress in Physical Geography 19:159-172

Cramer W, Bondeau A, Woodward FI, Prentice IC, Betts RA, Brovkin V, Cox PM, Fisher V, Foley JA, Friend AD, Kucharik C, Lomas MR, Ramankutty N, Sitch

S, Smith B, White A, Young-Molling C. 2001. Global response of terrestrial ecosystem structure and function to $CO_2$ and climate change: results from six dynamic global vegetation models. Global Change Biology 7:357-373

Cramer W, Bondeau A, Schaphoff S, Lucht W, Smith B, Sitch S. 2004. Tropical forests and the global carbon cycle: impacts of atmospheric carbon dioxide, climate change and rate of deforestation. Philosophical transactions of the royal society of London. Series B, Biological Sciences. 359:331-343

Daily GC. 1997. Countryside biogeography and the provision of ecosystem services. Pages 104–113 in P. Raven, editor. Nature and human society: The quest for a sustainable world. National Research Council, National Academy Press, Washington, D.C., USA.

DeFries RS, Houghton RA, Hansen MC, Field CB, Skole D, Townshend J. 2002. Carbon emissions from tropical deforestation and regrowth based on satellite observations for the 1980s and 1990s. PNAS 99:14256-14261

DeFries RS, Foley JA, Asner GP. 2004. Land-use choices: balancing human needs and ecosystem function. Frontiers in Ecology and the Environment 2:249-257

DeFries RS, Hansen A, Newton AC, Hansen MC. 2005. Increasing isolation of protected areas in tropical forests over the past twenty years. Ecological Applications 15:19-26

Dirzo R. 2001. Tropical Forests. Pages 251-276 in FS Chapin III, editor. Global Biodiversity in a Changing Environment, New York, New York: Springer-Verlag New York, Inc.

Dirzo R, Raven P. 2003. Global state of biodiversity and loss. Annual Review of Environment and Resources 28:137-167

Dixon RK, Brown S, Houghton RA, Solomon AM, Trexler MC, Wisniewski J. 1994. Carbon pools and flux of global forest ecosystems. Science 263:185–190

Fearnside PM, Guimarães WM. 1996. Carbon uptake by secondary forests in Brazilian Amazonia. Forest Ecology and Management 80:35-46

Field CB, Behrenfeld MJ, Randerson JT, Falkowski P. 1998. Primary production of the biosphere: integrating terrestrial and oceanic components. Science 281:237-240

Foley JA, DeFries R, Asner GP, Barford C, Bonan G, Carpenter SR, Chapin FS, Coe MT, Daily GC, Gibbs HK, Helkowski JH, Holloway T, Howard EA, Kucharik CJ, Monfreda C, Patz JA, Prentice C, Ramankutty N, Snyder PK. 2005. Global consequences of land use. Science 309:570-574

Foley JA, Asner GP, Costa MH, Coe MT, DeFries R, Gibbs HK, Howard EA, Olson S, Patz J, Ramankutty N, Snyder P. 2007. Amazonia revealed: forest degradation and loss of ecosystem goods and services in the Amazon Basin. Frontiers in Ecology 5:25-32

Gaston K. 2000. Global patterns of biodiversity. Nature 405:220-227

Gentry AH. 1988. Tree species richness of upper Amazonian forests. Proceedings of the National Academy of Sciences. 85:156-159

Gibbs HK, Brown S, Niles JO, Foley JA. 2007. Monitoring and estimating tropical forest carbon stocks: making REDD a reality. Environmental Research Letters 4:045023

Goldewijk KK. 2001. Estimating global land use change over the past 300 years: The HYDE Database. Global Biogeochemical Cycles 15:417-433

Grainger A. 2008. Difficulties in tracking the long-term global trend in tropical forest area. PNAS 105:818-823

Guariguata M, Ostertag R. 2001. Neotropical secondary forest succession: changes in structural and functional characteristics. Forest Ecology and Management 148:185-206

Hannah L, Midgley GF, Lovejoy T, Bond WJ, Bush M, Lovett JC, Scott D, Woodward FI. 2002. Conservation of biodiversity in a changing climate. Conservation Biology 16:264-168

Houghton RA, Boone RD, Melillo JM, Palm CA, Woodwell GM, Myers N, Moore B, Skole DL. 1985. Net Flux of Carbon Dioxide from Tropical Forests in 1980. Nature 316:617-620

Houghton RA. 2003. Revised estimates of the annual net flux of carbon to the atmosphere from changes in land use and land management 1850-2000. Tellus Series B – Chemical and Physical Meteorology 55:378-390

IPCC. 2002. Climate Change 2001: The Scientific Basis. Cambridge, MA: Cambridge University Press

Karsenty A. 2008. The architecture of proposed REDD schemes after Bali: Facing critical choices. International Forestry Review 10:443-457

Klein Goldewijk, K. 2001 Estimating global land use change over the past 300 years: the HYDE database. Global Biogeochemical Cycles 15:417–434

Körner C. 2007. The use of 'altitude' in ecological research. Trends in Ecology and Evolution 22:569-574

Lélé SM. 1991. Sustainable development: A critical review. World Development 19:607-621

Lewis SL, Phillips OL, Baker TR, Lloyd J, Malhi Y, Almeida S, Higuchi N, Laurance WF, Neill DA, Silva JNM, Terborgh J, Torres Lezama A, Vasquex Martinez R, Brown S, Chave J, Kuebler C, Núñez Vargas P, Vinceti B. 2004. Concerted changes in tropical forest structure and dynamics: evidence from 50 South American long-term plots. Philosophical Transactions of the Royal Society of London. Series B, Biological Sciences. 359:421-436

Malhi Y, Phillips OL. 2004. Tropical forests and global atmospheric change: a synthesis. Philosophical Transactions of the Royal Society of London. Series B, Biological Sciences. 359:549-555

Margulis L, Schwartz KV. 1998. Five Kingdoms, An Illustrated Guide to the Phyla of Life on Earth. New York: Freeman

May RM. 2000. The dimensions of life on Earth. In Nature and Human Society: The Quest for a SustainableWorld, ed. PH Raven, T Williams, pp. 30–45. Washington, DC: The National Academies Press

Mellilo JM, McGuire AD, Kicklighter DW, Moore BI, Vorosmarty CJ, Schloss AL. 1993. Global climate change and terrestrial net primary production. Nature 363:234–240

Mittermeier RA, Mittermeier CG, Brooks TM, Pilgrim JD, Konstant WR, da Fonseca GAB, Kormos C. 2003. Wilderness and biodiversity conservation. PNAS 100:10309-10313

Myers N, Mittermeier RA, Mittermeier CG. 2000. Biodiversity hotspots for conservation priorities. Nature 403:853-858

National Research Council (NRC). 1988. Biodiversity. ed. EO Wilson. Washington, DC: The National Academies Press

Nepstad DC, Verissimo A, Alencar A, Nobre C, Lima E, Lefebvre P, Schlesinger P, Potter C, Moutinho P, Mendoza E, Cochrane M, Brooks V. 1999. Large-scale impoverishment of Amazonian forests by logging and fire. Nature 398:505-508

Nepstad DC, Stickler CM, Soares-Filho B, Merry F. 2008. Interactions among Amazon land use, forests and climate: prospects for a near-term forest tipping point. Philosophical Transactions of The Royal Society of London. Series B, Biological Sciences. 363:1737-1746

Noble IR, Dirzo R. 1997. Forests as human-dominated landscapes. Science 277:522-525

Olson DM. 1998. The Global 200: a representation approach to conserving the Earth's most biologically valuable ecoregions. Conservation Biology 12:502-515

Paulay G. 1994. Biodiversity on oceanic islands: its origin and extinction. American Zoologist 34:134-144

Ramankutty N, Foley JA. 1999. Estimating historical changes in global land cover: Croplands from 1700 to 1992. Global Biogeochemical Cycles 13:997-1027

Ramankutty N, Gibbs HK, Achard F, DeFries D, Foley JA, Houghton RA. 2007. Challenges to estimating carbon emissions from tropical deforestation. Global Change Biology 13:51-66

Reid WV. 1992. How many species will be there? Pages 55-73, in: Whitmore TC, Sayer JA, editor, Tropical Deforestation and Species Extinction, Chapman and Hall , London

Rey Benayas JM, Martins A, Nicolau JM, Schulz JJ. 2007. Abandonment of agricultural land: an overview of drivers and consequences. CAB Reviews: Perspectives in Agriculture. 2:14-28

Rodrigues ASL, Andelman SJ, Bakarr MI, Boitani L, Brooks TM, Cowling RM, Fishpool LDC, da Fonseca GAB, Gaston KJ, Hoffmann M, Long JS, Marquest PA, Pilgrim JD, Pressey RL, Schipper J, Sechrest W, Stuart SN, Underhill LG, Waller RW, Watts MEJ, Yan X. 2004. Effectiveness of the global protected area network in representing species diversity. Nature 428:9-12

Rudel TK, DeFries R, Asner GP, Laurance WF. 2009. Changing drivers of deforestation and new opportunities for conservation. Conservation Biology 23:1396-1405

Sala OE, Chapin III FS, Armesto JJ, Berlow E, Bloomfield J, Dirzo R, Huber-Sanwald E, Huenneke LF, Jackson RB, Kinzig A, Leemans R, Lodge DM, Mooney HA, Oesterheld M, Poff NL, Sykes MT, Walker BH, Walker M, Wall DH. 2000. Global biodiversity scenarios for the year 2100. Science 287:1770-1774

Simberloff D. 1986. Are we on the verge of a mass extinction in tropical rain forests? Pages 165-80 in Elliott DK, editor. Dynamics of Extinction, Wiley, New York, New York, USA

Stickler CM, Nepstad DC, Coe MT, McGrath DG, Rodrigues HO, Walker WS, Soares-Filho BS, Davidson EA. 2009. The potential ecological costs and

cobenefits of REDD: a critical review and case study from the Amazon region. Global Change Biology 15:2803-2824

Turner III BL, Lambin EF, Reenberg A. 2007. The emergence of land change science for global environmental change and sustainability. PNAS 104:20666-20672

Uhl C. 1987. Factors controlling succession following slash-and-burn agriculture in Amazonia. 75:377-407

Vitousek PM, Ehrlich PR, Erhlich AH, Matson PA. 1986. Human appropriation of the products of photosynthesis. BioScience 36:368-373

Vitousek PM. 1994. Beyond global warming: Ecology and global change. Ecology 75:1861-1876

Vitousek PM, Mooney HA, Lubchenco J, Melillo JM. 1997. Human dominantion of Earth's ecosystems. Science 277:494-499

Willing MR, Kaufman DM, Stevens RD. 2003. Latitudina gradients of biodiversity: Pattern, process, scale, and synthesis. Annual Review of Ecology, Evolution, and Systematics. 34:273-309

Wright JS. 2005. Tropical forests in a changing environment. TRENDS in Ecology and Evolution 20:553-60

Wright JS, Stoner KE, Beckman N, Corlett RT, Dirzo R, Muller-Landau HC, Nuñez-Iturri G, Peres CA, Wang BC. 2007. The plight of large animals in tropical forests and the consequences for plant regeneration. Biotropica 39:289-291

Zarin DJ, Ducey MJ, Tucker JM, Salas WA. 2001. Potential Biomass Accumulation in Amazonian Regrowth Forests. Ecosystems 4:658-668

Zarin DJ, Davidson EA, Brondizio E, Vieira ICG, Sa T, Feldpausch T, Schuur EAG, Mesquita R, Moran E, Delamonica P, Ducey MJ, Hurtt GC, Salimon C, Denich M. 2005. Legacy of fire slows carbon accumulation in Amazonian forest regrowth. Frontiers in Ecology 3:365-369

## 1.3 Figures

**Figure 1.1:** Spatial scale of forest dynamics addressed by each chapter and the appendix in this dissertation.

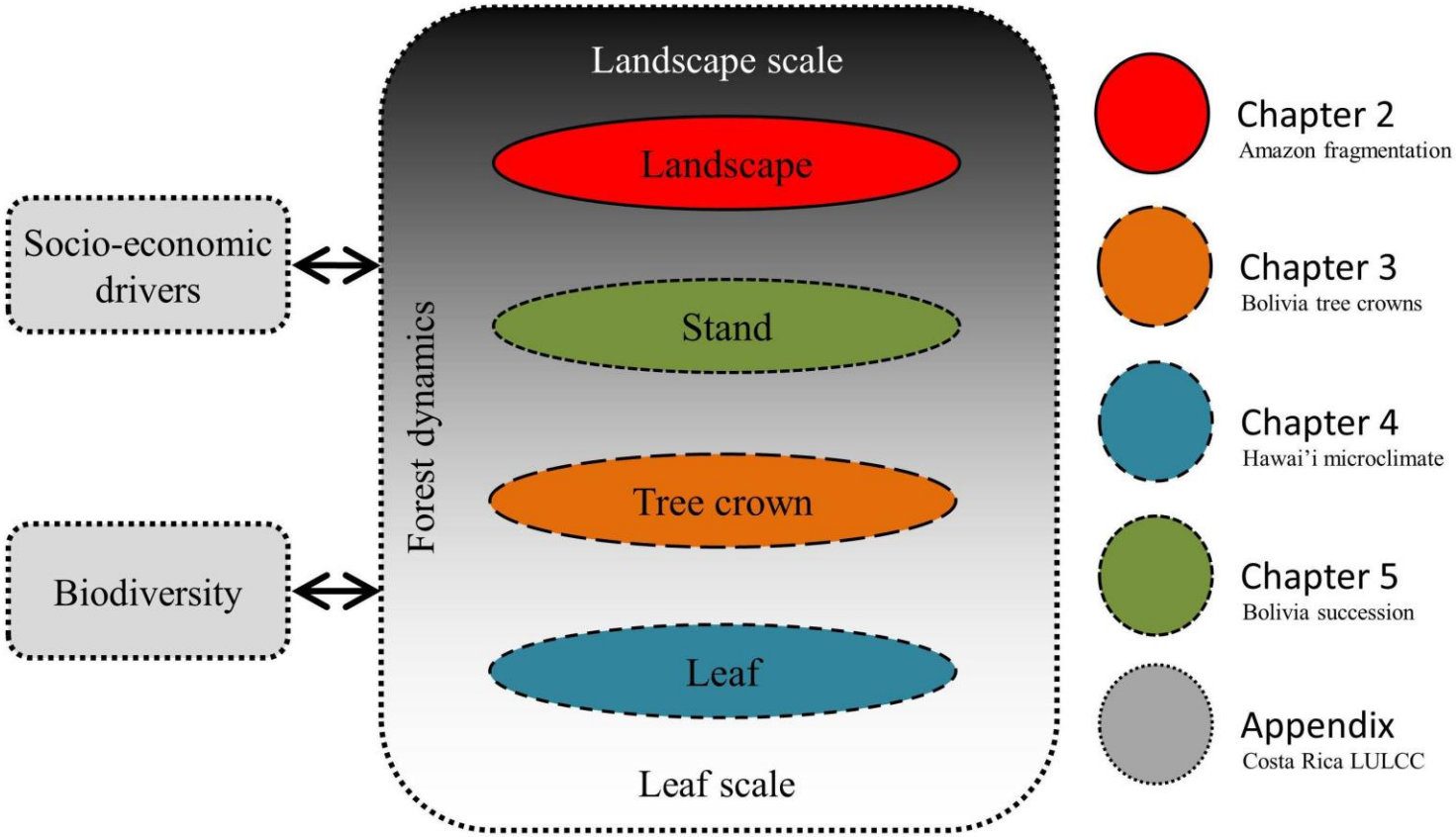

**Figure 1.2:** Interactions among themes related to forest dynamics across spatial and temporal scales addressed in this dissertation.

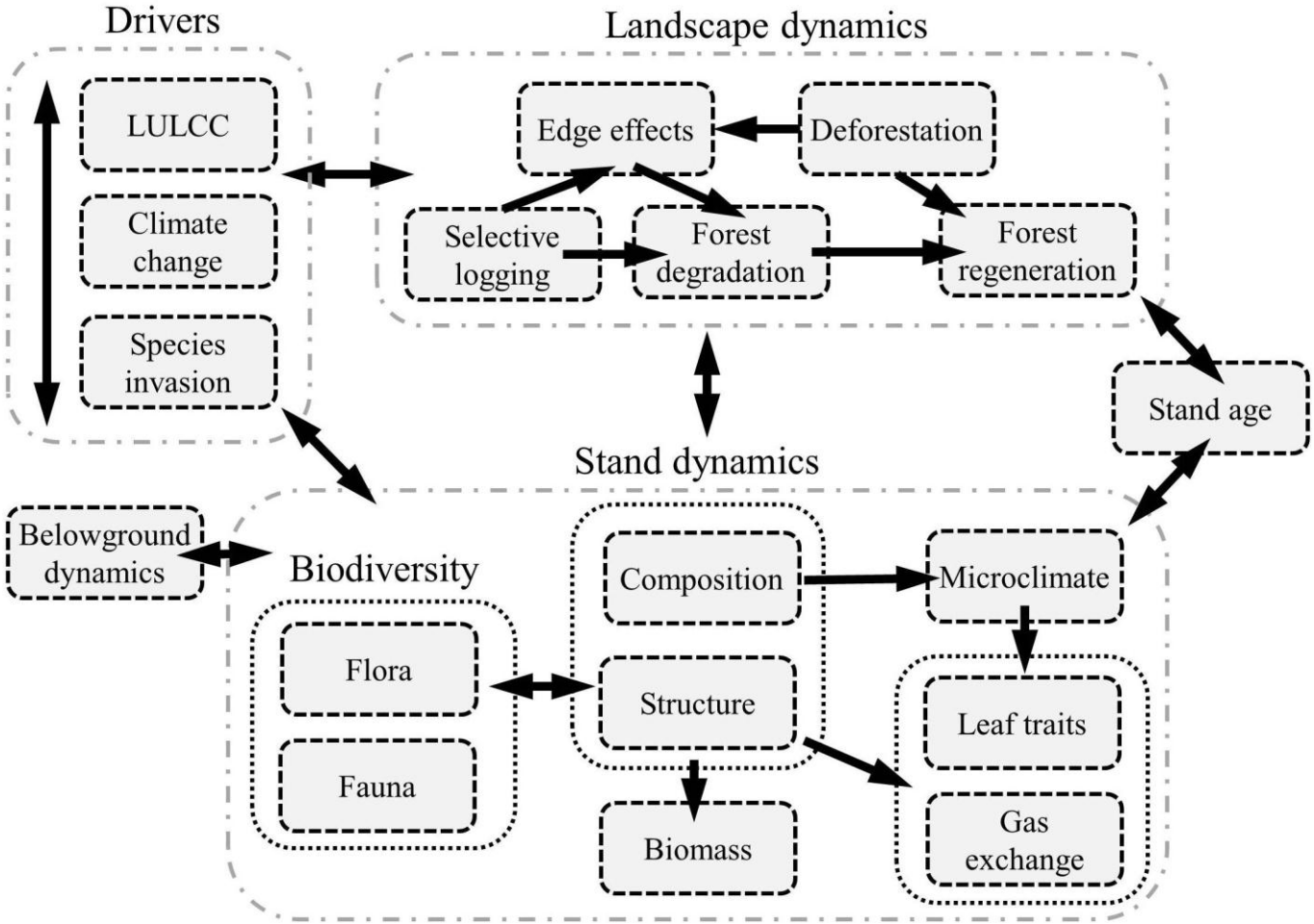

**Figure 1.3:** Spatial and temporal scale and resolution addressed by each chapter and the appendix in this dissertation.

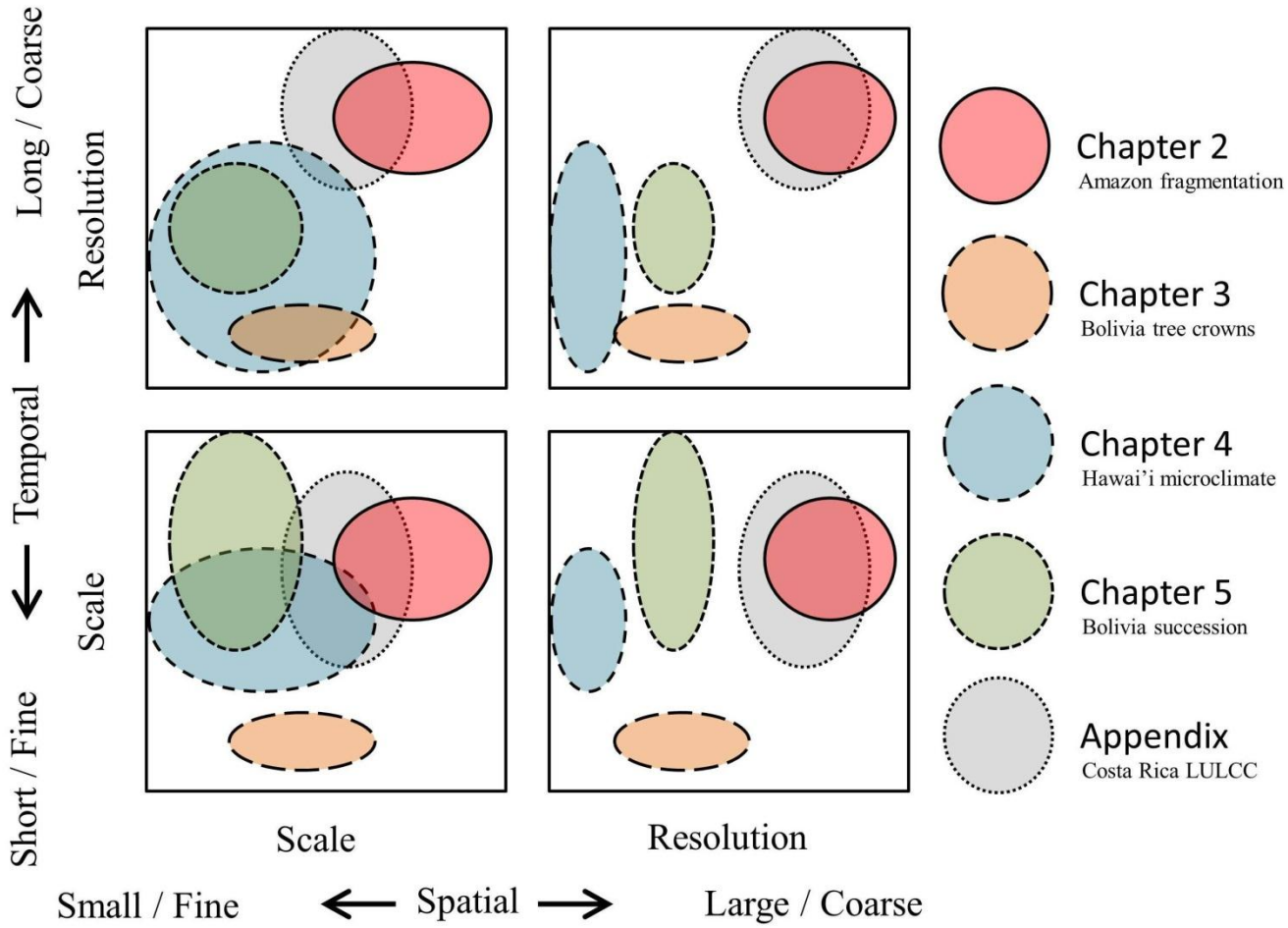

# CHAPTER 2

# FOREST FRAGMENTATION AND EDGE EFFECTS FROM DEFORESTATION AND SELECTIVE LOGGING IN THE BRAZILIAN AMAZON

## 2.1 Abstract

Forest fragmentation results from deforestation and disturbance, with subsequent edge effects extending deep into remaining forest areas. No study has quantified the effects of both deforestation and selective logging, separately and combined, on forest fragmentation and edge effects over large regions. The main objectives of this study were to: (1) quantify the rates and extent of forest fragmentation from deforestation and logging within the Brazilian Amazon, and (2) contextualize the spatio-temporal dynamics of this forest fragmentation through a literature review of potential ecological repercussions of edge creation. Using GIS and remote sensing, we quantified forest fragmentation - defined as both increases in the forest edge-to-area ratio and number of forest fragments - and edge-effected forest occurring from these activities across more than 1.1 million $km^2$ of the Brazilian Amazon from 1999 to 2002. Annually, deforestation and logging generated ~32,000 and 38,000 km of new forest edge while increasing the edge-to-area ratio of remaining forest by 0.14 and 0.15, respectively. Combined deforestation and logging increased the edge-to-area ratio of remaining forest by 65% over our study period, while generating 5539 and 3383 new forest fragments, respectively. Although we found that 90% of individual forest fragments were smaller than 4 $km^2$, we also found that 50% of the remaining intact forests were located in contiguous forest areas greater than 35,000 $km^2$. We then conducted a literature review documenting 146 edge effects and found that these penetrated to a median distance of 100 m, a distance encompassing 6.4% of all remaining forests in our study region in the year 2002, while 53% of forests were located within two km of an edge. Annually deforestation and logging

increased the proportion of edge-forest by 0.8% and 3.1%, respectively. As a result of both activities, the total proportion of edge-forest increased by 2.6% per year, while the proportion within 100 m increased by 0.5%. Over our study period, deforestation resulted in an additional 3000 $km^2$ of edge-forest, whereas logging generated ~20,000 $km^2$, as it extended deep into intact forest areas. These results show the large extent and rapid expansion of previously unquantified soft-edges throughout the Amazon and highlight the need for greater research into their ecological impacts.

*Keywords: Forest core, forest texture, landscape ecology, rainforest, remote sensing, sustainability*

## 2.2 Introduction

Forest fragmentation and edge effects from deforestation have been identified as one of the most pervasive and deleterious processes occurring in the tropics today (Gascon et al., 2000; Murcia, 1995; Skole and Tucker, 1993). Forest fragmentation results from the simultaneous reduction of forest area, increase in forest edge, and the sub-division of large forest areas into smaller non-contiguous fragments (Laurance, 2000). The detrimental effects of forest fragmentation from deforestation include increases in wildfire susceptibility (Alencar et al., 2004; Cochrane and Laurance, 2002; Cochrane et al., 2002) and tree mortality, changes in plant and animal species composition (Tabanez and Viana, 2000; Barlow et al., 2006; Cushman, 2006), seed dispersion (Rodríguez-Cabal et al., 2007; Cramer et al., 2007) and fruit and seed predation (Herrerías-Diego et al., 2008) and easier access to interior forest, leading to increased hunting and resource extraction (Peres, 2001) or conversion to agroscape (Kaimowitz and Angelsen, 1998). Forest fragmentation results in an increased proportion of the remaining forest being located in close proximity to the forest edge (Saunders et al., 1991). Detrimental edge effects extend into interior forest areas from these transition zones. While the majority of these effects are thought to extend no

further than 1 km (Murcia, 1995), some may extend as far as 5-10 km into intact forest areas (Curran et al., 1999). The negative impacts of edge effects on ecosystems include shifts in plant and animal community composition and changes in diversity (Benitez-Malvido and Martinez-Ramos, 2003; Cagnolo et al., 2006), increased rates of tree mortality (Nascimento and Laurance, 2004), and fire susceptibility (Cochrane and Laurance, 2002), altered microclimates (Williams-Linera et al., 1998), and increased carbon emissions (Laurance et al., 1997, Laurance and Williamson, 2001), primarily from increased mortality of large trees (Laurance et al., 2000).

Although research employing remote sensing and GIS have quantified significant fragmentation and potentially edge-effected forest from deforestation at small scales, few have been at the scale representative of the Amazon region. Large-scale impacts at the Amazon were highlighted by Skole and Tucker (1993) who showed that, in 1988, ~16,000 $km^2$ of remaining forest occurred within ~10,000 forest fragments <100 $km^2$, while the remaining 3,600,000 $km^2$ of intact forest occurred in a similar number of fragments. They calculated that potentially edge-effected forest (up to 1 km into interior forest) within these fragments affected an area 68% larger than that of the deforested area alone. Similar results from deforestation have been found at smaller scales. Forest subdivision was documented by Ranta et al. (1998) in 629 $km^2$ of the Brazilian Atlantic coastal region where the majority of forest fragments were found to be smaller than 30 ha, and by Cochrane (2001) for 1280 $km^2$ in Northeastern Pará where the majority of the remaining forests were located within a few large contiguous forest areas and that over 50% and ~85% of the remaining forest was within 300m and 1 km, respectively, of a forest edge. Cochrane et al. (2002) later studied 16,819 $km^2$ in the Sinop region of Mato Grosso, Brazil, and calculated that 52% of the remaining 12,271 $km^2$ of forests were within one km of the nearest edge.

In this study, we present selective logging as a previously unquantified driver of rapid and extensive forest fragmentation and subsequent edge effects in the Brazilian Amazon. Selective logging, which has only recently been mapped across the Brazilian Amazon, annually impacts as much forest area as the area converted to pasture or agriculture (Asner et al., 2005). In the Brazilian Amazon, only 2-9

merchantable species are removed per hectare of forest logged, but this process results in considerable ground and canopy damage (Asner et al., 2006; Pereira et al., 2002). Although the forest-to-logged forest transition is less abrupt than that between forest and pasture or agricultural areas, the effects of logging on forest ecological, hydrological, and microclimatic processes have been well documented (Uhl et al., 1991; Verıssimo et al., 1992). Selective logging has been shown to cause alterations in forest biophysical properties, including water and wind stress, and changes in micro-meteorological and aquatic systems (Pringle and Benstead, 2001), which may lead to an increased vulnerability to fires (Cochrane, 2001; Nepstad et al., 1999), as well as changes in overall forest structure and composition (Nepstad et al., 1992). Selective logging also has a direct impact on faunal populations, including insects (Lawton et al., 1998), primates (Johns and Johns, 1995), birds (Mason and Thiolay, 2001), bats (Soriano and Ochoa, 2001), and arboreal animals in general (Putz et al., 2001a,b). Like fragmentation, logging also leads to increased human access and reductions in animal populations and forest resources through hunting and extraction (Nepstad et al., 1992).

Although selective logging has been described as an integral large-scale driver of forest fragmentation (Gascon et al., 2000; Laurance, 2000), and Asner et al. (2006) have shown that timber extraction is occurring over large areas at high intensities, no study has yet quantified the extent and rate of forest fragmentation and edge effects from both deforestation and selective logging at large scales. The main objectives of this study were to: (1) quantify the rates and extent of forest fragmentation within the Brazilian Amazon, with an emphasis on comparing soft- and hard-edges, and (2) contextualize the spatio-temporal dynamics of this forest fragmentation through a literature review of potential ecological repercussions of edge creation. To address these objectives we present new data highlighting the intensity, longevity and fine-scale spatial distribution of canopy damage following selective logging, then we quantify the large-scale extent and annual rates of forest fragmentation – defined as both increases in the forest edge-to-area ratio and number of forest fragments – from deforestation (referred to as hard-edges) and selective logging (referred to as soft-edges) from 1999 to 2002 across 1.12 million $km^2$ of the Brazilian amazon “arc of

deforestation". We then conduct an extensive literature review to document the variety and intensity of measured edge effects, and to quantify the total area and annual change in the area of forest potentially degraded by edge effects extending from deforested and selectively logged areas.

## 2.3 Materials and Methods

### 2.3.1 Study region

The study region covered portions of four states (Acre, Mato Grosso, Pará, and Rondônia) in the Brazilian Amazon region which had deforestation and logging coverage over the study period 1999–2002. Areas with atmospheric interference (clouds or other) during any study year were removed from the analysis. The final study area encompassed over 1.12 million $km^2$. The selected area encompassed >80% of the deforestation (INPE, 2005) and selective logging (Asner et al., 2005) occurring within the Brazilian Amazon (Fig. 2.1). Although the majority of cloud interference problems were encountered in northern Pará, only a small section of northeastern Pará included significant incidence of logging or deforestation. Contiguous forested fragments smaller than 0.05 $km^2$ were excluded from our analysis as they frequently resulted from spatial misregistration errors.

### 2.3.2 Deforestation and logging maps

Maps of logging were obtained from the Carnegie Landsat Analysis System (CLAS), a system developed to identify forest disturbances and selective logging over large areas. A detailed description of the CLAS methodology, including the uncertainty analysis and validation effort, was provided in Asner et al. (2005). The final CLAS output is a map of logged areas within which canopy damage is quantified in each pixel, with a reported error of 11-14% (see Fig. 2.2). Maps of deforestation were obtained from the Program for Monitoring Deforestation in the Brazilian

Amazon (PRODES) of the Brazilian Institute for Space Research (INPE). PRODES deforestation maps in Geographic Information System (GIS) format are freely available at http://www.obt.inpe.br/prodes/, and are considered to be the best deforestation maps available for the Brazilian Amazon (Defries et al., 2005). The PRODES data used in this paper were accessed from September 2005 to May 2006. These data are subject to a 4% error from atmospheric conditions, spatial misregistration, or misclassification (INPE, 2005). PRODES began producing spatially accurate maps of annual deforestation in 2000–2001, whereas the year 2000 PRODES map represents cumulative deforestation from 1997 to 2000. In order to compare 1999–2000 CLAS logging to one year of PRODES deforestation, we calculated the mean annual change from the 1997 to 2000 PRODES data.

Both the deforestation and logging maps are based on 30-m resolution Landsat Enhanced Thematic Mapper Plus (ETM+) satellite imagery. The minimum deforested or logged area identified by the PRODES deforestation and CLAS logging was approximately 6 ha. We integrated the deforestation and logging maps in a GIS to quantify the impacts of deforestation with both new and up to three years of cumulative logging. We define new logging as logging occurring in the study year and cumulative logging as that occurring over multiple years. We quantified separately the fragmentation and edge effects of deforestation, new logging, and cumulative logging. As forest edge occurred simultaneously proximate to deforested and logged areas, we defined logging edge length and edge-forest extent as that which occurred in addition to that caused by deforestation through the specified study year.

### 2.3.3 Forest fragmentation and structure

We quantified forest structure at a fine-scale within logged areas and forest fragmentation at a large-scale for all forests within our study area. The effect of logging on fine-scale forest structure was investigated using canopy texture, which we define as the mean absolute difference in forest gap fraction between adjacent pixels, within a moving 6 x 6 pixel window. Forest canopy-gap fraction (e.g., canopy

openness *sensu* Pereira et al., 2002) is an indicator of forest structure that affects leaf physiology, forest carbon budgets, water balances, primary production, microclimate, and biodiversity (Brokaw, 1982; Mulkey and Pearcy, 1992). In this study, we used remotely sensed canopy-gap fraction images developed through extensive field work and described in detail by Asner et al. (2006). Canopy texture was used to quantify differences in the spatial distribution and extent of canopy damage between logged areas and intact forest. We used one-way ANOVA with Tukey's HSD post hoc test to evaluate significance of gap fraction and texture for up to two years post-logging. We randomly choose 25% of the available samples (n = 330,433) to limit the effects of spatial autocorrelation in our statistical comparison.

At the large-scale, we used two metrics of forest fragmentation: (1) the edge-to-area ratio (fragment edge/area) of all forest within our study area, hereafter referred to as edge-to- area fragmentation, and (2) the overall number of non-contiguous forest fragments, hereafter referred to as subdivision fragmentation. Changes in fragmentation were identified following 2000-2002 deforestation alone, and after including the additional impacts of new and cumulative logging. We quantified total edge length occurring from both deforestation and logging as well as natural sources (including transitions from forest to river or natural non-forested areas) and used temporal changes to discern anthropogenic impacts. The forest interface used in the calculations depended on the deforestation-logging combination because logging and the different ages of logged areas were either ignored or included as a source of additional forest edge interface over that of deforestation. We describe these combinations using a "D" for deforestation and an ''L'' for logging, followed by the included year (s). As the impact of a logged area would change with time post-harvest, we created combinations including and excluding older years of logging. These combinations were not necessary for deforestation, as we did not consider regeneration of deforested areas during our study period, although we recognize that soft- and hard-edge structure and influence changes with time (Didham and Lawton, 1999). The number of individual forested fragments, as well as their edge length and area, were calculated over the study area for the years 1997 and 2002. A maximum

area threshold of 350 $km^2$, which included 99.5% of all forest fragments, was used to exclude the very largest forest areas, which were contiguous between study states.

### 2.3.4 Forest edge effects

We limited our analysis to forested areas within two km of the nearest forest edge – hereafter referred to as edge-forests – based on the results of our spatial analysis and literature review, both of which showed that two km encompassed nearly all documented edge effects and potentially affected forest area in our study region (Fig. 2.3). Linear distance maps to the nearest forest edge were created for all deforestation–logging combinations at a spatial resolution of 100 x 100 m, the maximum possible considering computing requirements.

### 2.3.5 Literature review

We performed a literature review using academic search engines from December, 2005 to February, 2006 for the terms "forest fragmentation" and "edge effects" in peer-reviewed articles. We then iteratively scanned the bibliographies of the articles until no new relevant articles were identified. We recorded specific edge effects and the distance to which these effects penetrated the forest interior. All documented edge effects, including both temperate and tropical regions, were included in our review. We divided the reported impacts into four broad categories: (1) forest structure, (2) tree mortality, (3) forest microclimate, and (4) biodiversity.

## 2.4 Results

### 2.4.1 Forest fragmentation

At the fine-scale logging immediately increased the mean forest gap fraction from 14% to 22%, while doubling the mean canopy texture from 7% to 13% ($p < 0.05$; ANOVA). Changes in canopy-gap fraction and texture remained significant during the

two years following harvest (Tukey's HSD; $p < 0.05$). The largest decreases in canopy-gap fraction and texture occurred in the year immediately following logging, with the means decreasing from 13% and 22% to 8% and 15%, respectively. An example of the spatio-temporal dynamics of deforestation and logging is provided in Fig. 2.2.

Results from the large-scale analyses of edge-to-area and subdivision fragmentation are provided in Table 2.1 and Fig. 2.4. During our study period, forest area decreased 13% from deforestation and cumulative logging, while edge length increased 69%, resulting in an increase in edge-to-area frag- mentation of 61%. Annually new logging directly impacted about the same area as deforestation, while creating 117% more new forest edge. Subdivision from these activities increased the total number of forest fragments 74%, from 15,229 to 26,516 (Table 2.1). Annually new logging increased the number of forest fragments by 39%; however, when considered cumulatively (2000–2002), logging resulted in a 64% in- crease in total forest fragments. Although around 90% of individual forest fragments were smaller than 4 $km^2$ (Fig. 2.4A), more than 50% of total remaining forest occurred in fragments greater than 35,000$km^2$ (Fig. 2.4B).

In addition to large-scale subdivision fragmentation, individual forest fragments themselves became increasingly edge-to-area fragmented. Between 1997 and 2002, including deforestation only, the mean (std. dev.) area and perimeter of individual forest fragments decreased significantly from 3.5 (15.9) to 2.6 (13.7) $km^2$ and from 10.3 (28.4) to 9.8 (27.9) km, respectively, while the mean edge-to-area ratio increased from 9.3 (5.3) to 14.6 (11.3) (Tukey's HSD; $p < 0.05$). The addition of cumulative logging (2000–2002) did not significantly increase the edge-to-area fragmentation of these fragments over that of deforestation alone.

### 2.4.2 Forest edge effects

Results of the forest edge analysis are provided in Table 2.1 and Figs. 4 and 5. By the year 2002, including deforestation only, the proportion of edge-forests in the

study region had increased to 48%. Cumulative logging (2000-2002) further increased the proportion of edge-forest to 53% (Table 2.1), with 37% of remaining forest being within 1 km and 6.4% being within 100 m of the nearest edge (Fig. 2.4C), while more than 50% of all edge-forest occurred within 0.6 km of the nearest edge (Fig. 2.4D). The explicit spatial dynamics of edge-forest generation from deforestation, and new and cumulative logging are illustrated in Fig. 2.5. Annually, the total percentage of remaining forests less than two km from an edge increased by 2.6%, while the proportion within 100-m increased by 0.5% (Fig. 2.5). Deforestation increased the area of forest up to ~0.5 km, but decreased forest area from 0.5 to 2 km into interior forest, while new logging increased the forest area <1.8 km into intact forest areas, and then decreased the forest area up to 2 km study limit. Deforestation annually increased the area of forest within 100 m of the forest edge by 1800 $km^2$, while the addition of new and cumulative logging increased the forest area by 2500 and 4800 $km^2$, respectively (Fig. 2.5).

### 2.4.3 Literature review

The effects of edges on tropical and temperate forest attributes and function were abundantly documented in the literature (Figs. 3 and 6). Although our literature review initially identified hundreds of articles, only 62 of these provided explicit interior forest penetration distances for edge effects. Approximately 45% of all documented edge impacts extended ≤100 m, while 99% of documented edge impacts extended ≤ 2 km, into the surrounding forest. The 146 reported edge effects were divided about equally among four categories: (A) forest structure, (B) tree mortality, (C) microclimate, and (D) biodiversity (Fig. 2.6). Descriptive statistics for these categories are provided in Table 2.2, and complete references are provided in Supplementary Materials 2A.

Our review documented numerous impacts of hard-edges. In general, immediately following conversion of intact forest to pasture or agriculture, microclimatic alterations occur in the nearby surrounding forest edges through

increased penetration of sunlight and wind (Didham and Lawton, 1999). Air and soil moisture decrease (Williams-Linera et al., 1998), while there are increases in temperature (Cadenasso et al., 1997), vapor pressure deficit (Davies-Colley et al., 2000) and the availability of photosynthetically active radiation to the understory (Kapos, 1989), and throughout the forest edge (Young and Mitchell, 1994). Litterfall production increases (Sizer et al., 2000), as does the accumulated depth of the litter layer (Matlack, 1993), resulting in rapid increases in susceptibility to wildfire (Cochrane and Laurance, 2002), especially as forest edges are often located adjacent to agricultural or pasture lands that are often burned as part of their management (Peres, 2001).

Following edge creation, forest structure and composition can be altered both in interior forest (Mesquita et al., 1999) or at the forest edge (Didham and Lawton, 1999), as large trees often die off within 300m of the forest edge (Laurance et al., 2000), being replaced by densely spaced short-lived pioneers (Laurance et al., 2006), resulting in decreases in forest biomass (Nascimento and Laurance, 2004) and basal area (Harper et al., 2005). Tree mortality is also linked to positive feedbacks with fires (Cochrane, 2001), resulting in further loss of biomass (Laurance and Williamson, 2001) and carbon emissions to the atmosphere through increased turnover of necromass (Nascimento and Laurance, 2004). The change to a smaller statured forest (Didham and Lawton, 1999), sometimes containing plants having more chemical defenses (Hester and Hobbs, 1992), occurs through loss of native vegetation and often leads to an increased abundance of invasive species (Hobbs, 2001). Changes in structure and composition, accompanied by disruptions in plant–animal interactions (Rodríguez-Cabal et al., 2007), in turn, sometimes lead to invasion of disturbance-adapted animal species, including butterflies (Lovejoy et al., 1986), beetles (Didham, 1997; Nichols et al., 2007), pigs (Peters, 2000), birds (Hagan et al., 1996), frogs and lizards (Schlaepfer and Gavin, 2001), and mammals (Kinnaird et al., 2003), while insect biomass moves from the overstory to the understory (Malcolm, 1997).

Only four of the 62 reviewed articles addressed soft-edges. Pereira et al. (2002) and Asner et al. (2004) found that tree-felling gaps caused significant increases in

canopy openness for up to 100 m in the surrounding forest. Uhl and Buschbacher (1985) and Cochrane et al. (2004) highlighted the positive synergism between anthropogenic fires and wildfires in selectively logged forests. Given the paucity of literature on the ecological impacts of soft-edges and the very large length and area they occupy there is a clear need for additional studies of soft-edge impacts on biodiversity and ecosystem function.

## 2.5 Discussion

Although deforestation has been measured for decades, the full extent and spatial distribution of selective logging in the Amazon has only recently been mapped. Asner et al. (2005) showed the logging annually impacts a forest area equal in size (~12,000–19,000 $km^2$ annually) to that deforested. Subsequent analysis revealed that ≥76% of selective logging resulted in high levels of forest canopy damage, and that much of the area selectively logged was deforested within several years (Asner et al., 2006). Preliminary analysis of the selective logging data showed substantially different patterns in spatial distribution between selective logging and deforestation, which prompted the full spatial analysis presented in this study.

Traditionally, selective logging alone has not been considered as a source of forest fragments, as it does not generally result in a dramatic loss of vegetation cover. However, depending on harvest intensity, losses of 10–60% of canopy cover from logging operations are typical and logging activities cause marked disruption and small-scale fragmentation of the forest understory, mainly by roads, skidder tracks, and patios (e.g., Pereira et al., 2002). In addition, the results of our fine-scale analyses of fragmentation indicated that canopy damage in logged areas is intense and spatially distributed throughout the logged area. This combination indicates that logged areas could, for the reasons previously highlighted, result in extensive forest fragmentation and edge-effects. The detrimental impacts of selective logging may extend many years, especially when considering that many forest structural properties, such as deep

canopies, associated with wildlife habitat in intact forests, are not likely to be regained for 30–50 years or more following logging (Plumptre, 1996).

Canopy openings from logging disturbances are, however, far smaller than clearings for farms or ranches which generally lead to increased windspeeds, desiccation, and other microclimatic alterations, which in turn are key drivers of edge effects (see Laurance et al., 2002). In addition, forest edges adjoining farms or ranches are often repeatedly impacted by pasture burning, which can severely damage adjacent forests. Therefore, the penetration and magnitude of many edge effects are likely to be greater near forest to non-forest edges than near the edges of logged forest. However, large increases in fire susceptibility have been documented in forests (Cochrane et al., 2002) which result in edge-like effects following logging operations. Furthermore, the temporal trajectories of edge effects would differ, with some logged forests recovering or being managed, such as could potentially occur in over 50 million ha of National Forests (FLONAs) being established throughout the Brazilian Amazon (Veríssimo et al. 2002); while other logged areas undergo burning or subsequent deforestation.

Importantly, many species of forest-dependent fauna whose movements would be precluded by major clearings, such as cattle pastures or soy farms, probably do use logged forest (e.g. many understory birds, primates, and forest-interior insects such as certain beetles, ants, butterflies and euglossine bees; see Barlow et al., 2006, 2007 and Laurance et al., 2002), especially after a few years of forest recovery. Thus, logging alone is unlikely to isolate forest-dependent animal populations nearly to the extent of that caused by forest fragmentation from deforestation. Logging does, however, greatly facilitate hunting in some contexts (Walker, 2003), and in those cases the impacts of logging on hunted species, and the resulting fragmentation of their populations, could be far greater. Logged areas closer to settlements could result in increased hunting pressure, while those located further into forest interiors might cause a proportionally larger impact on remaining wildlife.

Edge effects can also be strongly influenced by local landscape and larger-scale climatic effects. For example, edge-related fires can penetrate up to a few kilometers into fragmented forests, and especially following logging, in more seasonal

parts of the Amazon, but are less important in less seasonal areas. The type of land-use surrounding fragments is also very important. Fragments encircled by pastures, which are often burned annually, are subjected to recurring disturbance from fires, whereas those adjoined by many crops may not experience recurring fires.

Logging edges differ from those of deforestation in several ways. First, the interface is forest-to-degraded-forest and a large variation in forest degradation exists. Second, these edges either recover through time (5–50 yrs depending on the edge effect), likely with reduced edge impact as the transition becomes less severe (Didham and Lawton, 1999), or become deforested and become hard-edges. However, logging in the Brazilian Amazon is an intense disturbance and many heavily logged areas could be considered hard-edges in some respects. It is recognized that deforestation is also dynamic, but at slower rates, with reforestation potentially occurring in many of these areas throughout the Amazon (Houghton et al., 2000), which could have a mitigating impact on the overall fragmentation caused by deforested areas. It would be of interest in future investigations of forest fragmentation to include more explicit recovery dynamics of deforested and selectively logged areas; however, the data for this analysis were not available for inclusion in the present study.

We found that rapid subdivision fragmentation occurred more from deforestation than from selective logging as logging extended deep into interior forests without disconnecting contiguous forest fragments. Deforestation tended to occur near previously deforested areas, and in 2002 actually reduced the percentage edge-forest as it homogenized the complex agroscape present at the exterior of larger forest fragments. Cumulative logging, however, as a result of penetrating deep into core forest areas generated 268% more edge forest than deforestation, while generating only 64% as many new non-contiguous forest fragments. Over our study period, not only was there a dramatic increase in the number of these forest fragments, but those fragments actually became much more fragmented than expected. In addition, we find that 90% of forest fragments across our 1.1 million $km^2$ study area fall under Laurance's (1998) fragment area threshold of 4 $km^2$, - beyond which detrimental effects become more pronounced. Fortunately, these fragments encompass only 5% of

the total remaining forest area. However, this percentage will increase as larger contiguous forest areas are subdivided into smaller fragments and forest edges continue to recede (Gascon et al., 2000).

More than 53% of the 700,000 $km^2$ of remaining forests in our total study area in 2002 were classified as edge-forests. Conversely, core forest area, defined as areas >2 km from the nearest forest edge, decreased from 56% to 49.7%, or by 84,303 km2, from 1997 to 2002. New logging resulted in an annual increase of edge-forest 24 times greater than that of deforestation alone, as logging extended more deeply into the interior core of remaining intact forest areas. However, the cumulative logged area was smaller than expected from the annual mean, as new logging grew from previously logged areas and thus continually consumed previously generated edge-forest. It is important to consider that our study period was only three years, while logging has likely been occurring in the region for a much longer time. For example, if assuming that logging during the past decade has occurred at an average intensity similar to that of our study period, and that the logged areas were not subsequently deforested, then there could be 260,000 km, representing a 40% increase in total existing edge length, of undocumented soft-edges bordering ≤10 year old logged areas. Within our study area, Skole and Tucker (1993) calculated 14% of remaining forests were edge-effected in 1988, using a definition of edge-forest as any forest areas within contiguous forest areas ≤100 $km^2$ and closer than 1 km to a forest edge. In 2002, 14 years later, our results from deforestation alone identified 36% of forest ≤1 km from an edge, an increase of 1.6% per year. Total forest fragments from deforestation were 8252 and ~23,000 in 1988 and 2002, respectively. However, we acknowledge that direct comparisons of our results to those of Skole and Tucker (1993) are difficult due to differences in edge-forest definition, study area and cloud coverage, but nonetheless, we find them useful to highlight general patterns.

## 2.6 Conclusions

Fragmentation of the Amazon is rapidly creating large areas of forest susceptible to edge effects, and is reducing the area of the remaining core forest. In total, we calculated that 53% of the remaining forests in more than 1.1 million $km^2$ were within 2 km and, ~37% were within 1 km of a forest edge. Moreover, 6.4% of all remaining forests were within 0.1 km of a forest edge, a distance shown in our literature review to undergo extensive edge impacts. Changes in edges are not cumulative because new logging and deforestation events consume older edges. Nonetheless, large forest tracts are being divided into smaller forested sections, which become increasingly vulnerable to wildfire, human encroachment, and reductions in biomass through increased mortality following micro-meteorological changes and/or wildfire.

Deforestation served as a driver of fragmentation primarily by increasing the area of edge-forest <500m fromthe nearest edge, while logging extended deeply into previously intact forest areas and created extensive edge-forest up to our two km study limit. Although logged forest habitat is a less damaging option to deforestation when considering ecosystem function, services or biodiversity, from the perspective of edge creation, it may pose a greater threat to forest sustainability than deforestation by increasing wildfire potential and accessibility deep within previously intact core forest areas. Both deforestation and logging contributed to the sub-division of remaining forest areas into smaller non-contiguous sections, though only the impacts of deforestation were statistically significant.

Although rapid and extensive fragmentation occurred throughout our study area, the majority of remaining forests were within large contiguous forested areas, and therefore not likely to be extensively degraded by the edge effects documented in our literature review. However, the rates of forest fragmentation will likely increase in the future as the remaining forested area is reduced, and as logging continues to penetrate into these previously intact core forests. The results of this study have wide-ranging implications for carbon sequestration and release, biodiversity conservation,

and ecological sustainability of ecosystems and human enterprises throughout the Brazilian Amazon.

## 2.7 Acknowledgements

We thank Rebecca Raybin for assistance with the literature review. We thank Angelica Almeyda, Lisa Curran, William Laurance, and Rob Pringle for helpful comments on the manuscript. This work was supported by NASA LBA-ECO grant NNG06GE32A and the Carnegie Institution.

## 2.8 References

Alencar A.A., Solórzano, L.A., Nepstad, D., 2004. Modeling forest understory fires in an eastern Amazonian landscape. Ecological Applications 14, 139-149.

Asner, G.P., Keller, M., Silva, J.N.M., 2004. Spatial and temporal dynamics of forest canopy gaps following selective logging in the eastern Amazon. Global Change Biology 10, 765-783.

Asner, G.P., Knapp, D.E., Broadbent, E.N., Oliveira, P.J.C., Keller, M., Silva, J.N.M., 2005. Selective logging in the Amazon. Science 310, 480-482.

Asner, G.P., Broadbent, E.N., Oliveira, P.J.C., Keller, M., Knapp, D.E., Silva, J.N., 2006. Condition and fate of logged forests in the Brazilian Amazon. Proceedings of the National Academy of Sciences 103, 12947-12950.

Barlow, J., Peres, C.A., Henriques, L.M.P., Stouffer, P.C., Wunderle, J.M., 2006. The responses of understory birds to forest fragmentation, logging and wildfires: An Amazonian synthesis. Biological Conservation 128, 182-192.

Barlow, J., Mestre, L.A.M., Gardner, T.A., Peres, C.A., 2007. The value of primary, secondary, and plantation forests for Amazonian birds. Biological Conservation 136, 212-231.

Benitez-Malvido, J., Martinez-Ramos, M., 2003. Impact of forest fragmentation on understory plant species richness in Amazonia. Conservation Biology 17, 389-400.

Brokaw, N.W., 1982. The definition of treefall gap and its effect on measures of forest dynamics. Biotropica 14, 158-160.

Cadenasso, M.L., Traynor, M.M., Pickett, S.T.A., 1997. Functional location of forest edges: gradients of multiple physical factors. Canadian Journal of Forest Research 27, 774-782.

Cagnolo, L., Cabido, M., Valladares, G., 2006. Plant species richness in the Chaco Serrano woodland from central Argentina: ecological traits and habitat fragmentation effects. Biological Conservation 132, 510-519.

Cochrane, M.A., 2001. Synergistic interaction between habitat fragmentation and fire in evergreen tropical forests. Conservation Biology 15, 1515-1521.

Cochrane, M.A., Laurance, W.F., 2002. Fire as a large-scale edge effect in Amazonian forests. Journal of Tropical Ecology 18, 311-325.

Cochrane, M.A., Skole, D.L., Matricardi, E.A.T., Barber, C., Chomentowski, W., 2002. Interaction and synergy between selective logging, forest fragmentation and fire disturbance in tropical forests: case study Mato Grosso, Brazil. CGCEO/RA03-02/w. Michigan State University, East Lansing, Michigan.

Cochrane, M.A., Skole, D.L., Matricardi, E.A.T., Barber, C., Chomentowski, W., 2004. Selective logging, forest fragmentation, and fire disturbance: implications of interaction and synergy. In: Zarin, D.J., Alavalapati, J.R.R., Putz, F.E., Schmink, M. (Eds.), Working Forests in the Neotropics: Conservation through Sustainable Management? Columbia University Press, New York, NY, pp. 310-324.

Cramer, J.M., Mesquita, R.C.G., Williamson, G.B., 2007. Forest fragmentation differentially affects seed dispersal of large and small-seeded tropical trees. Biological Conservation 137, 415-423.

Curran, L.M., Caniago, I., Paoli, G.D., Astianti, D., Kusneti, M., Leighton, M., Nirarita, C.E., Haeruman, H., 1999. Impact of El Nino and logging on canopy tree recruitment in Borneo. Science 286, 2184-2188.

Cushman, S.A., 2006. Effects of habitat loss and fragmentation on Amphibians: A review and prospectus. Biological Conservation 128, 231-240.

Davies-Colley, R.J., Payne, G.W., van Elswijk, M., 2000. Microclimate gradients across a forest edge. New Zealand Journal of Ecology 24, 111-121.

Defries, R., Asner, G.P., Achard, F., Justice, C., Laporte, N., Price, K., Small, C., Townshend, J., 2005. Monitoring tropical deforestation for emerging carbon markets. In: Mountinho, P., Schwartzman, S. (Eds.), Reduction of Tropical Deforestation and Climate Change Mitigation. IPAM, Washington, DC, pp. 1-27.

Didham, R.K., 1997. An overview of invertebrate responses to habitat fragmentation. In: Watt, A., Stork, N.E., Hunter, M. (Eds.), Forests and Insects. Chapman and Hall, London, pp. 201-218.

Didham, R.K., Lawton, J.H., 1999. Edge structure determines the magnitude of changes in microclimate and vegetation structure in tropical forest fragments. Biotropica 31, 17-30.

Gascon, C., Williamson, B.G., da Fonseca, G.A.B., 2000. Receding forest edges and vanishing reserves. Science 288, 1356-1358.

Hagan, J.M., Vander Haegen, M.W., McKinley, P.S., 1996. The early development of forest fragmentation effects on birds. Conservation Biology 10, 188-202.

Harper, K.A., MacDonald, S.E., Burton, P.J., Chen, J., Brosofske, K.D., Saunders, S.C., Euskirchen, E.S., Roberts, D., Jaiteh, M.S., Esseen, P.A., 2005. Edge

influence on forest structure and composition in fragmented landscapes. Conservation Biology 19, 768-782.

Herrerías-Diego, Y., Quesada, M., Stoner, K.E., Lobo, J.A., Hernández-Flores, Y., Montoya, G.S., 2008. Effects of forest fragmentation on fruit and seed predation of the tropical dry forest tree *Ceiba aesculifolia*. Biological Conservation 141, 241-248.

Hester, A.J., Hobbs, R.J., 1992. Influence of fire and soil nutrients on native and non-native annuals at remnant vegetation edges in the western Australian wheatbelt. Journal of Vegetation Science 3, 101-108.

Hobbs, R.J., 2001. Synergisms among habitat fragmentation, livestock grazing, and biotic invasions in southwestern Australia. Conservation Biology 15, 1522-1528.

Houghton, R.A., Skole, D.L., Nobre, C.A., Hackler, J.L., Lawrence, K.T., Chomentowski, W.H., 2000. Annual fluxes of carbon from deforestation and regrowth in the Brazilian Amazon. Nature 403, 301-304.

INPE., 2005. Prodes: assessment of deforestation in Brazilian Amazonia. Instituto Nacional de Pesquisas Espaciais (INPE), Sao Paulo, Brazil.

Johns, A.G., Johns, B.G., 1995. Tropical forest primates and logging: long-term coexistence? Oryx 29, 205-211.

Kaimowitz, D., Angelsen, A., 1998. Economic Models of Tropical Deforestation. A Review. Center for International Forestry Research Bogor, Indonesia.

Kapos, V., 1989. Effects of isolation on the water status of forest patches in the Brazilian Amazon. Journal of Tropical Ecology 5, 173-185.

Kinnaird, M.F., Sanderson, E.W., O'Brien, T.G., Wibisono, H.T., Woolmer, G., 2003. Deforestation trends in a tropical landscape and implications for endangered large mammals. Conservation Biology 17, 245-257.

Laurance, W.F., 2000. Do edge effects occur over large spatial scales? Trends in Ecology and Evolution 15, 134-135.

Laurance, W.F., Williamson, G.B., 2001. Positive feedbacks among forest fragmentation, drought, and climate change in the Amazon. Conservation Biology 15, 1529-1535.

Laurance, W.F., Laurance, S.G., Ferreira, L.V., Rankin-De Merona, J.M., Gascon, C., Lovejoy, T.E., 1997. Biomass collapse in Amazonian forest fragments. Science 278, 1117-1118.

Laurance, W.F., Ferreira, L.V., Rankin-De Merona, J.M., Laurance, S.G., 1998. Rainforest fragmentation and the dynamics of Amazonian tree communities. Ecology 79, 2032-2040.

Laurance, W.F., Delamonica, P., Laurance, S.G., Vasconcelos, H.L., Lovejoy, T.E., 2000. Rainforest fragmentation kills big trees. Nature, 404.

Laurance, W.F., Lovejoy, T.E., Vasconcelos, H.L., Bruna, E.M., Didham, R.K., Stouffer, P.C., Gascon, C., Bierregaard, R.O., Laurance, S.G., Sampaio, E., 2002. Ecosystem decay of Amazonian forest fragments: a 22-year investigation. Conservation Biology 16, 605-618.

Laurance,W.F., Nascimento, H.E.M., Laurance, S.G., Andrade, A.C., Fearnside, P.M., Ribeiro, J.E.L., Capretz, R.L., 2006. Rain forest fragmentation and the proliferation of successional trees. Ecology 87, 469-482.

Lawton, J.H., Bigness, D.E., Bolton, B., Bloemers, G.F., Eggleton, P., Hammond, P.M., Hodda, M., Holt, R.D., Larsen, T.B., Mawdsley, N.A., Stork, N.E., Srivastava, D.S., Watt, A.D., 1998. Biodiversity inventories, indicator taxa and effects of habitat modification in tropical forest. Nature 391, 72-76.

Lovejoy, T.E., Bierregaard Jr., R.O., Rylands, A.B., Malcom, J.R., Quintela, C.E., Harper, L.H., Brown Jr., K.S., Powell, A.H., Powell, G.V.H., Schubart, H.O.R., Hays, M.B., 1986. Edge and other effects of isolation on Amazon

forest fragments. In: Soulé, M.E. (Ed.), Conservation Biology: the Science of Scarcity and Diversity. Sinauer, Sunderland, Massachusetts, pp. 257-285.

Malcolm, J.R., 1997. Insect biomass in Amazonian forest fragments. In: Stork, N.E., Adis, J., Didham, R.K. (Eds.), Canopy Arthropods. Chapman and Hall, London, pp. 510-533.

Mason, D.J., Thiolay, J.M., 2001. Tropical forestry and the conservation of neotropical birds. In: Fimbel, R.A., Grajal, A., Robinson, J.G. (Eds.), The Cutting Edge: Conserving Wildlife in Logged Tropical Forests. Columbia University Press, New York, NY, pp. 167-191.

Matlack, G.R., 1993. Microenvironment variation within and among forest edge sites in the eastern United States. Biological Conservation 66, 185-194.

Mesquita, R.C.G., Delamonica, P., Laurance, W.F., 1999. Effect of surrounding vegetation on edge-related tree mortality in Amazonian forest fragments. Biological Conservation 91, 129-134.

Mulkey, S.S., Pearcy, R.W., 1992. Interactions between acclimation and photoinhibitation of photosynthesis of a tropical forest understory herb, Alocasia macrorrhiza, during simulated canopy gap formation. Functional Ecology 6, 719-729.

Murcia, C., 1995. Edge effects in fragmented forests: implications for conservation. Trends in Ecology and Evolution 10, 58-62.

Nascimento, H.E.M., Laurance, W.F., 2004. Biomass dynamics in Amazonian forest fragments. Ecological Applications 14, S127-S138.

Nepstad, D.C., Brown, F.I., Luz, L., Alechandre, A., Viana, V., Schwartzman, S., 1992. Biotic impoverishment of Amazonian forests by rubber tappers, loggers, and cattle ranchers. Advances in Economic Botany 9, 1-14.

Nepstad, D., Veríssimo, A., Alencar, A., Nobre, C., Eirivelthon, L., Lefebvre, P., Schlesinger, P., Potter, C., Moutinho, P., Mendoza, E., Cochrane, M., Brooks,

V., 1999. Large-scale impoverishment of Amazonian forests by logging and fire. Nature 398, 505-508.

Nichols, E., Larsen, T., Spector, S., Davis, A.L., Escobar, F., Favila, M., Vulinec, K.The Scarabaeinae Research Network, 2007. Global dung beetle response to tropical forest modification and fragmentation: a quantitative literature review and meta-analysis. Biological Conservation 137, 1-19.

Pereira Jr., R., Zweede, J., Asner, G.P., Keller, M., 2002. Forest canopy damage and recovery in reduced-impact and conventional selective logging in eastern Para, Brazil. Forest Ecology and Management 168, 77-89.

Peres, C.A., 2001. Synergistic effects of subsistence hunting and habitat fragmentation on Amazonian forest vertebrates. Conservation Biology 15, 1490–1505.

Peters, H.A., 2000. Clidemia hirta invasion at the Pasoh forest reserve: an unexpected plant invasion in an undisturbed tropical forest. Biotropica 33, 60-68.

Plumptre, A.J., 1996. Changes following 60 years of selective timber harvesting in the Budongo forest reserve, Uganda. Forest Ecology and Management 113, 201-213.

Pringle, C.M., Benstead, J.P., 2001. The effects of logging on tropical river ecosystems. In: Fimbel, R.A., Grajal, A., Robinson, J.G. (Eds.), The Cutting Edge: Conserving Wildlife in Logged Tropical forests. Columbia University Press, New York, NY, pp. 305-325.

Putz, F.E., Blate, G.M., Redford, K.H., Fimbel, R., Robinson, J., 2001a. Tropical forest management and conservation of biodiversity: an overview. Conservation Biology 15, 7-20.

Putz, F.E., Sirot, L.K., Pinard, M.A., 2001b. Tropical forest management and wildlife: silvicultural effects on forest structure, fruit production, and locomotion of arboreal animals. In: Fimbel, R.A., Grajal, A., Robinson, J.G. (Eds.), The Cutting Edge: Conserving Wildlife in Logged Tropical Forests. Columbia University Press, New York, NY, pp. 11-35.

Ranta, P., Blom, T., Niemela, J., Joensuu, E., Siitonen, M., 1998. The fragmented Atlantic rain forest of Brazil: size, shape and distribution of forest fragments. Biodiversity and Conservation 7, 385-403.

Rodríguez-Cabal, M., Aizen, M.A., Novaro, A.J., 2007. Habitat fragmentation disrupts a plant-disperser mutualism in the temperate forest of South America. Biological Conservation 139, 195-202.

Saunders, D.A., Hobbs, R.J., Margules, C.R., 1991. Biological consequences of ecosystem fragmentation: a review. Conservation Biology 5, 18-32.

Schlaepfer, M.A., Gavin, T.A., 2001. Edge effects on lizards and frogs in tropical forest fragments. Conservation Biology 15, 1079-1090.

Sizer, N.C., Tanner, E.V.J., Kossman Ferraz, I.D., 2000. Edge effects on litterfall mass and nutrient concentrations in forest fragments in central Amazonia. Journal of Tropical Ecology 16, 853-863.

Skole, D., Tucker, C., 1993. Tropical deforestation and habitat fragmentation in the Amazon: satellite data from 1978 to 1988. Science 260, 1905-1911.

Soriano, P.J., Ochoa, J.G., 2001. The consequences of timber exploitation for bat communities in tropical America. In: Fimbel, R.A., Grajal, A., Robinson, J.G. (Eds.), The Cutting Edge: Conserving Wildlife in Logged Tropical Forests. Columbia University Press, New York, NY, pp. 153-166.

Tabanez, A.A.J., Viana, V.M., 2000. Patch structure within Brazilian Atlantic forest fragments and implications for conservation. Biotropica 32, 925-933.

Uhl, C., Buschbacher, R.A., 1985. A disturbing synergism between cattle ranch burning practices and selective tree harvesting in the eastern Amazon. Biotropica 32, 925-933.

Uhl, C., Verissimo, A., Mattos, M., Brandino, Z., Vieira, I.C., 1991. Social, economic, and ecological consequences of selective logging in an Amazon frontier: the case of Tailandia. Forest Ecology and Management 46, 243-273.

Veríssimo, A., Barreto, P., Mattos, M., 1992. Logging impacts and prospects for sustainable forest management in an old Amazonian frontier: the case of Paragominas. Forest Ecology and Management 55, 169-199.

Verıissimo, A., Cochrane, M., Souza Jr., C., 2002. National forests in the Amazon. Science 297, 1478.

Walker,W., 2003. Mapping process to pattern in landscape change of the Amazonian frontier. Annuals of the Association of American Geographers 93, 376-398.

Williams-Linera, G., Dominguez-Gastelu, V., Garcia-Zurita, M.E., 1998. Microenvironment and floristics of different edges in a fragmented tropical rainforest. Conservation Biology 12, 1091-1102.

Young, A., Mitchell, N., 1994. Microclimate and vegetation edge effects in a fragmented podocarp-broadleaf forest in New Zealand. Biological Conservation 67, 63-72.

## 2.9 Tables

**Table 2.1:** Fragmentation statistics for all deforestation and logging combinations within our study region.

| Deforestation year (⩽)[a] | Logging year (s)[b] | ID | Forest area (km$^2$) | Edge length (km) | Edge-to-area ratio | Forest area ⩽ 2 km edge (km$^2$) | Forest area ⩽ 2 km edge (%) | Forest fragments (#) |
|---|---|---|---|---|---|---|---|---|
| 1997 | – | | 791 418 | 427 001 | 0.54 | 348 504 | 44.0% | 15 229 |
| 2000 | – | D0 | 758 474 | 455 954 | 0.60 | 345 563 | 45.6% | 17 594 |
| 2001 | – | D01 | 747 379 | 500 433 | 0.67 | 357 985 | 47.9% | 19 699 |
| 2002 | – | D012 | 733 626 | 543 638 | 0.74 | 348 589 | 47.5% | 23 133 |
| 2000 | 2000 | D0 L0 | 743 789 | 494 579 | 0.66 | 369 024 | 49.6% | 18 631 |
| 2001 | 2001 | D01 L1 | 733 772 | 542 186 | 0.74 | 369 678 | 50.4% | 20 463 |
| 2002 | 2002 | D012 L2 | 722 115 | 576 625 | 0.80 | 363 116 | 50.3% | 23 773 |
| 2001 | 2000–2001 | D01 L01 | 721 590 | 566 377 | 0.78 | 350 556 | 48.6% | 21 863 |
| 2002 | 2001–02 | D012 L12 | 710 628 | 605 112 | 0.85 | 370 503 | 52.1% | 24 943 |
| 2002 | 2000–2002 | D012 L012 | 699 855 | 621 713 | 0.89 | 368 150 | 52.6% | 26 516 |
| *Annual change* | | | | | | | | |
| New logging (Avg. 2000–2002) | | | −13 268 | 37 788 | 0.06 | 16 560 | 3.1% | 814 |
| Deforestation (Avg. 2000–2002) | | | −11 943 | 32 445 | 0.05 | 682 | 0.8% | 2109 |
| *Cumulative change*[c] | | | | | | | | |
| Deforestation (2000–2002) | | | −24 848 | 87 684 | 0.14 | 3026 | 1.9% | 5539 |
| Logging (2000–2002) | | | −33 771 | 78 075 | 0.15 | 19 561 | 5.1% | 3383 |

a Deforestation is always cumulative through study year.
b Signifies that logging is not included in the spatial analysis.
c Logging impacts are in addition to deforestation.

**Table 2.2:** Descriptive statistics of edge distance (m) into interior forest by disturbance category.

| Edge disturbance category | Distance (*m*) | | | | | N[a] |
|---|---|---|---|---|---|---|
| | Mean | Median | STD | Min | Max | |
| Forest structure | 124 | 100 | 169 | 5 | 1000 | 39 |
| Tree mortality | 430 | 300 | 391 | 10 | 1000 | 37 |
| Forest microclimate | 191 | 60 | 386 | 5 | 2400 | 35 |
| Biodiversity | 261 | 80 | 385 | 10 | 2000 | 35 |
| Total | 245 | 100 | 358 | 5 | 2400 | 146 |

References are provided in Appendix A.

a Number of individual edge effects documented in our literature review of 62 articles.

## 2.10 Figures

**Figure 2.1:** Interior and edge-forest (≤2 km edge) within our study area following deforestation and cumulative logging (2000-2002). White areas represent non-forest areas (i.e., pasture or agriculture) within our study area while grey areas represent those areas not included due to cloud interference or missing imagery. A map of the general study area is presented in Supplementary Materials 2.2.

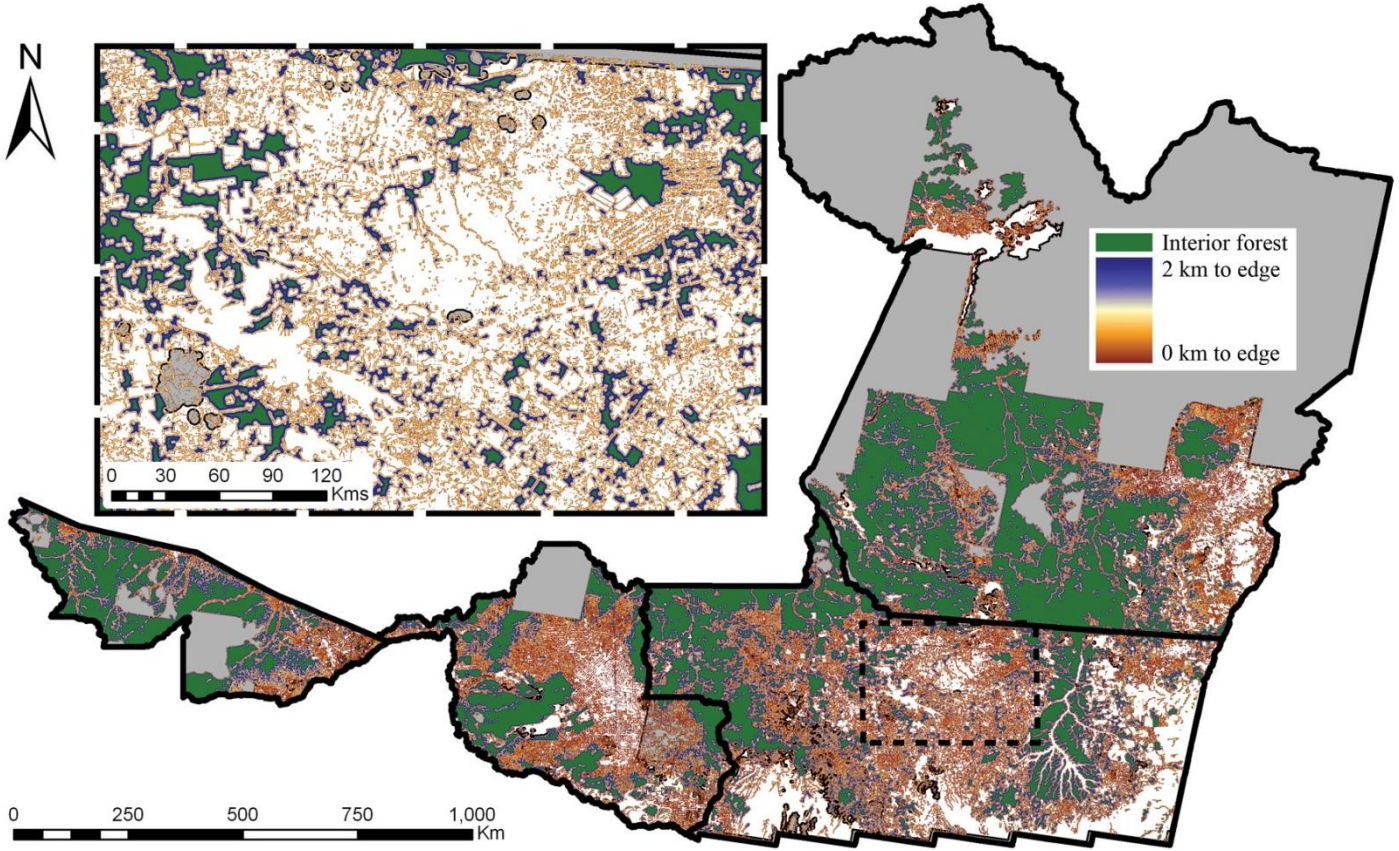

**Figure 2.2:** Example of spatio-temporal dynamics of deforestation and selective logging in the years 1999-2002 (A-D, respectively) in central Mato Grosso. Areas of deforestation and new logging are indicated by yellow and red arrows, respectively. Subdivided forest fragments are visible within logged areas

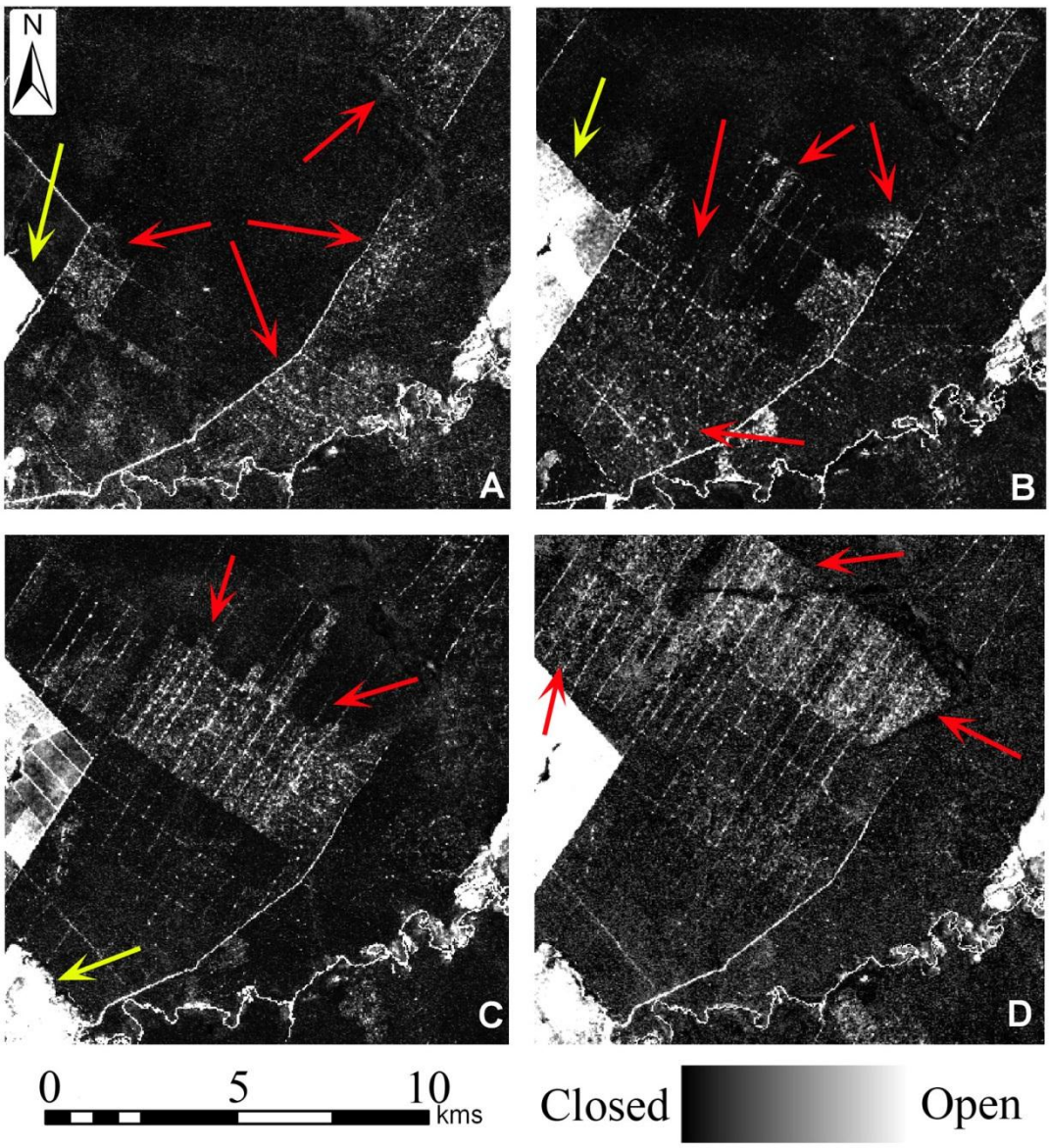

**Figure 2.3:** Total number (left) and cumulative percentage (right) of edge effects documented in our literature review. Arrows indicate the distance under which 99% of documented edge effects occurred. References are provided in Supplementary Materials 2.1.

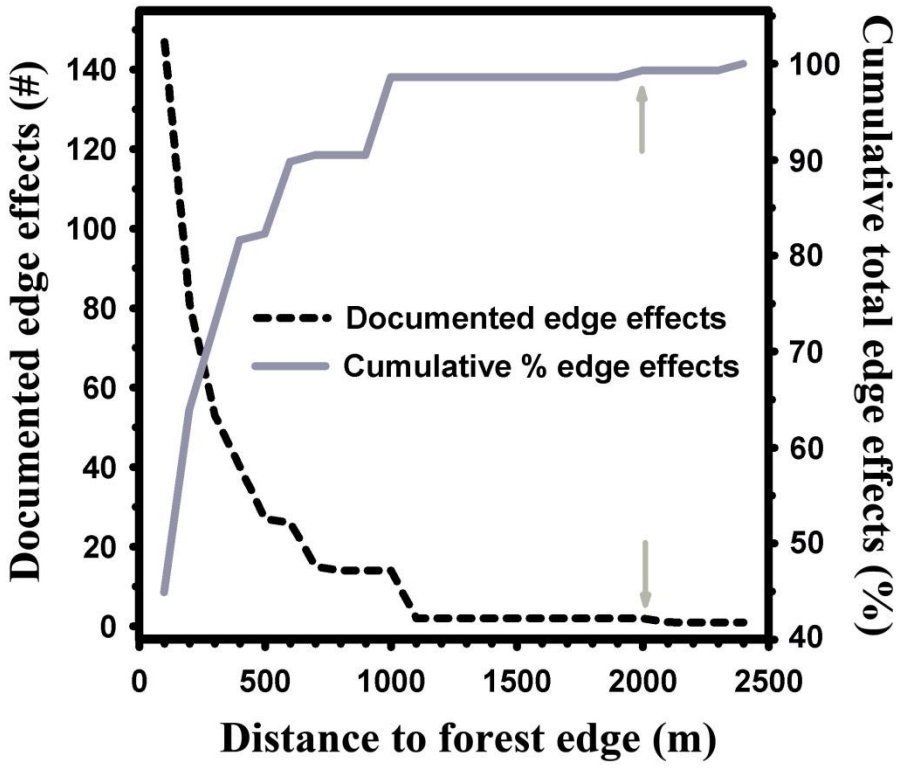

**Figure 2.4:** Cumulative percentage of (A) total non-contiguous forest fragments in our study region versus each fragment's area ($km^2$), (B) total forested area in our study region versus the area of individual non-contiguous forest fragments, (C) cumulative total forested area ($km^2$), and (D) total remaining forest, located within individual 100 m distance increments up to two km from the nearest forest edge. Logging impacts are in addition to those caused by deforestation.

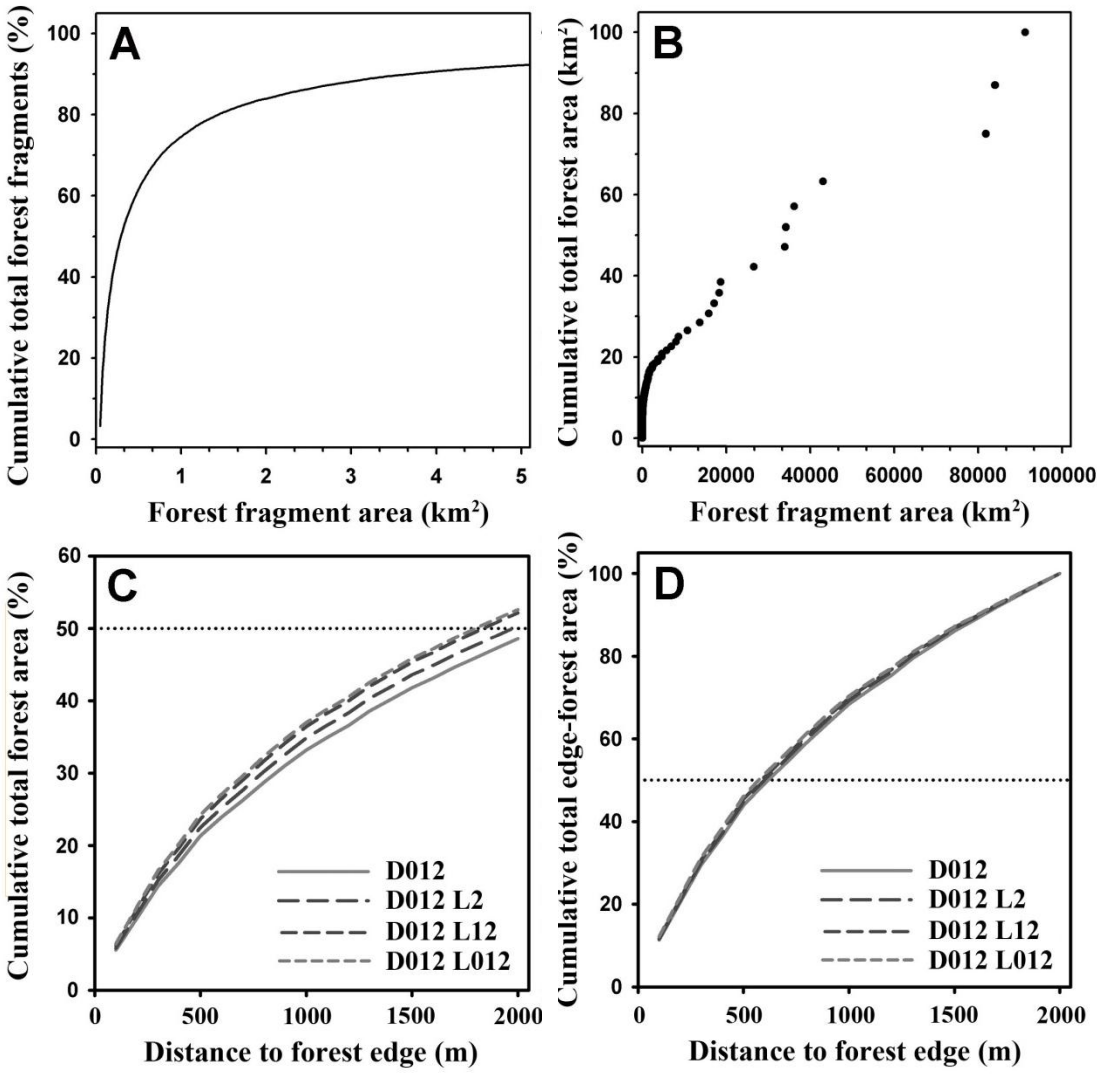

**Figure 2.5:** Mean annual change in edge-forest area and the percentage of total remaining forest impacted within individual 100 m distance increments up to two km into the forest interior. New logging and cumulative logging (2000–2002) impacts are in addition to those of deforestation.

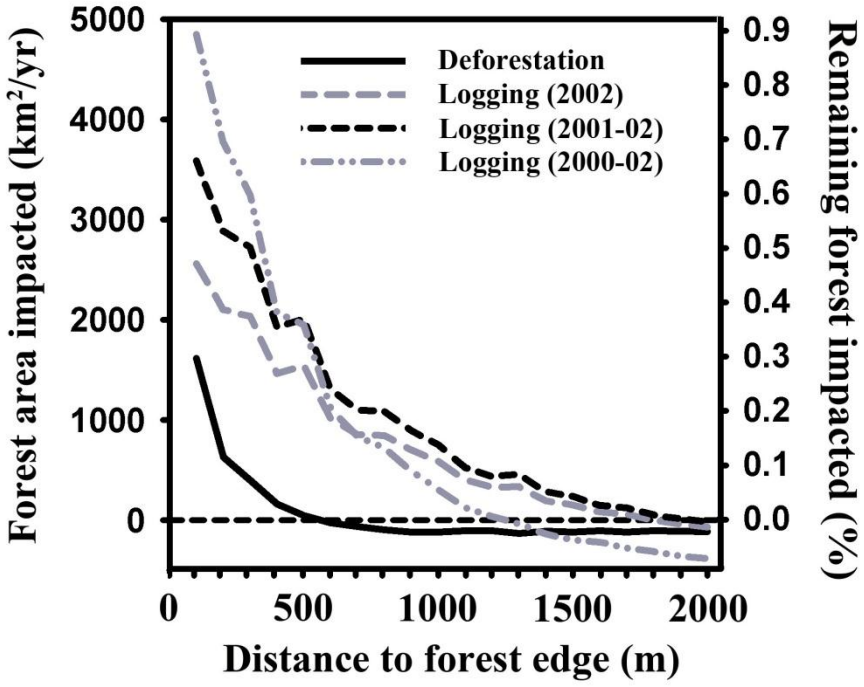

**Figure 2.6:** Literature review of edge effects divided into: (A) forest structure, (B) tree mortality, (C) forest microclimatic and (D) biodiversity disturbance categories. When multiple sources were identified the minimum (horizontal bar) and maximum (error bar) are provided. These effects are overlaid on area graphs to illustrate the cumulative percentage of remaining forest potentially impacted by each variable following year 2000–2002 deforestation (D012) and combined D012 and year 2000–2002 cumulative logging (CL012). The Y axis refers to the% remaining forest when logged areas are defined as either intact (D012) or degraded forest (D012–CL012). Complete references are provided in the Supplementary Materials

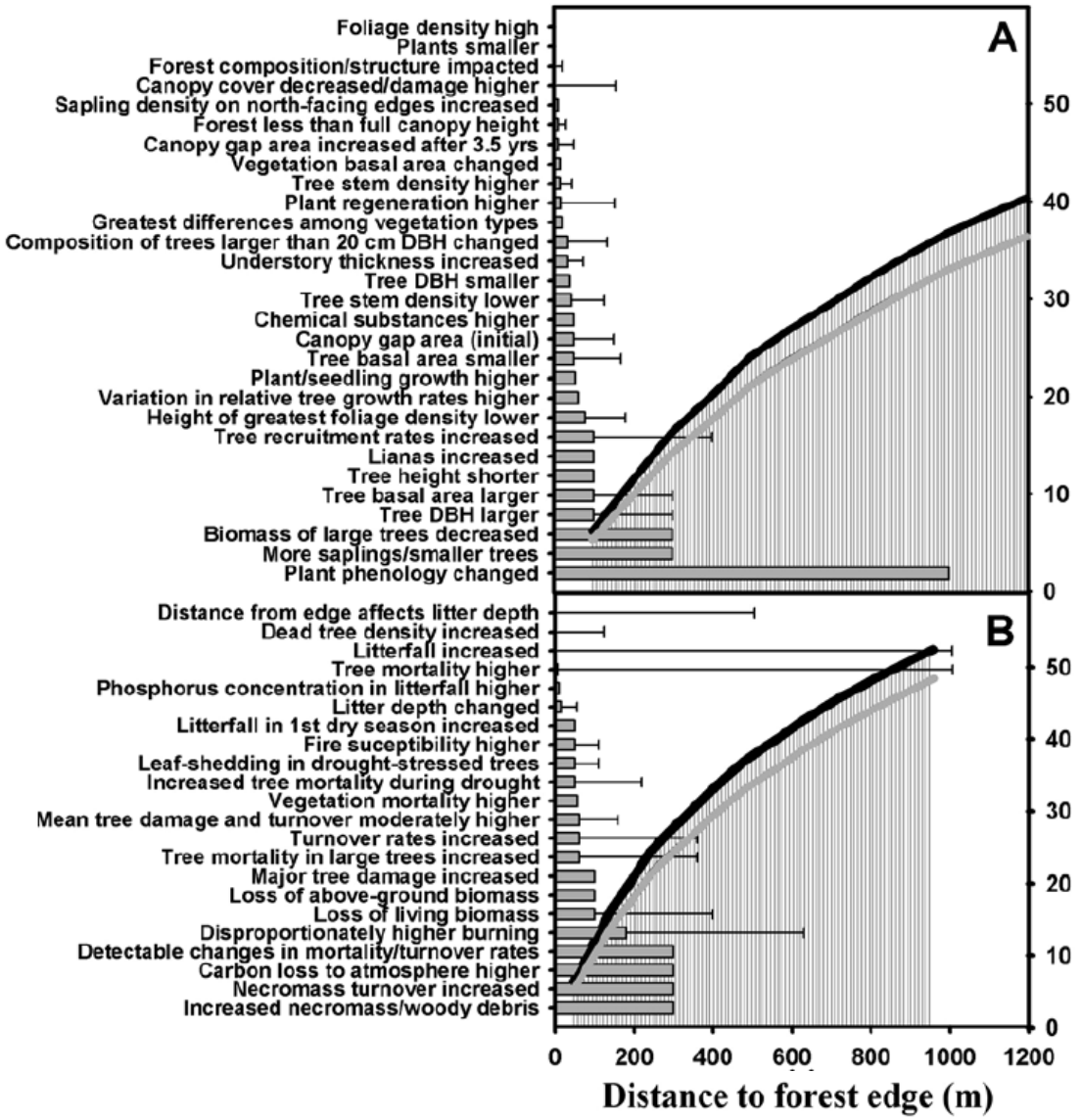

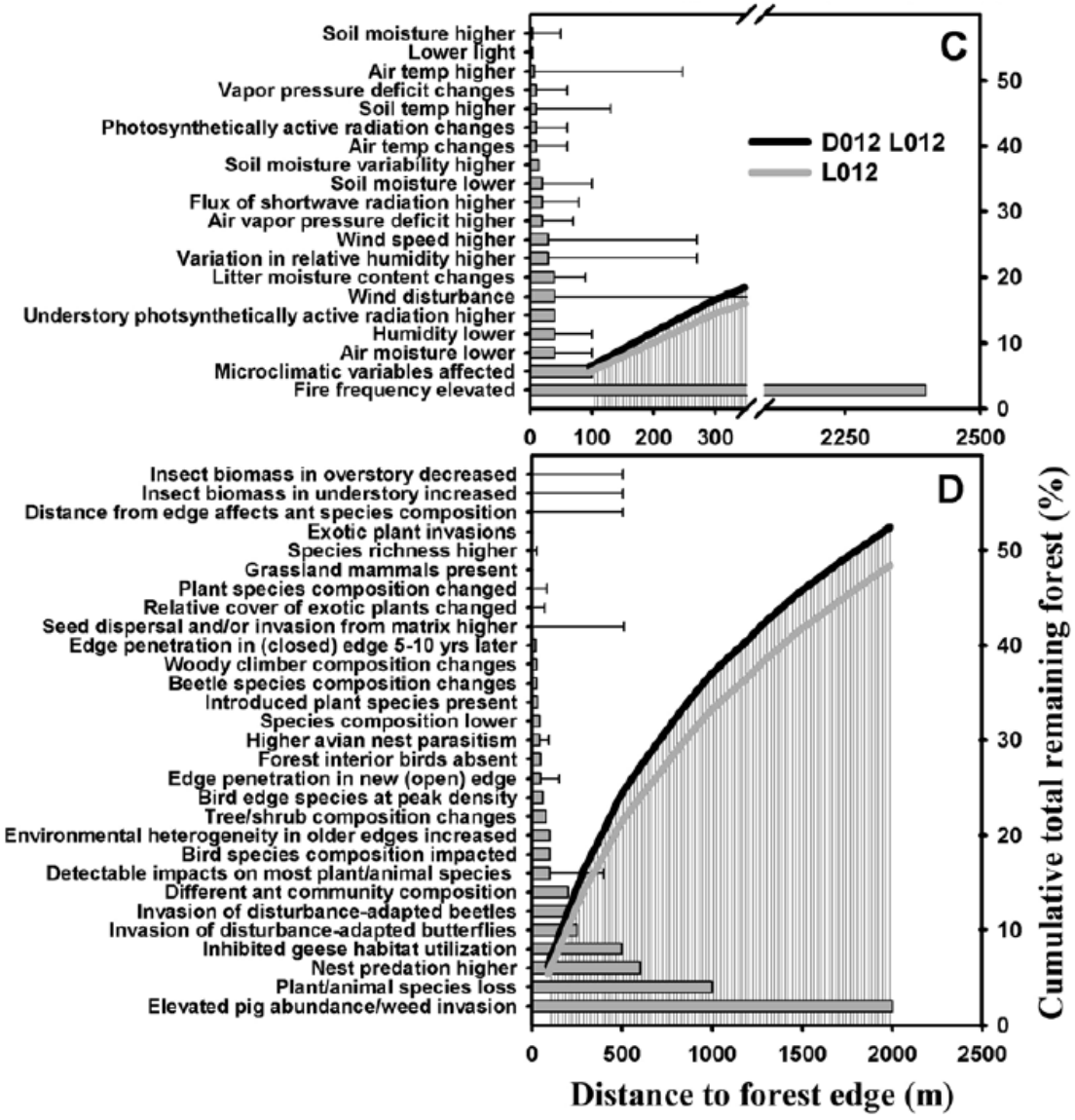
C
Soil moisture higher
Lower light
Air temp higher
Vapor pressure deficit changes
Soil temp higher
Photosynthetically active radiation changes
Air temp changes
Soil moisture variability higher
Soil moisture lower
Flux of shortwave radiation higher
Air vapor pressure deficit higher
Wind speed higher
Variation in relative humidity higher
Litter moisture content changes
Wind disturbance
Understory photsynthetically active radiation higher
Humidity lower
Air moisture lower
Microclimatic variables affected
Fire frequency elevated
D012 L012
L012
0
100
200
300
2250
2500
0
10
20
30
40
50
D
Insect biomass in overstory decreased
Insect biomass in understory increased
Distance from edge affects ant species composition
Exotic plant invasions
Species richness higher
Grassland mammals present
Plant species composition changed
Relative cover of exotic plants changed
Seed dispersal and/or invasion from matrix higher
Edge penetration in (closed) edge 5-10 yrs later
Woody climber composition changes
Beetle species composition changes
Introduced plant species present
Species composition lower
Higher avian nest parasitism
Forest interior birds absent
Edge penetration in new (open) edge
Bird edge species at peak density
Tree/shrub composition changes
Environmental heterogeneity in older edges increased
Bird species composition impacted
Detectable impacts on most plant/animal species
Different ant community composition
Invasion of disturbance-adapted beetles
Invasion of disturbance-adapted butterflies
Inhibited geese habitat utilization
Nest predation higher
Plant/animal species loss
Elevated pig abundance/weed invasion
0
500
1000
1500
2000
2500
0
10
20
30
40
50
Distance to forest edge (m)
Cumulative total remaining forest (%)

## 2.11 Supplementary Materials

**SM 2.1:** Tropical and temperate forest edge effects and sources for four disturbance categories. Data used for Fig. 6 of the main text.

| | Edge distance (m) | | |
|---|---|---|---|
| **Disturbance category and edge effect** | **Minimum** | **Maximum** | **Source** |
| **Forest structure** | | | |
| Plant phenology changed | 1000 | 5000 | Laurance and Williamson (2001); Curran et al. (1999) |
| More saplings/smaller trees | 300 | | Nascimento and Laurance (2004) |
| Biomass of large trees decreased | 300 | | Nascimento and Laurance (2004) |
| Tree DBH larger | 100 | 200 | Carvalho and Vasconcelos (1999) |
| Tree basal area larger | 100 | 200 | Carvalho and Vasconcelos (1999) |
| Tree height shorter | 100 | | Unwin (1989) |
| Lianas increased | 100 | | Laurance (1997) |
| Tree recruitment rates increased | 100 | 300 | Laurance et al. (1998a); Nascimento and Laurance (2004) |
| Height of greatest foliage density lower | 80 | 100 | Camargo and Kapos (1995) |
| Variation in relative tree growth rates higher | 60 | | Chen et al. (1992) |
| Plant/seedling growth higher | 53 | | Chen et al. (1992) |
| Tree basal area smaller | 50 | 120 | Unwin (1989); Chen et al. (1992) |
| Canopy gap area (initial) | 50 | 100 | Asner et al. (2004) |
| Chemical substances higher | 50 | | Hester and Hobbs (1992) |
| Tree stem density lower | 43 | 85 | Chen et al. (1992) |

| | Edge distance (m) | | |
|---|---|---|---|
| **Disturbance category and edge effect** | **Minimum** | **Maximum** | **Source** |
| Tree DBH smaller | 40 | | Carvalho and Vasconcelos (1999) |
| Understory thickness increased | 35 | 40 | Matlack, (1993); Malcolm (1994) |
| Composition of trees larger than 20 cm DBH changed | 35 | 100 | Hennenberg et al. (2005) |
| Greatest differences among vegetation types | 20 | | Mesquita et al. (1999) |
| Plant regeneration higher | 16 | 137 | Chen et al. (1992) |
| Tree stem density higher | 15 | 30 | Palik and Murphy (1990); Williams-Linera (1990); Ranney et al. (1981) |
| Vegetation basal area changed | 15 | | Ranney et al. (1981) |
| Canopy gap area increased after 3.5 yrs | 10 | 40 | Asner et al. (2004) |
| Forest less than full canopy height | 10 | 20 | Didham and Lawton (1999) |
| Sapling density on north-facing edges increased | 10 | | Fraver (1994) |
| Canopy cover decreased/damage higher | 5 | 150 | Laurance (1991); Malcolm (1994); Williams-Linera (1990); Chen et al. (1992); Miller and Lin (1985) |
| Forest composition/structure impacted | 5 | 15 | Williams-Linera (1990); Olander et al. (1998) |
| Plants smaller | 5 | | Davies-Colley et al. (2000) |
| Foliage density high | 5 | | Davies-Colley et al. (2000) |
| **Tree mortality** | | | |
| Increased necromass/woody debris | 300 | | Nascimento and Laurance (2004) |
| Necromass turnover increased | 300 | | Nascimento and Laurance (2004) |
| Carbon loss to atmosphere higher | 300 | | Nascimento and Laurance (2004) |
| Detectable changes in mortality/turnover rates | 300 | | Laurance et al. (1998b) |

| Disturbance category and edge effect | Edge distance (m) Minimum | Maximum | Source |
|---|---|---|---|
| Disproportionately higher burning | 180 | 450 | Cochrane (2001) |
| Loss of living biomass | 100 | 300 | Laurance and Williamson (2001) |
| Loss of above-ground biomass | 100 | | Laurance et al. (1998c) |
| Major tree damage increased | 100 | | Laurance et al. (1997a) |
| Tree mortality in large trees increased | 60 | 300 | Laurance et al. (2000c, 2001a) |
| Turnover rates increased | 60 | 300 | Laurance et al. (1998a,b) |
| Mean tree damage and turnover moderately higher | 60 | 100 | Laurance et al. (1998a,b) |
| Vegetation mortality higher | 56 | | Chen et al. (1992) |
| Increased tree mortality during drought | 50 | 170 | Laurance et al. (2001a); Laurance and Williamson (2001) |
| Leaf-shedding in drought-stressed trees | 50 | 60 | Laurance et al. (2001a); Laurance and Williamson (2001) |
| Fire susceptibility higher | 50 | 60 | Laurance and Williamson (2001) |
| Litterfall in 1st dry season increased | 50 | | Sizer et al. (2000) |
| Litter depth changed | 15 | 40 | Matlack (1993) |
| Phosphorus concentration in litterfall higher | 10 | | Sizer et al. (2000) |
| Tree mortality higher | 6 | 1000 | Ferreira and Laurance. (1997); Laurance (1997); Laurance et al. (1998a); Laurance and Williamson (2001); Nascimento and Laurance (2004); Chen et al. (1992) |
| Litterfall increased | 5 | 1000 | Sizer et al. (2000); Nascimento and Laurance. (2004); Laurance and Williamson (2001); Carvahlo et al. (1999) |
| Dead tree density increased | 5 | 120 | Williams-Linera (1990); Chen et al. (1992) |
| Distance from edge affects litter depth | 5 | 500 | Carvahlo et al. (1999) |

| Disturbance category and edge effect | Edge distance (m) Minimum | Maximum | Source |
|---|---|---|---|
| **Forest microclimate** | | | |
| Fire frequency elevated | 2400 | | Cochrane and Laurance (2002) |
| Microclimatic variables affected | 100 | | Lovejoy et al. (1986); Viana et al. 1997. |
| Air moisture lower | 40 | 60 | Matlack (1993) |
| Humidity lower | 40 | 60 | Kapos (1989); Williams-Linera et al. (1998) |
| Understory photosynthetically active radiation higher | 40 | | Kapos (1989) |
| Wind disturbance | 40 | 500 | Laurance (1991); Laurance et al. (1998a); Davies-Colley et al. (2000) |
| Litter moisture content changes | 39 | 50 | Matlack (1993) |
| Variation in relative humidity higher | 30 | 240 | Chen et al. (1995) |
| Wind speed higher | 30 | 240 | Chen et al. (1995) |
| Air vapor pressure deficit higher | 20 | 50 | Kapos (1989); Matlack (1993); Davies-Colley et al. (2000) |
| Flux of shortwave radiation higher | 20 | 60 | Chen et al. (1995) |
| Soil moisture lower | 20 | 80 | Kapos (1989); Camargo and Kapos (1995) |
| Soil moisture variability higher | 15 | | Chen et al. (1995) |
| Air temp changes | 10 | 50 | Young and Mitchell (1994) |
| Photosynthetically active radiation changes | 10 | 50 | Young and Mitchell (1994) |
| Soil temp higher | 10 | 120 | Davies-Colley et al. (2000); Williams-Linera et al. (1998); Chen et al. (1995) |
| Vapor pressure deficit changes | 10 | 50 | Young and Mitchell (1994) |

| Disturbance category and edge effect | Edge distance (m) Minimum | Maximum | Source |
|---|---|---|---|
| Air temp higher | 7 | 240 | Cadenasso et al. (1997); Williams-Linera (1990); Matlack (1993); Kapos (1989); Chen et al. (1995); Davies-Colley et al. (2000) |
| Lower light | 5 | | Davies-Colley et al. (2000) |
| Increased Nitrogen deposition | 20 | | Weathers et al. (2001) |
| Soil moisture higher | 5 | 44 | Camargo and Kapos (1995); Matlack (1993) |
| **Biodiversity** | | | |
| Elevated pig abundance/weed invasion | 2000 | | Peters (2000); Ickes and Williamson (2000) |
| Plant/animal species alterations | 1000 | | Skole and Tucker (1993); Chiarello (1999); Stevens and Husband (1998) |
| Nest predation higher | 600 | | Wilcove et al. (1986) |
| Inhibited geese habitat utilization | 500 | | Madsen (1985) |
| Changes in butterfly composition and abundance | 250 | | Lovejoy et al. (1986); Brown and Hutchings (1997) |
| Invasion of disturbance-adapted beetles | 200 | | Didham (1997); Didham et al. (1998) |
| Different ant community composition | 200 | | Carvalho and Vasconcelos (1999) |
| Detectable impacts (some seasonal) on plant/animal species | 100 | 300 | Laurance et al. (1997a); Schlaepfer et al. (2001) |
| Bird species composition impacted | 100 | | Ferris (1979) |
| Environmental heterogeneity in older edges increased | 100 | | Camargo and Kapos (1995) |
| Tree/shrub composition changes | 80 | | Hennenberg et al. (2005); Hill and Curran (2005) |
| Bird edge species at peak density | 60 | | Kroodsma (1982) |

| | Edge distance (m) | | |
|---|---|---|---|
| **Disturbance category and edge effect** | **Minimum** | **Maximum** | **Source** |
| Edge penetration in new (open) edge | 50 | 100 | Didham and Lawton (1999) |
| Forest interior birds absent | 50 | | Lovejoy et al. (1986) |
| Higher avian nest parasitism | 45 | 50 | Johnson and Temple (1990); Paton (1994) |
| Species composition lower | 45 | | Palik and Murphy (1990) |
| Introduced plant species present | 30 | | Olander et al. (1998) |
| Beetle species composition changes | 26 | | Didham and Lawton (1999) |
| Woody climber composition changes | 25 | | Hennenberg et al. (2005) |
| Edge penetration in (closed) edge 5-10 yrs later | 20 | | Didham and Lawton (1999) |
| Seed dispersal and/or invasion from matrix higher | 10 | 500 | Hester and Hobbs (1992); Willson and Crome (1989); Laurance (1991) |
| Relative cover of exotic plants changed | 10 | 60 | Fraver (1994) |
| Plant species composition changed | 10 | 75 | Fraver (1994); Wales (1972); Hennenberg et al. (2005); Bruna (1999) |
| Grassland mammals present | 10 | | Goosem (1997); Goosen and Marsh (1997) |
| Species richness higher | 10 | 15 | Matlack (1994); Ranney et al. (1981) |
| Exotic plant invasions | 10 | | Brothers and Spingarn (1992) |
| Distance from edge affects ant species composition | 5 | 500 | Carvalho and Vasconcelos (1999) |
| Insect biomass in understory increased | 5 | 500 | Malcolm (1997); Carvalho and Vasconcelos (1999) |
| Insect biomass in overstory decreased | 5 | 500 | Malcolm (1997); Carvalho and Vasconcelos (1999) |

**SM 2.2:** General study area and logging data used in this study as described in Asner et al. (2005).

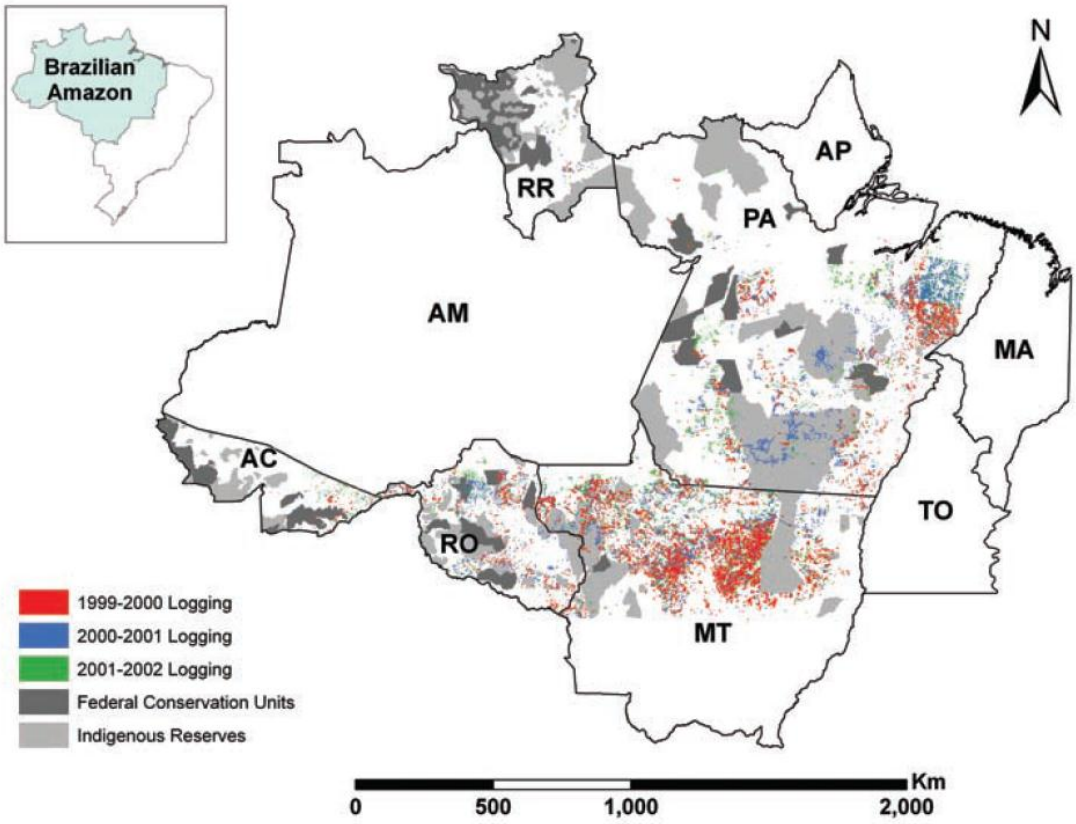


**Fig. 1.** Spatial distribution of selective logging in five timber-production states of the Brazilian Amazon for the year intervals 1999–2000 (red), 2000–2001 (blue), and 2001–2002 (green). The states of Amazonas (AM), Amapa (AP), Tocantins (TO), Maranhao (MA), and the southern non-forested part of Mato Grosso were not included in the analysis. Light gray areas show the extent of indigenous reserves; dark gray areas delineate federal conservation lands as of 1999 (*29*). RR, Roraima; PA, Pará; MT, Mato Grosso; RO, Rondônia; AC, Acre.

# CHAPTER 3

# SPATIAL PARTITIONING OF BIOMASS AND DIVERSITY IN A LOWLAND BOLIVIAN FOREST: LINKING FIELD AND REMOTE SENSING MEASUREMENTS

## 3.1 Abstract

Large-scale inventories of forest biomass and structure are necessary for both understanding carbon dynamics and conserving biodiversity. High-resolution satellite imagery is starting to enable structural analysis of tropical forests over large areas, but we lack an understanding of how tropical forest biomass links to remote sensing. We quantified the spatial distribution of biomass and tree species diversity over 4 ha in a Bolivian lowland moist tropical forest, and then linked our field measurements to high-resolution Quickbird satellite imagery. Our field measurements showed that emergent and canopy dominant trees, being those directly visible from nadir remote sensors, comprised the highest diversity of tree species, represented 86% of all tree species found in our study plots, and contained the majority of forest biomass. Emergent trees obscured 1–15 trees with trunk diameters (at 1.3 m, diameter at breast height (DBH)) ≥ 20 cm, thus hiding 30–50% of forest biomass from nadir viewing. Allometric equations were developed to link remotely visible crown features to stand parameters, showing that the maximum tree crown length explains 50–70% of the individual tree biomass. We then developed correction equations to derive aboveground forest biomass, basal area, and tree density from tree crowns visible to nadir satellites. We applied an automated tree crown delineation procedure to a high-resolution panchromatic Quickbird image of our study area, which showed promise for identification of forest biomass at community scales, but which also highlighted the difficulties of remotely sensing forest structure at the individual tree level.

*Keywords: Amazon, biomass, tree crown delineation, tropical forest, Quickbird satellite images*

## 3.2 Introduction

The spatial partitioning of biomass in tropical forests largely results from high species diversity, different survival strategies, and varying disturbance regimes (Whitmore, 1978). This partitioning plays a role in determining future forest structure, and thus biomass partitioning, by altering micro- climatic and biogeochemical conditions, and thus forest community dynamics (Brokaw, 1985; Kuppers, 1989; Whit- more, 1989; Guariguata et al., 1997). The resultant three-dimensional structure and composition of a forest partially defines its utility for human activities and the capacity of the forest to support animal and plant populations (Hansen et al., 1991). Forest structure also mediates carbon sequestration following both natural and anthropogenic disturbances (Cummings et al., 2002; Vieira et al., 2004). Few studies, however, have quantified how biomass is spatially distributed within tropical forests due to the complexity of multi-tiered canopies, large differences in tree diameter and height, and their generally large stature (Asner et al., 2002). A more accurate understanding of the three-dimensional partitioning of forest biomass would enhance our understanding of terrestrial carbon dynamics and provide insights into potential impacts of forest degradation (Phillips et al., 1998; Chambers et al., 2000; Keller et al., 2001).

Future approaches for rapid, cost-effective, fine-scale quantification of forest structure and diversity over large areas will likely rely on remotely sensed data. Excellent results are being derived from LiDAR (light detection and ranging) systems (Drake et al., 2002), and headway is being made on both manual and automated interpretation of high-resolution optical satellite imagery (Asner et al., 2002; Clark et al., 2004; Palace et al., 2008). However, a current limitation on all nadir- viewing sensors is imposed by the spatial arrangement of forest canopies, in particular where

larger diameter and taller canopy trees overtop numerous smaller individuals. Although the quantification of viewable versus total forest stems from nadir perspectives would be valuable for correction of remotely sensed data, no study has yet provided the integrated, detailed vertical and horizontal spatial analyses necessary to calibrate the relationship between remote sensing and tropical forest structure. Likewise, few studies have quantified the spatial distribution of tree species diversity as is relevant to nadir- viewing remote sensors. A better understanding of tree species spatial distribution and visibility to nadir sensors is relevant both to improving biomass estimations through better tree crown delineations and to forest management and biodiversity conservation.

In this study, we quantified the structural partitioning of forest biomass and species diversity in a tropical moist forest in lowland Bolivia by developing high-resolution, three-dimensional spatial maps of trees and their structural attributes within four 1-ha study plots. Principal questions addressed in our study were: (1) how is biomass distributed throughout the forest and by both tree-diameter and crown-position classes? (2) how is tree diversity distributed through these same classes? (3) how are tree stems and crowns spatially distributed throughout the stand? and (4) what implications do these results have for remote sensing of fine-scale forest structure and biomass?

## 3.3 Methods

### 3.3.1 Study area

This study was conducted in the timber concession of Agro-industria Forestal La Chonta Ltda., which encompasses 100,000 ha of forest in the Guarayos province of the department of Santa Cruz, Bolivia (158470 S, 628550 W; see Fig. 3.3). The elevation at the site is 400–600 m above sea level, with mildly undulating topography. Geologically, it is a continuation of the Brazilian shield with moderately fertile inceptisols and patches of black anthrosols throughout the concession (Calla, 2003;

Paz, 2003). Vegetation is classified as moist tropical semi-deciduous forest and has a biomass range of 73–190 mg/ha (Dauber et al., 2000). For trees ≥ 10 cm in diameter (at 1.3 meters diameter at breast height; DBH) the average tree density is 368 trees/ha, with mean basal area of 19.7 m2/ha, mean canopy height of 25 m, and on average 59 species/ha (all data for trees ≥10 cm in diameter at 1.3 m height from the ground (DBH); Pena-Claros et al., 2008). The average annual temperature is 25 $^{o}$C. Mean annual precipitation in the region is ~1580 mm, with 4 months receiving <100 mm (May–September) and 1 month (July) during which potential evapotranspiration exceeds rainfall (Pena-Claros, unpublished data). Seasonally deciduous and semi-deciduous forests like La Chonta provide about 45% of Bolivia's timber and encompass about 35% of the area designated for forest management (Superintendencia Forestal, 2002). The region is vulnerable to wildfires, and 30% of the concession was burned in 1995 (Cordero, 2000; Gould et al., 2002) and 2004 (C. Pinto, personal communication).

Four 100 m x 100 m (1 ha) and one 100 m x 50 m study plots were established within two ~27-ha stands belonging to the Long-term Silvicultural Research Program (LTSRP), established by the Instituto Boliviano de Investigación Forestal in different forest types within Bolivia (IBIF; more information available online at www.ibifbolivia.org.bo). The study plots had not been logged or burned in recent history. Initial plot locations were randomly selected, but then shifted so the edges of the 1-ha plots fell on established trails of the LTSRP plots (located every 50 m within the 450 m x 600 m LTSRP plots) reducing any possible impact related to human activities. All trees ≥20 cm in DBH within the 1-ha study plots had been mapped previously to a Cartesian coordinate system by IBIF technicians and identified to species level. The most abundant species in the plots were *Pseudolmedia laevis* (Moraceae), *Ampelocera ruizii* (Ulmaceae) and *Terminalia oblonga* (Combretaceae). The four 1-ha plots were used for all spatial analyses, while data from the fifth 0.5 ha plot was used to increase the sample size for development of allometric equations. Descriptive statistics of the four study plots is provided in Table 3.1.

### 3.3.2 Forest structure

Field data were collected from December 2005 through February 2006. For each tree, we measured the DBH, total tree height (from base of the trunk to the highest branch or foliage), height to the first large branch (defined as the first major trunk bifurcation), base to the crown (defined as the base of a sphere containing greater than 75% of the trees foliage), crown maximum length (m) and width (m), and horizontal offset (distance (m) and azimuth) of the crown center from the trunk location. For each tree, we also defined crown exposure using a five-point scale (Clark and Clark, 1992) in which 1 = no direct light or low amount of lateral light, 2 = intermediate or high amount of lateral light, 3 = vertical light in part of the crown, 4 = vertical light in the whole crown, and 5 = exposed crown with direct light coming from all directions.

The tree height, height to the first large branch, and crown base were estimated by two separate observers in 0.5 m increments. To correct for observer error, the observer- estimated heights (referred to as estimated heights) of 106 trees were regressed against height measurements made on the same trees using a handheld laser range finder (referred to as laser heights; impulse-200LR, laser technology Inc., Englewood, Colorado). The estimated height to the first branch showed a significant linear relationship with that of the laser range finder (estimated height = 1.48 + 0.85 × laser height, $r^2$ =0.88, $p < 0.0001$), and the estimated tree height had a significant linear relationship with laser total tree height (estimated total height = 0.745 + 0.89 × laser total height; $r^2$ =0.90, $p < 0.0001$). As the laser rangefinder was available only for the first portion of the field campaign, all height data collected thereafter were corrected using the regression equations described above. To ensure against gradual changes in estimated height accuracy during data collection, we calibrated our height estimates each morning prior to fieldwork by estimating the heights of 10–15 trees previously measured with the laser range finder. All subsequent statistical and descriptive analyses were conducted on the corrected height data. Crown length (transect of maximal distance) and width (perpendicular distance) were measured in the field using a 50-m measuring tape. A clinometer was used to identify the location

directly beneath the outermost edge of each tree crown. Error due to topography was minimized by holding the tape as horizontal as possible prior to recording the crown dimensions. Canopy center offset from the trunk was assessed by measuring the distance from the crown center point to the trunk base. Crown area was calculated assuming an oval shape with maximum crown length (L) and the perpendicular width (W) being the explanatory axes. Crown volume was calculated assuming a perfect spherical ellipsoid with width (W), length (L) and depth (D)being the three explanatory variables; crown depth was calculated as the difference between maximum tree height and crown base.

Forest biomass was calculated using six equations available in the literature (Brown, 1997; Araujo et al., 1999; Carvalho et al., 1988; Chave et al., 2005; see Supplementary Materials 3A for equations). Two biomass equations derived from Chave et al. (2005) required species-specific wood density values, which were largely unavailable at the species level. Therefore, we used wood density at the finest taxonomic resolution available via a web-based wood density database (http://www.worldagroforestrycentre.org/sea/Products/AFDbases/wd), which allowed us to obtain wood density data at the family, genus and species level for 52, 40 and 8% of the tree individuals in our study plots, respectively. It has been shown that wood density information at the order, family, genus and species levels contributed an additional 12.1, 13.3, 45.6 and 29.6%, respectively, of explanatory power over wood density variation (Baker et al., 2004; Slik, 2006). Consequently, we believe that our biomass estimates, which included wood density, provided a more accurate representation of tree biomass than those relying on DBH and height alone.

Separate one-way analyses of variance (ANOVA) among the five crown position classes were carried out for all structural parameters, followed by Tukey's HSD post hoc analyses when significant differences were found. All variables were log transformed prior to analysis to meet assumptions of data distribution normality. Optimal bi- and multi-variate power regression models were identified between all structural parameters using TableCurve 2D and 3D (Versions 5.01 and 4.0, respectively, Point Richmond, CA, USA: Systat, Inc.).

### 3.3.3 Forest composition

Species richness, abundance, diversity, and basal area ($m^2$/ha) were calculated for the four study plots, the five crown position classes, and for each DBH category. Diversity differences between the DBH and crown exposure classes were compared using the Shannon–Weiner diversity index. Changes in species composition between the crown exposure classes were compared using Sorensen's similarity index.

### 3.3.4 Spatial analyses

The Cartesian coordinate arrays from study plots 1–2 and 3–4 were geo-referenced to 22 and 17 differentially corrected GPS (Geographic Positioning System; Leica GS-50+, Leica Geosystems, St. Gallen, Switzerland) points, respectively. The grid points were converted to Universal Transverse Mercator (UTM; zone 20 South, datum WGS 1984) using linear regression. Root mean square errors (RMSE) for the regression equations were 5.6 and 6.1 m, respectively. Fine scale geo-referenced topographic data of the LTSRP plots was obtained from the Instituto Boliviano de Investigación Forestal (Vroomans, 2003), which was used to correct the vertical positioning of tree crowns prior to spatial analyses.

Following geo-rectification, maps of tree crown and trunk locations were created in a Geographic Information System (GIS; ArcInfo, Redlands, CA, USA). This process enabled vertical and horizontal spatial analysis of tree distributions and crown positions. The average distance between tree individuals within each of the five crown exposure classes was calculated using a linear least distance approach. Tree density was calculated for each crown exposure class and all classes together by first dividing each study plot into 5 × 5 m subsections and then counting all tree stems within 10 m of each subsection and dividing the number of tree stems by the search area (490 $m^2$). We then calculated histograms of the density distributions within each plot, ranging from 0 to 0.02 stems/$m^2$, for each crown exposure class. Density distributions were compared among crown exposure categories using separate one-way ANOVA ($N$ = 4 plots). The mean number of trees located beneath individual tree

crowns was calculated separately for each DBH and crown exposure class—henceforth referred to as obscured trees. Correlations between crown dimensions and the number of obscured trees were used to develop correction equations between nadir-visible trees and those identified and mapped in the field. These equations were developed for trees in crown exposure classes 3–5 only because the other exposure classes, by definition, were not visible to nadir-viewing optical remote sensors. We refer to biomass derived using the equation corrected for obscured tree stems as the corrected biomass. Field geo-referenced data of each plot were used to link the plot location to a Quickbird image acquired of our study area on 15 September 2005 at 4:37 pm GMT (11:00 am local time). The image acquisition angle was $< 5^{o}$ from nadir. The image was acquired at a resolution of 0.4 m panchromatic and 1.4 m multi-spectral. The image was geo-rectified using a first-degree linear regression model to 62 differentially corrected ground control points clustered around the study plots. The root mean square (RMS) error of the warp was 3.5 m, and the final projection was Universal Transverse Mercator (UTM; zone 20 South, datum WGS 1984).

Individual tree crowns were delineated in the panchromatic Quickbird imagery using an automated procedure developed by Palace et al. (2008). The procedure combines iterative detection of local maxima values with a 360 directional linear search algorithm to identify inter-pixel change events in the panchromatic image exceeding a defined threshold. No calibration to field data were conducted prior to image processing to assess the utility of the approach to areas not having extensive field data. The original algorithm was developed using field data from Cauaxi, Pará, Brazil (Palace et al., 2008), and was previously applied successfully at seven sites spanning the Amazon basin, indicating the robustness of the algorithm to provide landscape- level estimates of vegetation structure. However, this analysis used community-wide distribution comparisons rather than tree- to-tree comparisons, as we conducted in this study. As it is possible to achieve similar DBH distributions between RS and field assessments for the incorrect reason (e.g., some overestimates compensated by some underestimates), we seek to elucidate the forest DBH

distributions and resultant standing biomass estimates from RS using the spatially explicit analysis presented in this study.

Automated delineations of tree crowns were made as both polygons (incorporating the 360 search transects) and circles (using the average of the longest opposite ordinal transects as the radius). Individual tree crown area calculated from these methods was input into the allometric relationship between field-derived crown area and DBH to calculate remotely sensed DBH distributions over the study area. Both corrected and raw nadir-visible biomass data were calculated using the allometric crown area-to-biomass equations illustrated in Fig. 3.5. Crown area, DBH and biomass results were categorized to resolutions of 25 $m^2$, 10 cm and 1 Mg, respectively, based on a visual inspection of data distributions. Kolmogorov–Smirnov analyses were used to compare distributions of categorized tree abundances. Direct remote sensing to field comparison at the tree scale were conducted by randomly selecting tree individuals from crown exposure classes 3, 4 and 5, and then quantifying the number of remote sensing detections having their center point within the field-delineated tree crown. Remote sensing biomass calculations at the tree scale were made by inputting the summed area of all automated detections within that tree's crown into the corrected biomass. Paired t- tests and linear regressions were used to compare field derived individual crown area, DBH and biomass with the remote sensing polygon approach.

## 3.4 Results

### 3.4.1 Forest structure

The majority of the trees within the study plots had DBH values of 20–29 cm (Table 3.2). Basal area remained similar among DBH classes, showing only a 50% reduction as compared to the tenfold reduction in tree abundance and biomass. Across the four plots, there were more trees in the crown exposure class 3 (25%; trees receiving partially vertical light), followed by canopy position 5 (20%; emergent trees), while few trees (10%) had crowns located in crown exposure class 1 (Table

3.3). Basal area across our study plots was dominated by tree individuals in crown exposure class 5, which exceeded the summed basal area of all individuals in the other four crown exposure classes (Table 3.3).

Emergent trees (exposure class 5) are represented by trees belonging to a wider range of DBH classes, as indicated by the greater standard error value, than any other crown exposure class, and the percentage of trees belonging to crown exposure class 5 is larger as trees increase in size (Fig. 3.1). The majority of forest biomass was stored in trees in crown exposure class 4 and 5, in particular, exposure class 5 stored 139 Mg/ha, which was equal to the biomass found in all other crown positions combined (Table 3.3). Mean crown area and crown length of emergent trees was 228 $m^2$ and 17 m, respectively, while these variables for exposure class 4 were only 75 $m^2$ and 11 m, respectively. The maximum length of crowns of emergent trees was double that of crown position 4, though only smaller decreases were found from crown position 1–4. Maximum crown area increased from 146 to 357 to 1523 $m^2$ in crown exposure classes 1, 4 and 5, respectively (Table 3.3). The simplest biomass equations, which included only DBH (Supplementary Materials 3A, Eqs. A–D), produced lower biomass estimates than those incorporating wood density and tree height (Supplementary Materials 3A, Eqs. E and F), resulting in twofold differences in derived biomass.

The 216 allometric equations between forest structural variables are presented in the Supplementary Materials 3A. A subset of these equations was chosen based on their explanatory power and utility for linking nadir top-of-canopy visible parameters to field measurements which are provided in Table 3.4. All allometric relationships presented in Table 3.4, with the exception of DBH in crown exposure class 1, had *P*-values <0.001. For emergent trees, crown length and crown area had the greatest explanatory power of tree DBH ($R^2$ = 0.74 and 0.73, respectively).

### 3.4.2 Forest composition

A total of 59 tree species were found within our study area, dominated by *P. laevis* (Moraceae). Although tree abundance (20 cm DBH) varied threefold among study parcels, tree species richness varied far less with minimum and maximum species numbers of 26 and 37 found in study plots 3 and 4, respectively (Table 3.1). Species richness and stem abundance, 41 and 62, respectively, were greatest in DBH category 20–29 cm, and decreased rapidly to 25 and 30, respectively, in DBH category 30–39 cm. DBH categories greater than 70 cm were composed of fewer than five species. Species diversity followed a similar trend, but peaked in DBH category 50–59 cm (Table 3.2). For crown exposure classes, the highest species richness and diversity were found in emergent trees (35 spp.), followed by exposure class 3 (27 spp.; Table 3.3). Species composition was the least similar between crown exposure class 1 and 5, while species compositions were more similar for closer exposure classes (Table 3.5). The majority of tree species were represented within the emergent crown exposure class (Table 3.5). Cumulatively, from emergent through understory trees (classes 5, 5-4, 5-3, 5-2 and 5-1, respectively), we found that 59, 73, 86, 95 and 100% of all tree species were represented.

### 3.4.3 Spatial analyses

Tree individuals in crown exposure class 1 occurred approximately 27 m apart, while those in crown exposure class 5 occurred an average of 11 m apart (Table 3.3). Fig. 3.2 illustrates the distribution of tree stem density by crown position. The two-way ANOVA showed significant differences between tree densities in the five crown exposure classes at the 0.003 density class, with crown position 5 having the greatest abundance at this density. There were no significant differences among the five crown exposure classes at the other densities; although a trend was observed with the greatest area of zero stem density being found in crown exposure class 1.

A map of crown positions generated from the field data is provided in Fig. 3.3. The majority of obscured tree stems were located within smaller DBH classes (Fig.

3.4), where eight times as many trees in the 20–29 DBH class were obscured by trees in crown exposure class 5, as those in the 40–49 DBH class. The relationship between crown length or crown area and the total number of tree stems obscured is provided in Fig. 3.5 A and B, showing a minimum and maximum of 1–18 obscured tree stems. The nadir-viewable crown area and the crown exposure class had, as expected, a strong negative relationship with 100% of crown position 5 being visible, while only 55% and 60% of crown area in positions 3 and 4 was visible, respectively. Crown exposure classes 1 and 2 were almost entirely obscured by other crowns (Table 3.3).

Correction equations necessary to convert remotely sensed data to field-based structural data are illustrated in Fig. 3.5, and the equations are provided in the Supplementary Materials 3.1. Significant relationships were identified between crown length and crown area and the number of obscured trees (Fig. 3.5 A and B). Additional relationships were derived to relate crown length and area to basal area and biomass for both the nadir-visible trees and including the obscured trees (Fig. 3.5 C–F). Basal area and biomass estimates increased by 30–50%, largely depending on the crown area of the exposed tree crowns, when we included all obscured trees in comparison to calculations based only on nadir visible trees.

A total of 370 tree crowns were identified using the remote sensing methodology, although there were 531 tree crowns measured in the field (Fig. 3.6). The abundance of remotely identified trees in study plots 1, 3 and 4 represented less than half the trees identified in the field, while remote tree stem counts in study plot 2 was almost three times higher than the trees identified in the field (Table 3.1).

The remotely sensed circle and polygon delineation approach identified 70 and 108 trees having DBH < 20 cm, respectively. In the field trees with DBH < 20 cm were not included (Fig. 3.7A). These same approaches identified far fewer tree individuals in the 20–29 DBH class, with 43 and 59 trees identified using the circle and polygon approach, versus 249 trees identified in this class in the field, resulting in significantly different distributions. The remote sensing approaches identified trees with DBH values up to 110 cm, but identified few greater than this threshold (Fig. 3.7A). While crown areas from both the remotely sensed circle and polygon

approaches had significantly different (with greater and lower areas, respectively; see Table 3.6) crown area distributions from those of field measurements, the DBH distributions quantified from these areas do not differ between the remotely sensed polygon approach and field measurements (Table 3.7). While the nadir-visible biomass equations on the remote sensing circle approach did not significantly differ from field measurements, the polygon approach did so. When the corrected biomass equation, accounting for obscured trees, was used, stand biomass estimates from the remotely sensed circle approach significantly differed, while the polygon approach did not, from the field values (Table 3.7, Supplementary Materials 3C).

Direct comparisons between field-delineated tree crowns and remotely sensed crown polygons was conducted for 21, 21 and 42 trees for crown exposure classes 3, 4 and 5, respectively. Trees in exposure classes 1 and 2 were not used, as by definition, they are obscured from nadir-viewing remote sensors. Seventy-four percent of field-delineated tree crowns in crown exposure 5 had automated detections centered within them, while only 38% of crowns in exposure class 4 and 3 were detected via our remote sensing methodology. A significant linear relationship existed between emergent tree biomass calculated from field-measured variables and the biomass estimated from remotely identified crown polygons (remotely sensed polygon corrected biomass = 2.22 + 0.54 × field biomass; $R^2 = 0.42$, $P < 0.0001$), while non-significant relationships were found in exposure classes 3 and 4. Significant positive relationships were found between field-delineated crown areas and the number of remote circle and polygon detections within a given crown area (for crown exposure class 3: RS detections = 0.13 + 0.006 × field area; $R^2 = 0.68$, $P < 0.0001$; for class 4: RS detections = 0.11 + 0.007 × field area; $R^2 = 0.46$, $P < 0.015$; and for crown exposure class 5: RS detection = 0.496 + 0.003 × field crown area; $R^2 = 0.53$, $P < 0.0001$).

## 3.5 Discussion

Biomass inventories are needed to track forest carbon dynamics. High-resolution satellite imagery is starting to enable structural analysis of tropical forests over large areas, but we lack an understanding of how the spatial distribution of tropical forest biomass links to remote sensing. Furthermore, the high diversity of tree species present in tropical forests adds to their structural and spectral complexity, impeding many remote-sensing approaches. An increased understanding of how tree species diversity is distributed within the forest could assist in the development of methods which take advantage of this diversity. To interpret results from remote sensing, it is first necessary to understand how forest biomass and tree species diversity are horizontally and vertically distributed.

### 3.5.1 Spatial distribution of forest biomass

The highest tree abundance was found in the smallest DBH classes (Table 3.2), while basal area and biomass were more or less equally distributed among the different size classes. The distribution of stem abundance observed across DBH categories is typical of tropical forests (Cummings et al., 2002). Our vertical crown exposure data showed that the highest values of basal area, DBH, and total height occurred within emergent trees (Table 3.3), which encompassed about 58% of the total forest biomass found in our study sites, but represent only 20% of the 531 trees in our study plots. Other studies have highlighted large quantities of biomass being stored in emergent trees (Keller et al., 2001), but noted that emergent trees were quite rare.

An analysis across the Amazon showed that dry season length was positively correlated with percentage biomass stored in trees with diameters 50 cm, with a maximum storage of 41–45% biomass stored above that DBH threshold (Vieira et al., 2004). Our results are higher than these, and may be partly explained by the fact that our study location has a more pronounced dry season than any of the study sites addressed in the previous analysis. An alternate explanation would be the past land-use history in our study forest. Previous research has shown extensive distributions of

anthropogenic terra-preta soil containing 500-year-old pottery shards (Paz, 2003), suggesting that we may be seeing the remnant composition and forest structure of this period, especially as these trees may be many hundreds of years old (Chambers et al., 1998). Many of the largest trees in the forest are *Ficus* spp., known to be shade intolerant. These large trees show very little recruitment in the understory, implying that they became established under very different climatic conditions or disturbance regimes than at present or are the result of historical management practices. The significantly greater spatial clumping of emergent trees, as compared to all other crown exposure classes (Fig. 3.2), may be related to either past land-use history or the existence of fine-scale topo-edaphic gradients within our study plots (Vroomans, 2003; Paoli et al., 2008). The greater separation distance between understory tree stems in exposure class 1 may be explained by exclusion of tree stems smaller than our ≥20 cm DBH threshold.

Emergent trees had longer crown length and crown width, and consequently larger crown area, than trees in the other crown exposure classes (Table 3.3), likely due to the fact that trees expand their crowns when they reach the canopy of tropical forests (O'Brien et al., 1995; Poorter et al., 2005, 2006). The lack of correlation between DBH class and biomass resulted from larger DBH trees occurring at lower densities (Table 3.2).

### 3.5.2 Spatial distribution of forest diversity

Trees in the emergent tree class represented 59% of all species found in our study area, although they composed only 20% of the 531 trees >20 cm DBH within our study plots. When considering the three exposure classes likely viewable to a nadir remote sensor (exposure classes 5-3), we found that 86% of all tree species ≥20 cm DBH were represented. Thus the vast majority of tropical forest tree diversity for stems ≥20 cm DBH could be quantified and monitored using nadir viewing remote sensing techniques, such as the ones used in this study and in a study carried out in Hawaiian tropical forests (Carlson et al., 2007).

### 3.5.3 Linking field and remote sensing measurements

Since the emergent trees had the largest canopies and the tallest mean height, they obscured the largest number of understory trees (Fig. 3.4). Consequently, emergent trees obscure the understory biomass from nadir-viewing remote sensors, which resulted in an underestimation of biomass. It was possible with the first round of correction equations developed in this study to include the obscured trees so that the corrected biomass calculation did not differ significantly from the biomass estimations using field data (Table 3.7). These correction equations are inherently site-specific; consequently, the development of these types of spatial equations needs to be conducted for the large variety of forest types and forest ages found throughout the tropics to accurately determine full stand biomass from remote sensing. Forests having a greater stature or increased tree diversity would likely have greater standing biomass and diversity masked by overstory tree crowns. Understanding how the spatial distribution of biomass and tree species diversity differs among forest biomes and along climatic gradients, however, has not been well studied and is a topic we are currently investigating.

The automated crown delineation approach worked well at the community scale, although the circular crown measurement approach tended to over-estimate tree crown areas for smaller crowns, while erroneously dissecting larger crowns into multiple individuals. When remotely sensed tree crown area was converted to DBH using our allometric relationships, we found we had identified many tree individuals below our field diameter threshold of 20 cm. This is not unexpected, as our DBH threshold (≥20 cm DBH) meant that many small but nadir-visible tree crowns were not delineated and mapped in the field. This is apparent in the large open areas in Fig. 3.3 as compared with Fig. 3.6, where smaller crowns have been automatically delineated throughout the plots. Consequently, we suggest that future studies use crown exposure class instead of DBH to define sample trees, although we recognize the large (and sometimes infeasible) difficulties associated with such a survey. Even considering these differences, however, biomass estimated via remote sensing did not have significantly different distributions of biomass from those mapped in the field after

using our equations developed to correct for obscured trees. Our corrected biomass equation resulted in an increase of remotely estimated tree biomass of 30–50%, depending on the crown area. The utility of a crown-dependent conversion equation is highlighted in our clumping analysis, where it is shown that the forest in our study area is not homogeneous throughout the landscape, but rather varies in structure at fine spatial scales. Relationships between topography and forest structure and diversity, among other factors, have been identified within our study area (Vroomans, 2003) and warrant further investigation at larger scales via remote sensing.

Results from our remote sensing approaches were mixed at the tree-to-tree scale. Although the crown delineation program applied in this study captured many of the textural features of the Quickbird image, most of the larger emergent canopies were segmented into smaller crowns, while some smaller trees visually appeared to be merged. Our remote sensing analyses indicate that individual tree crowns are not easily quantified due to the highly heterogeneous matrix of shadows, intrinsic crown characteristics at the species level, multiple sub-crowns within a single tree, and canopy gap disturbances. Whether such problems would be exacerbated by the greater diversity and/or higher standing biomass typical of some tropical forests (Palace et al., 2008) would depend on the spatial distribution of tree diversity and biomass in those forests. For example, biomass uncertainty could be reduced in forests having fewer understory trees, such as some found in South East Asian. Our results do show, however, that even in these forests, which are noticeably more structurally heterogeneous than those in other areas of the Amazon, there is great potential for the approach to document larger-scale patterns in community structure and biomass. Further improvements to this technique will require: (1) a greater understanding of the spatial distribution of tree diversity and biomass in a variety of forest types, (2) the inclusion of spectral data to differentiate between adjacent tree crowns, and (3) improvement of the crown edge detection algorithm.

## 3.6 Conclusions

Improved understanding of the spatial distribution of forest species diversity and biomass will aid in the development of remote sensing approaches capable of rapidly and cost-effectively quantifying these factors over large areas of tropical forest. Such data are necessary for fine-scale forest management, biomass assessments, and conservation planning of tropical forests. In our study of a lowland moist semi-deciduous tropical forest in Bolivia, the upper-canopy and often emergent trees comprised the majority of the tree diversity and biomass. Trees with crowns visible to nadir remote sensors represented 86% of all tree species ≥20 cm DBH in our study plots. Emergent trees obscured many subordinate trees with DBH ≥20 cm, resulting in 30–50% of the forest biomass being hidden from nadir (e.g., satellite) view. Our allometric equations were specifically developed to link the portion of the forest that was remotely sensible to field parameters. Our subsequent correction equations allowed us to derive aboveground forest biomass, basal area, and tree density from only those tree crowns visible to the Quickbird satellite sensor. Although the automated crown detection algorithm employed here requires continued development, it did show promise for delivering high-resolution maps of forest structure. Our future efforts will focus on ways to improve both the satellite sensing approaches via enhanced algorithms and inclusion of spectral information, and their linkage to the full complexity of tropical forest diversity and biomass in three dimensions.

## 3.7 Acknowledgements

We thank the Instituto Boliviano de Investigación Forestal (IBIF) for field and logistical assistance and La Chonta Ltda. for allowing us access to their forest concession. We thank Don Ricardo Mendez for help with data collection. We thank Angelica Almeyda Zambrano for helpful comments and logistical support. This work

was supported by NASA LBA-ECO grant NNG06GE32A (LC-33) and the Carnegie Institution.

## 3.8 References

Araujo, T.M., Higuchi, N., Carvalho Jr., J.A., 1999. Comparison of formulae for biomass content determination in a tropical rain forest site in the state of Para, Brazil. For. Ecol. Manage. 117, 43–52.

Asner, G.P., Palace, M., Keller, M., Pereira Jr., R., Silva, J.N.M., Zweede, J.C., 2002. Estimating canopy structure in an Amazon forest from laser range finder and IKONOS satellite observations. Biotropica 34, 483–492.

Baker, T.R., Phillips, O.L., Malhi, Y., Almeida, S., Arroyo, L., Di Fiore, A., Erwin, T., Killeen, T.J., Laurance, S.G., Laurance,W.F., Lewis, S.L., Lloyd, J., Monteagudo, A., Neill, D.A., Patino, S., Pitman, N.C.A., Silva, J.N.M., Martinez, R.V., 2004. Variation in wood density determines spatial patterns in Amazonian forest biomass. Global Change Biol. 10, 545–562.

Brokaw, N., 1985. Gap-phase regeneration in a tropical forest. Ecology 66, 682.

Brown, S., 1997. Estimating Biomass and Biomass Change of Tropical Forests, A Primer. FAO Forestry Paper 134. United Nations Food and Agriculture Organization, Rome, 55 pp.

Calla, S.A., 2003. Arquelogía de ‘‘La Chonta’’. BOLFOR, Santa Cruz, Bolivia, 53 pp.

Carlson, K.C., Asner, G.P., Hughes, R.F., Ostertag, R., Martin, R.E., 2007. Hyperspectral remote sensing of canopy biodiversity in Hawaiian lowland rainforests. Ecosystems 10, 536–549.

Carvalho Jr., J.A., Higuchi, N., Araujo, T.M., Santos, J.C., 1988. Combustion completeness in a rainforest clearing experiment in Manaus, Brazil. J. Geophys. Res. 103, 13199–13915.

Chambers, J., Higuchi, N., Schimel, N., 1998. Ancient trees in the Amazon. Nature 391, 135–136.

Chambers, J.Q., dos Santos, J., Ribeiro, R.J., Higuchi, N., 2000. Tree damage, allometric relationships, and above-ground net primary production in central Amazon forest. For. Ecol. Manage. 5348, 1–12.

Chave, J., Andalo, C., Brown, S., Cairns, M.A., Chambers, J.Q., Eamus, D., Folster, H., Fromard, F., Higuchi, N., Kira, T., Lescure, J.-P., Nelson, B.W., Ogawa, H., Puig, H., Riera, B., Yamakura, T., 2005. Tree allometry and improved estimation of carbon stocks and balance in tropical forests. Oecologia 145, 87–99.

Clark, D.A., Clark, D.B., 1992. Life history diversity of canopy and emergent trees in a neotropical rain forest. Ecol. Monogr. 62, 315–344.

Clark, D.B., Castro, C.S., Alvarado, L.D.A., Reed, J.M., 2004. Quantifying mortality of tropical rain forest trees using high-spatial-resolution satellite data. Ecol. Lett. 7, 52–59.

Cordero,W., 2000. Determinación del daño causado por los incendios forestales ocurridos en los departamentos de Santa Cruz-Beni en los meses de agosto y septiembre de 1999. Informe Final. Corporación Andina de Fomento, Proyecto BOLFOR, & Geosystems. Santa Cruz, Bolivia, 43 pp.

Cummings, D.L., Boone Kauffman, J., Perry, D.A., Flint Hughes, R., 2002. Aboveground biomass and structure of rainforests in the southwestern Brazilian Amazon. For. Ecol. Manage. 163, 293–307.

Dauber, E., Teran, J., Guzman, R., 2000. Estimaciones de biomasa y carbono en bosques naturales de Bolivia. Superintendencia Forestal, Santa Cruz, Bolivia, 62 pp.

Drake, J.B., Dubayah, R.O., Clark, D.B., Blair, J.B., Hofton, M.A., Chazdon, R.L., Weishampel, J.F., Prince, S., 2002. Estimation of tropical forest structural characteristics using large-footprint lidar. Remote Sens. Environ. 79, 305–319.

Gould, K.A., Fredericksen, T.S., Morales, F., Kennard, D., Putz, F.E., Mostacedo, B., Toledo, M., 2002. Post-fire tree regeneration in lowland Bolivia, implications for fire management. For. Ecol. Manage. 165, 225–234.

Guariguata, M.R., Chazdon, R.L., Denslow, J.S., Dupuy, J.M., Anderson, L., 1997. Structure and floristics of secondary and old-growth forest stands in lowland Costa Rica. Plant Ecol. 132, 107–120.

Hansen, A.J., Spies, T.A., Swanson, F.J., Ohmann, J.L., 1991. Conserving biodiversity in managed forests, lessons from natural forests. BioScience 41, 382–392.

Keller, M., Palace, M., Hurtt, G., 2001. Biomass estimation in the Tapajos National Forest, Brazil, Examination of sampling and allometric uncertainties. For. Ecol. Manage. 154, 371–382.

Kuppers, M., 1989. Ecological significance of aboveground architectural patterns in woody plants. A question of cost-benefit relationships. Trends Ecol. Evol. 4, 375–379.

O'Brien, S.T., Hubbell, S.P., Spiro, P., Condit, R., Foster, R.B., 1995. Diameter, height, crown, and age relationships in eight neotropical tree species. Ecology 76, 1926–1939.

Palace, M., Keller, M., Asner, G.P., Hagen, S., Braswell, B., 2008. An analysis of Amazonian forest structure using an automated tree crown detection algorithm and IKONOS imagery. Biotropica 40, 141–150.

Paoli, G.D., Curran, L.M., Slik, J.W.F., 2008. Soil nutrients affect spatial patterns of aboveground biomass and emergent tree density in southwestern Borneo. Oecologia 155, 287–299.

Paz, C., 2003. Forest-use History and the Soils and Vegetation of a Lowland Forest in Bolivia. University of Florida, Gainesville, Florida, 67 pp.

Peña-Claros, M., Peters, E.M., Justianiano, M.J., Bongers, F., Blate, G.M., Fredericksen, T.S., Putz, F.E., 2008. Regeneration of commercial tree species

following silvicultural treatments in a moist tropical forest. For. Ecol. Manage. 255, 1283–1293.

Phillips, O.L., Malhi, Y., Higuchi, N., Laurance, W.F., Nunes, P.V., Vasquez, R.M., Laurence, S.G., Ferreira, L.V., Stern, M., Brown, S., Grace, J., 1998. Change in the carbon balance of tropical forests, evidence from long-term plots. Science 282, 439–442.

Poorter, L., Bongers, F., Sterck, F.J., Woll, H., 2005. Beyond the regeneration phase, differentiation of height-light trajectories among tropical tree species. J. Ecol. 93, 256–267.

Poorter, L., Bongers, L., Bongers, F., 2006. Architecture of 54 moist-forest tree species, traits, trade-offs, and functional groups. Ecology 87, 1289–1301.

Slik, J.W.F., 2006. Estimating species-specific wood density from the genus average in Indonesian trees. J. Trop. Ecol. 22, 481–482.

Superintendencia Forestal, 2002. Informe Anual Gestión 2002. Santa Cruz, Bolivia, 45 pp.

Vieira, S., Camargo, P.B., Selhorst, D., Silva, R., Hutyra, L., Chambers, J.Q., Brown, I.F., Higuchi, N., Santos, J., Wofsy, S., Trumbore, S.E., Martinelli, L.A., 2004. Forest structure and carbon dynamics in Amazonian tropical rain forest. Oecologia 40, 468–479.

Vroomans, V., 2003. Topografıa de las parcelas permanentes en la concesión forestal La Chonta y su efecto en la vegetación. Documento Técnico# 156/2003. Proyecto BOLFOR, Santa Cruz, Bolivia, 77 pp.

Whitmore, T.C., 1978. Gaps in the forest canopy. In: Tomlinson, P.B., Zimmerman, M. (Eds.), Tropical Trees as Living Systems. Cambridge University Press, New York, pp. 639–655.

Whitmore, T.C., 1989. Canopy gaps and the two major groups of forest trees. Ecology 70, 536.

## 3.9 Tables

**Table 3.1:** Abundance and structural variables (mean (±S.E.) for trees ≥20 cm in DBH in the four 1-ha plots included in this study

| Variable | Study plot | | | |
|---|---|---|---|---|
| | **1** | **2** | **3** | **4** |
| Tree abundance ( ≥ 20 cm DBH) | 119 | 66 | 162 | 184 |
| Richness | 32 | 31 | 26 | 37 |
| Diversity[a] | 2.76 | 3.15 | 1.79 | 2.39 |
| **Mean (±S.E.) percentage of tree stems in each crown exposure class** | | | | |
| Crown Exposure 5 | 31 (0.26) | 14 (0.21) | 27 (0.17) | 36 (0.20) |
| Crown Exposure 4 | 18 (0.15) | 13 (0.20) | 30 (0.19) | 48 (0.26) |
| Crown Exposure 3 | 22 (0.19) | 27 (0.41) | 33 (0.20) | 50 (0.27) |
| Crown Exposure 2 | 34 (0.29) | 10 (0.15) | 49 (0.30) | 36 (0.20) |
| Crown Exposure 1 | 14 (0.12) | 2 (0.03) | 23 (0.14) | 14 (0.08) |
| **Mean (±SE) of structural variables** | | | | |
| Basal area ($m^2$/ha) | 15.21 | 8.92 | 25.52 | 27.04 |
| Average DBH | 35.4 (2.0) | 37.0 (2.6) | 38.3 (1.7) | 37.3 (1.6) |
| Branch height | 9.7 (0.3) | 8.6 (0.5) | 9.7 (0.3) | 9.8 (0.3) |
| Crown base height | 12.8 (0.4) | 12.3 (0.6) | 13.8 (0.4) | 13.3 (0.3) |
| Total tree height | 19.7 (0.7) | 19.5 (0.9) | 22.7 (0.6) | 21.5 (0.6) |
| Crown length | 9.9 (0.5) | 11.3 (0.8) | 11.2 (0.5) | 11.5 (0.5) |
| Crown width | 6.9 (0.5) | 8.0 (0.7) | 7.9 (0.5) | 8.0 (0.4) |
| Crown depth | 6.1 (0.3) | 6.6 (0.5) | 8.0 (0.3) | 7.3 (0.3) |
| Crown area | 77.9 (13.8) | 96.8 (20.3) | 96.8 (13.1) | 91.8 (11.1) |
| Crown volume | 496.2 (130.1) | 702.1 (258.0) | 801.7 (167.8) | 639.9 (127.4) |
| Crowns detected remotely [b] | 64 | 186 | 58 | 62 |

[a] Shannon-Weiner diversity index.
[b] Number of individual tree crowns identified using automated delineation of the panchromatic Quickbird satellite image.

**Table 3.2:** Abundance, basal area and biomass per DBH classes present throughout the four 1-ha study plots

| DBH (cm) | Abundance (stems/ha) | Basal area ($m^2$/ha) | Biomass (± SE) (Kg/ha) [a] | Richness (4 ha) | Diversity (4 ha)[b] |
|---|---|---|---|---|---|
| 20 ≤ 29 cm | 61.75 | 2.92 | 26.69 (5.38) | 41 | 2.24 |
| 30 ≤ 39 cm | 30.00 | 2.80 | 29 (3.96) | 25 | 2.04 |
| 40 ≤ 49 cm | 13.25 | 2.12 | 23.31 (3.03) | 22 | 2.46 |
| 50 ≤ 59 cm | 9.25 | 2.10 | 24.7 (3.01) | 21 | 2.75 |
| 60 ≤ 69 cm | 5.50 | 1.82 | 23.08 (2.75) | 13 | 2.29 |
| 70 ≤ 79 cm | 1.75 | 0.73 | 9.62 (1.25) | 5 | 1.48 |
| 80 ≤ 89 cm | 1.50 | 0.84 | 11.69 (1.64) | 5 | 1.56 |
| 90 ≤ 99 cm | 1.50 | 1.02 | 14.06 (2.54) | 4 | 1.33 |
| 100 ≤ 109 cm | 0.75 | 0.59 | 8.6 (1.44) | 3 | 1.10 |
| 110 ≤ 119 cm | 1.50 | 1.52 | 22.31 (4.55) | 5 | 1.56 |
| 120 ≤ 129 cm | 1.25 | 1.46 | 22.01 (4.64) | 3 | 1.05 |
| 130 ≤ 139 cm | 0.25 | 0.36 | 6.3 (1.18) | 1 | 0.00 |
| ≥ 140 cm | 0.25 | 0.79 | 15.22 (3.69) | 1 | 0.00 |

[a] Mean and standard error of the five biomass equations described in the methods section.
[b] Shannon-Weiner diversity index

**Table 3.3:** Forest structure and crown characteristics per crown exposure class

| Variable | Crown exposure class | | | | |
|---|---|---|---|---|---|
| | **1 (Understory)** | **2** | **3** | **4** | **5 (Emergent)** |
| **Forest structure** | | | | | |
| Tree density (#/ha) | 53 | 129 | 132 | 109 | 108 |
| Richness | 14 | 26 | 27 | 26 | 35 |
| Total species represented (%) | 24 | 44 | 46 | 44 | 59 |
| Diversity [a] | 1.501 | 1.891 | 2.291 | 2.198 | 3.063 |
| Basal area ($m^2$/ha) | 0.58 | 2.01 | 2.75 | 3.91 | 9.92 |
| DBH (cm) *** | 23.2 (0.7) D | 27.0 (0.7) D | 30.8 (0.9) C | 40.3 (1.4) B | 60.8 (3.0) A |
| Biomass ± S.E. (Kg/ha) [b] | 5.92 (1.98) | 20.88 (5.34) | 29.8 (7.2) | 46.03 (9.45) | 138.9 (38.53) |
| **Crown structure** | | | | | |
| Branch height (m) *** | 7.8 (0.4) C | 8.2 (0.3) C | 8.0 (0.3) C | 10.8 (0.4) B | 12.7 (0.4) A |
| Total tree height (m) *** | 16.8 (0.6) C | 17.8 (0.4) C | 18.0 (0.5) C | 23.0 (0.6) B | 29.7 (0.8) A |
| Crown length (m) *** | 8.2 (0.4) C | 8.6 (0.3) C | 9.7 (0.4) C | 11.3 (0.4) B | 16.8 (0.9) A |
| Crown width (m) *** | 5.5 (0.3) C | 5.8 (0.2) C | 6.5 (0.3) C | 7.6 (0.3) B | 12.7 (0.9) A |
| Crown area ($m^2$) *** | 38.9 (3.8) C | 44.1 (3.5) C | 57.9 (5.7) C | 75.4 (5.4) B | 228.0 (28.4) A |
| Crown depth (m) *** | 5.7 (0.3) C | 5.7 (0.2) C | 6.0 (0.3) C | 7.7 (0.3) B | 10.5 (0.5) A |
| Crown volume ($m^3$) *** | 160.9 (20.9) C | 188.8 (21.6) C | 310.6 (67.6) C | 437.1 (47.6) B | 2,138.5 (346.6) A |
| Max (min) length (m) | 16.3 (3.5) | 20.5 (1.5) | 28.4 (2.0) | 24.4 (4.0) | 48.5 (2.7) |
| Max (min) width (m) | 12.0 (1.0) | 19.4 (1.0) | 25.0 (1.0) | 18.6 (1.4) | 40.0 (2.0) |
| Max (min) area ($m^2$) | 146 (5.5) | 312 (1.2) | 558 (3.5) | 357 (6.3) | 1,523 (4.7) |
| **Spatial distribution** | | | | | |
| Tree separation ± SE (m) [c] | 27.32 (11.54) | 13.27 (2.99) | 10.97 (1.22) | 14.19 (3.46) | 10.59 (0.87) |
| Nadir visible crown area ± SE (%) [d] | 20.14 (12.92) | 16.54 (2.49) | 53.91 (7.59) | 60.74 (5.55) | 100 (0) |

Data given are mean (±S.E.). When applicable, results of one-way ANOVA are given testing differences for the different variables among crown exposure classes. Different letters indicate significant differences; *p*-values: *$p < 0.05$, **$p < 0.01$, ***$p < 0.001$.

[a] Shannon-Weiner diversity index.

[b] Mean and standard error of the five biomass equations described in the methods section.

[c] Mean linear distance and standard error separating tree individuals across each of the 4 study plots.

[d] Mean and standard error crown area visible from a nadir perspective for all trees in each crown exposure class.

**Table 3.4:** Allometric relationships between crown width (*W*), length (*L*), and area (*A*) and tree DBH and tree total height (*H*)

| Variable | Crown exposure class | Crown width (m) | Crown length (m) | Crown area ($m^2$) |
|---|---|---|---|---|
| **DBH (cm)** | 5 | =21.96+3.02*W(0.68)*** | =10.55+2.97*L(0.74)*** | =16.35+3.44*A^0.5(0.73)*** |
| | 4 | =24.10+0.10*W(0.58)*** | =24.06+0.10*L^2(0.58)*** | =31.43+0.009*A^1.5(0.65)*** |
| | 3 | =22.79+0.07*W(0.51)*** | =11.60+1.94*L(0.47)*** | =23.91+0.11*A(0.43)*** |
| | 2 | =4.85+0.0004*W(0.49)*** | =15.91+1.26*L(0.27)*** | =24.84+0.001*A^2(0.53)*** |
| | 1 | NS | =19.12+0.47*L(0.08)* | NS |
| | All | =17.0+0.48*W(0.68)*** | =4.13+2.92*L(0.65)*** | =7.62+3.60*A^0.5(0.66)*** |
| **Tree height (m)** | 5 | =12.53+5.06*W^0.5(0.46)*** | =18.56+0.66*L(0.50)*** | =19.94+0.75*A^0.5(0.48)*** |
| | 4 | =15.98*0.97*W(0.23)*** | =14.38+0.77*L(0.27)*** | =14.57+1.07*A^0.5(0.27)*** |
| | 3 | =12.22+0.97*W(0.29)*** | =10.94+0.76*L(0.30)*** | =11.15+1.05*A^0.5(0.32)*** |
| | 2 | =14.37+0.58*W(0.10)*** | =12.22+0.63*L(0.19)*** | =15.59+0.48*A(0.16)*** |
| | 1 | =12.12+0.95*W(0.22)*** | NS | NS |
| | All | =14.05+0.96*W(0.41)*** | =11.57+0.89*L(0.46)*** | =12.61+1.09*A(0.45)*** |

For sample sizes in each crown exposure class refer to Table 3. $r^2$ values are provided in parenthesis and p-values are coded as follows: *p < 0.05, ***p < 0.001; NS = non-significant and are provided following each equation.

**Table 3.5:** Sorensen's index of species composition similarity between crown position classes

| | **Crown exposure class** | | | |
|---|---|---|---|---|
| | **1** | **2** | **3** | **4** |
| **2** | 0.45 | 1 | | |
| **3** | 0.44 | 0.57 | 1 | |
| **4** | 0.25 | 0.62 | 0.53 | 1 |
| **5** | 0.2 | 0.43 | 0.45 | 0.59 |

**Table 3.6:** Remote sensing (RS) and field delineated crown area ($m^2$), tree diameter (cm) and individual tree biomass (Mg) statistics

| | **Min.** | **Max.** | **Mean** | **Std. Dev.** |
|---|---|---|---|---|
| RS polygon crown area | 1.13 | 333 | 75.1 | 78.9 |
| RS circle crown area | 1.13 | 1052 | 234.3 | 240.9 |
| Field crown area | 0 [a] | 1524 | 90.8 | 157.4 |
| | | | | |
| RS polygon DBH | 11.5 | 73.3 | 33.8 | 17.2 |
| RS circle DBH | 11.5 | 124.4 | 53.6 | 30.6 |
| Field DBH | 11.0 | 200.0 | 37.0 | 21.1 |
| | | | | |
| RS polygon biomass | 0.06 | 6.86 | 1.00 | 1.47 |
| RS circle biomass | 0.06 | 21.52 | 3.02 | 4.52 |
| Field biomass | 0.08 | 62.55 | 1.95 | 0.08 |

[a] No crown area present due to damage.

**Table 3.7:** Kolmogorov–Smirnov comparison D values between remote sensing (circle and polygon approaches) and field measurement distributions across the four 1-ha study plots

| | **RS Circle vs. RS Polygon** | **RS Circle vs. Field** | **RS Polygon vs. Field** |
|---|---|---|---|
| Crown area ($m^2$) | 0.5366 *** | 0.3659 ** | 0.3902 ** |
| DBH (cm) | 0.3571 ns | 0.3571 ns | 0.4286 ns |
| Remotely visible biomass (Mg) | 0.3889 ** | 0.2500 ns | 0.3333 * |
| Corrected biomass (Mg) | 0.611 *** | 0.5278 *** | 0.1667 ns |

*$p < 0.05$; **$p < 0.01$; ***$p < 0.001$.

## 3.10 Figures

**Figure 3.1:** Cumulative percentage of total woody stems ≥20 cm in diameter (DBH) within individual crown exposure classes along a DBH gradient. Crown exposure classes 1–5 are completely shaded to fully exposed tree crowns.

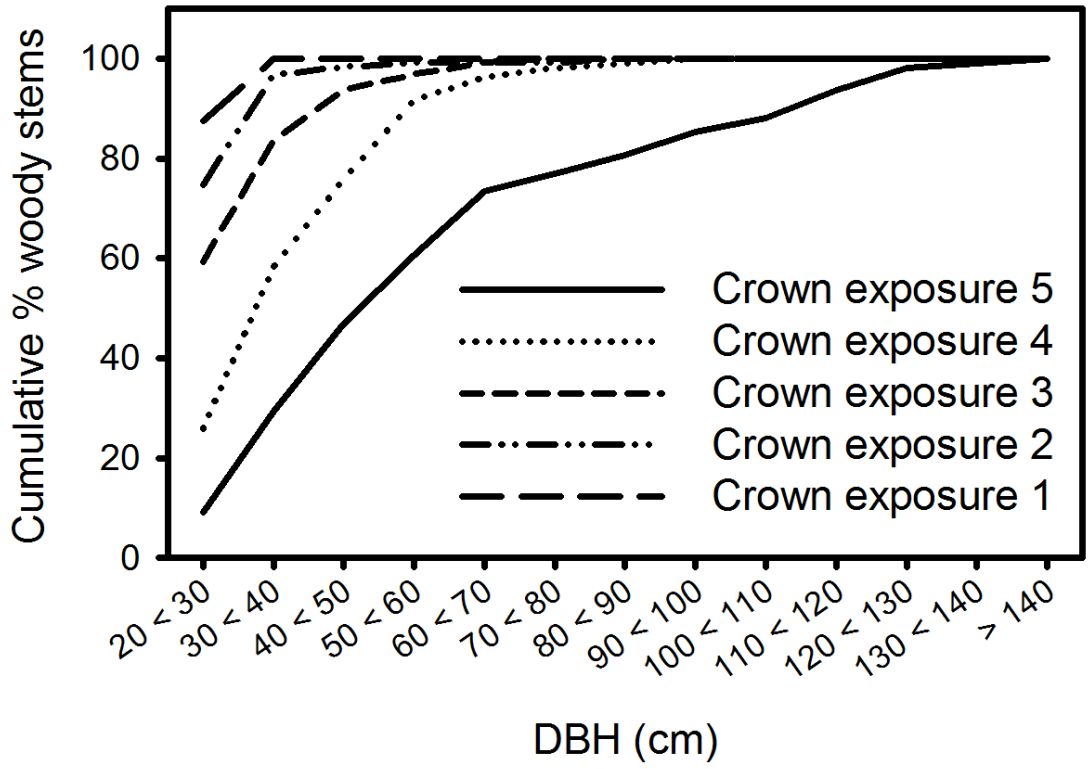

**Figure 3.2:** Tree stem density by crown exposure class and for all exposure classes combined. Areas having no individuals are represented as a density of zero. Error bars represent standard deviation of the mean among the four one ha study plots. The asterisk represents significant differences among crown positions ($P < 0.05$).

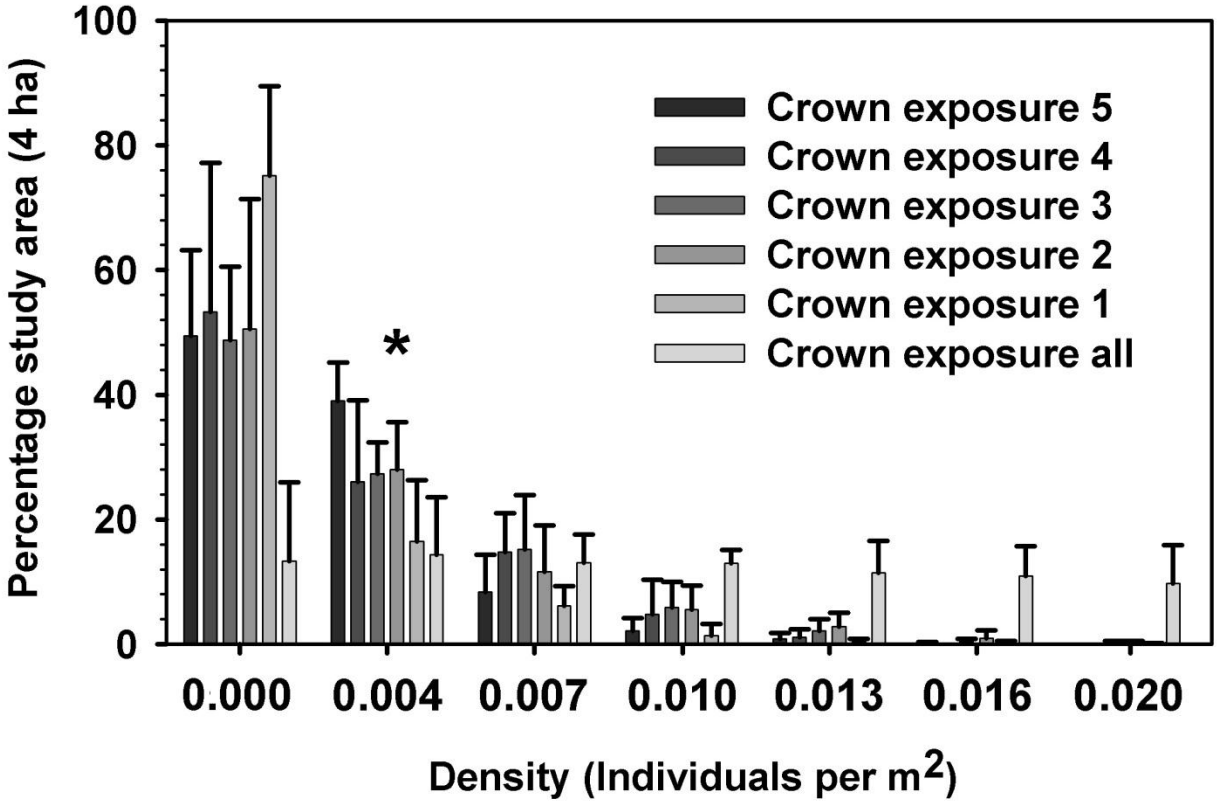

**Figure 3.3:** Field geolocated tree crowns (DBH ≥20 cm) in crown exposure classes 1 (shaded understory) through 5 (emergent) for the four study plots. Crown delineations are overlaid on the panchromatic Quickbird satellite image. Areas within each plot but outside delineated tree crowns represent crowns of trees not meeting our DBH ≥20 cm threshold.

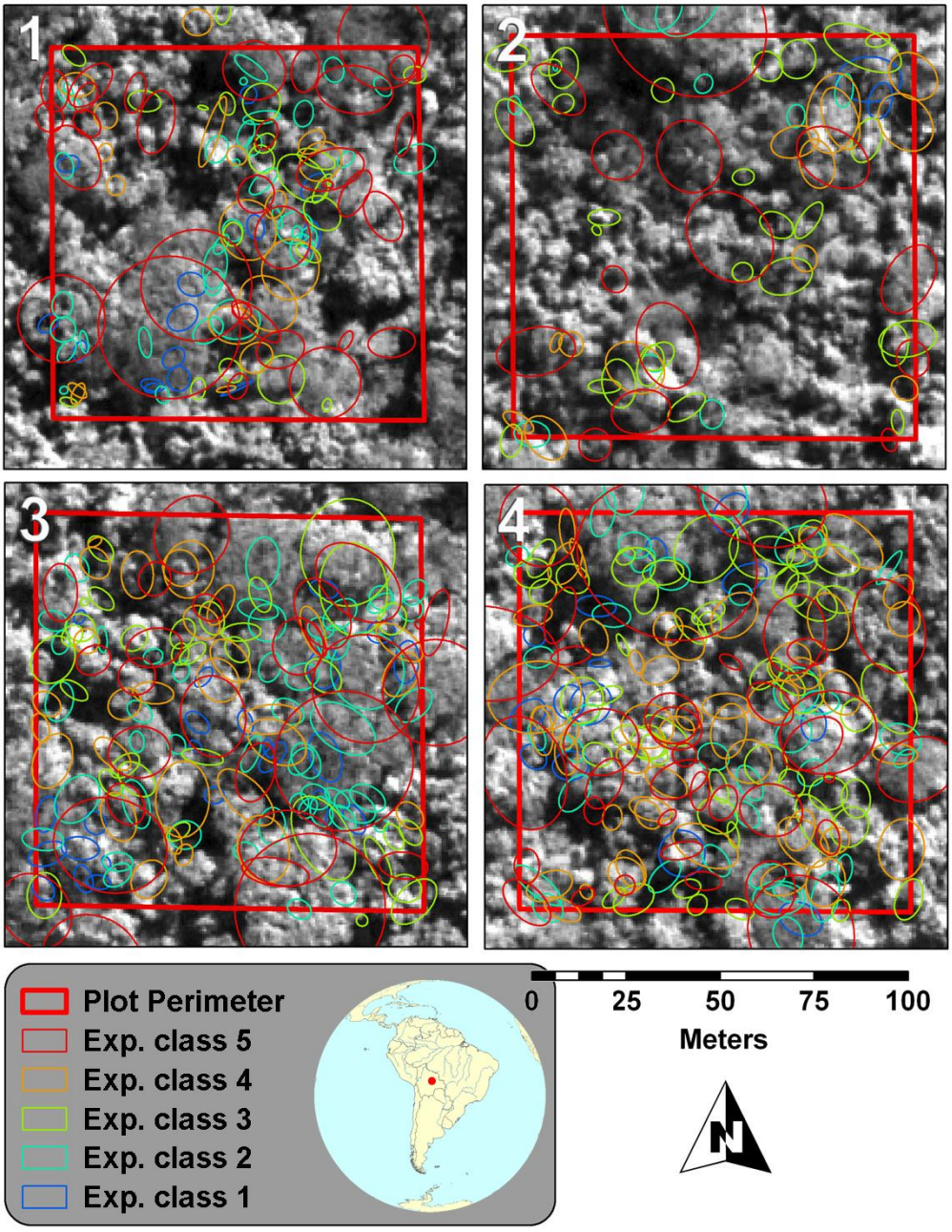


.

**Figure 3.4:** Mean number of stems covered by trees belonging to crown exposure class 5, 4 and 3. Error bars represent standard errors of the mean.

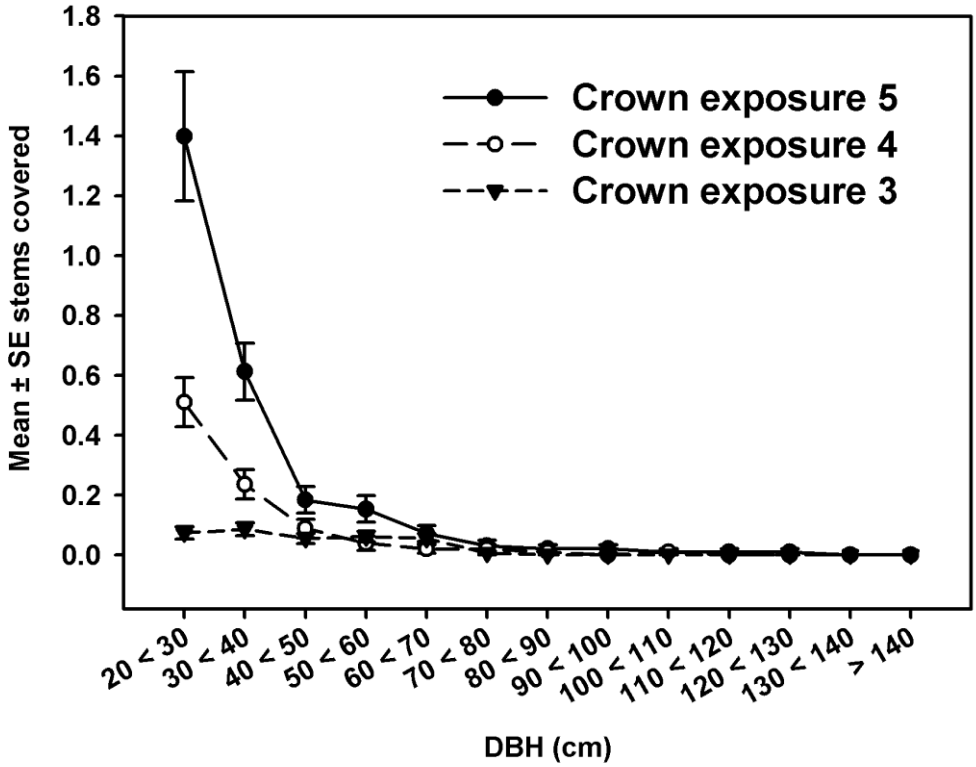

**Figure 3.5:** Correction factors for obscured understory trees for: tree abundance (A and B), basal area (C and D) and biomass (E and F) for trees with DBH ≥20 cm using crown length and crown area. Equations are provided in Supplementary Materials 3C. STD represents the standard deviation of the six biomass equations used in the analysis and is provided to indicate the potential error in the biomass estimation.

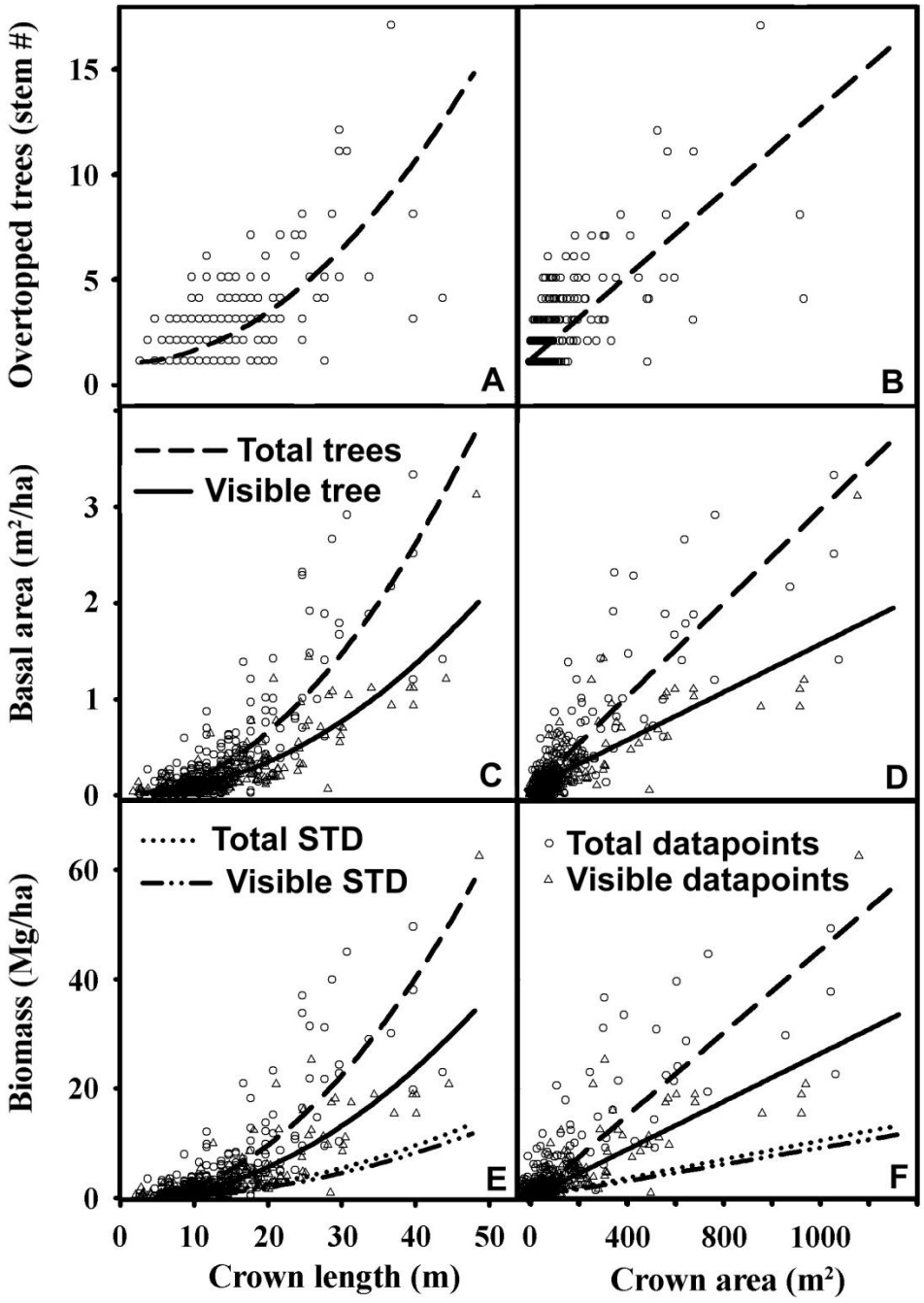

**Figure 3.6:** Automated circle and polygon crown delineations in study plots 1–4 (top left corner) overlaid on the panchromatic Quickbird satellite image.

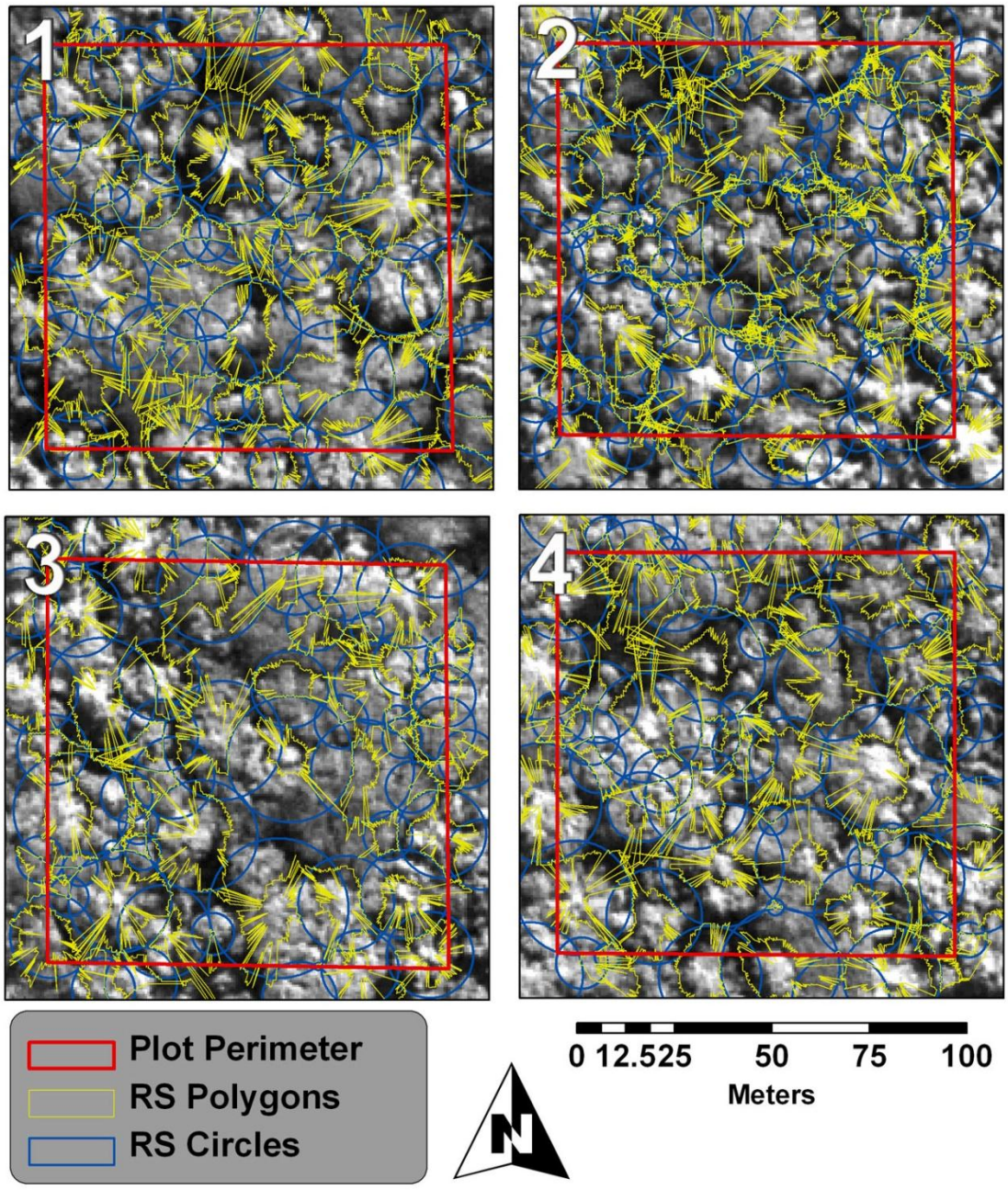

**Figure 3.7:** Abundance of trees by 10 cm DBH classes (a) and biomass (Mg) (b). The x-axis labels represent the lower limit of the size class. Biomass derived using remote sensing circle and polygon approaches is calculated using the corrected biomass equation incorporating obscured tree stems provided in Supplementary Materials 3C.

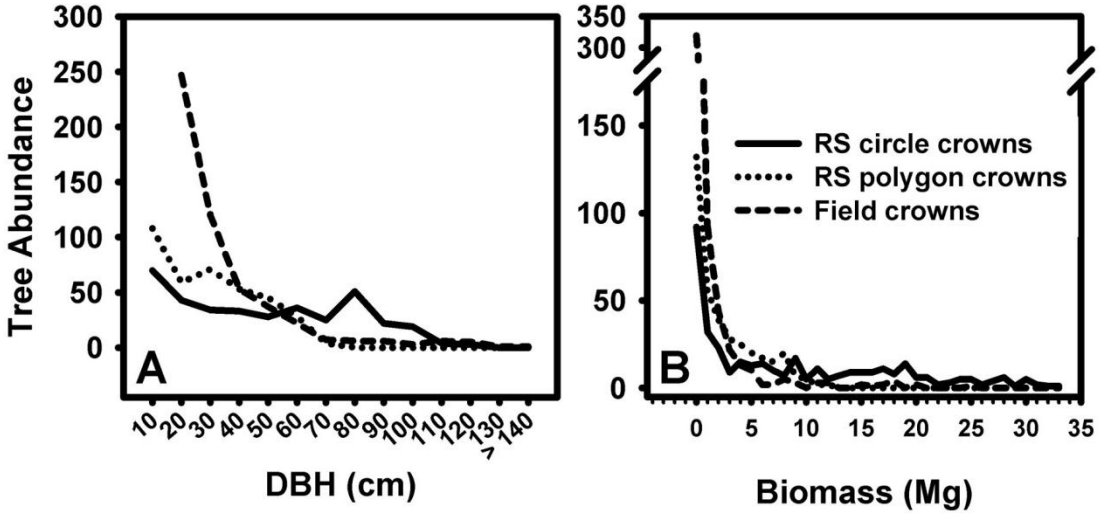

## 3.11 Supplementary Materials

**SM 3.1:** Above ground biomass equations found in the literature (kg). $\rho$ = wood density ($g/cm^3$), DBH = Bole diameter at breast height (1.3 m; cm), H = Total tree height (m).

| ID | Equation | References |
|---|---|---|
| A | $M=42.69+(-12.8)*DBH+1.242*DBH^2$ | Brown (1997) |
| B | $M=\exp[-2.134+2.53*\ln(DBH)]$ | Brown (1997) |
| C | $M=0.6*(4.06*DBH^{1.76})$ | Araujo et al. (1999) |
| D | $M=1000*0.6*\exp[3.323+2.546*\ln(DBH/1000)]$ | Carvalho et al. (1998) |
| E | $M=0.112*(\rho*DBH^2*H)^{0.916}$ | Chave et al. (2005) |
| F | $M=0.0509*(\rho*DBH^2*H)$ | Chave et al. (2005) |

**SM 3.2:** Bivariate power regressions between all forest structural variables. R values are presented in parentheses and P value significance is provided as:* = $p < 0.05$, ** = $p < 0.01$, *** = $p < 0.001$, NS = non-significant, following each equation.

| | Variable | Crown Position | Tree Total (TT) | Depth (m) (D) | Length (m) (L) | Width (m) (W) | Area ($m^2$) (A) | Volume ($m^3$) (V) |
|---|---|---|---|---|---|---|---|---|
| Height (m) | DBH (cm) | 5 | =29.2+0.001*TT$^3$(0.58)*** | =29.27+0.81*D^1.5(0.37)*** | =10.55+2.97*L(0.74)*** | =21.96+3.02*W(0.68)*** | =16.35+3.44*A^0.5(0.73)*** | =26.12+0.95*V0.5(0.71)*** |
| | | 4 | =28.21+0.001*TT$^3$(0.35)*** | =33.85+0.006*D^3(0.30)*** | =24.06+0.10*L^2(0.58)*** | =25.59+0.198*W(0.59)*** | =31.43+0.009*A^1.5(0.65)*** | =31.78+0.015*V(0.61)*** |
| | | 3 | =12.38+0.97*TT(0.23)*** | =20.5+1.58*D(0.17)*** | =11.60+1.94*L(0.47)*** | =16.22+2.23*W(0.35)*** | =23.91+0.11*A(0.43)*** | =19.89+0.74*V^0.5(0.41)*** |
| | | 2 | =21.00+0.001*TT$^3$(0.41)*** | =23.74+0.08*D^2(0.15)*** | =15.91+1.26*L(0.27)*** | =23.57+0.03*W^2.5(0.44)*** | =24.84+0.001*A^2(0.53)*** | =24.52+0.001*V^1.5(0.56)*** |
| | | 1 | =15.17+0.46*TT(0.19)*** | =21.51+0.02*D^2.5(0.13)** | =19.12+0.47*L(0.08)* | ns | ns | =22.29+0.0004*V^1.5(0.10)** |
| | | All | =23.42+0.001*TT$^3$(0.56)*** | =29.76+0.008*D^3(0.35)*** | =4.13+2.92*L(0.65)*** | =11.55+3.29*W(0.62)*** | =7.62+3.60*A^0.5(0.66)*** | =17.67+0.94*V^0.51(0.67)*** |
| | First Branch (FB) | 5 | =-4.70+3.21*TT$^{0.5}$(0.33)*** | =10.15+0.19*D(0.05)* | ns | ns | ns | ns |
| | | 4 | =-3.57+2.96*TT$^{0.5}$(0.28)*** | =9.94+0.008*D^2(0.03)*** | ns | ns | ns | ns |
| | | 3 | =-21.54+14.75*TT$^{0.24}$(0.41)*** | =6.15+0.32*D(0.08)** | ns | ns | ns | ns |
| | | 2 | =-19.70+12.18*TT$^{0.29}$(0.39)*** | ns | ns | ns | ns | ns |
| | | 1 | =-6.08+3.41*TT$^{0.5}$(0.39)*** | ns | ns | ns | ns | ns |
| | | All | =-6.17+3.44*TT$^{0.5}$(0.45)*** | =6.87+0.36*D(0.12)*** | =7.66+0.17*L(0.06)*** | =8.8+0.67*W(0.01)* | =7.89+0.20*A^0.5(0.05)*** | =9.14+5.2e-04*V(0.05)*** |
| | Canopy Base (CB) | 5 | =-10.26+5.20*TT$^{0.5}$(0.69)*** | =8.89+2.37*D^0.5(0.14)*** | =12.78+0.30*L(0.28)*** | =14.07+0.29*W(0.23)*** | =13.43+0.33*A^0.5(0.26)*** | =4.47+5.51*V0.13(0.28)*** |
| | | 4 | =-7.03+4.43*TT$^{0.5}$(0.59)*** | =12.14+0.25*D(0.06)* | =10.71+0.30*L(0.11)*** | =11.46+0.35*W(0.09)*** | =10.88+0.40*A^0.5(0.11)*** | =11.0+0.42*V0.35(0.10)*** |
| | | 3 | =-7.50+4.50*TT$^{0.5}$(0.70)*** | =8.86+0.44*D(0.15)*** | =8.28+0.28*L(0.15)*** | =8.9+0.41*W(0.14)*** | =10.46+0.02*A(0.14)*** | =9.42+0.15*V0.5(0.19)*** |
| | | 2 | =-9.95+5.08*TT$^{0.5}$(0.63)*** | ns | =9.01+0.26*L(0.06)** | ns | =11.06+6.54e-06*A^2(0.08)*** | =11.15+1.59e-09*V3(0.07)** |
| | | 1 | =0.70+0.57*TT(0.67)*** | ns | ns | ns | ns | ns |
| | | All | =-9.35+4.94*TT$^{0.5}$(0.74)*** | =9.27+0.53*D(0.20)*** | =8.54+0.42*L(0.29)*** | =9.75+0.45*W(0.25)*** | =9.04+0.51*A0.5(0.27)*** | =8.24+0.78*V0.32(0.29)*** |
| | Tree Total (TT) | 5 | | =-1.67+9.8*D^0.5(0.69)*** | =18.56+0.66*L(0.50)*** | =12.53+5.06*W^0.5(0.46)*** | =19.94+0.75*A^0.5(0.48)*** | =1.14+10.01*V^0.15(0.64)*** |
| | | 4 | | =12.12+1.37*D(0.67)*** | =14.38+0.77*L(0.27)*** | =15.98+0.97*W(0.23)*** | =14.57+1.07*A^0.5(0.27)*** | =11.34+1.61*V^0.34(0.52)*** |
| | | 3 | | =8.86+1.57*D(0.69)*** | =10.94+0.76*L(0.30)*** | =12.13+0.99*W(0.29)*** | =11.15+1.05*A^0.5(0.32)*** | =12.58+0.41*V^0.5(0.52)*** |
| | | 2 | | =10.75+1.22*D(0.44)*** | =12.22+0.63*L(0.19)*** | =14.37+0.59*W(0.10)*** | =15.59+0.48*A(0.16)*** | =12.53+0.42*V^0.5(0.35)*** |
| | | 1 | | =8,93+1.39*D(0.53)*** | ns | ns | ns | =12.14+0.42*V^0.5(0.26)*** |
| | | All | | =9.26+1.65*D(0.71)*** | =11.57+0.89*L(0.46)*** | =14.07+0.97*W(0.41)*** | =12.61+1.09*A(0.45)*** | =5.96+3.55*V^0.26(0.63)*** |
| Crown | Depth (D) | 5 | | | =5.15+0.33*L(0.41)*** | =6.47+0.32*W(0.37)*** | =5.80+0.37*A^0.5(0.40)*** | =2.31*V^0.22(0.63)*** |
| | | 4 | | | =3.28+0.43*L(0.23)*** | =4.03+0.55*W(0.20)*** | =6.13+0.026*A(0.23)*** | =-3.39+3.09*V^0.23(0.65)*** |
| | | 3 | | | =2.14+0.40*L(0.29)*** | =2.78+0.52*W(0.28)*** | =2.23+0.56*A^0.5(0.31)*** | =2.78+0.23*V^0.5(0.58)*** |
| | | 2 | | | =2.86+0.33*L(0.17)*** | =3.70+0.25*W(0.13)*** | =3.03+0.43*A^0.5(0.17)*** | =2.27+0.28*V^0.5(0.52)*** |
| | | 1 | | | =3.82+0.24*L(0.08)* | =3.65+0.41*W(0.14)*** | =2.8+0.51*A^0.5(0.20)*** | =1.99+0.32*V^0.5(0.55)*** |
| | | All | | | =2.71+0.42*L(0.39)*** | =3.85+0.46*W(0.35)*** | =3.14+0.52*A^0.5(0.39)*** | =1.56*V^0.28(0.68)*** |
| | Length (L) | 5 | | | | =4.02+0.999*W(0.89)*** | =0.31+1.19*A^0.5(0.94)*** | =5.56+0.307*V^0.5(0.91)*** |
| | | 4 | | | | =2.83+1.127*W(0.71)*** | =0.91+1.28*A^0.5(0.90)*** | =1.86*V^0.31(0.71)*** |
| | | 3 | | | | =2.79+1.088*W(0.68)*** | =1.14+1.25*A^0.5(0.86)*** | =4.55+0.36*V^0.5(0.78)*** |
| | | 2 | | | | =3.07+0.978*W(0.63)*** | =1.02+1.23*A^0.5(0.86)*** | =3.57+0.42*V^0.5(0.74)*** |
| | | 1 | | | | =3.29+0.949*W(0.51)*** | =1.04+1.25*A^0.5(0.80)*** | =3.51+0.42*V^0.5(0.65)*** |
| | | All | | | | =3.08+1.05*W(0.83)*** | =1.41+1.20*A^0.5(0.94)*** | =1.74*V^0.32(0.88)*** |
| | Width (W) | 5 | | | | | = -1.37+1.10*A^0.5(0.98)*** | =2.08+0.29*V^0.5(0.91)*** |
| | | 4 | | | | | = -0.42+0.98*A^0.5(0.94)*** | =1.04*V^0.34(0.73)*** |
| | | 3 | | | | | = -0.46+0.99*A^0.5(0.93)*** | =2.34+0.28*V^0.5(0.82)*** |
| | | 2 | | | | | = -0.62+1.03*A^0.5(0.92)*** | =1.67+0.34*V^0.5(0.73)*** |
| | | 1 | | | | | = -1.04+1.26*A^0.5(0.71)*** | =1.46+0.34*V^0.5(0.74)*** |
| | | All | | | | | =-0.9+1.06*A^0.5(0.97)*** | =0.78*V^0.4(0.88)*** |
| | Area (A) | 5 | | | | | | =8.37+0.60*V^0.79(0.94)*** |
| | | 4 | | | | | | =8.22+1.01*V^0.70(0.88)*** |
| | | 3 | | | | | | =1.42*V^0.68(0.93)*** |
| | | 2 | | | | | | =1.19*V^0.71(0.82)*** |
| | | 1 | | | | | | =1.26*V^0.69(0.81)*** |
| | | All | | | | | | =0.81*V^0.75(0.93)*** |

is greater than 128, 149, 178, 152, 63 (670 total) for crown positions 5-1 and all, respectively.

**SM 3.3:** Correction equations for converting nadir top-of-canopy estimations based on the single visible tree crown (RS) to corrected forest biomass incorporating obscured tree stems ≥ 20 cm DBH (FB). *P*-values are provided following each equation and $R^2$ values are provided in parentheses. * = $P < 0.05$, ** = $P < 0.01$, *** = $P < 0.001$. NS = non-significant. $N \geq 314$.

| **Variables** | **Crown Length (m)** | **Crown Area ($m^2$)** |
|---|---|---|
| Obscured trees (stem #) | FB = 1.02+0.006*L^2 (0.56)*** | FB = 1.17+0.01*A (0.62)*** |
| Basal area ($m^2$/ha) | FB = 40.21+16.3*L^2 (0.66)*** | FB = 486.67+24.31*A (0.69)*** |
| | RS = 161.6+8.65*L^2 (0.74)*** | RS = 449.4+12.47*A (0.72)*** |
| Biomass (Mg/ha) | FB = -562.09+25.49*L^2 (0.62)*** | FB = 148.37+37.92*A (0.65)*** |
| | RS = -420.27+14.17*L^2 (0.70)*** | RS = 55.63+20.4*A (0.67)*** |

# CHAPTER 4

# PREDICTING LEAF TRAIT VARIATION IN A HAWAIIAN RAINFOREST UNDERSTORY: A MICROCLIMATE MODELING APPROACH BASED ON FUSION OF AIRBORNE LIDAR AND HYPERSPECTRAL IMAGERY

## 4.1 Abstract

We develop and validate a high-resolution three-dimensional model of forest interior light and air temperature for a tropical forest in Hawaii along an elevation gradient varying greatly in forest structure but not species composition. Our microclimate models integrate high-resolution airborne waveform light detection and ranging data (LiDAR) and hyperspectral imagery with detailed microclimate measurements. We then integrate modeled microclimate with spatially explicit measurements of leaf traits, including gas exchange and structure. Our results highlight the importance of: (a) species differences in leaf traits, with species explaining up to 65% of the variation in some leaf traits; (b) differences between exotic and native species, with exotic species having greater maximum rates of assimilation and foliar $\delta^{15}N$ values; (c) structural factors, with foliar %N and light saturation of photosynthesis decreasing in mid-canopy locations; (d) microclimate factors, with foliar %N and light saturation increasing with growth environment illumination; and (e) decreases in mean annual temperature with elevation resulting in closure of the nitrogen cycle, as indicated through decreases in foliar $\delta^{15}N$ values. The dominant overstory species (*Metrosideros polymorpha*) did not show plasticity in photosynthetic capacity, whereas the dominant understory species (*Cibotium glaucum*) had higher maximum rates of assimilation in more illuminated growth environments. The approach developed in this study is among the highest resolution three-dimensional models of forest microclimate and ecophysiology we identified in the literature. The feasibility of this study highlights the potential of new airborne sensors to quantify forest productivity at spatial and temporal scales not previously possible.

Results provide insights into the function of a native species dominated Hawaiian forest undergoing simultaneous biological invasion and climatic change.

*Key words: canopy structure, climate change, direct and diffuse light, induction rate, photosynthetic active radiation (PAR), sun fleck, tropical forest*

## 4.2 Introduction

Tropical forests cover 11.7% of the land surface area (Potter et al. 1993), contain 57% of above- and 27% of belowground carbon (Dixon et al. 1994), and are important contributors to the global carbon cycle (Cramer et al. 2004; Field et al. 1998). Carbon fluxes and overall productivity within these forests are highly dependent on light and temperature regimes (Boisvenue and Running 2006), which are projected to change in the future (Hulme and Viner 1998, Hansen et al. 2010, Mercado et al. 2009). Light within a forest understory is considered to be the most important (Mercado et al. 2009), and limiting (Stadt et al. 2005), environmental factor influencing photosynthesis and carbon gain (Araujo et al. 2008; Ellsworth and Reich 1992; Kull 2002). Overall, light penetration to a tropical forest understory is among the lowest of terrestrial ecosystems, and that light which does exist is highly variable temporally, due to time of day, season or climatic conditions, and is highly dependent on the structure and density of both the forest under- and overstory (Chazdon and Pearcy 1991; Montgomery 2004). However, in spite of light limitation the understory can make substantial contributions to overall forest productivity. For example, Sampson et al. (2006) calculated understory plants contributed up to 28% of a deciduous forest's gross primary productivity due to understory penetration by diffuse radiation.

Variation in microclimate often results in predictable changes in leaf traits (Poorter et al. 2006). The established paradigm is that photosynthesis is N limited (Evans 1989), and numerous studies have shown the significant positive relationship

between leaf N content and maximum photosynthesis capacity ($A_{max}$) (Chazdon and Field 1987; Evans and Poorter 2001; Evans 1989), in spite of species differences (Walters and Field 1987). Given this, forest canopies should optimize both the distribution of their leaves for high light capture efficiency and leaf photosynthetic rates according to their irradiance growth environment (Field 1983; Laisk et al. 2005; Meir et al. 2002). Canopy optimization of N distribution and photosynthetic capacity to light availability has been shown within a variety of crop and forest stands (Dang et al. 1997; Ellsworth and Reich 1993; Hirose et al. 1989; Hollinger 1989).

It remains unclear, however, how foliar acclimation and development adjusts to differing types, and variability, of irradiance (Meir et al. 2002; Bai et al. 2008), and especially when considering communities of diverse species, although the importance of such differences has been demonstrated (Chazdon and Field 1987). Understanding drivers of leaf trait variation in different species, or functional groups (Poorter et al. 2006), is especially relevant in highly taxonomically and architecturally diverse, but highly light limited, tropical forest understory environments. A number of factors diminish the strength of relationships between light availability and investment in photosynthetic capacity, including light saturation, partitioning of nitrogen for non-photosynthesis activities, leaf aging, and position (Field 1983), or variation in temperature, wind speed, precipitation and nutrient availability, as well as species differences (Dang et al. 1997).

Ecosystem processes, including overall productivity (Baldocchi and Harley 1995), within tropical forests occur within a complex three-dimensional architecture (Koetz et al. 2007). Interactions between architecture and microclimate require further study (Gastellu-Etchegorry and Trichon 1998). Failure to include spatial data on forest architecture, for example, can result in large errors from simple big-leaf models (Baldocchi and Harley 1995, Knohl and Baldocchi 2008). Attempts to estimate daily light regimes using traditional methods, such as hemispherical photographs, have resulted in inaccurate values, up to 107% greater than those shown from understory photosynthetic active radiation (PAR) sensors (Johnson and Smith 2006). Light regime modeling approaches explicitly integrating manually collected leaf area

distributions showed greatly improved results (Aubin et al. 2000; Gersonde et al. 2004).

High-resolution light detection and ranging (LiDAR) sensors allow incorporation of spatially explicit information into microclimate models at scales infeasible through field data collection. Airborne LiDAR has recently been used to accurately estimate forest height (Hudak et al. 2002; Sexton et al. 2009), biomass (Asner et al. 2008a; Boudreau et al. 2008), and architecture (Omasa et al. 2007), including gap dynamics (Kellner and Asner 2009; Koukoulas and Blackburn 2004). The capacity to quantify forest structure over large areas at high resolutions has led to insights into ecosystem function (Asner, et al. 2008a,b), including patterns of canopy height heterogeneity not visible at smaller scales (Vitousek et al. 2009). Discrete LiDAR – in which a small number of individual laser pulses are used (Lim et al. 2003), has more recently, been combined with hyperspectral imagery and used to generate maps of leaf chlorophyll (Thomas et al. 2006), providing insights into flux tower measurements of gross ecosystem productivity (Thomas et al. 2009). Koetz et al. (2006) used physically based radiative transfer models to invert large footprint wLiDAR accurately estimating forest biophysical parameters, including leaf area index (LAI), tree height, and general interior forest architecture.

Waveform LiDAR (wLiDAR) represents an advance over discrete LiDAR sensors as it records a higher point cloud per area, allowing more accurate estimations of forest understory architecture (Asner et al. 2007). This could lead to a better understanding of forest productivity if data approximates the fine scales at which canopy microclimate and ecophysiology are determined. Parker et al. (2001) used wLiDAR, one of the first attempts integrating this technology, to estimate nadir light transmittance statistics for two forest stands; however, a horizontal resolution of 10 m made detailed forest interior studies infeasible.

In this research, we develop a new approach to map forest leaf area (2D) and leaf density (3D) at very high spatial scales. Using these maps, we develop and validate a three-dimensional model of direct and diffuse light transmittance and air temperature throughout a tropical rainforest in Hawaii. We then couple the

microclimate models with detailed spatially explicit measurements of plant ecophysiological characteristics across a community of native and invasive species to understand structural, taxonomic, and climatic determinants of ecophysiological properties. The selected study forest, a model ecosystem having a near mono-dominant canopy species and both invasive and native species coupled with an extraordinary elevation gradient along the slope of Mauna Kea volcano, enables addressing questions related to relationships among forest structure, climate and ecophysiology not feasible in other systems. The specific research objectives of this study are to: (i) develop and validate a high resolution three-dimensional model of forest microclimate using a coupled airborne LiDAR – hyperspectral sensor; and then to (ii) integrate remote sensing information and modeled microclimate data to better understand the taxonomic, structural and microclimatic determinants of foliar ecophysiology in our study area.

This study represents a development and validation step towards a rapid large-scale remote sensing based approach to model detailed forest productivity. Johnson and Smith (2006) have highlighted the need for such data. In addition, Alton et al. (2007) state that understanding how climate change will interact with plant photosynthesis a key issue requiring further study. An approach built off an airborne system allows for rapid and economic collection of detailed forest structural measurements, and thereby models of microclimate and foliar ecophysiology, over a wide variety of forest types. Such efforts will enable a more unified understanding of climate change effects on the three-dimensional dynamics of forest photosynthesis and physiology at larger scales. For example, such information would be appropriate for integration with flux towers, which are providing significant insight into forest productivity dynamics (Schwalm et al. 2010).

## 4.3 Materials and methods

### 4.3.1 Study design

Figure 4.1 presents the overall study design and we describe in detail each individual component of the flowchart below. We combined airborne remote sensing data with detailed spatially explicit measurements of forest microclimate and ecophysiology. We then developed detailed spatio-temporal models of microclimate and used these models to understand variation in foliar ecophysiology. We parameterized and validated remote sensing and modeling components using extensive field data.

### 4.3.2 Study site

This study took place in a portion of the 5,016 ha State of Hawaii Hilo Forest Reserve and Laupahoehoe Natural Area Reserve, designated as a Hawaii Experimental Tropical Forest (HETF) of the US Forest Service (USFS), located on the North Hilo coast of the island of Hawai'i, Hawai'i. This reserve is also the location of a newly established Hawaii Permanent Plot Network (HIPPNET) and Center for Tropical Forest Science (CTFS) research plot (www.ctfs.si.edu). The reserve encompasses an elevation gradient from 600–1800 m elevation, with overall gradients in temperature and precipitation of 13-18°C and 2000-3500 mm, respectively (Giambelluca et al. 2011). A 2.5 km long by 800 m wide study transect was established in the northern central portion of the reserve extending from 1005 to 1343 m elevation (Fig. 4.2), corresponding to a mean annual temperature of 16.2 to 17.5 °C, respectively, comparable to the projected increases in global temperature over the next century (Nozawa et al. 2001). While three distinct substrate ages exist within the reserve: 4-14, 14-25 and 25-65 ty (ty = 1000 yrs.), resulting from previous lava flows, the study transect was located entirely on youngest flow (4-14 ty). The transect consisted of two soil types, the lower half resting on the Akaka soil (rAK) and the upper half on Honokaa silty clay loam (HTD) – both considered well drained with moderate available water capacity (websoilsurvey.nrcs.usda.gov/ accessed [06/02/2011]). The

study transect was situated to keep the native Hawaiian tree *Metrosideros polymorpha v. glaberrima* (Myrtaceae) constant as the dominant – to the near exclusion of all others - canopy species. Above ground biomass (AGB) across the study transect ranged from approximately 500 Mg $ha^{-1}$ at 1000 m to 250 Mg $ha^{-1}$ at 1300 m (Asner et al. 2008a), simultaneous to a reduction in average canopy height from 24 to 14 m (Fig. 4.3).

The lower portion of the transect begins above a biological invasion front ending around 900 m dominated by *Psidium cattleianum* (Myrtaceae) and *Ficus rubiginosa* (Moraceae) and ends below an area of natural *M. polymorpha* dieback (Mueller-Dombois 1987). Understory plant composition is dominated by tree ferns (*Cibotium* sp.), and the small trees *Cheirodendron trigynum ssp. Trigynum* (Araliaceae), *Ilex anomala* (Aquifoliaceae), *Myrsine lessertiana* (Myrsinaceae) and *Coprosma rhynchocarpa* (Rubiaceae). The primary animal source of disturbance – constant throughout the study transect - consists of non-native feral pigs (*Sus scrofa*) which root the forest floor and propagate invasive species (Stone et al. 1992).

### 4.3.3 Study plots

Study plots were established at low (~1000 m) and high (~1300 m) elevations and positioned to encompass the range of forest structure found in the study transect. Six plots were located between 1000-1050 m and five between 1250-1300 m elevations. We established a two meter by 30 meter transect within each study plot ($N = 8$). Data were collected for each stem greater than 0.5 m in height and included elevation (1000 or 1300 m), species, native vs. non-native status, height (m), and diameter (cm; at breast height when applicable). Volume ($cm^3$) was calculated as basal area ($cm^2$) multiplied by height (cm). Density (D = no. of individuals/1000 $m^2$), dominance (Do = $\sum$ volume of all individuals/1000 $m^2$) and frequency (F = # of transects containing the species) were calculated for each species. An importance value (IV) was calculated for each species using relative percent values (R; versus median of all species) as:

$$IV = [RD * 100] + [RDo * 100] + [RF * 100]$$

modified from (Busby et al. 2010; Curtis and McIntosh 1951). Georeferenced marker stakes were established within each study plot using a differentially corrected geographic positioning system (GPS) unit (GS-50+, Leica Geosystems AG, St. Gallen, Switzerland) incorporating multiple-bounce filtering. Following 6 to 8 hours of 5 second interval GPS data collection per marker ($N$ = 10) final post-differential correction horizontal (XY) and vertical (Z) uncertainty (cm±std. dev.) were 19±13 and 33±24 cm, respectively.

### 4.3.4 Georeferencing

All interior forest measurements were georeferenced in three dimensions (3D) for integration with remote sensing data. The georeferencing procedure consisted of mounting a laser rangefinder with integrated inclinometer and 3D compass (Trupulse 360B, Laser Technology Inc., Centennial, Colorado 80112 USA) using filter mode and reflectors to avoid erroneous pulse returns on a tripod a known height (mh; cm) directly above a study plot marker stake. Position data returned from the Trupulse included the straight-line distance (sd; m), inclination (inc; °) and azimuth (az; °) from magnetic north. Prior to offset calculations, azimuth was adjusted to degrees from true north by adding a declination of 9.75° (www.ngdc.noaa.gov/geomagmodels/struts/calcIGRFWMM). Locations of offset locations were then calculated from the marker stake as:

$$hd = sd * \cos(inc)$$
$$x\ offset = hd * \sin(az)$$
$$y\ offset = hd * \cos(az)$$
$$z\ offset = sd * \sin(inc) + mh$$

where hd = horizontal distance (m), and x, y and z offsets are in meters from the marker stake. An accuracy assessment of geolocation offsets showed single offsets

were accurate to < 30 cm 3D over a wide range of distances (11-22 m), whereas double offsets, required in only a few instances when the marker stake had an obstructed view of the measurement location, were accurate to < 64 cm 3D.

### 4.3.5 Climate measurements

Both top-of-canopy (TOC) climate and interior forest microclimate measurements were collected. TOC measurements were acquired continuously by stations at 1052 (i.e., low), 1180 (i.e., mid), and 1353 (i.e., high) m elevation - evenly spaced along the transect. TOC sensors at low and high-elevations consisted of a total quantum sensor (SQ-110, Apogee Instruments, Inc., Logan, Utah, 84321 USA), temperature and relative humidity, a sonic anemometer and precipitation (WXT-510, Vaisala Inc., Helsinki, Finland) downloaded to a datalogger (CR-200, Campbell Scientific, Inc., Logan, Utah, 84321, USA). The mid-elevation sensor array consisted of a direct/diffuse quantum sensor (BF3, Delta-T Devices Ltd., Cambridge, United Kingdom), a total quantum sensor (LI-190, LICOR Ltd, Lincoln, Nebraska 68504, USA), and temperature and relative humidity sensors (HMP45C-L20, Vaisala Inc., Helsinki, Finland) downloaded to a datalogger (CR-3000, Campbell Scientific, Inc., Logan, Utah, 84321, USA). Climate data collected every 15 seconds was averaged to a one-minute interval, with the exception of rainfall data that was the sum total each minute. Four mobile interior forest micro-climate stations were constructed, each consisting of a quantum sensor (SQ-110, Apogee Instruments, Inc., Logan, Utah, 84321 USA), a temperature and relative humidity sensor (HOBO U23-002, Onset Computer Corp., Bourne, Massachusetts, 02532 USA) and a cup anemometer (200-WS-01, Novalynx Corp., Auburn, California, 95602 USA). PAR and windspeed data were downloaded to a datalogger (CR-10x, Campbell Scientific, Inc., Logan, Utah, 84321, USA) while temperature and relative humidity data were internally logged. Microclimate data were logged every 15 seconds and averaged to one-minute intervals. In addition, PAR data were logged every three seconds for the first five minutes of each hour.

TOC PAR sensors were intercalibrated using known clear sky days to the mid-elevation quantum sensor, which was recalibrated annually, and calibration drift was removed using a clear sky PAR model coded in R and modified from equations provided by Apogee Inc. (Supplementary Materials 4E; American Society of Civil Engineers 2005). This model uses day of year, time of day, latitude, longitude, elevation, air temperature, and relative humidity as input variables and has been validated to estimate clear sky PAR within 3% at solar noon. Interior forest quantum sensors were intercalibrated weekly in an open field for two hours with data logged every 15 seconds averaged to one-minute intervals and returned for recalibration several times a year.

### 4.3.6 Leaf traits

Leaf trait measurements included light, $C0_2$ and induction gas exchange response curves, foliar mass per area, elemental C and N percentage, and $\delta^{13}C$ and $\delta^{15}N$ stable isotopes. Foliar gas exchange measurements were acquired using a LI-6400 portable infrared gas analyzer (LI-COR Ltd., Lincoln, Nebraska, 68504 USA) on the dominant species identified by the species importance values. Single and double rope tree climbing techniques were used to collect *in situ* foliar gas exchange above 2.5 m in height, while tripods were used below that height. Additional data collected at each measurement location was: (a) species, (b) time and date, (c) diameter at breast height (DBH) (d) height of measurement, and (e) total height of plant. Photographs were collected for identification by botanists at the University of Hawaii – Hilo in cases where the species was not identified in the field. Gas exchange measurements were acquired at ambient leaf temperature - between 23 and 27 °C - on mature leaves with relative humidity maintained between 65-75% and following a minimum 30-minute LI-COR 6400 stabilization period. Most measurements were conducted with the cuvette leaf area at capacity (6 $cm^2$), however when leaves smaller than six $cm^2$ were used leaf area was measured in the field and gas exchange measurements were adjusted accordingly. Each of the three response curves were collected on separate

leaves located immediately adjacent to each other and having similar characteristics. Curves were measured between the hours of 09:00 and 16:00 at a flow rate of 400 (mol air $s^{-1}$).

Light response curves were collected at a constant reference chamber $C0_2$ concentration (μmol C02 $mol^{-1}$ air) of 400 and by increasing the photosynthetic photon flux density (PPFD or Q; μmol $m^{-2}$ $s^{-1}$) – i.e., encompassing the 400 to 700nm wavebands - stepwise from zero through saturating PPFD using the following increments: 0, 20, 40, 60, 80, 100, 130, 160, 200, 250, 300, 400, 800, and 1600. Measurements at each PPFD were logged when gas exchange was stable as indicated by: (a) visually stable intracellular $C0_2$ concentration (Ci; μmol $C0_2$ mol $air^{-1}$) and net $C0_2$ assimilation rates (A; μmol $C0_2$ $m^{-2}$ $s^{-1}$) values, (b) a total coefficient of variation (CV) % - calculated as the sum of $C0_2$ and $H_20$ CV % - of less than 0.1% and (c) following a min-max wait time of 3-10 minutes, respectively. $C0_2$ response curves, C02 assimilation rates versus the intracellular C02 concentration (A-Ci), were collected at saturating PPFD + 200 (μmol $m^{-2}$ $s^{-1}$) identified by the light response curve. Following a five-minute stabilization period at a reference chamber $C0_2$ concentration (μmol C02 $mol^{-1}$ air) of 100, $C0_2$ concentration was increased stepwise through the following increments: 100, 300, 600, 900, 1200, and 1500. Measurements were logged at each increment using the same criteria as for light response curves, but with min-max time adjusted to 3-5 minutes, respectively. Induction response curves were collected following a five-minute stabilization period at a PPFD of 20. During the last 30 seconds of stabilization, measurements were logged every two seconds, following which PPFD was increased directly to 1300, and logging continued every two seconds for 3-5 minutes. Prior to analysis measurements from the light and $C0_2$ response curves were normalized for differences in leaf temperature to A at 25°C through a custom version of the SiB2 photosynthesis model (Sellers et al. 1996) coded in IDL (Interactive Data Language, ITTVIS, Inc., Boulder, CO, 2000-2010) and provided by Dr. Berry (Dept. of Global Ecology, Carnegie Institution for Science, Stanford, CA).

Normalized light (AQ) and $C0_2$ (ACi) response curves were fit through non-linear parameterization using the LI-COR Photosynthesis software (Ver 1.0, LI-COR Ltd., Lincoln, Nebraska, 68504 USA) freely available for download at: ftp://ftp.licor.com/perm/env/LI-6400/Software/analysis_software/Photosynthesis.exe [accessed 06/03/2011]. AQ curves were fit to:

$$A = \frac{\emptyset * Q}{\left[1 + \left(\frac{\emptyset * Q}{A_{max}}\right)^{p}\right]^{1/p}} + A_0$$

where A (i.e., $A_{area}$) is the net $C0_2$ assimilation (µmol $C0_2$ $m^{-2}$ $s^{-1}$) per area, $A_{max}$ is the maximum rate of A (the asymptote), ∅ is the apparent quantum efficiency (i.e., the initial slope of the fit hyperbola), p is the curve convexity parameter, $A_0$ is the dark respiration rate (µmol $C0_2$ $m^{-2}$ $s^{-1}$) and Q is the incident photosynthetic photon flux density (PPFD; µmol $m^{-2}$ $s^{-1}$). In addition, the light compensation point and light saturation estimate (µmol $m^{-2}$ $s^{-1}$) were calculated as Q value at which A = zero and the linear intersection of ∅ and $A_0$ with $A_{max}$, respectively.

ACi curves were fit to a biochemical model of photosynthesis developed by Farquhar et al. (1980) and updated to account for triose-phosphate limitation (TPU) as described in Long and Bernacchi (2003), where net $C0_2$ assimilation (A) per area, dependent solely on mesophyll processes, is determined by the minimum of three potential limiters: Rubisco activity ($V_{c,max}$; Wc), RuBP regeneration ($J_{max}$; Wj) or the regeneration and utilization of inorganic triose-phosphate ($V_{TPU}$; Wp). Limitation typically shifts from Wc to Wj to Wp with increasing Ci, calculated by:

$$W_c = \frac{Vc_{max} * C_i}{\left[C_i + K_c(1 + {}^{O}/_{K_o})\right]}$$

where $V_{c,\,max}$ is the maximum rate of carboxylation by Rubisco (µmol C02 $m^{-2}$ $s^{-1}$), Kc and Ko are the Michaelis-Menten constants of Rubisco for $C0_2$ and $0_2$, respectively and O is the stroma $0_2$ concentration (Pa).

$$W_j = \frac{J * C_i}{4.5 * C_i + 10.5 * \Gamma)}$$

where τ is the specificity factor for Rubisco, Γ = 0.5*O/τ, and J, the whole chain electron transport rate, is:

$$J = \frac{Q_2 + J_{max} - \sqrt{(Q_2 + J_{max})^2 - 4\theta_{PSII} Q_2 J_{max}}}{2\theta_{PSII}}$$

with $\theta_{PSII}$ = curvature factor, $Q_2$ = incident quanta available to PSII, and $Q_2 = Q \propto_1 \emptyset_{PSII,max} \beta$, where $\propto_1$=leaf absorptance, $\emptyset_{PSII,max}$ = max quantum yield of PSII, and β = fraction absorbed light accessible by PSII.

$$W_p = \frac{3 * TPU}{\left(1 - \frac{\Gamma}{C_i}\right)}$$

where Vo is the rate of oxygenation of Rubisco and TPU is rate of triose phosphate utilization (µmol C02 $m^{-2}$ $s^{-1}$). The determination of A at Ci (x) is:

$$A = \left(1 - \frac{\Gamma}{C_i}\right) \times \min(W_c, W_j, W_p) - R_{day}$$

where $R_{day}$ represents the $C0_2$ released through non-photorespiration processes (µmol C02 $m^{-2}$ $s^{-1}$).

Induction response data were analyzed through non-linear parameterization of a two parameter modified rectangular hyperbola model in JMP software (V. 7. SAS Institute Inc., Cary, NC, 1989-2007) developed for induction response analysis (Hunt et al. 1991; Poorter and Oberbauer 1993). The model is defined as:

$$A_t = \frac{A_{max} * k_i * t}{A_{max} + k_i * t}$$

where $A_t$ is assimilation at time t (seconds), $k_i$ is the induction curve convexity, t is seconds post-PPFD increase and $A_{max}$ is net $C0_2$ assimilation per unit area. Using the output $A_{max}$ value, the input data were then converted to induction state, redefining A as percentage of $A_{max}$ at time t (seconds) post-induction, and the equation was then reparameterized using an $A_{max}$ equal to 100% to obtain $k_{is}$ - a value comparable across leaves varying in $A_{max}$. Output results for statistical analysis were the estimated $A_{max}$, $k_i$, $k_{is}$, and time (seconds) to 50% induction state (IS 50%) calculated as:

$$t = -\frac{IS * A_{max}}{(IS - 100)K_i}$$

where t is time post induction in seconds, IS equals the induction state (%), and $A_{max}$ and $k_i$ are as defined above.

All leaves on which gas exchange measurements were conducted were collected and scanned at 600 dpi (x9575, Lexmark International, Inc., Lexington, KY 40550 USA) for leaf area calculation in Photoshop (CS, Adobe Systems Inc., San Jose, CA 95110, USA) within 12 hours. Leaves were then oven dried at 55 °C for 48-56 hours, weighed (0.01mg; Mettler Toledo AG245), and ground to a fine powder using a Wiley Mill (Thomas Scientific, Swedesboro, NJ 08085) fitted with a 40 inch to a mesh screen. Samples were analyzed for carbon (C) and nitrogen (N) percentage and $\delta^{13}C$ and $\delta^{15}N$ values using a Vario Microcube elemental analyzer (Elementar Analysensysteme GmbH, Hanau, Germany) coupled with an isotope ratio mass spectrometer (Isoprime, Manchester, United Kingdom) operating in continuous flow mode at the Stable Isotope Laboratory (www.tulane.edu/~brosenhe/SILT_U) at Tulane University. Samples were normalized to international isotope scales by bracketing with USGS-40 and USGS-41 glutamic acid standards (calibrated to the international VPDB ($\delta^{13}C$) and AIR ($\delta^{15}N$) scales) and repeated analysis of sorghum flour was used to assess instrumental drift during runs as well as differences between runs. Stable isotope data are expressed using "delta" notation (Ometto et al. 2006).

Additional variables were defined as follows: specific leaf area (SLA) is the projected leaf area per unit leaf dry mass ($cm^2\ g^{-1}$) (Evans and Poorter 2001; Liu et al. 2010; Martin and Asner 2009), leaf mass per area (LMA; $g\ m^{-2}$) (Cordell et al. 1998), $N_{area}$ is nitrogen content per area ($g\ m^{-2}$) (Cordell et al. 1998; Dang et al. 1997; Ellsworth and Reich 1993), photosynthetic nitrogen use efficiency (PNUE) is the ratio of $A_{max}$ to $N_{area}$ ($\mu mol\ C0_2\ s^{-1}\ mol^{-1}$ N) (Cordell et al. 1998; Funk and Vitousek 2007), water use efficiency (WUE) is the ratio of $A_{area}$ to transpiration rate ($\mu mol\ C0_2$ per mmol $H_2O$) under saturating PAR (Funk and Vitousek 2007), and $A_{mass}$ is the ratio of $A_{max}$ to unit leaf dry mass ($nmol\ C0_2\ g^{-1}\ s^{-1}$) (Ellsworth and Reich 1992). We also calculated the ratio of IS50% / $A_{max}$, to understand optimization of induction response time, which we included in the AIC and best subsets regression analyses.

### 4.3.7 Airborne remote sensing

The study transect was imaged by the Carnegie Airborne Observatory (CAO) in January 2008 at a height of 500±50 meters. The CAO integrates a high-fidelity hyperspectral imager (HiFIS) having 72 bands distributed from 368-1040 nm, a full waveform Light Detection and Ranging (wLiDAR) scanner operating at 1064 nm and 100 kHz and a Global Positioning System-Inertial Measurement Unit (GPS-IMU). An automated processing stream incorporates ortho-georectification and atmospheric correction for a final spatial accuracy of < 15 cm in 3D (Asner et al. 2007). HiFIS data had a final spatial resolution of 1.25 meters while wLiDAR data were collected at 0.56 meters. wLiDAR pre-processing included noise reduction, deconvolution, waveform registration and angular rectification (Wu et al. 2011). wLiDAR point clouds were processed to proportional data by summing points within 0.56 x 0.56 x 0.15 meter (XYZ) voxels, and dividing each voxel's value by the summed total points in each 0.56 x 0.56 m vertical profile throughout the study transect. Ground and tree crown topography maps were generated through analysis of point cloud data. Solar azimuth at time of data collection was calculated in IDL using solar geometry and tree crown topography.

Leaf area index (LAI; $m^2$ leaf area / $m^2$ ground area) was calculated using paired LAI-2000 (LICOR Ltd., Lincoln, Nebraska 68504, USA) units in remote mode for 49 locations randomly distributed throughout the study transect at a height of 155 cm. We calculated a map of the top-of-canopy cosine angle to the sun using the tree (primarily *Metrosideros polymorpha*) canopy topography maps and per-pixel acquisition time. HiFIS data were interpolated to 0.56 m from 1.25 m spatial resolution to be directly comparable with the wLiDAR data using the nearest neighbor method. The modified red edge normalized difference vegetation index (mNDVI):

$$mNDVI_{705} = \frac{\rho_{750} - \rho_{705}}{\rho_{750} + \rho_{705} - 2\rho_{445}}$$

was run on the image and we then removed the effect of shade through a linear regression between mNDVI extracted for a 2 meter radius surrounding each LAI field location and the cosine value (P-value < 0.0001; $R^2$ = 0.5367), then calculated LAI as the linear relationship between field calculated LAI values and the difference between the cosine predicted mNDVI value and that calculated from the image. The final relationship was highly significant (P-value < 0.01; $R^2$ = 0.3401; $N$ = 49) and was applied to the entire HiFIS image to derive a detailed LAI map of the study area.

Leaf area density (LAD) - defined as $m^2$ of leaf area per $m^3$ of volume - was calculated throughout the study area using the proportional data derived from the corrected wLiDAR points. Three-dimensional maps of LAD were calculated by converting two-dimensional LAI values from $m^2$ to pixel scale (0.56 x 0.56 m = 0.3136 $m^2$) and distributing the leaf area across the vertical profile according to the proportion values obtained from the waveform LiDAR proportion maps at a vertical resolution of 0.15 meters, as below:

$$LAD(x) = LAI * 0.3136 * pwf(x)$$

where LAD = leaf area ($m^2$) within the vertical profile (0.56 x 0.56 m) at height *x* to *x* + 0.15 meters, LAI = leaf area index ($m^2$ leaf / $m^2$ ground area), and *pwf* = proportion waveform LiDAR points occurring at *x*.

The wLiDAR correction process was validated for this study site using field leaf area density profiles ($N$ = 13) ranging from 10 to 24 m in height with horizontal and vertical resolution of a 0.2463 $m^2$ and 0.5 m, respectively. Field LAD profiles were collected across diverse forest structure types by establishing and rappelling off horizontal Tyrolean rope traverses between tree canopies, collecting all leaves and measuring their collection height using an ultrasonic range finder (SONIN, Inc., Charlotte, NC 28277 USA) with a sonic target to reduce erroneous returns. Leaves were stored in zip lock bags with moist paper towels until leaf area ($cm^2$) was calculated within 24 hours using a LI-3100 (LICOR Ltd, Lincoln, Nebraska 68504, USA). A significant linear relationship was shown between the cumulative percentage of leaf area identified rebinned to comparable vertical (0.5 m) and horizontal (pixel area of 0.3136 $m^2$) resolution ($P$-value < 0.0001; $R^2$ = 0.4960; $N$ = 404), and no significant difference in LAD values was identified in a matched pairs analysis ($P$-value > |t| = 0.1253; $N$ = 404). Virtual forests were then generated through integration of the surface elevation and 3D LAD ($cm^2$) data, which were used in the subsequent modeling analyses.

### 4.3.8 Interior forest microclimate modeling

Interior forest climate data were compared to interpolated TOC climate data at each study plot center point. TOC values were derived from the weighted average – based on elevation - of the most proximate pair of TOC sensors. For example, for a position located between the mid and high TOC towers the interpolated TOC values would be:

$$p = \frac{(TOC_{interior} - TOC_{mid})}{(TOC_{high} - TOC_{mid})}$$

$$TOC_{interp} = (TOC_{high} * p) + (TOC_{mid} * (1 - p))$$

Interpolated total PAR values were proportioned according to diffuse and direct PAR measured at the mid elevation tower which was the only location with a BF3 direct vs. diffuse sensor installed. Separate direct and diffuse PAR models were developed. Direct PAR utilized solar azimuth and elevation calculated through interpolation of JPL planetary ephemeris (DE405; http://ssd.jpl.nasa.gov) using IDL code modified from that provided by Craig Markwardt (http://cow.physics.wisc.edu/~craigm).

The direct PAR model calculated the distribution of leaf area density at 0.25 m increments from zero to 100 m distance from the sensor directly towards the sun position, which was calculated at one-minute intervals. Leaf area density (LAD) was then adjusted according to its distance from the sensor using the following equation:

$$DirSF = \sum(-k * sd * LAD(x))$$

where DirSF is the direct structure factor, k is the extinction parameter set to 0.025, sd is the straight-line distance from the sensor (x), and LAD is the leaf area density ($cm^2$) encountered at distance (x). DirSF calculation was limited to the daytime, defined as solar elevations >= 25°. The diffuse PAR model used the same approach for each location to calculate the diffuse structure factor (DifSF) but averaged DirSF values from 36 combinations of azimuth and elevation (> 22.5 °) equally distributed across a hemisphere above the sensor.

Total interior forest PAR was modeled at one-hour intervals using the averaged PAR and structure data. Interior PAR was calculated:

$$tPAR_{int(t)} = a + b * tPAR_{TOC}(t) - c * tDirSF + d * DifSF$$

$$PAR_{int(t)} = 1.09 * ((tPAR_{int(t)} * 0.24 + 1)\text{^}(1/0.24))$$

The constants a-d equal: 2.3638, 0.3633, 0.0304 and 3.792E-04, respectively. $tPAR_{toc}$ and tDirSF represent power transformed (t; i.e., (U^λ)-1/ λ) versions of the raw variables conducted to normalize residual distributions using lambda values of 0.28 and 0.44, respectively. Parameterization was conducted in JMP on a randomly selected 50% of the available interior forest data during daylight hours. The remaining data were used to validate the model. Both the parameterization model (*P*-value < 0.0001, $R^2$ = 0.6566, *N* = 355) and validation (*P*-value < 0.0001, $R^2$ = 0.6622, *N* = 371) were highly significant.

Average air temperature was predicted at each sensor location using the environmental lapse rate calculated at 30-minute increments as follows:

$$Temp_{pred(t)} = (INT_{elev} - MID_{elev}) * MLR(t) + MID_{temp}(t)$$

where $Temp_{pred}$ is the predicted air temperature (°C) at time t and $INT_{elev}$ is the elevation at the interior forest sensor. $MID_{elev}$ and $MID_{temp}$ is the elevation and air temperature at the mid elevation climate tower, and MLR is the mean environmental lapse rate calculated among the high, mid and low elevation climate towers. This relationship was highly significant (*P*-value < 0.0001, $R^2$ = 0.7975, *N* = 4713).

The final forest interior air temperature model compared the measured versus the predicated air temperatures as influenced by DirSF and DifSF as:

$$\left(\frac{Temp_{meas}}{Temp_{pred}}\right) = a - b * \sqrt{DirSF} + c * DifSF$$

The constants a-c equal: 1.014, 6.1687E-04, and 4.984E-06, respectively. The sample size was reduced as DirSF was calculated for daytime hours only. The model was parameterized and validated as described for PAR above and was highly significant (*P*-value < 0.0001, $R^2$ = 0.8914, *N* = 1529).

### 4.3.9 Data integration

An overview of the data integration approach used is illustrated in Fig. 4.1. For each location where ecophysiology data were collected, 4400 minutes of daytime climate data were randomly selected between December 17$^{th}$, 2010 and June 1$^{st}$, 2011, averaged to half hour intervals, and the following variables were calculated using the field data collection, climate models and remote sensing data: (a) ground elevation (m), (b) canopy, plant and leaf height above forest floor (m), (c) DBH (cm), (d) mean and standard deviation of modeled available photosynthetic photon flux density (PPFD), and (d) modeled average air temperature (°C). Highly correlated variable groups were identified using Pearson correlation analysis (> 0.7; see supplementary materials 4A), resulting in the final selection of the leaf trait predictor variables: (a) leaf height, (b) PPFD mean and (c) std. dev., and (d) mean air temperature. Ground elevation, although highly correlated with mean air temperature, was included as well to account for potential unquantified variation in climate and forest dynamics along the elevation gradient.

Predictor variables were transformed in R, when appropriate, to have a normal distribution and the importance of all variables on each ecophysiology variable was assessed using: (a) community scale; best subsets multiple regressions in R with the most significant combinations of predictor variables identified using the adjusted $R^2$ value, and (b) for the dominant canopy and understory species - *Metrosideros polymorpha* (Ohia) and *Cibotium glaucum* (Hapu'u), respectively – and the entire species community, linear regressions between selected ecophysiological variables and leaf height, PPFD mean, and air temperature mean. Separate general linear models were fit in R to understand differences due to the following classifications: (a) species, (b) life-form, (c) exotic vs. native, (d) height strata, (e) canopy position, and (f) *M. polymorpha* or other. Life forms were defined as herb, fern, liana, shrub, tree fern, understory tree or canopy tree. Height strata were defined as ground, mid or upper. Canopy positions were defined as understory or canopy. Models were compared using Akaike Information Criteria (AIC; Mazerolle 2006; Mutua 1994) and weight (Anderson 2008), which adjusts for differences in parameter size, using

identical data sets. AIC provides a method to compare relative model goodness of fit for a specific foliar variable, with models $\Delta_i > 10$ above the minimum AIC having little support (Burnham and Anderson 2004). For our analysis, we kept the two best models and discarded those having AIC values $\Delta_i > 20$.

We sought to identify groups having similar ecophysiological characteristics using two approaches. We used principal components analysis (PCA; Reich et al. 1999) to assess if general trends in ecophysiological variables ($N$=22) existed. We then identified significant correlations between PCA axes and box-cox transformed, for increase normality, PPFD and air temperature. We clustered the foliar dataset into three groups through *k*-means analysis using the first three PCA axes and compared ecophysiological, structural, and climatic variables among these groups using one-way ANOVAs and Pearson tests.

## 4.4 Results

### 4.4.1 Plant diversity and structure

Total canopy height declined from 20.4±8.1 m at 1000-1049 m elevation to 13.2±5.7 m at 1300-1349 m elevation (Fig. 4.3). Leaf area index remained constant across the study area (3.9±1.4 $m^{-2}$ $m^{-2}$). A total of 24 species were identified in the plant diversity transects (Table 4.1). Importance values ranged widely, with *Metrosideros polymorpha* (Ohia), *Cibotium glaucum* (Hapu'u) and *Cheirodendron trigynum* (Olapa) identified as the three most important species. The canopy was comprised almost exclusively of Ohia, although Ohia seedlings and saplings also existed in more open understory environments, with the next strata comprised mostly of Olapa, *Coprosma rhynocarpa* (Pilo), and *Ilex anomala* (Kawau). A final strata occurring at 3-5 m height consisted almost entirely of Hapu'u. Species growing below 2 m included an abundance of the exotic species *Hedychium gardnerianumi* (Invasive Ginger) and occasional *Psidium cattleianum* (Guava) individuals. Open wet areas at low elevations were dominated by the exotic species *Persicaria punctata* (Smartweed)

below 1 meter height, with shrubs including young Ohia and the exotic species *Clidemia hirta*.

### 4.4.2 Microclimate

Table 4.2 summarizes mean top of canopy climatic conditions recorded at the low, mid and high elevation towers between December 17$^{th}$, 2010 and May 16$^{th}$, 2011. Seasonal dynamics of PPFD and air temperature are provided in Fig. 4.4 and diurnal dynamics are provided in Fig. 4.5. Measured mean air temperature dropped from 15.93 to 14.13 °C from the low to high elevation tower respectively. The low elevation tower received 58% more rainfall than the high elevation tower. Total daytime PAR was nearly equal among the low, mid and high elevation locations with the mean diffuse percentage equaling 66% of daily PAR.

### 4.4.3 Leaf trait variation

Foliar C:N was highly correlated with SLA. $A_{max}$ was significantly correlated with foliar %N and all $C0_2$ response variables, but not with leaf mass per area (LMA). Day respiration, however, was correlated with LMA (see supplementary materials 4B for all Pearson correlations). General linear model results of categorical variables are presented in Table 4.3, with the most significant classifications being species (22/22), life form (18/22), and height strata (6/22). Elevation class was the most significant predictor of foliar $\delta^{15}N$ values. Both species and height strata were the most significant predictors of the light compensation point. Exotic versus native species, respectively, had significantly ($\alpha$=0.05) greater foliar %N (2.0±0.8 vs. 1.4±0.50), $\delta^{15}N$ (-0.75±1.8 vs. -2.7±1.8), IS50% (29.6±16.8 vs. 14.5±12.9) and $A_{max}$ (6.8±5.0 vs. 3.6±1.8), but significantly lower day respiration (-0.34±0.28 vs. -0.52±0.24). In addition, $Vc_{max}$ (19.3±14.0 vs. 12.0±6.6), $J_{max}$ (14.7±10.5 vs. 9.4±5.8), and TPU (3.4±2.5 vs. 2.1±1.1) were significantly higher for exotic as compared to native species.

The best subsets multiple regression analysis revealed strong climatic and structural determinants of foliar ecophysiology (Table 4.4). Most leaf traits were correlated with leaf height (20 of 24), followed by modeled mean PPFD (14 of 24), elevation (7 of 23), and modeled mean air temperature (7 of 24). Of all leaf traits, leaf height was most significantly correlated with foliar %C (positive; adj-$R^2$ = 0.40), followed by SLA (negative; Adj-$R^2$=0.35) and IS50% (negative; Adj-$R^2$=0.36). $A_{max}$, and associated %N, were strongly positively correlated with modeled mean PPFD, and foliar C:N was negatively correlated with modeled mean PPFD. While $\delta^{15}N$ was significantly positively correlated with modeled mean air temperature (Adj-$R^2$=0.28), $\delta^{13}C$ was not correlated with any structural or climatic variables. Rates of respiration increased with modeled air temperature but decreased with increasing leaf height.

Linear regressions between leaf traits and the predictor variables defined above were conducted for *M. polymorpha* (Ohia) and *C. glaucum* (Hapu'u), the overstory and understory species having the greatest importance values (Table 4.1), as well as across the entire community (Table 4.7). Significant positive relationships existed between modeled mean PPFD and $A_{max}$ across the community (Adj-$R^2$=0.26), and at the species scale for *M. polymorpha* (Adj-$R^2$=0.13) and *C. glaucum* (Adj-$R^2$=0.40). Light saturation was most strongly correlated with modeled air temperature for *C. glaucum*. The dynamic response time (IS50%) of *C. glaucum* increased in higher modeled light environments, while that of *M. polymorpha* did not. Although increases in foliar C:N were shown at the community level (Adj-$R^2$=0.18), no such relationships existed within the individual species.

### 4.4.4 Leaf trait clusters

Principal components 1-3 encompassed 33.7%, 17.4%, and 10.6%, respectively, for a cumulative total of 62.6% of the variation (see supplementary materials 4.3 for eigenvectors). Linear regression analysis revealed PCA axis one to have a significant positive correlation with modeled mean PPFD [*F*-ratio (*P*-value) = 38.6 (<0.0001), Adj-$R^2$=0.39, *P*=<0.0001, *DF* = 77], while PCA axis two and axis

three did not have significant correlations with modeled mean PPFD [*F*-ratio (*P*-value) = 2.5 (0.12) and 3.6 (0.06), respectively]. Multiple regression analysis using modeled mean PPFD and modeled mean air temperature as predictors and each individual PCA axis as the response revealed PCA axis one to have a significant positive relationship with modeled mean PPFD but not with modeled mean air temperature [model Adj-$R^2$=0.35, $P$< 0.0001; MM-PPFD and MM-air temperature $F$ ($P$) = 22.2 (<0.0001) and 0.04 (0.85), respectively] while PCA axis two had a significant positive relationship with air temperature, but not PPFD [model Adj-$R^2$=0.17, $P$=0.0003; MM-PPFD and MM-air temperature *F*-ratio (*P*-value) = 0.03 (0.8741) and 10.6 (0.0017), respectively] (see supplementary materials 4D). PCA axis three was not significantly correlated with MM-PPFD, MM-air temperature or any other spatial or structural variables.

*K*-means analysis of these axes revealed three distinct groups within the foliar dataset (Table 4.4 and Fig. 4.6), which following analysis – see below - were found to be sorted by growth light environment (Table 4.5). The low light cluster had lower maximum rates of photosynthesis (i.e., $A_{max}$ and $A_{mass}$), including light saturation, but was able to reach $A_{max}$ quickly as compared to the medium and high light clusters. Leaves in this cluster had higher leaf mass per area, foliar %C, and water use efficiency (WUE) and lower foliar %N, and photosynthetic nitrogen use efficiency (PNUE). The high light cluster had very high rates of $A_{max}$ (and $A_{mass}$), PNUE, light saturation, triose phosphate utilization (TPU), $Vc_{max}$, and $J_{max}$. While many values were similar to other clusters, the medium light cluster was distinguished by intermediate values of $A_{max}$, $A_{mass}$, PNUE, induction response time (IS50%), and lower values of $Vc_{max}$, $J_{max}$, light compensation and saturation, and WUE. The medium light cluster had the lowest leaf mass per area.

We identified taxonomic, climatic and structural differences among the clusters (Table 4.5). The low light cluster was comprised of all tall plants with large DBH values whose sampled leaves occurred in low and less variable (i.e., low modeled standard deviation of PPFD) light environments. This cluster was composed entirely of native species and dominated by the dominant canopy species *Metrosideros*

*polymorpha* and the understory tree fern *Cibotium glaucum*. The medium light cluster was dominated by native species growing in light environments intermediate between the low- and high-modeled light clusters and often situated within the mid height strata. The high light cluster, similar in many respects to the medium light cluster, was composed of low height plants - the lowest strata of the forest - in high, but variable, modeled light environments. Composition of this cluster had abundant exotic species, including Kahili Ginger (*Hedychium gardnerianum*) and Strawberry Guava (*Psidium cattleianum*). It is likely that an additional cluster exists composed of top of canopy full sunlight Ohia leaves. Our sampling effort did however include such leaves, but on Ohia trees located in gaps or between taller Ohia individuals where rope traverses were feasible. It was not feasible in this study to sample leaves located at the top of canopy position in the tallest emergent Ohia individuals.

In general, leaves from any individual species were grouped in the same cluster (78±18%; Table 4.1). A significant positive relationship between $A_{max}$ (log-transformed) and mean modeled PPFD was found across the community the entire dataset (Adj-$R^2$=0.25, $P$ = < 0.0001, $N$ = 152). However, individual clusters had different $A_{max}$ to mean modeled PPFD relationships. No significant relationship existed for cluster one ($P$=0.2766, $N$ = 152), but a significant positive relationship existed for cluster two (Adj-$R^2$=0.16, $P$ = < 0.0072, $N$ = 44) and cluster three (Adj-$R^2$=0.26, $P$ = < 0.0040, $N$ = 30) (Fig. 4.7).

## 4.5 Discussion

The main components of this project were: (1) development of a two-dimensional map of leaf area index using airborne hyperspectral imagery; (2) derivation of a three-dimensional leaf area density map through integration of the two-dimensional leaf area index map with vertical profiles provided through airborne waveform LiDAR; (3) coding and validation of photosynthetic active radiation and air temperature microclimate models integrating top-of-canopy climate measurements

with forest structure from the leaf area density map; and (4) integrating modeled microclimate information with remote sensing and detailed field data to predict leaf traits and gas exchange dynamics for a suite of species occurring within a range of forest structural types (i.e., closed, open) along an elevation gradient.

### 4.5.1 Remote sensing

While passive and active remote sensing techniques have proven very useful for large-scale analyses (Asner et al. 2005), remote sensing studies have historically been limited in their ability for finer scale analyses of ecosystem function. Recent advances have increased the capacity of remote sensing to integrate with ecosystems at scales appropriate for detailed functional analysis (Chambers et al. 2007). Space-borne hyperspectral imaging resulted in development of techniques to link remote sensing more directly to plant physiological traits (Asner et al. 2004, 2005). Airborne hyperspectral analysis provided finer spatial resolution studies, allowing detection of species composition and foliar properties (Carlson et al. 2007). Studies using large footprint LiDAR (Koetz et al. 2007) showed the utility of three-dimensional structural information, and airborne platforms have now integrated hyperspectral sensors with light detection and ranging (LiDAR) systems (Asner et al. 2007). With this fusion, simultaneous analysis of ecosystem structure and foliar traits has become feasible (Asner et al. 2008).

A primary objective of many remote sensing studies has been to understand forest function in three dimensions spatially (Omasa et al. 2007). Efforts to better understand spatial properties of ecosystem dynamics, including productivity and canopy chemistry (Asner and Martin 2008), however, has been limited due to the difficulty of acquiring maps of forest interior structure and leaf area distribution (Houldcraft et al. 2005). In tropical forests especially, this difficulty has stemmed from the rapid extinction of the LiDAR signal in the dense overstory, and by the difficulties associated with collecting field parameterization and validation data within forest canopies (Laman 1995). Methods developed in this project have helped

surmount some canopy access issues, in particular, intra-crown access using vertical transects off horizontal Tyrolean traverses.

Spatial resolution represents a serious obstacle to fully understanding forest dynamics. Interior forest light is known to be the primary limiter of photosynthesis in many tropical forests understories (Whitmore 1996). The distribution of foliage within a forest plays an integral role in light distribution (Chazdon et al. 1988; Chen et al. 1994; Montgomery 2004). Light that does reach the understory arrives as either direct or diffuse radiation, and global increases in diffuse radiation are predicted for the next 100 years (Mercado et al. 2009). Baldocchi and Wilson (2001) highlighted this importance through a modeling analysis which showed that differences in leaf distribution throughout the forest vertical profile can alter forest net primary productivity (NPP) by up to 50%, largely through alteration of available photosynthetic active radiation (PAR) (Chazdon and Pearcy 1986a,b). Without an improved understanding of interactions between leaf area density distribution and light major errors will continue to exist in forest productivity models. However, no significant advances have been made in modeling 3D interior forest light dynamics at fine scales, although advances using medium-large footprint LiDAR are ongoing (Parker et al. 2001; Thomas et al. 2006). This has been due to several reasons including: (1) fine spatial scale of leaf area density determining direct light, and (2) the lack of a waveform LiDAR equipped remote sensing platform (Mallet and Bretar 2009) and decomposition algorithms (Wu et al. 2011) enabling detailed 3D analyses at a high spatial resolution. However, even field-based approaches have encountered difficulties and required inclusion of extensive stand structural information (Sonohat et al. 2004).

The recent development of the Carnegie Airborne Observatory (CAO; Asner et al. 2007) integrating high pulse count waveform LiDAR with a hyperspectral sensor has begun to overcome limitations to forest interior microclimate modeling. The data collected for this study is among the highest spatial resolution available and allows us to test the feasibility of modeling microclimate dynamics at a temporal and spatial scale directly comparable to the scale of a leaf's growth environment. Future

improvements to the PPFD and air temperature microclimate models we develop and parameterize in this study would include the use of interior forest PAR sensors distinguishing between direct and diffuse light and parameterization for other tropical forests with differing structure and gap dynamics (Kellner and Asner 2009). This would allow for an improved understanding of interactions between forest structure and the direct/diffuse light ratio versus the approach used in our study that combined direct and diffuse light as total photosynthetic active radiation (PAR).

### 4.5.2 Sources of leaf trait variation

Many factors influence a leaf's physiological traits, including: (1) structural parameters, such as the plant's height (Kenzo et al. 2006); and (2) site specific differences, such as general climate (Reich et al. 1996) or soil fertility (Ordoñez et al. 2009). Inter-species differences (Hikosaka 2004), result from divergent competitive growth strategies (Poorter et al. 2006) or simply life form (Wright et al. 2005), while intra-species occur as individual plants optimize their nutrient allocation to maximize productivity (Field and Mooney 1986; Hirose and Werger 1987; Hollinger 1989). The importance of vertical distributions in leaf traits, representing broad changes in micro-climate (Kumagai et al. 2001) and hydraulic limitations (Taylor and Eamus 2008), has been identified in many studies (Domingues et al. 2005). Leaves positioned in the upper canopy generally increase net $CO_2$ uptake while those situated in the lower canopy have reduced (or negative) uptake as the proportion of maintenance respiration costs are increased relative to C gain (Ellsworth and Reich 1993). Surprisingly, our analysis showed no correlation between leaf height and mean daily PPFD (see Appendix 4.1). This difference is likely due to the forest structure in our study area, having a low LAI open canopy with dispersed tall relatively small DBH trees, differing from those in many tropical areas that have very high LAI canopies with heavily shaded forest interiors. Given this, horizontal differences in topography, low to mid-story leaf area, and gap dynamics may be dominant controls over microclimate variation, rather than vertical gradients as found in other studies in tropical forests

(Domingues et al. 2005). A broad suite of leaf traits have been shown to co-vary, including positive relationships between foliar %N and $A_{max}$ (Field and Mooney 1986; Reich et al. 1997), as we likewise find in this study (see Appendix 4.2). This relationship partly results from the availability of photosynthetic enzymes limiting photosynthetic capacity (Field 1983). In addition to leaf N concentration and $A_{max}$, leaf photosynthetic induction rates, i.e., the activation and synthesis of photosynthesis related biochemical components and stomatal movements (Pearcy 1990) vary with both species and growth light environment (Bazzaz and Carlson 1982; Portes et al. 2008).

### 4.5.3 Species and structure

The single greatest source of leaf trait variation found in our study was inter-species differences (Table 4.3). Wright et al. (2004) used a global database of leaf traits, including 2,548 species, and found large variation among functional groups but strong co-variation among leaf traits, consistent with changes in species growth strategies along a continuous 'leaf economics spectrum' (Wright et al. 2004), constructing short lived, low LMA, high $A_{max}$ leaves to long lived, high LMA, low $A_{max}$ leaves. Likewise, Popma et al. (1992) found variation among species resulted from specialization to different growth environments, with gap-independent species producing nutrient poor leaves with low photosynthetic rates. In addition, they found that species adapted growing in a wide range of light environments show larger phenotypical plasticity in leaf traits. Markesteijn et al. (2007) also found leaf trait variation among 43 tropical forest tree species to be dominated by inter-species differences, with short-lived pioneer species having the greatest leaf trait plasticity.

Many studies in Hawaii have focused on differences between species of exotic and native origin (Hughes and Denslow 2005). This topic is of conservation importance as many native ecosystems are undergoing invasion in which native dominated species composition becomes altered or dominated by exotic species, resulting in changes in composition, structure, and other ecological properties

(Vitousek et al. 1987). Among other reasons, exotic species may invade native ecosystems following disturbance or when native communities have low resource use resulting in resource availability – termed the 'fluctuating resource hypothesis' (Funk and Vitousek 2007). Funk and Vitousek (2007) studied the resource use efficiency (RUE) of invasive and native species and found that invasive species used limiting resources more efficiently, as indicated by higher photosynthetic rates ($A_{max}$), higher photosynthetic nitrogen use efficiency (PNUE), although water use efficiency (WUE) was not different. Asner et al. (2006) used remote sensing coupled with the CASA carbon cycle model and found that growth rates of *Myrica faya*, an invasive species, were 16-44% higher than *Metrosideros polymorpha*. In our study, exotic species exhibited significantly greater rates of photosynthesis and nutrient use, including higher foliar %N and $A_{max}$. These findings are in line with other studies showing higher growth rates on non-resource limited sites, a reasonable assumption for our study area given the young age of the substrate. The lack of resource limitation is also exhibited in the non-significance of PNUE between our exotic and native species, a result found by Funk and Vitousek (2007).

### 4.5.4 Light and air temperature

Photosynthetic active radiation is a dominant limiting factor to total forest photosynthesis (Whitmore, 1996; Kull 2002; Graham et al. 2003) and its availability plays a major role in survival, growth, ecology and physiology of forest plants (Chazdon and Pearcy 1986a; Myneni and Ganapol 1992), especially in the understory (Capers and Chazdon 2004). Photosynthetic active radiation dynamics vary greatly between forests of different stand architecture, even when species composition remains the same (Sonohat et al. 2004). In addition to light, air temperature is a primary determinant of photosynthesis and respiration (Berry and Bjorkman 1980) and increases in mean annual temperature (MAT) have been shown to correspond to increased total net primary productivity (Raich et al. 2006). We see the importance of these two environmental gradients expressed in our PCA analysis, with axis one being

significantly correlated with modeled light and axis two correlated with modeled temperature. The fact that the first two axes encompass only 51% of the variability in leaf traits across our community may be partly explained by the exclusion of species, identified as a significant source of leaf trait variation, from the PCA. Preliminary analysis on our dataset does reveal the possibility of models with greater significance (PCA 1 vs. MM-PPFD; Adj-$R^2$=0.58, $P$<0.0001, $DF$=77) and merits further investigation.

Differences in light and temperature in the plant growth environment are directly correlated with changes in leaf photosynthetic capacity, as well as a broad suite of ecophysiological characteristics (Wright et al. 2004, 2005). Field (1983) showed that plants optimize the distribution of N within their leaves according to the distribution of daily photosynthetic active radiation. Evans and Poorter (2001) found that photosynthesis was three times greater in ten dicotyledonous $C_3$ species grown under 1000 versus 200 µmol $m^{-2}$ $s^{-1}$ PPFD, however photosynthesis per unit leaf dry mass was not significantly different due to increased specific leaf area (SLA) but constant nitrogen concentration. Hollinger (1989) showed that leaf N content and $A_{max}$ followed vertical gradients according to available PPFD in the forest canopy. However, relationships are not linear and photosynthesis of plants located in the understory often become light saturated at less than half of full sunlight intensity (Lambers et al. 1998). This may partly explain the low correlation we found between mean PPFD and light saturation at the community scale.

In our study, most leaf traits did follow vertical gradients, as shown by the significance of leaf height, but were also simultaneously correlated with light and air temperature; likely resulting from inconsistencies in the leaf height to PPFD relationship – which will be focus of future studies. Chazdon and Field (1987) found that in understory plants the light environment was only able to explain a maximum of 35.1% of the variation in $A_{max}$, indicating that other determinants, including climatic variation, topography or resource competition, were playing important roles. They also found that understory plants (versus plants growing in open gap environments) were less able to adjust $A_{max}$ to variation in the light intensity of their growth

environment, although compensation through increased light use efficiency was possible (Chazdon and Pearcy 1986b). Similar to their results, however, we found that modeled light variability did not significantly correlate to Amax, while simpler measures, such as canopy openness in their study, or in the case of our study modeled mean daily PPFD, did. This is similar to the percentage of variation in $A_{max}$ explained for the *C. glaucum*, the dominant understory species in our study area. While direct radiation accounts for between 10 to 80% of total understory irradiance, and in some cases the majority of carbon fixation (Chazdon 1986, Pearcy and Calkin 1983, Pearcy 1990), it arrives to the understory of a forest within an intact canopy in the form of sun flecks lasting from seconds to minutes (Chazdon and Fetcher 1984). Thus, it is to the advantage of understory plants to develop the foliar capacity to rapidly use short temporal bursts of light (i.e., sunflecks) (Chazdon and Pearcy 1986a).

In our study, we found a positive correlation between modeled PPFD and time to reach 50% maximum assimilation rate (IS50%), differing from Rijkers et al. 2000 who found no differences in time to reach 90% maximum assimilation in spite of large differences in $A_{max}$. At first, this relationship appears to indicate that the dominant control over induction response time is the maximum photosynthetic rate of the leaf - although the Pearson correlation of 0.22 is low (Appendix 4.2), and $A_{max}$ is related to species differences and the illumination of the growth environment. However, further analysis shows that while $A_{max}$ is related positively with growth environment, IS50% is more related to leaf height where it declines with height, although leaf height does have a significant negative correlation with modeled illumination environment. Given the low Pearson correlation, there is an opportunity to identify where leaves simultaneously maintain high maximum photosynthesis rates and rapid induction response times using the ratio of IS50% / $A_{max}$ – which we consider a measure of induction response efficiency (i.e., lower values = more efficient). Our results show increasing induction response efficiency with increasing leaf height and in higher modeled light growth environments, but decreasing efficiency with increasing modeled air temperature. The relationship with increasing leaf height is logical as PPFD actually decreases at the base of the Ohia canopy prior to increasing near the

top-of-canopy. Decreasing efficiency in warmer environments also makes sense as increased availability of nutrients could results in reduced requirement for resource use optimization. As a plant likely shifts a range of leaf traits simultaneously, we expected to find a patter of increasing water use efficiency (WUE) simultaneous to induction response efficiency. A linear regression analysis showed this significant negative relationship between them (Adj-$R^2$=0.17, $P$ = < 0.0001, $N$ = 90), indicating simultaneous increases in light and water use efficiency. Similar to the findings of Funk and Vitousek (2007), we did not find significant differences in either water use efficiency or induction response efficiency between exotic and native species.

### 4.5.5 Stable isotopes

Foliar $\delta^{13}C$ is typically thought to represent changes in foliar water use efficiency (WUE) resulting from differences in water availability (Seibt et al. 2008) or structural differences in the leaf (Bonal et al. 2007). Variation in foliar $\delta^{13}C$ due to differences in atmospheric isotopic composition (i.e., increased respired versus atmospheric $C0_2$) would be unlikely to have an effect higher than 3-5 meters (Ometto et al. 2002) and leaf height was a non-significant predictor of variation in foliar $\delta^{13}C$. Our $\delta^{13}C$ values were similar to those reported in the Amazon (Ometto et al. 2006). However, for *M. polymorpha* – the canopy dominant in our study area, different conclusions regarding determinants of $\delta^{13}C$ variation have been found. Vitousek et al. (1990) found that, for Ohia (*M. polymorpha*), internal $C0_2$ resistance to diffusion resulting from increased leaf mass per area (LMA) was a primary factor determining variation in $\delta^{13}C$, similar to the results found by Körner and Diemer (1987) who identified a pattern of increasing elevation, LMA, and $\delta^{13}C$. In addition, a positive relationship between increased carboxylation efficiency and leaf area based N content, associated with increasing elevation, was found to result in significantly less negative foliar $\delta^{13}C$ values (Cordell et al. 1999). Both studies agree that species differences is likely a primary factor determining $\delta^{13}C$, but is often overlooked during analysis, and Seibt et al. (2008) argues the potential for species differences in mesophyll

conductance may mask trends in WUE. This is highlighted in our study, as only species differences (or as lumped into life-form groupings) were able to explain variation in foliar $\delta^{13}C$, with no correlations found between foliar $\delta^{13}C$ and any other leaf trait or predictor variable, including modeled mean PPFD or air temperature. As water is in abundant supply across the entire study area this result most likely represents maximized species variability when no potentially cofounding variation in water availability exists. We did find, however, that photosynthetic WUE increased significantly with increasing height in the canopy. We explain this as representing simultaneous increases in hydraulic limitations to water availability (Panek 1996) and shifts in species composition from fast growing less efficient species in the understory to, primarily, *M. polymorpha*, a slow growing canopy species with low photosynthetic capacity and high leaf mass per area (LMA) (Cordell et al. 1999).

Foliar $\delta^{15}N$ represents an integrative measure of ecosystem dynamics over time (Adams and Grierson 2001), among other things. In our study, foliar $\delta^{15}N$ had no correlation with species but was significantly explained by air temperature. As decreasing foliar $\delta^{15}N$ is generally considered to represent a tightening of the N cycle (Austin and Vitousek 1998), the positive relationship between foliar $\delta^{15}N$ increasing with air temperature may indicate increased N availability at lower elevations resulting from faster nutrient cycling, including decomposition (Vitousek et al. 1989). This is further indicated by the lack of species significance and the significant multiple regression (Adj-$R^2$=0.30, $P$=<0.0001, DF=97) for foliar $\delta^{15}N$ which showed that leaf height was non-significant ($F$=0.69, $P$-value=0.41) while air temperature was highly significant ($F$=42.04, $P$-value=<0.0001) (see Fig. 4.8). These results are similar to those reported by Craine et al. (2009) and Amundson et al. (2003), who both reported a positive relationship between mean annual temperature (MAT) and foliar $\delta^{15}N$. Foliar $\delta^{15}N$ values in our study were more depleted than those reported in parts of the Amazon (Ometto et al. 2006), similar to those reported by Martinelli et al. (1999) for *M. polymorpha*, but more negative than those reported by Cordell et al. (1999) which were collected at a different study site in Hawaii. This may be partly due to our study area having a comparatively young substrate, as compared to older substrates in the

Amazon, and therefore a more conservative nitrogen cycle (Martinelli et al. 1999). Other sources of variation may include differences in rainfall (Austin and Vitousek 1998) or increased microbial activities at higher mean annual temperature (i.e., lower elevations) resulting in soil $^{15}N$ enrichment through the preferential loss of isotopically lighter nitrogen gases (Martinelli et al. 1999).

### 4.5.6 Clusters

Leaves may be stratified across light and temperature gradients due to changes in species composition based on each preferred growth environment or acclimation of individual leaves within a species (Reich et al. 1994). In our study area, simultaneous changes in species composition and leaf trait acclimation were evident. The community $A_{max}$ to light relationship occurred in part due to transitions from low to medium to high light clusters of species (Reich et al. 1994). The response of each cluster differed however, similar to findings by Reich et al. (1998a; 1998b), with those species growing in the highest light environments having significant correlations between light and $A_{max}$. Such differences are similar to those identified during forest succession, with shifts occurring from pioneer to climax species having differing capacities to acclimate to their irradiance growth environments (Poorter et al. 2006). Kuppers et al. (1996) used both successional and light classes to show a reduction in the time to reach 50% induction state (IS50%) from pioneer through late successional species, but increasing time to reach IS50% with increasing light. Our results highlight that the acclimation capacity may differ regardless of the leaf trait cluster – based on mean values - to which a species is assigned. For example, *M. polymorpha*, a dominant overstory species, did not increase $A_{max}$ with increases in light, while *C. glaucum* did. Ecologically, such changes make sense as species adapted to low light growth environments will require greater acclimation ability to take advantage of forest disturbances (Reich et al. 1994), i.e., including tree fall gaps, which result in large, but potentially short, increases in incident radiation both within the gaps and within the surrounding forest (Denslow et al. 1990).

## 4.6 Conclusions

We developed and validated a high-resolution three-dimensional model of microclimate through airborne waveform LiDAR hyperspectral fusion in a native dominated Hawaiian rainforest. Using this model, we show that a broad suite of leaf traits, occurring across species clusters, as well as within individual species, can be predicted by the modeled light and modeled air temperature of the growth environment. At the community scale, we show that correlations between the maximum rate of photosynthesis ($A_{max}$) occurs both through shifts in species clusters, as well as through acclimation of individuals leaves within a species to its growing environment. This relationship differs between species with different competitive growth strategies, with no acclimation occurring in the dominant overstory species *M. polymorpha*, but significant acclimation (i.e., plasticity) occurring in the dominant understory species *C. glaucum*. However, the greatest factor contributing to leaf trait variation was identified as inter-species variability. Analysis of stable isotopes shows that while foliar $\delta^{13}C$ is determined by inter-species differences (and in particular life form) in leaf physiology, foliar $\delta^{15}N$ is determined by ecosystem differences in nutrient cycling resulting from differences in mean annual temperature along the elevation gradient. While no significant differences in resource use efficiency were identified between exotic and native species, we did find that species in general increased their light and water resource use efficiency simultaneously related to leaf height in general, the illumination state of their growth environment, and more broadly, to ecosystem changes in nutrient availability related to decreasing modeled air temperature associated with increasing elevation. The results of this study serve to develop and validate new tools useful for investigating ecosystem function at high spatial and temporal resolutions as well as provide insights into an ecosystem undergoing rapid degradation through species invasion and climate change. Future work built off this study will include full forest productivity modeling under different disturbance and climate change scenarios.

## 4.7 Acknowledgements

We give thanks to the following individuals for support in the lab and in the field and for their numerous insights during the course of this project: A. Wolf, A. Uowolo, B. Ostertag, B. Hwang, B. Paritosh, C. Williams, C. Lunch, D. Freyberg, D. Gelber, M. Gilbert, D. Leopold, E. Davidson, F. Inman-Narahari, F. Hughes, H. Farrington, H. Tidwell, J. Broadbent, J. Funk, J. Johnson, J. Kellner, J. Price, K. Brauman, K. Turbo, L. Fortini, M. Tweiten, P. Vitousek, R. Naesborg, R. Dirzo, S. Almeyda, T. Priest, T. Tobeck, J. Berry, J. Bingham, and G. Woods. We give thanks to the staff of Department of Biology at Stanford University, Institute of Pacific Islands Forestry (IPIF) and the Hilo office of the Department of Forestry and Wildlife (DOFAW) for logistical support throughout. We thank Stanford University, the National Science Foundation (NSF), the Department of Energy (DOE), the National Aeronatics and Space Agency (NASA) and the Carnegie Institution for Science for financial support. We thank W. Clark, N. Dickson and M. Holbrook for help during the writing process. Analysis and writing was partially conducted while E. Broadbent was a doctoral fellow and A. Almeyda Zambrano was a Giorgio Ruffolo Fellow in the Sustainability Science Program at Harvard University. Support from Italy's Ministry for Environment, Land and Sea is gratefully acknowledged.

## 4.8 References

Adams MA, Grierson PF (2001) Stable isotopes at natural abundance in terrestrial plant ecology and ecophysiology: an update. Plant Biology 3:299-310.

Alton PB, North PR, Los SO (2007) The impact of diffuse sunlight on canopy light-use efficiency, gross photosynthetic product and net ecosystem exchange in three forest biomes. Global Change Biology 13:776-787.

American Society of Civil Engineers (2005) The ASCE standardized reference evapotranspiration equation. Reston, Virginia USA.

Amundson R, Austin AT, Schuur EA, Yoo K, Matzek V, Kendall C, Uebersax A, Brenner D, Baisden WT (2003) Global patterns of the isotopic composition of soil and plant nitrogen. Global Biogeochemical Cycles 17: 1031-1042.

Anderson DR (2008) Model-based inference in the life sciences: a primer on evidence. Springer: New York, New York.

Araujo WL, Dias PC, Moraes GA, Celin EF, Cunha RL, Barros RS, DaMatta FM (2008) Limitations to photosynthesis in coffee leaves from different canopy positions. Plant physiology and biochemistry 46:884-890.

Asner GP, Martin RE, Carlson KM, Rascher U, Vitousek PM (2006) Vegetation-climate interactions among native and invasive species in Hawaiian rainforest. Ecosystems 9:1106-1117.

Asner GP, Martin RE (2008) Spectral and chemical analysis of tropical forests: Scaling from leaf to canopy levels. Remote Sensing of Environment 112:3958-3970.

Asner GP, Hughes FR, Varga TA, Knapp DE, Kennedy-Bowdoin T (2008a) Environmental and biotic controls over aboveground biomass throughout a tropical rain forest. Ecosystems 12:261-278.

Asner GP, Hughes RF, Vitousek PM, Knapp DE, Kennedy-Bowdoin T, Boardman J, Martin RE, Eastwood M, Green RO (2008b) Invasive plants transform the three-dimensional structure of rain forests. Proceedings of the National Academy of Sciences 105:4519-4523.

Asner GP, Knapp DE, Jones M, Kennedy-Bowdoin T, Martin RE, Field CB, Boardman J (2007) Carnegie airborne observatory: in-flight fusion of hyperspectral imaging and waveform light detection and ranging for three-dimensional studies of ecosystems. Journal of Applied Remote Sensing 1:013536.

Asner GP, Nepstad D, Cardinot G, Ray D (2004) Drought stress and carbon uptake in an Amazon forest measured with spaceborne imaging spectroscopy.

Proceedings of the National Academy of Sciences of the United States of America 101:6039-6044.

Asner GP, Carlson KM, Martin RE (2005) Substrate age and precipitation effects on Hawaiian forest canopies from spaceborne imaging spectroscopy. Remote Sensing of Environment 98:457-467.

Aubin I, Beaudet M, Messier C (2000) Light extinction coefficients specific to the understory vegetation of the southern boreal forest, Quebec. Canadian Journal of Forest Research 30:168-177.

Austin AT, Vitousek P (1998) Nutrient dynamics on a precipitation gradient in Hawai'i. Oecologia 113:519-529.

Bai KD, Liao DB, Jiang DB. (2008) Photosynthetic induction in leaves of co-occurring *Fagus lucida* and *Castanopsis lamontii* saplings grown in contrasting light environments. Trees-Structure and Function 22:449-462.

Baldocchi DD, Harley PC (1995) Scaling carbon dioxide and water vapour exchange from leaf to canopy in a deciduous forest: model testing and application. Plant Cell and Environment 18:1157-1174.

Baldocchi DD, Wilson KB (2001) Modeling $C0_2$ and water vapor exchange of a temperate broadleaved forest across hourly to decadal time scales. Ecological Modelling 142:155-184.

Bazzaz FA, Carlson RW (1982) Photosynthetic acclimation to variability in the light environment of early and late successional plants. Oecologia 54:313-316.

Berry J, Bjorkman O (1980) Photosynthetic response and adaptation to temperature in higher plants. Annual Review of Plant Physiology 31:491-543.

Boisvenue C, Running SW. 2006. Impacts of climate change on natural forest productivity – evidence since the middle of the 20$^{th}$ century 12:862-882.

Bonal D, Born C, Brechet C, Coste S, Marcon E, Roggy JC, Guehl JM (2007) The successional status of tropical rainforest tree species is associated with

differences in leaf carbon isotope discrimination and functional traits. Annals of Forest Science 64:169-176.

Boudreau J, Nelson RF, Margolis HA, Guindon L, Kimes DS (2008) Regional aboveground forest biomass using airborne and spaceborne LiDAR in Quebec. Remote Sensing of Environment 112:3876-3890.

Burnham KP, Anderson DR (2004) Multimodel inference: understanding AIC and BIC in model selection. Sociological Methods and Research 33:261-304.

Busby PE, Vitousek P, Dirzo R (2010) Prevalence of tree regeneration by sprouting and seeding along a rainfall gradient in Hawai'i. Biotropica 42:80-86.

Carlson KM, Asner GP, Hughes RF, Ostertag R, Martin RE (2007) Hyperspectral remote sensing of canopy biodiversity in Hawaiian lowland rainforests. Ecosystems 10:536-549.

Capers RS, Chazdon RL (2004) Rapid assessment of understory light availability in a wet tropical forest. Agricultural and Forest Meteorology 123:177-185.

Chambers JQ, Asner GP, Morton DC, Anderson LO, Saatchi SS, Espirito-Santo FD, Palace M, Souza C (2007) Regional ecosystem structure and function: ecological insights from remote sensing of tropical forests. Trends in Ecology and Evolution 22:414–423.

Chazdon RL, Fletcher N (1984) Photosynthetic light environments in a lowland tropical forest in Costa Rica. The Journal of Ecology 72:553-564.

Chazdon RL (1986) Light variation and carbon gain in rain forest understorey palms. The Journal of Ecology 74:995-1012.

Chazdon RL, Field CB (1987) Determinants of photosynthetic capacity in six rainforest Piper species. Oecologia 73:222–230.

Chazdon RL, Pearcy RW (1986a) Photosynthetic responses to light variation in rainforest species. I. Induction under constant and fluctuating light conditions. Oecologia 69:517-523.

Chazdon RL, Pearcy RW (1986b) Photosynthetic responses to light variation in rainforest species: II carbon gain and photosynthetic efficiency during lightflecks. Oecologia 69:524–531.

Chazdon RL, Pearcy RW (1991) The Importance of Sunflecks for Forest Understory Plants. BioScience 41:760-766.

Chazdon RL, Williams K, Field CB (1988) Interactions between Crown Structure and Light Environment in Five Rain Forest Piper Species. American Journal of Botany 75:1459-1471.

Chen SG, Shao BY, Impens I, Ceulemans R (1994) Effects of plant canopy structure on light interception and photosynthesis. Journal of Quantitative Spectroscopy and Radiative Transfer 52:115-123.

Cordell S, Goldstein G, Mueller-Dombois D, Webb D, Vitousek PM (1998) Physiological and morphological variation in Metrosideros polymorpha, a dominant Hawaiian tree species, along an altitudinal gradient: the role of phenotypic plasticity. Oecologia 113:188-196.

Cordell S, Goldstein G, Meinzer FC, Jandley LI (1999) Allocation of carbon and nitrogen in leaves of Metrosideros polymorpha regulates carboxylation capacity and $\delta^{13}C$ along an altitudinal gradient. Functional Ecology 13:811-818.

Cramer W, Bondeau A, Schaphoff S, Lucht W, Smith B, Sitch S (2004) Tropical forests and the global carbon cycle: impacts of atmospheric carbon dioxide, climate change and rate of deforestation. Philosophical transactions of the Royal Society of London. 359:331-343.

Craine JM, Elmore AJ, Aidar MP, Bustamante M, Dawson TE, Hobbie EA, Kahmen A, Mack MC, McLauchlan KK, Michelsen A, Nardoto GB, Pardo LH, Peñuelas J, Reich PB, Schuur EA, Stock WD, Templer PH, Virginia RA, Welker JM, Wright IJ (2009) Global patterns of foliar nitrogen isotopes and

their relationships with climate, mycorrhizal fungi, foliar nutrient concentrations, and nitrogen availability. The New Phytologist 183:980-992.

Curtis JT, McIntosh RP (1951) An upland forest continuum in the prairie-forest border region of Wisconsin. Ecology 32:476–496.

Dang QL, Margolis HA, Sy M, Coyea MR, Collatz JG, Walthall CL (1997) Profiles of photosynthetically active radiation, nitrogen and photosynthetic capacity in the boreal forest: Implications for scaling from leaf to canopy. Journal of Geophysical Research 102:28845-28859.

Denslow JS, Schultz JC, Vitousek PM, Strain BR (1990) Growth Responses of Tropical Shrubs to Treefall Gap Environments. Ecology 71:165-179.

Dixon RK, Brown S, Houghton RA, Solomon AM, Trexler MC, Wisniewski J (1994) Carbon pools and the flux of global ecosystems. Science 263:185-190.

Domingues TF, Berry JA, Martinelli LA, Ometto JP, Ehleringer JR (2005) Parameterization of canopy structure and leaf-level gas exchange for an Eastern Amazonian Tropical Rain Forest. Earth Interactions 9:1-23.

Ellsworth D, Reich P (1993) Canopy structure and vertical patterns of photosynthesis and related leaf traits in a deciduous forest. Oecologia 96:169-178.

Ellsworth D, Reich P (1992) Leaf mass per area, nitrogen content and photosynthetic carbon gain in *Acer saccharum* seedlings in contrasting forest light environments. Functional Ecology 6:423–435.

Evans JR (1989) Photosynthesis and nitrogen relationships in leaves of C3 plants. Oecologia 78:9-19.

Evans J, Poorter H (2001) Photosynthetic acclimation of plants to growth irradiance: the relative importance of specific leaf area and nitrogen partitioning in maximizing carbon gain. Plant Cell and Environment 24:755-767.

Farquhar GD, Caemmerer SV, Berry JA (1980) A Biochemical Model of Photosynthetic $C0_2$ Assimilation in Leaves of C3 Species. Planta 149:78-90.

Field CB (1983) Allocating leaf nitrogen for the maximization of carbon gain: leaf age as a control on the allocation program. Oecologia 56:341-347.

Field CB, Mooney HA (1986) The photosynthesis–nitrogen relationship in wild plants. On the Economy of Plant Form and Function (ed. T. Givnish), pp. 25-55. Cambridge University Press, Cambridge.

Field CB, Behrenfeld MJ, Randerson JT, Falkowski P (1998) Primary production of the biosphere: integrating terrestrial and oceanic components. Science 281: 237-240.

Funk JL, Vitousek PM (2007) Resource-use efficiency and plant invasion in low-resource systems. Nature 446:1079-1081.

Gastellu-Etchegorry J, Trichon V (1998) A modeling approach of PAR environment in a tropical rain forest in Sumatra: application to remote sensing. Ecological Modelling 108:237-264.

Gersonde R, Battles JJ, O'Hara KL (2004) Characterizing the light environment in Sierra Nevada mixed-conifer forests using a spatially explicit light model. Canadian Journal of Forest Research 34:1332-1342.

Giambelluca TW, Chen Q, Frazier AG, Price JP, Chen Y-L, Chu P-S, Eischeid J, Delparte D. 2011. The Rainfall Atlas of Hawai'i. http://rainfall.geography.hawaii.edu. [accessed June 1st 2012]

Graham E, Mulkey SS, Kitajima K, Phillips NG, Wright SJ (2003) Cloud cover limits net CO2 uptake and growth of a rainforest tree during tropical rainy seasons. Proceedings of the National Academy of Sciences 100:572-576.

Hansen J, Ruedy R, Sato M, Lo K (2010) Global surface temperature change. Reviews of Geophysics 48:1-29.

Hikosaka K (2004) Interspecific difference in the photosynthesis–nitrogen relationship: patterns, physiological causes, and ecological importance. Journal of Plant Research 117:481-494.

Hirose T, Werger M (1987) Maximizing daily canopy photosynthesis with respect to the leaf nitrogen allocation pattern in the canopy. Oecologia 72:520–526.

Hirose T, Werger MJ, van Rheenen JW (1989) Canopy development and leaf nitrogen distribution in a stand of *Carex acutiformis*. Ecology 70:1610-1618.

Houldcroft CJ, Campbell CL, Davenport IJ, Gurney RJ, Holden N (2005) Measurement of canopy geometry characteristics using LiDAR laser altimetry: a feasibility study. IEEE Transactions on Geoscience and Remote Sensing 43:2270–2282.

Hollinger DY (1989) Canopy organization and foliage photosynthetic capacity in a broad-leaved evergreen montane forest. Functional Ecology 3:53-62.

Hudak AT, Lefsky MA, Cohen WB, Berterretche M (2002) Integration of lidar and Landsat ETM+ data for estimating and mapping forest canopy height. Remote Sensing of Environment 82:397-416.

Hughes RF, Denslow JS (2005) Invasion by an $N_2$-fixing tree alters function and structure in wet lowland forests of Hawaii. Ecological Applications 15:1615-1628.

Hulme M, Viner D (1998) A climate change scenario for the tropics. Climatic Change 39:145-176.

Hunt R, Hand DW, Hannah MA, Neal AM (1991) Response to $CO_2$ enrichment in 27 herbaceous species. Functional Ecology 5:410-421.

Johnson DM, Smith WK (2006) Low clouds and cloud immersion enhance photosynthesis in understory species of a southern Appalachian spruce-fir forest (USA). American Journal of Botany 93:1625-1632.

Kellner JR, Asner GP (2009) Convergent structural responses of tropical forests to diverse disturbance regimes. Ecology letters 12:887-897.

Kenzo T, Ichie T, Watanabe Y, Yoneda R, Ninomiya I, Koike T (2006) Changes in photosynthesis and leaf characteristics with tree height in five dipterocarp species in a tropical rain forest. Tree physiology 26:865-873.

Knohl A, Baldocchi DD (2008) Effect of diffuse radiation on canopy gas exchange processes in a forest ecosystem. Journal of Geophysical Research 113:1-17.

Koetz B, Morsdorf F, Sun G, Ranson K, Itten K, Allgöwer B (2006) Inversion of a lidar waveform model for forest biophysical parameter estimation. IEEE Geoscience and Remote Sensing Letters 3:49-53.

Koetz B, Sun G, Morsdorf F, Ranson K, Kneubuhler M, Itten K, Allgöwer B. (2007) Fusion of imaging spectrometer and LIDAR data over combined radiative transfer models for forest canopy characterization. Remote Sensing of Environment 106:449-459.

Körner C, Diemer M (1987) In situ photosynthetic responses to light, temperature and carbon dioxide in herbaceous plants from low and high altitude. Functional Ecology 1:179-194.

Koukoulas S, Blackburn GA (2004) Quantifying the spatial properties of forest canopy gaps using LiDAR imagery and GIS. International Journal of Remote Sensing 25:3049-3072.

Kull O (2002) Acclimation of photosynthesis in canopies: models and limitations. Oecologia 133:267-279.

Kumagai T, Kuraji K, Noguchi H, Tanaka Y, Tanaka K, Suzuki M (2001) Vertical profiles of environmental factors within tropical rainforest, Lambir Hills National Park, Sarawak, Malaysia. Journal of Forest Research 6:257-264.

Küppers M, Timm H, Orth F, Stegemann J, Stober R, Schneider H, Paliwal K, Karunaichamy KS, Ortiz R (1996) Effects of light environment and successional status on lightfleck use by understory trees of temperate and tropical forests. Tree Physiology 16:69-80.

Laisk, A., Eichelmann, H., Oja, V., Rasulow, B., Padu, E., Bichele, I., Pettai, H. & Kull, O. (2005) Adjustment of leaf photosynthesis to shade in a natural canopy: rate parameters. Plant, Cell and Environment, 28, 375-388.

Lambers H, Chapin FS, Pons TL (1998) Plant physiological ecology. Springer, New York, New York.

Laman TG (1995) Safety recommendations for climbing rain forest trees with“ single rope technique.” Biotropica 27:406-409.

Liu F, Yang W, Wang Z, Xu Z, Liu H, Zhang M, Liu Y, An S, Sun S (2010) Plant size effects on the relationships among specific leaf area, leaf nutrient content, and photosynthetic capacity in tropical woody species. Acta Oecologica 36:149-159.

Lim K, Treitz P, Wulder M, St-Onge B, Flood B (2003) LiDAR remote sensing of forest structure. Progress in Physical Geography 27:88-106.

Long SP, Bernacchi CJ (2003) Gas exchange measurements, what can they tell us about the underlying limitations to photosynthesis? Procedures and sources of error. Journal of Experimental Botany 54:2393-2401.

Mallet C, Bretar F (2009) Full-waveform topographic lidar: State-of-the-art. ISPRS Journal of Photogrammetry and Remote Sensing 64:1-16.

Markesteijn L, Poorter L, Bongers F (2007) Light-dependent leaf trait variation in 43 tropical dry forest tree species. American Journal of Botany 94:515-525.

Mazerolle MJ (2006) Improving data analysis in herpetology: using Akaike’s Information Criterion (AIC) to assess the strength of biological hypotheses. Amphibia-Reptilia 27:169-180.

Martin RE, Asner GP (2009) Leaf chemical and optical properties of metrosideros polymorpha across environmental gradients in Hawaii. Biotropica 41:292-301.

Martinelli LA, Piccolo MC, Townsend AR, Vitousek PM, Cuevas E, Mcdowell W, Robertson GP, Santos OC, Treseder K (1999) Nitrogen stable isotopic

composition of leaves and soil: tropical versus temperate forests. Biogeochemistry 46:45-65.

Meir R, Kruijt B, Broadmeadow M, Barbosa E, Kull O, Carswell F, Nobre A, Jarvis PG, Meir P (2002) Acclimation of photosynthetic capacity to irradiance in tree canopies in relation to leaf nitrogen concentration and leaf mass per unit area. Plant, Cell and Environment 25:343-357.

Mercado LM, Bellouin N, Sitch S, Boucher O, Huntingford C, Wild M, Cox PM (2009) Impact of changes in diffuse radiation on the global land carbon sink. Nature 458:1014-1017.

Montgomery R (2004) Effects of understory foliage on patterns of light attenuation near the forest floor. Biotropica 36:33-39.

Mueller-Dombois D (1987) Natural dieback in forests. BioScience 37:575-583.

Mutua FM (1994) The use of the Akaike Information Criterion in the identification of an optimum flood frequency model. Hydrological Sciences 39:235-244.

Myneni RB, Ganapol BD (1992) Remote sensing of vegetation canopy photosynthetic and stomatal conductance efficiencies. Remote Sensing of Environment 42:217-238.

Nozawa T, Emori S, Numaguti A, Tsushima Y, Takemura T, Nakajima T, Abe-Ouchi A, Kimoto M (2001) Projections of future climate change in the 21st century simulated by the CCSR/NIES CGCM under the IPCC SRES scenarios. In Present and future of modelling global environmental change–toward integrated modelling. Matsuno T, Kida H [Eds.]. Terrapub. Tokyo, Japan. pp. 15-28.

Omasa K, Hosoi F, Konishi A (2007) 3D lidar imaging for detecting and understanding plant responses and canopy structure. Journal of Experimental Botany 58:881-898.

Ometto JP, Flanagan BL, Martinelli LA, Moreira MZ, Higuchi N, Ehleringer JR (2002) Carbon isotope discrimination in forest and pasture ecosystems of the Amazon Basin, Brazil. Global Biogeochemical Cycles 16:1-10.

Ometto JP, Ehleringer JR, Domingues TF, Berry JA, Ishida FY, Mazzi E, Higuchi N, Flanagan LB, Nardoto GB, Martinelli LA (2006) The stable carbon and nitrogen isotopic composition of vegetation in tropical forests of the Amazon Basin, Brazil. Biogeochemistry 79:251-274.

Ordoñez JC, Bodegom PM, van Witte JP, Wright IJ, Reich PB, Aerts R (2009) A global study of relationships between leaf traits, climate and soil measures of nutrient fertility. Global Ecology and Biogeography 18:137-149.

Panek J (1996) Correlations between stable carbon-isotope abundance and hydraulic conductivity in Douglas-fir across a climate gradient in Oregon, USA. Tree Physiology 16:747-755.

Parker G, Lefsky M, Harding D (2001) Light transmittance in forest canopies determined using airborne laser altimetry and in-canopy quantum measurements. Remote Sensing of Environment 76:298–309.

Pearcy RW, Calkin H (1983) Carbon dioxide exchange of $C_3$ and $C_4$ tree species in the understory of a Hawaiian forest. Oecologia 58:19-25.

Pearcy R (1990) Sunflecks and photosynthesis in plant canopies. Annual Review of Plant Biology 41:421-453.

Poorter L, Oberbauer SF (1993) Photosynthetic induction responses of two rainforest tree species in relation to light environment. Oecologia 96:193-199.

Poorter L, Bongers L, Bongers F (2006) Architecture of 54 moist-forest tree species: traits, trade-offs, and functional groups. Ecology 87:1289-1301.

Potter CS, Randerson JT, Field CB, Matson PM, Vitousek PM, Mooney HA, Klooster SA (1993) Terrestrial ecosystem production: A process model based on global satellite and surface data. Global Biogeochemical Cycles 7:811-841.

Popma J, Bongers F, Werger MJ (1992) Gap-dependence and leaf characteristics of trees in a tropical lowland rain forest in Mexico. Oikos 63:207-214.

Portes MT, Alves TH, Souza GM (2008) Time-course of photosynthetic induction in four tropical woody species grown in contrasting irradiance habitats. Photosynthetica 46:431-440.

Raich JW, Russell AE, Kitayama K, Parton WJ, Vitousek PM (2006) Temperature influences carbon accumulation in moist tropical forests. Ecology 87:76-87.

Reich PB, Walters MB, Ellsworth DS, Uhl C (1994) Photosynthesis-nitrogen relations in Amazonian tree species. I. Patterns among species and communities. Oecologia 97:62-72.

Reich PB, Oleksyn J, Tjoelker MG 1996. Needle respiration and nitrogen concentration in Scots pine populations from a broad latitudinal range: a common garden test with field grown trees. Functional Ecology 10:768-776.

Reich PB, Walters MB, Ellsworth DS (1997) From tropics to tundra: global convergence in plant functioning. Proceedings of the National Academy of Sciences 94:13730-13734.

Reich PB, Ellsworth DS, Walters MB (1998a) Leaf structure (specific leaf area) modulates photosynthesis-nitrogen relations: evidence from within and across species and functional groups. Functional Ecology 12:948-958.

Reich PB, Walters MB, Ellsworth DS, Vose JM, Volin JC, Gresham C, Bowman WD (1998b) Relationships of leaf dark respiration to leaf nitrogen, specific leaf area and leaf life-span: a test across biomes and functional groups. Oecologia 114:471-482.

Reich PB, Ellsworth DS, Walters MB, Vose JM, Gresham C, Volin JC, Bowman WD (1999) Generality of leaf trait relationships: a test across six biomes. Ecology 80:1955-1969.

Reitberger J, Schnörr C, Krzystek P, Stilla U (2009) 3D segmentation of single trees exploiting full waveform LiDAR data. ISPRS Journal of Photogrammetry and Remote Sensing 64:561-574.

Rijkers T, Vries PJ, de Pons TL, Bongers F (2000) Photosynthetic induction in saplings of three shade-tolerant tree species: comparing understory and gap habitats in a French Guiana rain forest. Oecologia 125:331-340.

Sampson DA, Janssens IA, Ceulemans R (2006) Under-story contributions to stand level GPP using the process model SECRETS. Agricultural and Forest Meteorology 139:94-104.

Schwalm CR, Williams CA, Schaefer K, Arneth A, Bonal D, Buchmann N, Chen J, Law BE, Lindroth A, Luyssaert S, Reichstein M, Richardson AD (2010) Assimilation exceeds respiration sensitivity to drought: A FLUXNET synthesis. Global Change Biology 16:657-670.

Seibt U, Rajabi A, Griffiths H, Berry JA (2008) Carbon isotopes and water use efficiency: sense and sensitivity. Oecologia 155:441-454.

Sellers P, Randall D, Collatz GJ, Berry JA, Field CB, Dazlich DA, Zhang C, Collelo GD, Bounoua L (1996) A revised land surface parameterization (SiB2) for atmospheric GCMS. Part I: model formulation. Journal of Climate 9:676-705.

Sexton J, Bax T, Siqueira P, Swenson J, Hensley S (2009) A comparison of LiDAR, radar, and field measurements of canopy height in pine and hardwood forests of southeastern North America. Forest Ecology and Management 257:1136-1147.

Sonohat G, Balandier P, Ruchaud F (2004) Predicting solar radiation transmittance in the understory of even-aged coniferous stands in temperate forests. Annals of Forest Science 61:629-641.

Stadt KJ, Lieffers VJ, Hall RJ, Messier C (2005) Spatially explicit modeling of PAR transmission and growth of Picea glauca and Abies balsamea in the boreal forests of Alberta and Quebec. Canadian Journal of Forest Research 35:1-12.

Stone CP, Cuddihy LW, Tunison JT (1992) Responses of Hawaiian ecosystems to removal of feral pigs and goats. In Alien plant invasions in native ecosystems of Hawaii. Stone CP, Scott JM [eds.] University of Hawaii Press. Honolulu, HI USA. pp. 666-704.

Taylor D, Eamus D (2008) Coordinating leaf functional traits with branch hydraulic conductivity: resource substitution and implications for carbon gain. Tree Physiology 28:1169-1177.

Thomas V, Finch D, McCaughey J, Noland T, Rich L, Treitz P (2006) Spatial modelling of the fraction of photosynthetically active radiation absorbed by a boreal mixedwood forest using a lidar–hyperspectral approach. Agricultural and Forest Meteorology 140:287-307.

Thomas V, McCaughey JH, Treitz P, Finch DA, Noland T, Rich L (2009) Spatial modelling of photosynthesis for a boreal mixedwood forest by integrating micrometeorological, LiDAR and hyperspectral remote sensing data. Agricultural and Forest Meteorology 149:639-654.

Todd KW, Csillag F, Atkinson PM (2003) Three-dimensional mapping of light transmittance and foliage distribution using LiDAR. Canadian Journal of Remote Sensing 29:544-555.

Vitousek PM (1984) Litterfall, nutrient cycling, and nutrient limitation in tropical forests. Ecology 65:285-298.

Vitousek PM, Walker LR, Whiteaker LD, Muller-Dombois D, Matson PM (1987) Biological invasion by *Myrica faya* alters ecosystem development in Hawaii. Science 238:802-804.

Vitousek PM, Shearer G, Kohl DH (1989) Foliar $\delta^{15}N$ natural abundance in Hawaiian rainforest: patterns and possible mechanisms. Oecologia 78:383-388.

Vitousek PM, Field CB, Matson PA (1990) Variation in foliar $\delta^{13}C$ in Hawaiian Metrosideros polymorpha: a case of internal resistance? Oecologia 84:362-370.

Vitousek PM, Asner GP, Chadwick OA, Hotchkiss S (2009) Landscape-level variation in forest structure and biogeochemistry across a substrate age gradient in Hawaii. Ecology 90:3074-3086.

Walters M, Field CB (1987) Photosynthetic light acclimation in two rainforest *Piper* species with different ecological amplitudes. Oecologia 72:449-456.

Whitmore TC (1996) A review of some aspects of tropical rain forest seedling ecology with suggestions for further enquiry. In The ecology of tropical forest tree seedlings. Swaine MD [ed.], Parthenon. Paris, France. pp. 3-39.

Wright IJ, Reich PB, Westoby M, Ackerly DD, Baruch Z, Bongers F, Cavender-Bares J, Chapin T, Cornelissen JH, Diemer M, Flexas J, Garnier E, Groom PK, Gulias J, Hikosaka K, Lamont BB, Lee T, Lee W, Lusk C, Midgley JJ, Navas ML, Niinemets U, Oleksyn J, Osada N, Poorter H, Poot P, Prior L, Pyankov VI, Roumet C, Thomas SC, Tjoelker MG, Veneklaas EJ, Villar R (2004) The worldwide leaf economics spectrum. Nature 428:821-827.

Wright IJ, Reich PB, Cornelissen JH, Falster DS, Garnier E, Hikosaka K, Lamont BB, Lee W, Oleksyn J, Osada N, Poorter H, Villar R, Warton DI, Westoby M (2005) Assessing the generality of global leaf trait relationships. The New Phytologist 166:485-496.

Wu J, van Aardt J, McGlinchy J, Asner GP (2011) A robust signal processing chain for small-footprint waveform LiDAR. IEEE Transactions on Geoscience and Remote Sensing 99:1-14.

## 4.9 Tables

**Table 4.1:** Plant diversity transects. Density (# individuals / 1000 $m^2$), volume (basal area * height $cm^3$), frequency (% transects occurring). Species are ranked by their importance value (IV). Sampled (cluster) = whether foliar samples were collected and to which cluster the species was assigned.

| Family | Genus | Species | Common name | Status | Life-form | Density | Vol. ($cm^3$) | Freq. (%) | Height (m) | DBH (cm) | IV | Rank | Cluster |
|---|---|---|---|---|---|---|---|---|---|---|---|---|---|
| Myrtaceae | *Metrosideros* | *polymorpha* | Ohia | Native | Canopy tree | 85 | 1108099715 | 100 | 11.63±8.51 | 63.72±66.07 | 3522722 | 1 | 1 |
| Cibotiaceae | *Cibotium* | *glaucum* | Hapu'u-pulu | Native | Tree fern | 250 | 20514819 | 100 | 2.79±1.97 | 14.25±7.8 | 66115 | 2 | 1 |
| Araliaceae | *Cheirodendron* | *trigynum* | Olapa | Native | Understory tree | 137 | 4620076 | 100 | 4.54±3.36 | 4.99±5.02 | 15285 | 3 | 1 |
| Polygonaceae | *Persicaria* | *punctata* | Water smartweed | Exotic | Herb | 4533 | 7120 | 37.5 | 0.5±0 | 0.2±0 | 12379 | 4 | |
| Rubiaceae | *Coprosma* | *rhyncocarpa* | Pilo | Native | Understory tree | 91 | 1382914 | 100 | 3.8±2.83 | 3.73±3.5 | 4871 | 5 | 3 |
| Aquifoliaceae | *Ilex* | *anomala* | Hawai'i holly | Native | Understory tree | 50 | 894898 | 75 | 3.13±2.42 | 4.13±5.94 | 3151 | 6 | 1 |
| Zingiberaceae | *Hedychium* | *gardnerianum* | Kahili ginger | Exotic | Herb | 506 | 244571 | 50 | 1.54±0.32 | 1.99±0.07 | 2262 | 7 | 2 |
| Dryopteridaceae | *Dryopteris* | *wallichiana* | Laukahi | Native | Fern | 98 | 398655 | 75 | 0.86±0.28 | 7.17±1.99 | 1703 | 8 | 3 |
| Aspleniaceae | *Asplenium* | *contiguum* | Asplenium | Native | Fern | 59 | 179112 | 50 | 0.81±0.24 | 6.78±1.28 | 842 | 9 | |
| Pandanaceae | *Freycinetia* | *arborea* | Ie'ie | Native | Liana | 148 | 12729 | 37.5 | 0.78±0.35 | 1.04±0.32 | 526 | 10 | 3 |
| Rosaceae | *Rubus* | *hawaiensis* | Akala | Native | Shrub | 67 | 9096 | 62.5 | 1.01±0.41 | 0.93±0.96 | 354 | 11 | 2,3 |
| Celastraceae | *Perrottetia* | *sandwicensis* | Olomea | Native | Understory tree | 11 | 49204 | 50 | 3.4±1.95 | 2.8±2.05 | 300 | 12 | 2,3 |
| Dryopteridaceae | *Dryopteris* | *glabra* | Kilau | Native | Fern | 33 | 30152 | 50 | 0.8±0.25 | 2.53±2.71 | 298 | 13 | |
| Cyatheaceae | *Cyathea* | *cooperi* | Australian Tree Fern | Exotic | Tree fern | 4 | 62924 | 12.5 | 1.15±0.49 | 12.5±0.71 | 240 | 14 | |
| Myrtaceae | *Psidium* | *cattleianum* | Strawberry Guava | Exotic | Understory tree | 30 | 11007 | 37.5 | 1.7±1.1 | 1.03±0.64 | 203 | 15 | 3 |
| Rubiaceae | *Psychotria* | *hawaiiensis* | Kopiko | Native | Understory tree | 11 | 27416 | 37.5 | 2.8±1.86 | 2.28±1.59 | 202 | 16 | |
| Athyriaceae | *Athyrium* | *microphyllum* | Akolea | Native | Fern | 13 | 13534 | 50 | 0.8±0.3 | 3.83±1.33 | 193 | 17 | |
| Melastomataceae | *Clidemia* | *hirta* | Koster's curse | Exotic | Shrub | 41 | 13686 | 12.5 | 1.19±0.59 | 1.29±0.91 | 184 | 18 | 2 |
| Rutaceae | *Melicope* | *clusiifolia* | Alani | Native | Understory tree | 9 | 32768 | 12.5 | 4.25±1.5 | 3±1.41 | 156 | 19 | |
| Liliaceae | *Astelia* | *menziesiana* | Painiu | Native | Herb | 2 | 33450 | 12.5 | 1±0 | 14 | 141 | 20 | |
| Ericaceae | *Vaccinium* | *calycinum* | Ohelo | Native | Shrub | 28 | 664 | 12.5 | 1.15±0.36 | 0.4±0.23 | 107 | 21 | |
| Rubiaceae | *Hedyotis* | *hillebrandii* | Manono | Native | Understory tree | 4 | 5431 | 25 | 2±2.12 | 1.9±1.56 | 86 | 22 | 3 |
| Apocynaceae | *Alyxia* | *olviformis* | Maile | Native | Liana | 13 | 41 | 12.5 | 1±0 | 0.2±0 | 64 | 23 | |
| Campanulaceae | *Clermontia* | *parviflora* | Haha | Native | Shrub | 2 | 576 | 12.5 | 1.5±0 | 1.5 | 36 | 24 | |

**Table 4.2:** Mean ± standard deviation daytime (sun elevation > 25° C) climatic conditions at top of canopy tower locations between Dec 17th 2010 and June 19th 2011. Rainfall is the total over this period.

| | Climate tower location | | |
|---|---|---|---|
| **Climate variables** | **Low (1052 m)** | **Mid (1180 m)** | **High (1353 m)** |
| Air temperature (°C) | 17.48±1.99 | 16.87±2.04 | 16.23±2.15 |
| Relative humidity (%) | 79.25±11.34 | 85.41±13.50 | 77.23±12.13 |
| Windspeed (m $s^{-1}$) | 2.46±1.75 | 2.97±1.31 | 2.05±1.31 |
| Wind direction (° True North) | 258±43 | 280±66 | 252±96 |
| Direct PPFD (%) | | 34±35 | |
| Diffuse PPFD (%) | | 66±35 | |
| PPFD (µmol $m^{-2}$ $s^{-1}$) | 932±572 | 909±556 | 937±559 |
| Rainfall (mm total) | 684.41 | | 399.79 |

**Table 4.3:** General linear model results for leaf traits versus taxonomic, ecological and structural categories (# parameters). Data is the Akaike Information Criteria (AIC) (adj-$R^2$) degrees of freedom and *P*-value. AIC allows intra-row comparisons and models > 20 above the minimum AIC have been removed.

| Foliar variable | Species (14) | Life-form (7) | Strata (3) | Canopy (2) | *M. polymorpha* (2) | Status (2) | Elevation (2) |
|---|---|---|---|---|---|---|---|
| %C | **424 (0.505) 87****** | | | 452 (0.274) 99**** | | | |
| %N | 134 (0.435) 87**** | **130 (0.427) 94****** | 146 (0.303) 98**** | | | | |
| C:N | **733 (0.466) 87****** | 738 (0.406) 94**** | 752 (0.291) 98**** | | 747 (0.319) 99**** | | |
| $\delta^{13}C$ | 313 (0.356) 83**** | **309 (0.339) 90****** | | | | | |
| $\delta^{15}N$ | | | | | | 393 (0.136) 95*** | **376 (0.273) 95****** |
| Light Saturation (AQ) | **1356 (0.259) 86***** | 1372 (0.077) 93* | 1369 (0.071) 97* | 1368 (0.072) 98** | 1371 (0.04) 98* | | 1372 (0.029) 98* |
| Light Compensation (AQ) | **563 (0.333) 86****** | 568 (0.255) 93**** | **563 (0.265) 97****** | 570 (0.206) 98**** | 574 (0.174) 98**** | | |
| Convexity (AQ) | 508 (0.113) 87* | **497 (0.149) 94**** | | | 499 (0.091) 99** | | |
| Respiration (AQ) | **-16 (0.37) 86****** | -3 (0.239) 93**** | 0 (0.182) 97**** | 6 (0.122) 98*** | 5 (0.135) 98**** | | |
| Amax (AQ) - All | **433 (0.528) 87****** | 479 (0.203) 94*** | | | | 479 (0.166) 99**** | |
| $Vc_{max}$ (Aci) | **668 (0.342) 84****** | 687 (0.15) 91** | | | | | |
| $J_{max}$ (Aci) | **644 (0.234) 84***** | 652 (0.119) 91** | | | | 653 (0.063) 96** | 650 (0.091) 96** |
| TPU (Aci) | **328 (0.343) 84****** | 348 (0.144) 91** | | | | | |
| Convexity (Induction %) | **19 (0.338) 78****** | 37 (0.14) 85** | | | 38 (0.08) 90** | | |
| IS 50% (Induction) | **724 (0.312) 77****** | | 740 (0.094) 88** | 728 (0.19) 89**** | 742 (0.062) 89** | 735 (0.127) 89*** | 737 (0.112) 89*** |
| WUE | **369 (0.175) 80**** | | | **369 (0.08) 92**** | | | |
| SLA | **928 (0.645) 81****** | 954 (0.506) 88**** | | | | | |
| LMA | **864 (0.587) 82****** | 887 (0.446) 89**** | | | | | |
| $N_{area}$ | **99 (0.334) 81****** | 103 (0.256) 88**** | | | | | |
| PNUE | **882 (0.407) 81****** | 904 (0.198) 88*** | | | | | |
| $A_{mass}$ | **926 (0.653) 82****** | 984 (0.316) 89**** | | | | | |
| IS50% / $A_{max}$ | **487 (0.149) 77*** | | | 483 (0.079) 89** | | | 480 (0.105) 89*** |

AQE = Apparent quantum efficiency; TPU = Triose phosphate utilization; IS = Induction state; PPFD = Photosynthetic photon flux density; WUE = Water use efficiency; SLA = Specific leaf area; LMA = Leaf mass per area; PNUE = Photosynthetic nitrogen use efficiency. P-values < 0.05 = *, < 0.01 = **, < 0.001 = *** and < 0.0001 = ****. Status = invasive or native; Strata = low, mid or overstory position; Position = canopy or not; *M. polymorpha* = yes or no. ϕ = Smartweed (*Persicaria punctata*) has been removed from the dataset.

**Table 4.4:** Best subsets models of leaf traits versus structural and modeled mean and standard deviation (SD) photosynthetic photon flux density (PPFD; µmol $m^{-2}$ $s^{-1}$) and air temperature (°C). Data represents the *t*-ratio (*F*-ratio) and *P*-value significance, with increasing *, **, ***, ****, and ϕ representing *P*-values of 0.1, 0.05, 0.01, 0.001, and < 0.0001, respectively.

| Leaf traits | Elevation (m) | Leaf height (m) | Modeled in growth environment | | | $R^2$ | Adj-$R^2$ | P-value | N |
|---|---|---|---|---|---|---|---|---|---|
| | | | PPFD mean | PPFD SD | Air temp mean | | | | |
| %C | | 7.33 (53.78) ϕ | | | | 0.377 | 0.369 | ϕ | 101 |
| %N | | -4.15 (17.22) ϕ | 1.81 (3.28) * | | | 0.288 | 0.273 | ϕ | 97 |
| C:N | | 5.01 (25.06) ϕ | -1.12 (1.25) ns | | | 0.313 | 0.299 | ϕ | 98 |
| $\delta^{13}C$ | | | | | | | | ns | 96 |
| $\delta^{15}N$ | | 0.89 (0.7834) ns | | | 6.15 (37.85) ϕ | 0.291 | 0.276 | ϕ | 96 |
| Light Saturation (AQ) | | -2.2 (4.85) ** | 1.5 (2.24) ns | | | 0.131 | 0.112 | **** | 95 |
| Light Compensation (AQ) | -1.84 (3.37) * | 7.09 (50.26) ϕ | | | | 0.355 | 0.342 | ϕ | 98 |
| AQE (x100) | | | | | | | | ns | 97 |
| Convexity (AQ) | | 2.46 (6.06) ** | 2.69 (7.24) *** | | | 0.085 | 0.066 | ** | 98 |
| Respiration (AQ) | 1.75 (3.06) * | -3.72 (13.82) **** | | | 1.50 (2.25) ns | 0.231 | 0.206 | ϕ | 97 |
| $A_{max}$ € | | | 5.63 (31.71) ϕ | | 1.69 (2.87) ns | 0.326 | 0.318 | ϕ | 186 |
| $Vc_{max}$ (Aci) | 2.89 (8.35) *** | 2.19 (4.78) ** | | | 4.51 (20.33) ϕ | 0.276 | 0.253 | ϕ | 97 |
| $J_{max}$ (Aci) | 2.36 (5.58) ** | 2.20 (4.82) ** | | | 3.98 (15.81) ϕ | 0.250 | 0.226 | ϕ | 98 |
| TPU (Aci) | 2.10 (4.43) ** | | | | 3.78 (14.29) **** | 0.224 | 0.208 | ϕ | 98 |
| Convexity (Induction %) | 2.12 (4.50) ** | 4.16 (17.31) ϕ | -1.71 (2.91) * | | | 0.352 | 0.330 | ϕ | 90 |
| IS 50% (Induction) | -2.58 (6.64) ** | -4.27 (18.26) ϕ | 1.76 (3.09) * | | | 0.380 | 0.360 | ϕ | 89 |
| WUE | | 3.24 (10.49) *** | 0.67 (0.45) ns | | | 0.115 | 0.095 | *** | 93 |
| SLA | | -6.86 (47.03) ϕ | -1.77 (3.15) * | | | 0.360 | 0.346 | ϕ | 93 |
| LMA | | 6.74 (45.49) ϕ | | | | 0.326 | 0.319 | ϕ | 96 |
| $N_{area}$ | | 2.58 (6.66) ** | 3.00 (9.05) *** | | | 0.106 | 0.086 | *** | 93 |
| PNUE | | -2.85 (8.15) *** | 1.42 (2.01) ns | | | 0.172 | 0.154 | **** | 93 |
| $A_{mass}$ | | -4.70 (22.12) ϕ | 2.09 (4.39) ** | | | 0.346 | 0.331 | ϕ | 94 |
| IS50% / $A_{max}$ | | -3.04 (9.24) *** | -3.31 (10.99) *** | | 3.82 (14.59) **** | 0.184 | 0.155 | **** | 89 |

AQE = Apparent quantum efficiency, TPU = Triose phosphate utilization, IS = Induction state, PPFD = Photosynthetic photon flux density, WUE = Water use efficiency, SLA = Specific leaf area, LMA = Leaf mass per area, PNUE = Photosynthetic nitrogen use efficiency. € = $A_{max}$ values combined from light response and induction response curves.

**Table 4.5:** Predictors of Hapu'u (*Cibotium glaucum*) and Ohia (*Metrosideros polymorpha*) leaf traits. Data represents the slope (adj-$R^2$) degrees of freedom and *P*-value of linear regressions.

| Leaf traits | Leaf height (m) | Modeled in growth environment | |
|---|---|---|---|
| | | PPFD mean | Air temp mean |
| A. *Metrosideros polymorpha* | | | |
| $A_{max}$ * | NS | 0.01 (0.131) 25 * | NS |
| Light saturation * | NS | NS | NS |
| Day respiration * | NS | NS | NS |
| Convexity ε ** | NS | NS | NS |
| IS 50% ε | -0.56 (0.151) 20 * | NS | NS |
| C:N | NS | NS | NS |
| $\delta^{13}C$ | NS | NS | NS |
| $\delta^{15}N$ | 0.14 (0.129) 22 * | NS | NS |
| A. *Cibotium glaucum* | | | |
| $A_{max}$ * | -1.18 (0.262) 13 * | 0.02 (0.403) 13 ** | 2.28 (0.61) 13 *** |
| Light saturation * | -179.25 (0.281) 13 * | 2.8 (0.335) 13 * | 345.79 (0.647) 13 *** |
| Day respiration * | 0.11 (0.636) 12 *** | NS | NS |
| Convexity ε ** | NS | NS | NS |
| IS 50% ε | NS | 0.12 (0.271) 12 * | 12.19 (0.347) 12 * |
| C:N | NS | NS | NS |
| $\delta^{13}C$ | NS | NS | NS |
| $\delta^{15}N$ | NS | 0.02 (0.269) 13 * | NS |
| B. Community | | | |
| $A_{max}$ * | -0.14 (0.053) 97 * | 0.01 (0.261) 97 **** | 1.67 (0.155) 97 **** |
| Light saturation * | -11.56 (0.053) 96 * | 0.49 (0.063) 96 ** | 91.59 (0.062) 96 ** |
| Day respiration * | -0.02 (0.167) 96 **** | 0 (0.043) 96 * | NS |
| Convexity ε ** | 0.02 (0.084) 88 ** | NS | NS |
| IS 50% ε | -1.11 (0.124) 87 *** | 0.03 (0.037) 87 * | 8.22 (0.133) 87 *** |
| C:N | 0.97 (0.181) 97 **** | -0.03 (0.077) 97 ** | NS |
| $\delta^{13}C$ | NS | NS | NS |
| $\delta^{15}N$ | NS | 0.01 (0.13) 93 *** | 1.55 (0.289) 93 **** |

* and ε = calculated from light or inductance response curves, respectively. P-values < 0.05 = *, < 0.01 = **, < 0.001 = *** and < 0.0001 = ****. ** = convexity of raw inductance data.

**Table 4.6**: Leaf trait mean ± standard deviation for *K*-means low, medium and high modeled light clusters and results of among cluster one-way ANOVAs sorted by the adjusted $R^2$ value.

| Leaf traits | Modeled light environment | | | Adj-$R^2$ | *P*-value |
|---|---|---|---|---|---|
| | Low | Medium | High | | |
| Cluster size (*N*) | 40 | 22 | 15 | | |
| $A_{max}$ (AQ) | 3.2±1.2 | 3.4±0.9 | 7.4±1.7 | 0.64 | < 0.0001 |
| $A_{mass}$ | 30.4±13.2 | 55.4±18.2 | 110.8±42.7 | 0.64 | < 0.0001 |
| PNUE | 34.8±15.8 | 45.2±18.4 | 85±30.3 | 0.47 | < 0.0001 |
| LMA | 108.8±18.7 | 64.4±16.6 | 77.3±36.1 | 0.44 | < 0.0001 |
| %C | 47.8±1.4 | 44.5±1.9 | 45.6±2.6 | 0.40 | < 0.0001 |
| SLA | 95±18.7 | 166.2±47 | 154.5±65.7 | 0.40 | < 0.0001 |
| Light Saturation (AQ) | 227.9±157.6 | 221.8±124.4 | 554.9±225.4 | 0.37 | < 0.0001 |
| C:N | 40.2±10.3 | 26.7±6.8 | 27.1±10.6 | 0.32 | < 0.0001 |
| IS 50% (Induction) | 8.3±4.2 | 22.3±13.9 | 26.2±18.9 | 0.31 | < 0.0001 |
| TPU (Aci) | 2±1 | 1.7±0.8 | 3.7±1.6 | 0.30 | < 0.0001 |
| %N | 1.3±0.3 | 1.9±0.7 | 1.9±0.6 | 0.27 | < 0.0001 |
| $Vc_{max}$ (Aci) | 12±6.1 | 9.2±4.3 | 20.5±9.2 | 0.26 | < 0.0001 |
| $J_{max}$ (Aci) | 9.6±5.2 | 6.9±3.6 | 16.3±9.2 | 0.23 | < 0.0001 |
| Light Compensation (AQ) | 9.4±3.8 | 5.7±2.7 | 8.2±3.3 | 0.17 | 0.0004 |
| WUE | 6.9±1.6 | 5.2±1.5 | 5.6±1.9 | 0.15 | 0.0008 |
| Respiration (AQ) | -0.5±0.2 | -0.4±0.2 | -0.5±0.2 | 0.14 | 0.0017 |
| Convexity (Induction %) | 0.5±0.3 | 0.3±0.2 | 0.4±0.3 | 0.14 | 0.0017 |
| $\delta^{13}C$ | -30.2±1.3 | -31.1±1.8 | -30.1±1.1 | 0.06 | 0.0427 |
| $\delta^{15}N$ | -2.8±1.6 | -2.8±1.9 | -2.3±1.7 | NS | NS |
| AQE (x100) (AQ) | 6.8±2.5 | 6.5±0.9 | 6.7±0.8 | NS | NS |
| Convexity (AQ) | 3.3±3.2 | 2.6±2.1 | 1.9±1 | NS | NS |
| $N_{area}$ | 1.4±0.3 | 1.2±0.7 | 1.3±0.4 | NS | NS |

AQE = Apparent quantum efficiency; TPU = Triose phosphate utilization; IS = Induction state; PPFD = Photosynthetic photon flux density; WUE = Water use efficiency; SLA = Specific leaf area; LMA = Leaf mass per area; PNUE = Photosynthetic nitrogen use efficiency.

**Table 4.7**: Forest elevation, structure and micro-climate mean ± standard deviation (SD) for low, medium and high light environment *K*-means clusters and results of among cluster one-way ANOVAs. Categorical classifications are % true and differences among clusters are assessed using the Pearson test.

| **Variables** | **Modeled light environment** | | | **Adj-$R^2$** | ***P*-value** |
|---|---|---|---|---|---|
| | **Low** | **Medium** | **High** | | |
| Cluster size (*N*) | 40 | 22 | 15 | | |
| Elevation (m) | 1176±124 | 1173±124 | 1090±105 | NS | NS |
| Canopy height (m) | 21.6±6.8 | 18.4±8.2 | 21.1±9.6 | NS | NS |
| Total plant height (m) | 12.8±9.5 | 2.7±2.4 | 2.6±1.6 | 0.33 | < 0.0001 |
| Leaf height (m) | 7.5±5.1 | 1.5±0.5 | 1.8±1.2 | 0.38 | < 0.0001 |
| DBH (cm) | 57.3±59.7 | 9.3±4.5 | 11.2±2.7 | 0.26 | < 0.0001 |
| Airborne LAI ($m^2$) | 4.1±0.3 | 4.1±0.4 | 4.1±0.3 | NS | NS |
| Modeled Mean PPFD (µmol $m^{-2}$ $s^{-1}$) | 173±27.8 | 226±94.5 | 318±203.2 | 0.21 | < 0.0001 |
| Modeled SD PPFD (µmol m-2 s-1) | 98±14.4 | 121±40.0 | 157±75.5 | 0.21 | < 0.0001 |
| Modeled Mean temp (°C) | 16.9±0.5 | 17±0.7 | 17.6±0.7 | 0.13 | 0.0018 |
| | | | | **ChiSquare** | ***P*-value** |
| Native spp. (%) | 100 | 87 | 67 | 13.4 | 0.0013 |
| *M. polymorpha* (%) | 45 | 0 | 7 | 18.7 | < 0.0001 |
| Canopy position (%) | 78 | 42 | 7 | 44.4 | < 0.0001 |
| Height strata: Upper (%) | 53 | 27 | 0 | 33.5 | < 0.0001 |
| Height strata: Middle (%) | 40 | 43 | 47 | - | - |
| Height strata: Lower (%) | 8 | 30 | 53 | - | - |

## 4.10 Figures

**Figure 4.1:** Overview of remote sensing and field data integration and analysis. Hyperspectral and waveform light detection and ranging (LiDAR) data were collected simultaneously using the Carnegie Airborne Observatory (CAO) while discrete LiDAR was collected separately. Field data collected for parameterization and validation included: (a) LAI-2000 for leaf area index (LAI; two-dimensional), (b) vertical leaf area density (LAD; three-dimensional) transects, (c) microclimatic data, and (d) leaf trait measurements throughout the study transect. Leaf traits included chemical and gas exchange analyses. Microclimate data included modeled daytime mean and standard deviation photosynthetic photon flux density (PPFD) and modeled mean daytime air temperature. Spatial data included location, elevation and forest structural information. Taxonomic data included species, native vs. exotic status, and life form. Principal component analysis (PCA) axes were input into *k*-means analysis to identify ecophysiological similar clusters that were explained through differences in microclimate, taxonomy and spatial location.

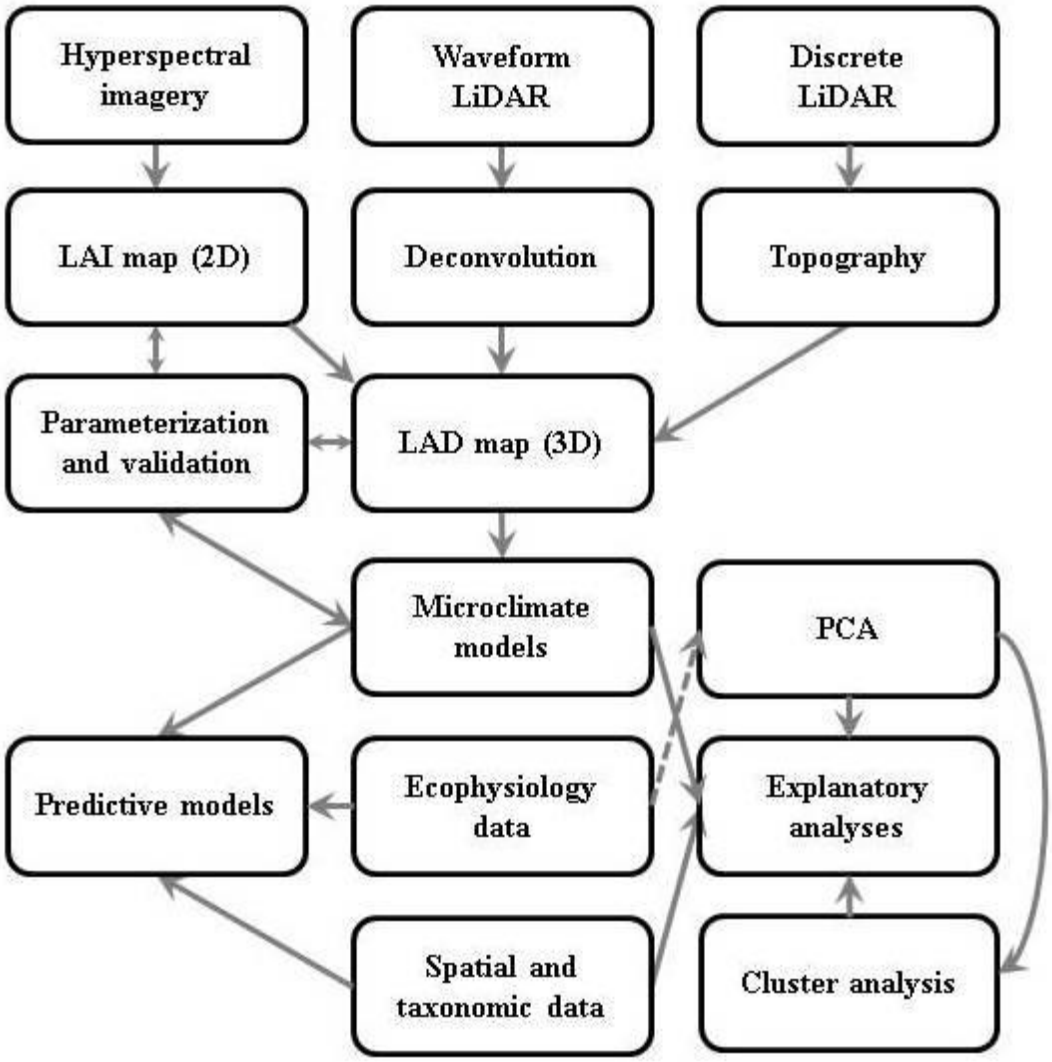

**Figure 4.2:** Study area (C) located within the Hawaii Experimental Tropical Forest (B) in Laupahoehoe, Hawai'i (A). Inset C provides tree height at 1.25 x 1.25 m resolution, with heights ranging from 0 m (black) to 40 m (white).

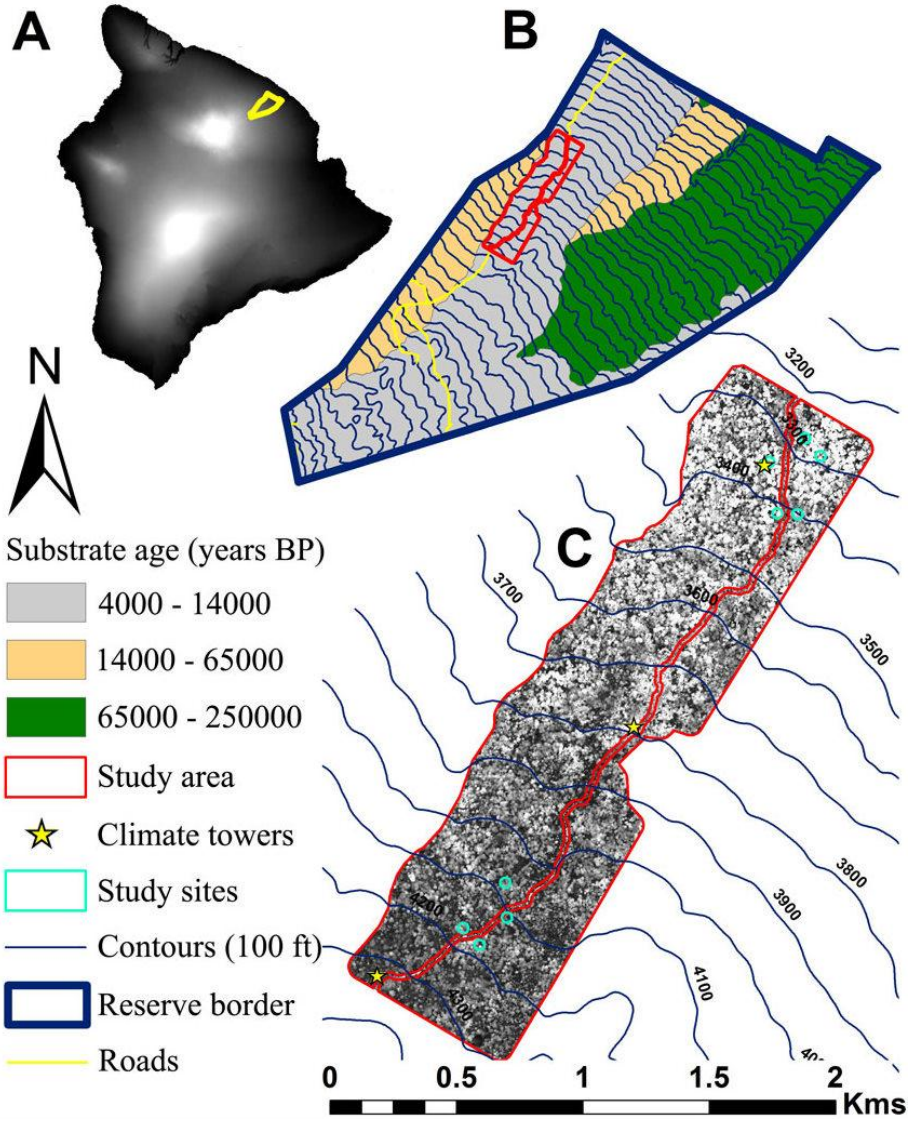

**Figure 4.3:** Tree height (m) and leaf area index (LAI; $m^2$ $m^{-2}$) for 50 m elevation classes. Data derived from airborne hyperspectral imagery (1.25 x 1.25 m resolution) with $N$ > 500,000 pixels per elevation class.

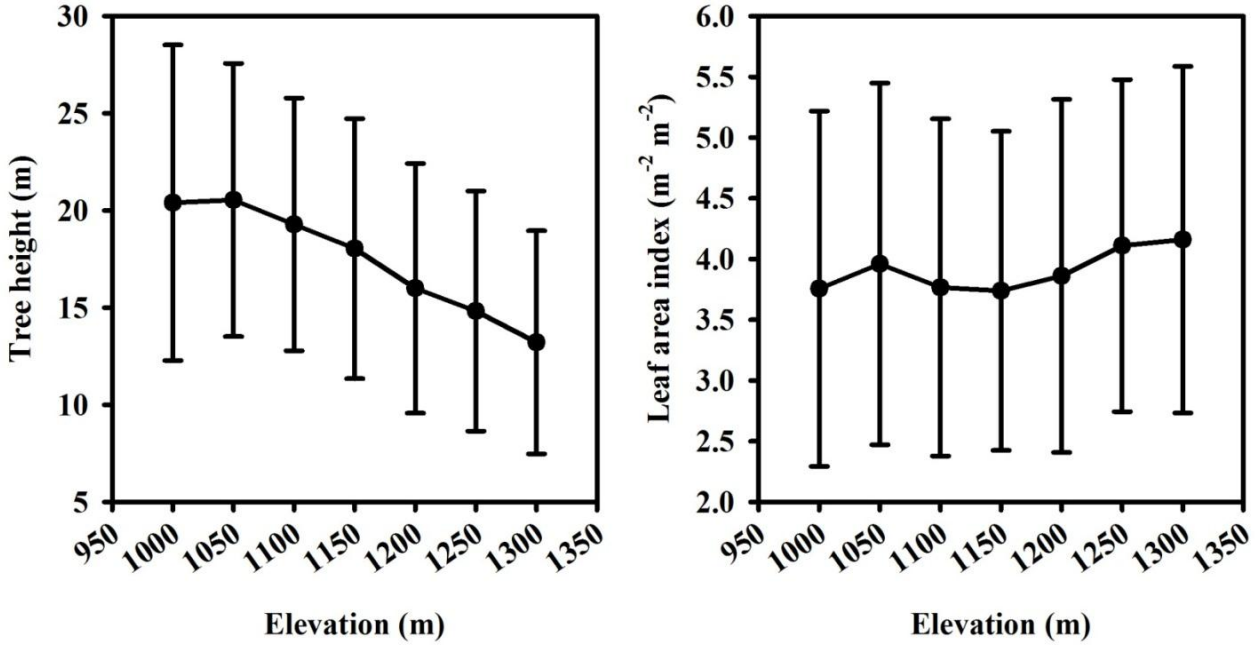

**Figure 4.4:** Measured daily average daytime (solar elevation > 25°) photosynthetic photon flux density (PPFD; μmol $m^{-2}$ $s^{-1}$), diffuse PPFD (%), and air temperature (°C) at the mid elevation top-of-canopy climate tower. Julian dates extend from January 1st, 2010 (40179 JD) through June 17th, 2011 (40711 JD).

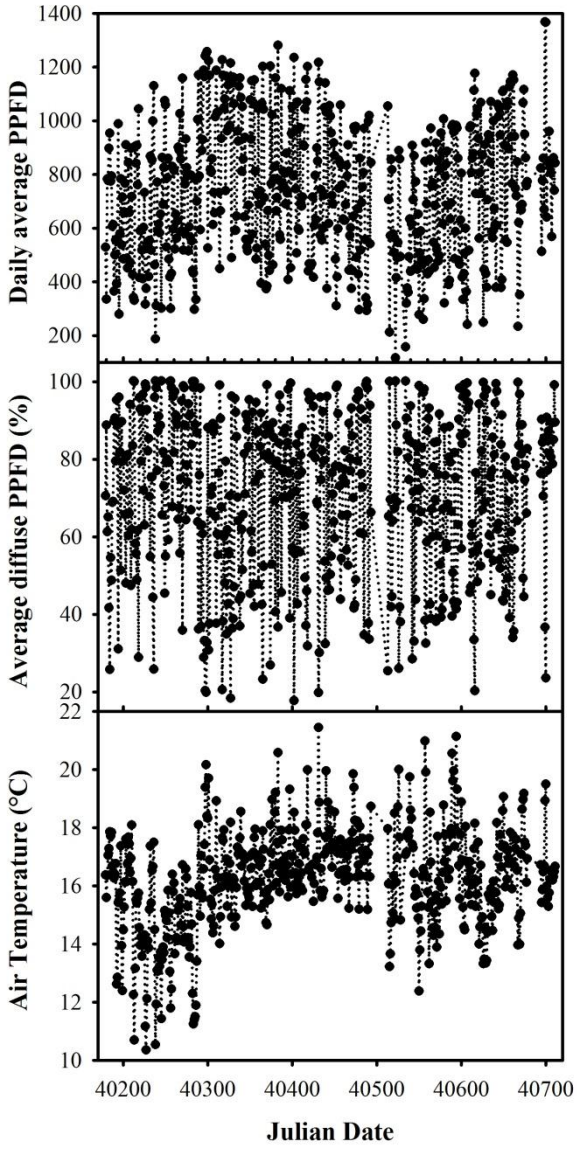

**Figure 4.5:** Measured hourly mean daytime (solar elevation > 25°) photosynthetic photon flux density (PPFD; µmol $m^{-2}$ $s^{-1}$), diffuse PPFD (%), and air temperature (°C) at mid elevation top-of-canopy climate tower.

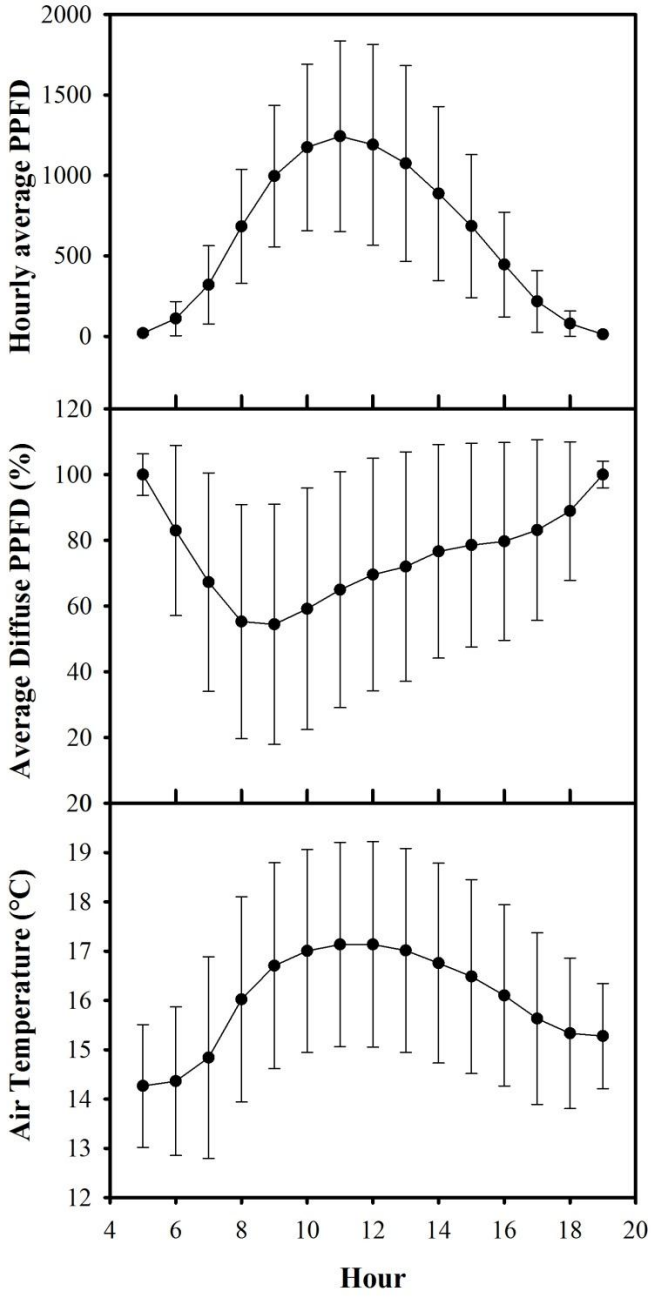

**Figure 4.6:** Principal leaf trait clusters identified through *k*-means analysis. Low, medium and high light clusters are represented by the colors red, blue, and green, respectively.

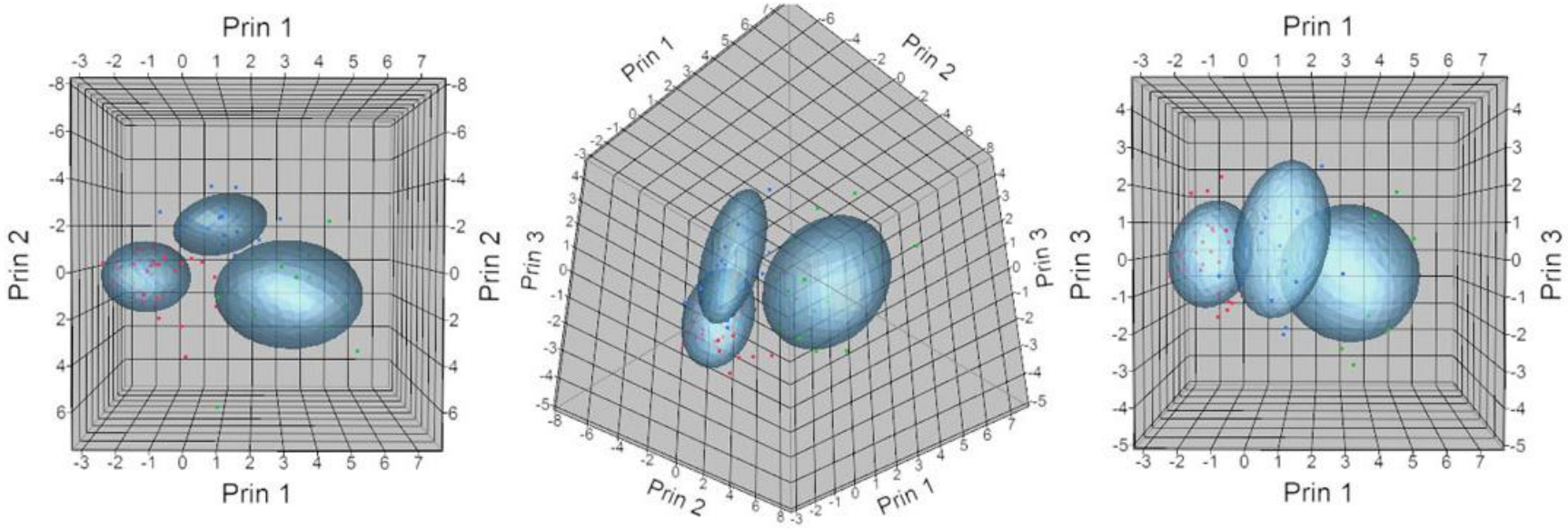

**Figure 4.7:** Relationships (log-log regressions) between $A_{max}$ (maximum μmol $C0_2$ $m^{-2}$ $s^{-1}$) and modeled mean daily PPFD (μmol $m^{-2}$ $s^{-1}$) for the entire community and modeled low, medium and high light leaf trait clusters. Regressions for the community and modeled medium and high light leaf trait clusters are significant ($P < 0.05$).

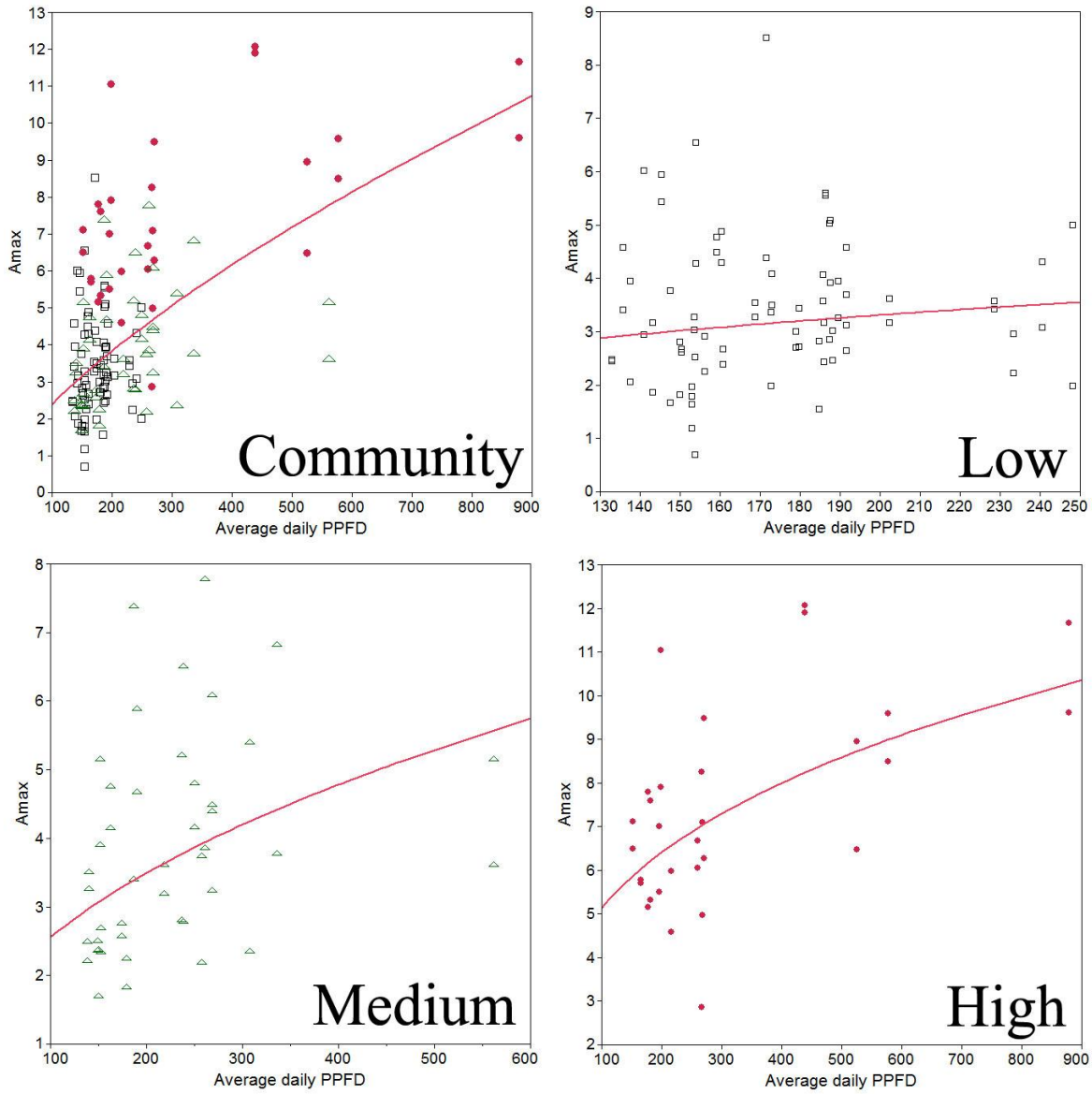

**Figure 4.8:** Relationship of multiple regression foliar $\delta^{15}N$ residuals versus modeled mean daytime air temperature (°C) and leaf height (m).

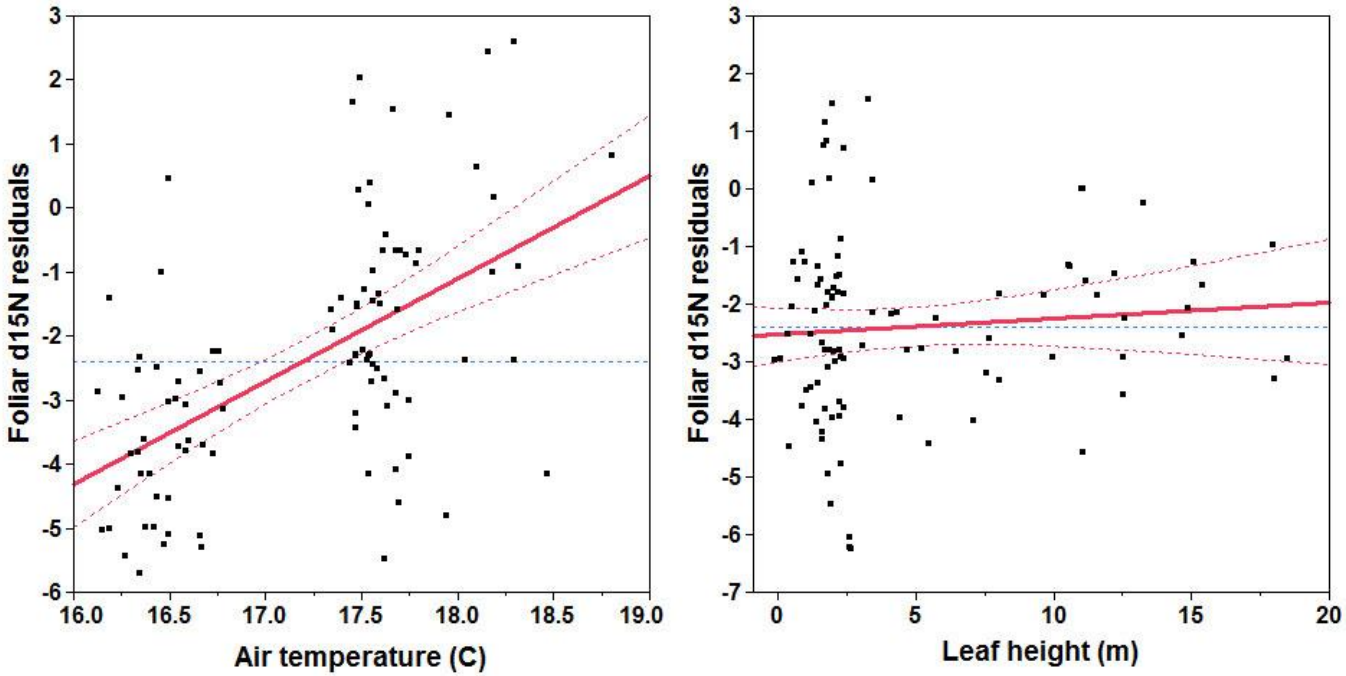

## 4.11 Supplementary Materials

**SM 4.1:** Pearson correlations between elevation and forest structure variables and modeled mean and standard deviation (SD) photosynthetic photon flux density (μmol $m^{-2}$ $s^{-1}$) and air temperature (°C). *P*-value significance increases from white (<0.05), light grey (< 0.01) to dark grey (< 0.001). Row numbers refer to numbered column variables.

| Variables | 1 | 2 | 3 | 4 | 5 | 6 | 7 | 8 |
|---|---|---|---|---|---|---|---|---|
| 1. Elevation (m) | | | | | | | | |
| 2. Canopy height (m) | -0.56 | | | | | | | |
| 3. Plant height (m) | | 0.27 | | | | | | |
| 4. Leaf height (m) | | 0.31 | 0.93 | | | | | |
| 5. Total canopy height (%) | 0.28 | -0.22 | 0.79 | 0.83 | | | | |
| 6. DBH (cm) | | | 0.8 | 0.82 | 0.74 | | | |
| 7. Modeled mean PPFD | -0.39 | | -0.48 | -0.52 | -0.59 | -0.52 | | |
| 8. Modeled SD PPFD | -0.55 | | -0.53 | -0.6 | -0.61 | -0.53 | 0.85 | |
| 9. Modeled mean air temp | -0.92 | 0.43 | -0.21 | -0.25 | -0.42 | -0.32 | 0.69 | 0.76 |

**SM 4.2:** Pearson correlations between foliar variables. *P*-values < 0.05, 0.01, 0.001 and 0.0001 are represented by increasing shades of grey. Row numbers refer to numbered column variables.

| | 1 | 2 | 3 | 4 | 5 | 6 | 7 | 8 | 9 | 10 | 11 | 12 | 13 | 14 | 15 | 16 | 17 | 18 | 19 | 20 |
|---|---|---|---|---|---|---|---|---|---|---|---|---|---|---|---|---|---|---|---|---|
| 1. C % | | | | | | | | | | | | | | | | | | | | |
| 2. N % | -0.24 | | | | | | | | | | | | | | | | | | | |
| 3. C:N | 0.37 | -0.87 | | | | | | | | | | | | | | | | | | |
| 4. $\delta^{13}C$ | | | | | | | | | | | | | | | | | | | | |
| 5. $\delta^{15}N$ | | 0.31 | -0.29 | | | | | | | | | | | | | | | | | |
| 6. Light Saturation (AQ) | | 0.27 | -0.32 | | 0.28 | | | | | | | | | | | | | | | |
| 7. Light Comp. (AQ) | 0.41 | -0.36 | 0.38 | | | -0.22 | | | | | | | | | | | | | | |
| 8. Convexity (AQ) | | | | | | -0.5 | | | | | | | | | | | | | | |
| 9. Respiration (AQ) | -0.36 | 0.35 | -0.36 | | | | -0.86 | | | | | | | | | | | | | |
| 10. Amax (AQ) | | 0.39 | -0.37 | | 0.35 | 0.85 | -0.25 | -0.26 | 0.29 | | | | | | | | | | | |
| 11. Vcmax (Aci) | | 0.29 | -0.21 | | 0.27 | 0.45 | | | | 0.69 | | | | | | | | | | |
| 12. Jmax (Aci) | | 0.24 | | | 0.23 | 0.37 | | | | 0.61 | 0.98 | | | | | | | | | |
| 13. TPU (Aci) | | 0.3 | -0.22 | | 0.28 | 0.48 | | | | 0.73 | 0.98 | 0.95 | | | | | | | | |
| 14. Convexity (Ind. raw) | 0.23 | | | | | 0.27 | | | | 0.43 | 0.41 | 0.37 | 0.39 | | | | | | | |
| 15. IS 50% (Ind.) | -0.55 | 0.28 | -0.3 | | 0.29 | 0.21 | | | | 0.22 | | | | -0.5 | | | | | | |
| 16. WUE | 0.4 | | | | | | | | | | | | | 0.32 | -0.46 | | | | | |
| 17. SLA | -0.41 | 0.44 | -0.51 | | | | -0.32 | | 0.25 | | | | | | | | | | | |
| 18. LMA | 0.45 | -0.51 | 0.59 | | | | 0.42 | | -0.37 | | | | | | | | -0.92 | | | |
| 19. Narea | | 0.53 | -0.36 | | 0.3 | | | | | | 0.22 | 0.23 | 0.21 | | | | -0.45 | 0.42 | | |
| 20. PNUE | -0.33 | | | | | 0.65 | -0.25 | -0.29 | 0.21 | 0.77 | 0.43 | 0.36 | 0.49 | 0.26 | 0.34 | | 0.53 | -0.47 | -0.4 | |
| 21. Amass | -0.26 | 0.51 | -0.5 | | 0.27 | 0.69 | -0.31 | -0.23 | 0.32 | 0.87 | 0.56 | 0.46 | 0.61 | 0.33 | 0.36 | | 0.6 | -0.56 | | 0.84 |

TPU = Triose phosphate utilization; IS = Induction state; WUE = Water use efficiency; SLA = Specific leaf area; LMA = Leaf mass per area; PNUE = Photosynthetic nitrogen use efficiency.

**SM 4.3:** Leaf trait principal component analysis (PCA) eigenvectors. PCA 1 and 2 have significant positive relationships with modeled mean photosynthetic photon flux density (μmol $m^{-2}$ $s^{-1}$) and modeled mean air temperature (°C), respectively.

| **Foliar variables** | **PCA 1** | **PCA 2** | **PCA 3** |
|---|---|---|---|
| %C | -0.12561 | 0.27258 | 0.11704 |
| %N | 0.23549 | -0.27856 | 0.21494 |
| C:N | -0.24773 | 0.29564 | -0.0541 |
| $\delta^{13}C$ | -0.00599 | 0.27701 | -0.07444 |
| $\delta^{15}N$ | 0.2006 | -0.06256 | 0.04016 |
| Light Saturation (AQ) | 0.25381 | 0.17838 | -0.32197 |
| Light Compensation (AQ) | -0.24622 | 0.17904 | -0.0774 |
| AQE (x100) | 0.00441 | 0.05646 | -0.34937 |
| Convexity (AQ) | -0.1033 | -0.0795 | 0.41917 |
| Respiration (AQ) | 0.24404 | -0.1407 | 0.18253 |
| $A_{max}$ € | 0.32548 | 0.17753 | -0.09415 |
| $Vc_{max}$ (Aci) | 0.27112 | 0.23879 | 0.21301 |
| $J_{max}$ (Aci) | 0.23556 | 0.25331 | 0.24395 |
| TPU (Aci) | 0.28428 | 0.21586 | 0.18983 |
| Convexity (Induction %) | 0.16278 | 0.28224 | 0.13882 |
| IS 50% (Induction) | 0.07844 | -0.28451 | -0.15312 |
| WUE | -0.07849 | 0.08228 | 0.14378 |
| SLA | 0.19106 | -0.26865 | -0.17269 |
| LMA | -0.18336 | 0.3099 | 0.14023 |
| $N_{area}$ | 0.10962 | -0.12966 | 0.36804 |
| PNUE | 0.28129 | 0.17249 | -0.28471 |
| $A_{mass}$ | 0.34059 | 0.07366 | -0.10055 |

**SM 4.4:** Relationships between multiple regression residuals of axis one and two of principal component analysis (PCA) of foliar ecophysiological variables versus box-cox transformed modeled mean photosynthetic photon flux density (µmol $m^{-2}$ $s^{-1}$) and modeled mean air temperature (°C).

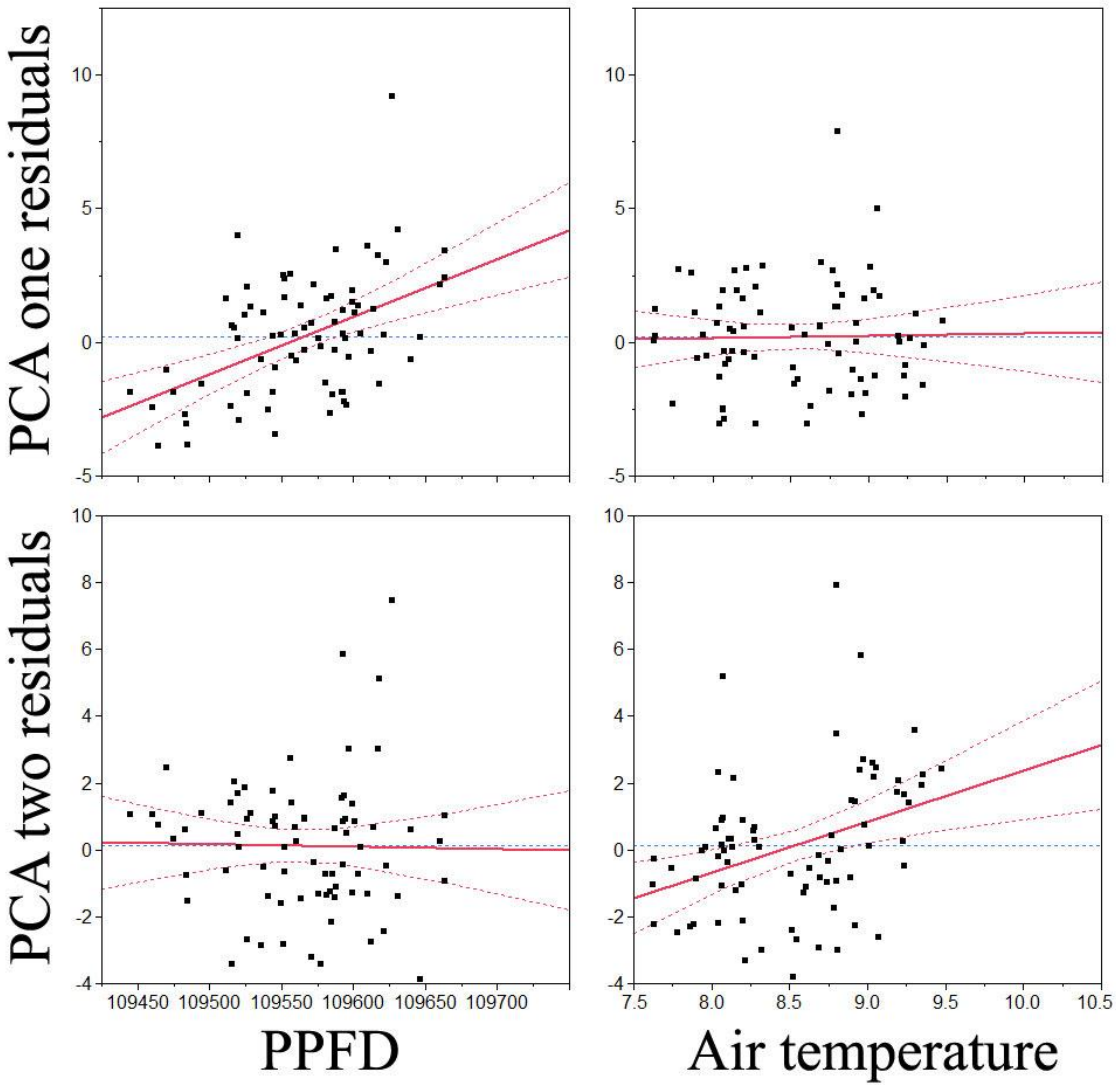

**SM 4.5:** Clear sky top-of-canopy photosynthetic active radiation (PAR) model coded in R language. This model was used to validate calibration of top-of-canopy PAR sensors at each climate tower.

```
# Author: Eben Broadbent
# Contact: eben.broadbent@gmail.com
# Date: 03/05/2012
# Description: Coded in R by Eben Broadbent (PhD candidate at Stanford Biology)
#  from an Excel version of equations provided by Jacob Bingham
(Jacob.Bingham@apogeeinstruments.com,
# Application Engineer at Apogee Inc.) of Apogee Instruments (www.apogeeinstruments.com).

# Instructions for Calculating Quantum Sensor Accuracy:
#  1 - Comparison must be made on a clear, non-polluted, summer day within two hours of solar noon.
#  2 - Sensor must be level and perfectly clean. Enter your measured solar radiation in the blue cell
below.
#  3 - Enter input parameters in green cells below.
#  4 - Difference between the model and your sensor is shown in the yellow cell below.
#  5 - If the measured value is more than 5 % different than the estimated value on replicate days,
contact Apogee for recalibration.

#Definitions:
#          Latitude =          latitude of the measurement site [degrees]
#                    (positive for Northern hemisphere, negative for Southern hemisphere)
#          Longitude =         longitude of the measurement site [degrees]
#          Longitudetz =       longitude of the center of the local time zone [degrees]
#                    (expressed as positive degrees west of the standard meridian in Greenwich, England)
#                    Examples: 75, 90, 105, and 120 for Eastern, Central, Rocky Mountain, and Pacific
time zones in the US
#                              0 for Greenwich, England; 345 for Paris, France; 255 for Bangkok, Thailand
#          Elevation =         elevation of the measurement site [meters]
#          Day of Year =       numeric day of the year (0-365)
#          Time of Day =       numeric time of the day in tenths of hours (0-24.0)
#          Daylight Savings =          correction to account for daylight savings time (enter 1 if on
daylight savings time, 0 if not)
#          TA =      air temperature at the time of measurement [C] (if air temperature is not available,
leave cell blank)
#          RH =      relative humidity at the time of measurement [%] (if relative humidity is not
available, leave cell blank)
#          Measured PPF =  measured value of photosynthetic photon flux [mmol m-2 s-1] from the
sensor being tested
#          Model Estimated PPF =     estimated photosynthetic photon flux [mmol m-2 s-1] incident on a
horizontal plane for clear sky conditions
#          Difference from Model =   difference in percent between the measured and estimated values of
radiation

#Definitions:
#          Solar Constant = solar constant for the mean distance between the Earth and sun
#          Energy in PAR = average energy content of photosynthetically active radiation (PAR)
#          PAR / Solar =       ratio of photosynthetically active radiation (PAR) to incoming shortwave
radiation (SWi)
#          Kt =      atmospheric turbidity coefficient (1 for clean air)
#          dr =      inverse relative distance factor for the distance between the Earth and sun
```

```
#          d =       solar declination
#          eqt =     equation of time
#          Solar N =          time of solar noon
#          Solar Z =          solar zenith angle
#          Kb =      clearness index for direct beam radiation
#          Kd =      transmissivity index for diffuse radiation
#          PB =      barometric pressure of the measurement site (kPa)
#          eA =      air vapor pressure (kPa)
#          w =       precipitable water in the atmosphere (mm)
#          SWa =     extraterrestrial radiation (W m-2)

# Reference:
#  The ASCE Standardized Reference Evapotranspiration Equation. 2005. American Society of Civil Engineers. Reston, Virginia, USA.

# Coding notes:
#  Run on .csv sheet containing over 800,000 rows and 20 columns of met data. will run in < 1 minute.
# Set working directory (where input and output files are stored/written to)
setwd("")
# Open .csv table (must have column names as defined below, including columns created for output of modeled variables)
datain <- read.csv('Input Met Data.csv', header=TRUE, colClasses = "character")
colnames(datain)

# User defined variables
D9  = 41.7                              # Latitude =          41.7  (from http://itouchmap.com/latlong.html)
D10 = 111.8                             # Longitude =         111.8 (from http://itouchmap.com/latlong.html)
D11 = 105                               # Longitudetz =       105  (150 = Hawaii time zone) (http://clearskycalculator.com/longitudeTZ.htm)
D12 = 1400                              # Elevation =         1400   (from Google Earth)
D13 = as.numeric(datain$day_of_year)          # Day of Year =             172  (input from 10 minute measurements)
D14 = round(as.numeric(datain$day_hours),1)     # Time of Day =         13.5 (input from 10 minute measurements) (HI correction applied, 3 hours difference)
D15 = 0                                 # Daylight Savings = 0 (Hawaii does not observe daylight savings time (thus = 0): http://www.timetemperature.com/tzus/hawaii_time_zone.shtml)
D16 = as.numeric(datain$mid_Ta)               # TA =   25 (input from 10 minute measurements)
D17 = as.numeric(datain$mid_rH)               # RH =   30  (input from 10 minute measurements)

# test values of user defined variables (for copy / paste into R cmd line)
# D9=41.7;D10=111.8;D11=105;D12=1400;D13=172;D14=13.5;D15=1;D16=25;D17=30 # Apogee test
# D9=19.95;D10=-155.28;D11=150;D12=1155;D13=172;D14=12;D15=0;D16=25;D17=60 # Hawaii test

# Constants:
Q2 =      1367.8 # Solar Constant (W m-2)
Q3 =      218000 # Energy in PAR (J mol-1)
Q4 =      0.45        # PAR / Solar (J J-1)
Q5 =      1.0           # Kt

# Calculated Parameters:
Q8 = 1+0.033*cos(((2*pi)/365)*D13) # dr
```

```
Q9 =
asin(0.39785*sin((278.97+0.9856*D13+1.9165*sin((356.6+0.9856*D13)*(pi/180)))*(pi/180)))*180/pi
# delta
Q10 = (5.0323-
430.847*cos(((2*pi*D13)/366)+4.8718)+12.5024*cos(2*(((2*pi*D13)/366)+4.8718))+18.25*cos(3*(((
2*pi*D13)/366)+4.8718))-
100.976*sin(((2*pi*D13)/366)+4.8718)+595.275*sin(2*(((2*pi*D13)/366)+4.8718))+3.6858*sin(3*(((
2*pi*D13)/366)+4.8718))-12.47*sin(4*(((2*pi*D13)/366)+4.8718)))/60 # eqt
Q11 = 12+D15-(Q10/60)-((D11-D10)/15) # Solar N
Q12 = acos(sin(D9*(pi/180))*sin(Q9*(pi/180))+cos(D9*(pi/180))*cos(Q9*(pi/180))*cos((D14-
Q11)*(pi/12)))*(180/pi) # Solar Z

T8 = 101.325*((288-0.0065*(D12-0))/288)^(9.80665/(0.0065*287)) # Pb
T9 = 0.61121*exp((17.502*D16)/(240.97+D16))*(D17/100.0) # ea
T10 = 0.14*T9*T8+2.1 # w
T11 = 0.98*exp(((-0.00146*T8)/(Q5*sin((90-Q12)*(pi/180))))-0.075*(T10/sin((90-
Q12)*(pi/180)))^0.4) # kb

T12 = 0.18+0.82*T11 # kd, assumes <= 0.15 kb value

T11g = which(T11 > 0.15)
if (is.na(T11g[1]) == FALSE) {T12[T11g]  = 0.35-0.36*T11[T11g]}  # kd, adjusts for those having kb
not <= 0.15

T13 = Q2*Q8*cos(Q12*(pi/180)) # Swa

Model_Estimated_SW  = (T11+T12)*T13
Model_Estimated_PPF = (Q4/(0.000001*Q3))*(T11+T12)*T13 # umol m-2 s-1

# Write modeled PAR data into the data table
datain$Clearsky_PAR_modeled <- Model_Estimated_PPF
datain$Clearsky_SW_modeled  <- Model_Estimated_SW

# Create modeled parameter table
model_vals <-
cbind(datain$timestamp_1min,Q8,Q9,Q10,Q11,Q12,T8,T9,T10,T11,T12,T13,Model_Estimated_SW,M
odel_Estimated_PPF)

# Write out .csv
write.csv(datain, file = "Output MET with modeled.csv", row.names = FALSE)
write.csv(model_vals, file = "Model_parameters.csv", row.names = FALSE)
```

# CHAPTER 5

# PREDICTORS OF LEAF TRAIT VARIATION IN TREE SPECIES DURING FOREST SUCCESSION IN THE BOLIVIAN AMAZON

## 5.1 Abstract

Secondary forests encompass large areas of the tropics and play an important role in the global carbon cycle. During secondary forest succession, simultaneous continuous changes occur in stand structural attributes, soil properties, and in the composition of tree species, among other factors. Most studies classify tree species into categories based on their regeneration requirements. We use a high-resolution secondary forest chronosequence to assign tree species to a continuous gradient in species successional status assigned according to their distribution across the chronosequence. Species successional status, not stand age or differences in stand structure or soil properties, was found to be the best predictor of leaf trait variation. Foliar $\delta^{13}C$ had a significant positive relationship with species successional status, indicating changes in foliar physiology related to growth and competitive strategy, but was not correlated with stand age, whereas soil $\delta^{13}C$ dynamics were largely constrained by plant species composition. Foliar $\delta^{15}N$ had a significant negative correlation with both stand age and species successional status, resulting – most likely - from a large initial burning enrichment in both soil $^{15}N$ and $^{13}C$ and not closure of the nitrogen cycle. Foliar %C was not correlated with either stand age or species successional status but was found to have significant phylogenetic signal. Results from this study are relevant to understanding the dynamics of tree species growth and competition during forest succession and highlight possibilities of, and potentially confounding signals affecting, the utility of leaf traits to understand community and species dynamics during secondary forest succession.

*Key words: Community composition; foliar properties; forest succession; stable isotopes; swidden agriculture*.

## 5.2 Introduction

Secondary forests encompass a large and expanding portion of tropical forests worldwide (Asner et al. 2009). These forests provide valuable ecosystem services (Chazdon 2008), including biodiversity corridors and refugia (Moran et al. 2000), wildlife habitat, water filtration, and forest products (Wadsworth 1997). In addition, carbon uptake by secondary forests is an important factor in greenhouse gas emissions (Fearnside and Guimaraes 1996), with 30% of deforested areas in the Brazilian Amazon having been abandoned and now in some stage of regrowth (Houghton et al. 2000). Forest regeneration following slash-burn agriculture is of particular importance, as this activity has resulted in 50% of annual deforestation and 25% of estimated carbon emissions in Asia (Lawrence 2005). Due to their fast growth rates, these forests may help alleviate deforestation and degradation pressure on existing old-growth forests (Guariguata and Ostertag 2001). Given the importance of secondary forests, a detailed understanding of the successional processes governing the development of their structure, soil properties and species composition is critical. However, in spite of numerous studies on successional processes, substantial uncertainty exists regarding their growth rates (Fearnside and Guimaraes 1996), nutrient dynamics (Ostertag et al. 2008), and the interactions between land use history and successional trajectories (Guariguata and Ostertag 2001). This is, in part, a result of the numerous factors influencing regeneration, including soil type (Moran et al. 2000) and nutrient availability (Quesada et al. 2009), previous land use intensity (Gehring et al. 2005), fire history (Davidson et al. 2005), topography (Castilho et al. 2006), and distance to seed trees (Guevara et al. 1986).

During secondary forest succession, changes in stand structural attributes are simultaneous with changes in soil properties and species composition. Succession is

typically divided into distinct structural phases characterized by a unique suite of species (Budowski 1965) traditionally divided into successional / functional guilds (Finegan 1984, 1996; Kennard 2002; Pinard et al. 1999). The first phase of succession lasts only 1-5 years and is dominated by herbs, shrubs and climbers. During the second phase, from approximately 3-30 years following abandonment, pioneer species, with low wood density, rapid growth rates and high light requirements, develop a short stature closed canopy resulting in phase one species being shaded out. A transition then occurs within the pioneer species regeneration guild from short-lived 'pioneers of initiation' to longer-lived 'pioneers of exclusion' (Denslow 1996) species which, while still having high light requirements and rapid growth rates, are able to gain taller statures more typical of an old growth forest. In the final phase slow growing shade tolerant species with high wood density replace the pioneers, as most pioneer species seedlings are incapable of growing in the increasingly shaded understory, (Denslow 1987; Denslow and Guzman 2000), resulting in a composition similar to an old growth forest (Finegan 1996; Peña-Claros 2003). Waring and Running (2007) refer to the structural phases of forest succession as stand initiation, stem exclusion and understory reinitiation phases, with the final old growth stage, in both stand structure and composition, being reached 100 to 400 years post-abandonment.

At the species scale, forest succession theory has typically grouped species according to regeneration requirements into species successional categories or guilds (Swaine and Whitmore 1988). Although common, this approach is limited and studies are beginning to investigate the dynamics and ecological implications of approaches incorporating more detailed species successional classifications (Chazdon et al. 2010; Reich et al 1995). Such studies have the potential to elucidate gradients of change in successional species not easily seen when using categorical classifications (Peña-Claros 2003). New approaches have started by increasing the number of successional categories (Chazdon et al. 2010), referred to as plant functional types, and by developing continuous gradients of successional status using multi-variate methods (Peña-Claros 2003; Poorter et al. 2004). An improved understanding of how

successional status affects leaf traits in secondary forests is necessary given: (a) an increased interest in linkages between plant functional traits and species assembly processes (Garnier et al. 2004; Poorter 2007); and (b) the increasing use of leaf traits as indicators of ecosystem nutrient cycling and limitation (Davidson et al. 2007).

Foliar properties, including nutrients and isotopes, are being increasingly used to describe the dynamics of plant communities (Gusewell 2004; Koerselman and Meuleman 1996) and may provide new insights into community successional dynamics (Garnier et al. 2004). Within most terrestrial ecosystems, nitrogen (N) and phosphorus (P) availability are the primary limiters of plant growth (Gusewell 2004) and the foliar N:P ratio has been of particular focus (Townsend et al. 2007). Its use has highlighted changes from a conservative N cycle in early secondary sites to a conservative P cycle later in succession (Davidson et al. 2007), with an increase in the foliar N:P ratio being used to indicate a shift to P limitation on ecosystem processes (Tessier and Raynal 2003). Co-limitation by N and P is also possible (Davidson and Howarth 2007), similar to that which can occur during primary succession (Hedin et al. 2003). Further insights into ecosystem dynamics have been revealed by combining foliar nutrient concentrations with carbon and nitrogen stable isotopes. The carbon isotope ratio ($\delta^{13}C$) is representative of leaf intercellular processes and water use efficiency, integrating photosynthetic activity throughout the leaf's lifespan (Dawson et al. 2002). Foliar $\delta^{13}C$ is correlated with a broad range of plant functional characteristics, including leaf size and thickness, stomatal density, and gas exchange metabolism (Dawson et al. 2002) and leaf mass per area (LMA; Vitousek et al. 1990). The nitrogen stable isotope ratio functions as more of an ecosystem scale integrator determined by internal processes and varying input-output balances, with decreasing foliar $\delta^{15}N$ generally representing a tightening of the N cycle (Compton et al. 2007).

Although leaf traits have potential to improve our understanding of forest succession dynamics, few studies have been conducted on the factors, including stand or soil properties, constraining leaf trait variation (Dawson et al. 2002, Compton et al. 2007, Chazdon et al. 2010). In particular, few studies have investigated the drivers - including soil isotope variation (Billings and Richter 2006, Schedlbauer and Kavanagh

208) - of foliar isotope variation within different successional tree species during succession (Pardo et al. 2002, Bonal et al. 2007). We use a high-resolution forest succession chronosequence following slash-burn agriculture to evaluate the biotic and abiotic predictors of leaf trait variation in 20 tropical tree species encompassing a continuous gradient from early to late successional status. Biotic predictors include stand structural characteristics, taxonomic and phylogenetic analyses, and species successional position, calculated as the stand age at which each species becomes most abundant. Abiotic predictors include a suite of soil properties, including fertility and structure measurements. Our overarching research question is whether leaf trait variation during forest succession is explained principally by changes in: (a) stand age, (b) forest structure, or (c) soil properties, or, alternatively, by (d) shifts along a continuous gradient of species varying in environmental niche preference and growth strategy? In addition, we investigate phylogenetic signal as a predictor of leaf trait variation. Results from this study are relevant to better understanding forest regeneration following disturbance, a carbon sink of global importance, as well as forest community and species dynamics in general.

## 5.3 Materials and Methods

### 5.3.1 Study Sites

This study was carried out in the community of Molienda (municipality of Bolpebra and department of Pando) in the Bolivian Amazon (11°26’28.189” S, 69°09’30.06” W). The forest is considered lowland tropical moist forest with mildly undulating topography, has a mean annual rainfall of 1800 mm, and has a pronounced dry season extending from May to September (Beekma et al. 1996). In this community, most households rely on slash-and-burn agriculture as their principal food source, with preference to opening agricultural areas within primary forest. Patches of current slash-and-burn agriculture, usually less than 3 ha in extent - hereafter referred to as agriculture, and successional forests growing on abandoned agricultural fields are

dispersed throughout the primary forest, which dominates the landscape. Forest stands used in this study were identified through interviews with long-term residents. Information of each stand was cross-validated using important historical events and through triangulation via interviews with multiple community members. Only stands with similar topography, hydrology, and land use history were included. Stands were distributed widely throughout the landscape to minimize spatial auto-correlation. In total, 15 successional stands, with stand ages ranging from 4-47 years, and two primary forest stands were identified, giving this chronosequence among the highest temporal resolutions and range (Chazdon et al. 2007) identified in our literature review. As no age could be defined for primary forests data from these stands was used principally for phylogenetic signal analysis for which stand age estimation was not necessary. All stands were initially primary forest, which was cleared, burnt and then used for growing beans, corn, rice and yucca for 2-4 years prior to abandonment. No stands underwent wildfires, logging, or had been reentered for agricultural use post-abandonment. These stands, being first-cycle, are therefore representative of the lowest intensity of proceeding land use in the Amazon (Gehring et al. 2005). All stands were less than three hectares in extent and were surrounded by primary forest.

### 5.3.2 Forest structure and composition

Forest inventories were conducted using one 10 x 80 meter transect located diagonally across each stand. The transect location was randomly selected within each stand with the requirement that all transect area was at least 20 m from the stand edge. All trees, both living and dead, >= 2 m in height were measured. Botanical samples were collected and brought to the Centro de Investigación y Preservación de la Amazonia (CIPA) herbarium in Cobija, Bolivia for identification. All trees were mapped to Cartesian coordinates within each transect and, for each tree, we quantified diameter at breast height (DBH; 1.3m; cm), height (m), and crown exposure (CE), defined using a five-point scale (Clark and Clark 1992) in which 1 = no direct light or low amount of lateral light, 2 = intermediate or high amount of lateral light, 3 =

vertical light in part of the crown, 4 = vertical light in the whole crown, and 5 = exposed crown with direct light coming from all directions (i.e., emergent). Liana infestation was defined for each tree using a scale of 1 = none, to 4 = completely covered. The approximate percentage of each tree's crown volume was estimated for the following four categories: new, senescent, and mature leaves or no leaves present. Wood density was estimated for all tree species at the highest taxonomic resolution possible using the web-based wood density database (World Agroforestry Center 2010), and information derived from Nogueira et al. (2007) and Fearnside (1997). In cases where species identification was not available (29% of living stems), individuals were given the mean calculated wood density of the forest stand. Biomass (kg) was calculated using the equation for tree biomass described in Chave et al. (2005):

$$Biomass = 0.0509 \times Wood\ Density \times DBH^2 \times Tree\ Height \quad (1)$$

For each stand we also calculated the average and maximum tree height and DBH which we refer to as $height_{avg}$, $height_{max}$, $DBH_{avg}$, and $DBH_{max}$, respectively, and used the mean value of all trees within each stand to describe the other stand structural variables.

We used the Shannon Weiner index to compare compositional diversity among forest stands. The Chao-Jaccard (CJ) dissimilarity index (zero = no dissimilarity, one = complete dissimilarity) was run between all stand ages (excluding dead stems) (Chao et al. 2005) using the *vegdist* and *mantel* tests in the 'vegan' package in R. Significance of compositional differences among all stand ages was tested using the Pearson method of the Mantel test with 1000 permutations. We developed a continuous metric, termed species successional status, calculated separately for each tree species as the median stand age in which the each species occurred. Species successional status had a significant positive relationship with stand age (Adj-$R^2$ = 0.48, $P < 0.0001$, $N = 1479$; see Fig. 5.1), while the lower $R^2$ value indicated that tree species occurred across a wide range of stand ages enabling the subsequent comparative analyses of the effects of stand age and species successional status on leaf

trait variation. This approach differs from that of Peña-Claros (2003), and used by Poorter (2004), which used correspondence analysis to assign a value of 0 (earliest) to 100 (latest) for successional status, as it directly provides a successional status age for each species enabling direct comparison with measurements of stand structure and soil properties. Species data from primary forest stands were not used in the calculation of successional age as stand age was unknown.

### 5.3.3 Soil properties

Soil cores (2 x 4 ″; AMS, Inc., American Falls, ID) were collected for three randomly chosen locations at depths of 0-10, 10-20, and 20-30 cm. Soil samples were then aggregated for each depth in the field, oven dried at 50 °C for 72 hours, lightly ground and sieved to 2 mm to remove coarse particles, including roots and stones. Mineral fractions weighing ~150 grams were placed into 50 ml polypropylene centrifuge tubes for transportation to the Department of Global Ecology for further analysis. pH was measured on fresh soil samples in solution immediately following collection using a hand-held pH meter (Hanna Instruments, Inc.,Woonsocket, RI). Bulk density was determined using the approach described in (Elmore and Asner 2006) using the soil corer to obtain a soil from a known volume for each depth. Bulk density samples were oven dried at 70 °C for 96 hours, and sieved to 2 mm to remove roots and stones. The mineral fraction of the soil sample was weighed using a portable electronic scale (Ohaus, Inc., Pine Brook, NJ). The volume of fractions larger than 2 mm was recorded using the displacement method. The bulk density per depth was calculated as the mineral fraction sample mass divided by the volume (170-206 ml), adjusted for the volume of the large fraction (mean±standard deviation was 2.6±1.4 % of volume). Soil mass was calculated as Mg $ha^{-1}$ to 30 cm depth using the average of the three bulk density measurements and adjusted for the mass > 2 mm.

Following return to the Department of Global Ecology, Stanford, CA the soil samples were ground to a fine powder using a Wiley Mill and elemental content (%C; %N) for carbon and nitrogen and $\delta^{13}C$ and $\delta^{15}N$ isotope ratios were quantified using a

Carlo Erba EA 1110 C:N combustion (NC2500, CE Instruments, Milan, Italy) coupled with an isotope ratio mass spectrometer (IRMS Delta Plus, Finnigan Mat, San Jose, CA) operating in a continuous flow mode. Standards used for carbon and nitrogen isotopes are PDB and AIR, respectively. Data are expressed in δ (‰) notation (Martinelli et al. 1999, Ometto et al. 2006) where:

$$\delta = (R_{sample}/R_{standard} - 1) * 1000 \quad (2)$$

with R equal to the ratio of $^{13}C$:$^{12}C$ or $^{15}N$:$^{14}N$ for the sample and standard. In this context, a positive δ value means the sample has more of the heavier isotope than the standard and vice-versa. We use the terminology of enrichment (i.e., positive value or less negative trend; becoming heavier) or depletion (i.e., negative value or more negative trend; becoming lighter) of the heavier isotope versus the standard as described by Dawson et al. (2002). Individual soil depths were then aggregated and homogenized to get average 0-30 cm depth soil samples. These samples were measured for extractable phosphorus using the weak Bray and Sodium Bicarbonate methods (ppm; P1 and P2, respectively), soil pH (saturated paste method), extractable cations (ppm; K, Mg, Ca, Na and H) using 1.0 ammonium acetate @ pH 7.0, and soil texture using NaHexametaphosphate + hydrometer (%) at A&L laboratories (Modesto, CA). Cation exchange capacity (CEC) was calculated as the sum of K, MG, Ca, Na and H (meq/100g). All variables were converted from meq/100g, % or ppm to a 0-30 cm per hectare scale using the soil mass (kg $ha^{-1}$).

### 5.3.4 Foliar properties

Tree species selected for foliar analyses were identified to encompass a wide taxonomic range and to be present in as many age stands as possible. Two to three top of canopy trees of each study species were randomly chosen from each stand provided the particular species was present. In total, 149 tree individuals encompassing 20 species, or approximately 10% of all tree species, were selected. From these

individuals we collected 10-15 fully expanded mature leaves from two separate locations within the full sunlight portion of each individual's crown either by hand or using a shotgun. Leaf samples were oven dried at 60 °C for 72 hours, sealed in plastic bags and stored in an air-conditioned room prior to transportation to the Carnegie Institution's Department of Global Ecology at Stanford University. Foliar samples were aggregated to the scale of sample tree and ground to a fine powder using a Wiley Mill (Thomas Scientific, Swedesboro, NJ). Foliar N (TKN; mg $g^{-1}$) and P (TKP; mg $g^{-1}$) were extracted using a sulfuric acid/hydrogen peroxide digest and quantified using simultaneous colorimetric N and P analyses on an Alpkem rapid flow autoanalyzer (OI Analytical, College Station, TX), using the ammonium molybdate ascorbic acid method (Kuo 1996). Elemental content (%C; %N) for carbon and nitrogen and $\delta^{13}C$ and $\delta^{15}N$ isotope ratios were quantified on leaf samples aggregated from each tree using a C:N combustion analyzer coupled with an isotope ratio mass spectrometer as described in the soil methods. In all subsequent sections, foliar C:N refers to % measurements and foliar N:P ratio refers to Alpkem measurements.

### 5.3.5 Statistical analysis

Statistical analyses for this and all following sections were carried out using JMP v.7.0.1 (SAS Institute, Inc.) and in R v.2.9.2 (http://www.R-project.org). Summary statistics in the following sections refer to mean ± standard deviation. First, we measured overall changes in stand structural and soil properties through regressions versus stand age. Soil analyses are aggregated soil depth samples, with the exception - when indicated - of a multiple regression analysis for soil $\delta^{13}C$ and $\delta^{15}N$ including stand age, soil depth (5, 15 and 25 cm) and their interaction as predictor variables. While we compared secondary forest values with those from the primary forest plots using a two-sided t-test, results from these analyses were used for descriptive purposes only given the small primary forest sample size ($N = 2$ for soils and stand values). Second, we investigated relationships between leaf traits and a suite of predictor variables. Leaf traits were treated as response variables and

included: (a) %C, %N, and their ratio; (b) N (mg $g^{-1}$), P (mg $g^{-1}$), and their ratio; and (c) the stable isotope ratios $\delta^{13}C$ and $\delta^{15}N$. Potential predictors of leaf trait variation were: (a) stand age, (b) stand structure, (c) soil properties, and (d) species successional status. Third, to test for changes in plant isotope fractionation during succession – potentially indicative of changes in the importance of mycorrhizal fungi (Compton et al. 2007) – linear regressions were run between foliar-minus-soil isotope values, referred to as $\Delta\delta^{13}C_{plant\text{-}soil}$ or $\Delta\delta^{15}N_{plant\text{-}soil}$ (Amundson et al. 2003), and stand age and species successional status.

Whereas stand age and species successional status were individual values, the stand structure and soil properties groups were each composed of 18 unique, but often correlated, variables (Tables 1 and 2). To summarize each of these groups we used the first two axes of separate Principal Components Analyses (PCAs) (Marisol et al. 2011). To identify the most important predictor variables for each leaf trait we used the *bestglm* command (best subsets approach) based on the Akaike Information Criteria (AIC) in R and then used changes in the adjusted $R^2$ value to select the best number and combination of predictor variables for each leaf trait. Pearson correlations were used to assess relationships among all predictor variables. We further explored relationships between leaf traits, individual stand, and soil variables through regression analysis. To directly test the importance of stand age versus species successional status on leaf trait variation we used the ANOVA command in R to compare linear regression models including only stand age or species successional status to a model including both variables. To test if individual species followed the same relationships as those found across the species community we used linear regressions between leaf traits and stand age for four species (*Cecropia polystachya*, *Miconia* sp., *Jacaranda cuspidifolia* and *Inga* sp.) representing early to later successional statuses and occurring across a wide range of stand ages. In the case of foliar $\delta^{13}C$, in which intra-species patterns opposed those at the community scale, we ran an additional multiple linear regression model using stand age, species successional status and their interaction as predictor variables. Data for leaf trait analyses were transformed, when significantly different from normal as indicated

using the *shapiro.test* command in R, using either the Box Cox, logarithmic, square root, or exponential transformation in R.

Third, we tested separately for taxonomic and phylogenetic sources of leaf trait variation, similar to the approach used by Swenson and Enquist (2007). Taxonomic differences in each leaf trait were tested using a Kruskal-Wallis test in R. A phylogram of phylogenetic relationships among our study species, based on molecular data compiled into a mega-tree, was constructed using Phylomatic (www.phylodiversity.net/phylomatic/), which is a standard approach used in over 46 peer-reviewed articles (www.citeulike.org/group/4921/library/). Further relationships among the Fabaceae were resolved following the Tree of Life Web Project (www.tolweb.org/Fabaceae) and Wojciechowski et al. (2004), and among Moraceae following Zerega et al. (2005). Angiosperm node ages were calculated from Wikstrom et al. (2001) and Hedges et al. (2006) (www.timetree.org). The resultant phylogeny had five (of 18) soft polytomies the ages of which were estimated using Phylocom BLADJ (Branch Length ADJuster; www.phylodiversity.net/bladj; Webb et al. 2008), following which the phylogeny was converted to an ultrametric tree (i.e., branch lengths consistent with estimated relative time of divergence; see Appendix 5.1).

Tests for phylogenetic signal (i.e., do related taxa have more similar leaf traits) were run separately for each leaf trait and for species successional status using the *phylosignal* module of the *picante* package in R (Kembel et al. 2010). The *phylosignal* module tests for the presence of phylogenetic signal by comparing observed patterns of a leaf trait to a null model produced by randomly shuffling taxa labels across the tips of the phylogenetic tree (Blomberg et al. 2003), providing a *P*-value of signal significance, which does not provide information about trait evolution, and a *K*-statistic which tests for evolutionary processes by comparing trait data to an evolutionarily null model in which a *K*-statistic of one is equal to a Brownian motion model of evolution (Blomberg et al. 2003). Although *K*-statistic values greater than one indicate conservatism of traits versus random or convergent evolution (~0), we do

not purport to make any evolutionary arguments in this study (Ackerly 2009), given the incomplete status of our phylogenetic tree (Davies et al. 2011).

## 5.4 Results

### 5.4.1 Forest structure and composition

Forest structure and species richness and diversity information for all study sites is summarized in Table 5.1. Data were collected from 17 stands encompassing secondary forest ages 4 to 47 and two primary forest stands. We identified 205 species from 1,892 individual trees. The most abundant species was *Jacaranda cuspidifolia* (Bignoniaceous) which had 157 individuals and dominated the developing stand stage. One hundred and thirty eight of our species were represented by less than five individuals, while 78 were represented by only one. The average tree crown contained 65%, 8% and 4% of mature, senescent and new leaves, respectively, while 23% of the crown volume remained vacant. Three distinct phases were identified within our chronosequence (Fig. 5.2), corresponding to stand initiation, stem exclusion and understory reinitiation stages (Waring and Running 2007). During phase one the percentage of dead trees decreased rapidly from greater than 60% to less than 10% in the 4 and 7 year old stands, respectively. Phase two demonstrated a stem exclusion peak as shown through an increase, then decrease, in understory stem density. Phase three showed a steady increase in understory stem density with little stem mortality. Biomass increased according to a positive Michaelis-Menten asymptotic relationship with stand age during forest succession, while both tree height and DBH for the entire community and for emergent trees only, exhibited significant linear and quadratic relationships (Fig. 5.3). Peaks in tree height and DBH were found between 30-40 years post-abandonment. The Pearson mantel statistic showed significant changes in community composition among the study stands for the entire community ($R = 0.37$, $P = 0.001$, $N = 1892$) and within emergent trees only ($R = 0.43$, $P = 0.001$, N = 1892). While the entire tree species community became more similar to primary forest

species composition ($R^2$ = 0.75, $P$ < 0.0001, $N$ = 15) during succession, no such pattern was shown in the emergent trees, which remained completely dissimilar (i.e., Chao-Jaccard = 1) at all stand ages. Stand age had significant positive correlations with both species richness ($R^2$ = 0.62, $P$ < 0.0001, $N$ = 15) and species diversity ($R^2$ = 0.64, $P$ < 0.0001, $N$ = 15), as did species richness and diversity ($R^2$ = 0.93, $P$ < 0.0001, $N$ = 14). The standard error of species successional statuses, calculated across all stems in each stand, had a significant negative relationship with stand age ($R^2$ = 0.38, $P$ < 0.0001, $N$ = 14; Fig. 5.1). While rate of taxonomic compositional change was greatest following 20 years (Fig. 5.3), the rate of change in stand mean successional status was greatest prior to 10 years after which it reduced greatly (Fig. 5.1).

Structure PCA axes 1-3 explained 47%, 24%, and 9% of variation across all stand structural variables (see Table 5.1), respectively. PCA axis one had strong positive correlations with biomass, basal area, species diversity and $height_{max}$ and negative correlations with number of dead trees and the % crown with senescent leaves (Appendix 5.2). As the strongest correlations were with biomass, we refer to this as the biomass axis. PCA axis two had strong positive correlations with % crown with no leaves, $DBH_{avg}$ and $height_{avg}$ and negative correlations with tree density, liana infestation, and % crown with mature leaves. As the strongest correlations were with $height_{avg}$ and $DBH_{avg,}$ we refer to this axis as the structure axis. While the biomass axis had a significant positive linear relationship with stand age (PCA1 = -4.20 + 0.17 * Stand age, $R^2$ = 0.71, $P$ < 0.0001, $N$ = 15) the structure axis did not. Secondary forests, as compared to primary forests, had significantly lower biomass (178±110 vs. 304±31), wood density (528±75 vs. 604±4), $DBH_{max}$ (54.8±22.1 vs. 80.2±2.6), % crown in mature leaves (64.5±9.8 vs. 71.5±1.84) and greater mean crown exposure class (2.86±0.65 vs. 1.8±0.14), liana infestation (1.71±0.30 vs. 1.45±0.07) and % crown in senescent leaves (8.4±2.7 vs. 5.3±1.1).

### 5.4.2 Soil properties

Soil properties for all study sites are summarized in Table 5.2 and Figure 5.4. Significant relationships were found between stand age and soil mass (Mg ha-1) (positive, $R^2 = 0.55$, $P = 0.0058$, $N = 12$), soil $\delta^{13}C$ (negative, $R^2 = 0.45$, $P = 0.0171$, $N = 12$), CEC (positive, $R^2 = 0.31$, $P = 0.0592$, $N = 12$) and soil N (positive, $R^2 = 0.34$, $P = 0.0461$, $N = 12$). Strong positive trends were found, significant following exclusion of the youngest successional site, between stand age and soil carbon (Mg ha-1), ($R^2 = 0.31$, $P = 0.0589$, $N = 12$) - but not soil organic matter (%) or %C. A negative trend was identified between soil base saturation and stand age ($R^2 = 0.29$, $P = 0.0854$, $N = 11$). No significant relationships were found between stand age and soil P1, P2, or sand, silt and clay content (Mg ha-1), although soil P1 had a significantly negative relationship (with a trend in P2) with soil clay content ($R^2 = 0.38$, $P = 0.0321$, $N = 12$) which was not correlated with stand age. While soil %C had no correlation with bulk density, a strong negative trend was found between soil organic matter (%) and bulk density ($R^2 = 0.26$, $P = 0.0921$, $N = 12$). The multiple regression model of soil $\delta^{15}N$ which included soil depth was highly significant ($R^2 = 0.23$, $P = 0.0285$, $N = 38$), and showed a negative and positive relationship between soil $\delta^{15}N$ and stand age (*t*-ratio = -2.07, *F*-ratio = 4.29, *P*-value = 0.0459) and depth (*t*-ratio = 2.25, *F*-ratio = 5.08, *P*-value = 0.0307), respectively, and no significant interaction (although see Fig. 5.5 for trend). While the model of soil $\delta^{13}C$ was also significant ($R^2 = 0.28$, $P = 0.0111$, $N = 37$), only a positive relationship between $\delta^{13}C$ (which became less negative) and soil depth was found (*t*-ratio = 2.81, *F*-ratio = 7.90, *P*-value = 0.0083) - although a negative trend was found between soil $\delta^{13}C$ (which became more negative) and stand age (*t*-ratio = -1.70, *F*-ratio = 2.90, *P*-value = 0.0983) which was significant when aggregated as described above. Soil $\delta^{15}N$ within the secondary forest stands at mean 7.5, 15 and 25 cm depths were 8.25±1.26, 9.24±1.20, and 9.32±0.97 (‰), respectively, and soil $\delta^{13}C$ values at these depths were -28.43±0.46, -28.14±0.96, and -27.50±0.99 (‰), respectively. However, recognizing the sample size constraints ($N = 6$), no pattern of increasing soil $\delta^{15}N$ was found within the two primary forest stands ($P = 0.3594$) with soil $\delta^{15}N$ of 9.15±0.07, 9.65±0.49, and 8.60±0.28 (‰) for the three

depths, respectively, while soil $\delta^{13}C$ did become significantly less negative with depth ($R^2$ = 0.83, $P$ = 0.0079, $N$ = 6; varying from -28.3 to -26.4 from 7.5 to 25 cm depth, respectively).

Soil PCA axes 1-3 explained 30%, 22%, and 15% of variation across all soil property variables, respectively. Soil PCA axis one was positively correlated with P1, P2, C, Mg, CEC, base cations, and sand content and negatively correlated with stable isotopes, and silt and clay content (Appendix 5.2). As the strongest correlations were with the soil texture, measures we refer to this axis as the soil texture axis. Soil PCA axis two was positively correlated with C, N, $\delta^{13}C$, K, MG, H, and negatively correlated with $\delta^{15}N$. As strong correlations were identified throughout this group, and in particular with soil C, we refer to this axis as the soil fertility axis (Schoenholtz et al. 2000). While the texture axis had no significant relationship with stand age, the soil fertility axis had a significant positive linear relationship (PCA-2 = -2.73 + 0.10 * Stand age, $R^2$ = 0.42, $P$ < 0.0313, $N$ = 11). Secondary forests, as compared to primary forests, had significantly lower soil $\delta^{13}C$ (-28.20±0.53 vs. -27.25±0.21 (‰), respectively) and higher P2 (10.66±3.24 vs. 7.45±0.64, respectively).

### 5.4.3 Leaf traits

The tree species, and their descriptive statistics, selected for inclusion in foliar analyses are provided in Table 5.3. While most leaf traits were significantly inter-correlated, foliar $\delta^{15}N$ was only correlated with foliar %C (Appendix 5.3). Prior to assessing leaf trait relationships with our six predictor variables, we used Pearson correlations to understand their relationships (Appendix 5.4). Stand age was significantly correlated with all of the predictor variables except for soil texture, which was only correlated with the stand structure axis. Species successional status was correlated with both the stand biomass and soil texture axes. The best subsets regression using these predictor variables showed that while stand age had two significant relationships with leaf traits, specifically positive with foliar $\delta^{13}C$ (i.e., less negative) and negative with $\delta^{15}N$, species successional status had five significant

relationships, with foliar N (+), %N (+), C:N (-), N:P (+) and $\delta^{13}C$ (more negative) (Table 5.4 and Fig. 5.6). Foliar $\delta^{15}N$ had a significant positive relationship with soil $\delta^{15}N$ ($R^2 = 0.246$, $P < 0.0001$, $N = 232$) whereas none was found between foliar and soil $\delta^{13}C$. A significant negative correlation, although weak, was found between $\Delta\delta^{15}N_{plant\text{-}soil}$ and stand age ($R^2 = 0.029$, $P = 0.0089$, $N = 232$, but after exclusion of the youngest stand $R^2 = 0.119$, $P < 0.0001$, $N = 204$) and species successional status ($R^2 = 0.118$, $P < 0.0001$, $N = 232$), whereas a significant negative correlation was found only between $\Delta\delta^{13}C_{plant\text{-}soil}$ and species successional status ($R^2 = 0.149$, $P < 0.0001$, $N = 227$) (Fig. 5.7). Secondary forests, as compared to primary forests, had significantly higher foliar N (1.89±0.88 vs. 1.62±0.53), N:P (17.98±6.61 vs. 15.31±3.51), and %C (51.98±2.63 vs. 49.52±2.78) and lower foliar $\delta^{15}N$ (3.74±1.56 vs. 5.75±2.00).

The stand biomass and structure axes had significant correlations with foliar $\delta^{15}N$ - positive and negative, respectively - and soil texture had a significant positive correlation with foliar P and negative correlation with foliar N:P. Of all leaf traits only foliar %C was not significantly correlated with at least one predictor variable. For all leaf traits, species successional status had significantly higher explanatory power than stand age (Appendix 5.5). We then tested if correlations in leaf traits with stand age found across the species community also occurred within four individual species. No species had a significant relationship between foliar N, P, or N:P and stand age. Three species of four (*Inga* sp. being the exception) had significant negative relationships between foliar $\delta^{15}N$ and stand age ($R^2$ ranged from 0.19-0.26) and two species (*Miconia* sp. and *Jacaranda cuspidifolia*) had significant positive relationships between foliar $\delta^{13}C$ (less negative) and stand age ($R^2$ ranged from 0.09-0.13). Last, we tested for taxonomic and phylogenetic leaf trait signal. Although significant differences existed among species for all foliar variables ($R^2 = 0.38$ to 0.54, $P < 0.0001$), significant phylogenetic signal (i.e., more than by chance alone) was found for only foliar %C ($K = 1.2272$, $P = 0.0073$). We do not make a case for phylogenetic trait conservatism or any evolutionary arguments, especially as our significant *K*-statistic value was only marginally larger than one.

## 5.5 Discussion

In this study, we have used a high-resolution forest succession chronosequence to evaluate potential predictors of leaf trait variation. Specifically, we analyzed correlations among leaf traits and stand age, species successional status, and PCA derived axes of stand biomass and structure and soil texture and fertility. While all leaf traits, with the exception of foliar % C, had significant correlations with at least one predictor variable, the strongest relationships were found between foliar stable isotopes and stand age and species successional status. Although our discussion focuses on leaf trait variation during secondary forest succession, we also discuss patterns identified in stand structure and composition and soil properties, focusing on variation in soil $\delta^{13}C$ and $\delta^{15}N$.

### 5.5.1 Stand structure and composition

The rapid decline in dead stems in the early stages of succession were likely a result of both remnant dead stems from the slash and burn cycle and rapid turnover in species composition during the first 10 years of succession. Areas having undergone multiple slash and burn cycles would be less likely to have remnant dead trees, however our plots had undergone only one year of agriculture prior to abandonment. Krach et al. (1993) documented rapid turnover in species composition during the early stages of succession (< 10 years) which, subsequently, slowed dramatically. Our results however showed a rapid species turnover, as shown through decreases in composition differences as compared to primary forest, beginning 15 years post-abandonment. These differences may be due to methodological differences, with Krach et al. (1993) focusing only on cover of dominant species and our analyses using all stems within the forest stand while we analyze all stems within each stand. However, we did see a pattern of rapid change during the first 10 years when we look at changes in stand mean species successional status simultaneous with a reduction in the successional status variance. Such changes are in line with those predicted by the "Initial Floristic Composition" (IFC) hypotheses, which states that early successional

stands will contain a large proportion of the species dominating in later stages of succession (van Breugel et al. 2007). In our case, the rapid reduction in the early stages is due to high mortality of early pioneer species while the high variance in the early succession is due to the prevalence of later succession species. In older stands, pioneer species have died off due to differences in growth rates, longevity and shade-tolerance (Gómez-Pompa and Vázquez-Yanes 1981), reducing the variance of successional status in those stands.

Further insights are possible by separating overstory species from the community in general. The increase in community species richness was not seen in the overstory, whereas slight increases in diversity were seen. This represents a continual shift in overstory composition. However, the increasing species richness differs from that postulated by the IFC hypotheses, as new species are continually added throughout succession and earliest stands having low richness and high dominance by a few short-lived pioneers. The species similarity changes are on par with those hypothesized by Waring and Running (2007). Although the understory approximated primary forest composition after only 50 years, the overstory remained completely different (Fig. 5.3), similar to that found by Peña-Claros (2003). Waring and Running state that primary forest composition will be attained between 100-400 years post-abandonment. However, it is not possible to simply extrapolate vertical growth rates of shade tolerant trees now dominate in the understory to predict composition changes in the overstory as many have negligible growth rates (Blundell and Peart 2004), with changes occurring in pulse events following disturbance related gap openings (Canham 1988).

By 50 years, our secondary forests were similar in structure to our primary forest plots. Biomass was nearing the asymptote and average tree height and DBH had both begun to decrease. Similar dynamics have been seen during succession in the Amazon (Peña-Claros 2003, Denslow and Guzman 2000), with the earlier stages of succession having the greatest rates of biomass accrual (Silver et al. 2000). This relationship has been described as resulting from die-off of pioneer species simultaneous to establishment of long lived shade tolerant species, with more than 200

years being estimated to be required to attain primary forest biomass (Saldarriaga 1985). We found a quadratic relationship between stand age and the height of our emergent trees in which the mean height of emergent trees attained maximum values in intermediate stands. We postulated this to result from early successional species, with no recruitment in the understory, prior to species turnover to dominance by shade tolerant species (Saldarriaga 1985, Uhl et al. 1988). We found indications towards this occurring with the trees contributing the most to overstory composition in the intermediate aged stands to be early successional species growing past their identified species successional statuses ($R^2$ = 0.42, $P$ = 0.0658, $N$ = 13).

### 5.5.2 Soil properties

Changes in soil properties during secondary forest succession typically include increases in soil carbon (Silver et al. 2000) - although the opposite was found by Schedlbauer and Kavanagh (2008) who explained that active non-crystalline clays and aluminum-humus linkages may have resulted in higher carbon stability during land use than that found in other studies, increasing extractable soil N and decreasing P stocks (Feldpausch et al. 2004), and decreases in bulk density (Paul et al. 2002) [but see Werner (1984)] – among other possibilities (Ostertag et al. 2008). Generally, rapid decreases in total soil organic carbon (SOC) occur within the first 50 years following forest conversion, followed by slower losses until reaching a new lower equilibrium after 100 years. However, forest soils have significant memory and forest derived SOC represents >80% of the total pool if cultivation occurs for less than 5 years (Awiti et al. 2008). Global patterns of soil nitrogen are primarily controlled by mean annual precipitation and temperature that determine input from atmospheric deposition and N fixation, but during the slash-and-burn process, significant ecosystem nitrogen is lost through biomass removal, volatilization from combustion (Kauffman et al. 1995), and denitrification and leaching (Keller et al. 1993). During stand development, we found significant increases in soil mass that, in part, resulted in increasing pools of carbon and nitrogen, but not phosphorus. Feldpausch et al. (2004)

identified similar patterns during young successional stands (< 14 years), with soil nitrogen increasing but phosphorus moving from below- to above-ground. Such dynamics are typical during succession as available soil phosphorus declines during nutrient redistribution from vegetation growth due to virtually no primary minerals remaining in the highly weathered soils (Markewitz et al. 2004). Soil nitrogen, however, can increase through symbiotic nitrogen fixation, especially during early stages of succession (Cleveland et al. 1999, Rastetter et al. 2001) and atmospheric deposition (Holland et al. 1999). These changes were highlighted by the soil fertility axis, driven largely through N, increasing with stand age. Reductions in soil $\delta^{15}N$, although a non-significant negative trend with stand age, also formed an important contributor of the soil fertility axis.

Soil $\delta^{15}N$ is determined by the equilibrium of $\delta^{15}N$ inputs, outputs and internally through redistribution via plant uptake (Amundson et al. 2003; see theoretical fig. 5.7) and most soils have positive $\delta^{15}N$ values due to accumulated losses (Handley and Raven 1992). In general, ecosystems with high rates of nitrogen fractionation resulting in soil $^{15}N$ enrichment are viewed as having a leaky or open N cycle, typically with abundant N, versus ecosystems with a conservative or closed N cycle, and therefore reduced N loss, having reduced $^{15}N$ enrichment (Robinson 2001, Davidson et al. 2007). Input processes include: (a) soil $^{15}N$ depletion through atmospheric inputs, including from precipitation (Garten 1991), combustion (Andreae et al. 1988), and nitrogen deposition (Piccolo et al. 1994); and (b) soil $^{15}N$ enrichment via symbiotic nitrogen fixation related fractionation during uptake (Delwiche et al. 1979, Yoneyama et al. 1993, Hobbie and Colpaert 2003, Hobbie and Ouimette 2009). Output processes include: (a) soil $^{15}N$ enrichment through selective loss of $^{14}N$ during decomposition related nitrification and denitrification (Piccolo et al. 1994, 1996), including gaseous $^{14}N$ losses to the atmosphere (Houlton et al. 2006); and (b) soil $^{15}N$ enrichment through hydrologic leaching loss of $^{15}N$ depleted nitrogen (relative to the soil) produced during nitrification, denitrification and ammonia volatilization (Austin and Vitousek 1998). Redistribution processes include: (a) soil $^{15}N$ enrichment through discrimination against $^{15}N$ during biological nitrogen fixation, or creation of $^{15}N$

depleted compounds during decomposition and stabilization, and subsequent loss and/or assimilation of leachate from such activities at depth resulting in soil $^{15}N$ depletion (Hobbie and Ouimette 2009); and (b) discrimination against $^{15}N$ during plant uptake resulting in redistribution of depleted $^{15}N$ from mineral soil at depth to plant biomass and eventually to the surface horizon (Compton et al. 2007).

Patterns of soil $\delta^{15}N$ in depth profiles, now well established (Nadelhoffer and Fry 1988, Piccolo et al. 1996), result from multiple factors, including: (a) the soil surface can become $^{15}N$ depleted as litterfall accumulates at the soil surface while deeper soils can become $^{15}N$ enriched due to increased mycorrhizal fungal activity (Hobbie and Ouimette 2009); (b) N loss from nitrification and denitrification can result in either: (i) a steady soil $^{15}N$ enrichment with depth given abundant N availability (Hobbie and Ouimette 2009); or (ii) enriched soil $^{15}N$ at intermediate depth in arbuscular mycorrhizal (AM) systems and/or sites of higher available nitrogen (Schuur and Matson 2001); and/or (c) increases in soil fungi with depth resulting in soil $^{15}N$ enrichment (Wallender et al. 2009). Differences in soil texture may also play a role in defining soil $\delta^{15}N$, with increasing clay % generally accompanying soil $^{15}N$ enrichment (Delwiche and Steyn 1970), as well as land use intensity altering soil $\delta^{15}N$ (Koerner et al. 1999). Of particular importance, burning alters the $^{15}N$ pattern in soil profiles by eliminating the most $^{15}N$ depleted organic layer (Hobbie and Ouimette 2009) resulting in significant soil $\delta^{15}N$ enrichment in the upper 20 cm (Boeckx et al. 2005).

In our secondary forest stands, soil $\delta^{15}N$ both decreased with stand age and increased with soil depth. In the primary forest however, we found that soil $\delta^{15}N$ was greatest at intermediate depth followed by decreases as would be expected for AM systems or those with higher N availability (Schuur and Matson 2001). Differences along the stand age gradient were unlikely a result of chronosequence errors as no significant gradients in soil clay content were found (Delwiche and Steyn 1970). The pattern of soil $^{15}N$ enrichment with depth may develop rapidly due to the large soil $^{15}N$ enrichment in the upper 20 cm from combustion fractionation during the burning process (Boeckx et al. 2005), preferentially moving $^{14}N$ downwards. Such dynamics

would occur most rapidly during the agricultural phase and in early successional stands with less well developed root mats and reduced bulk density but continue throughout all stands. Although no significant interaction effect was found showing reduced profile significance with stand age, as would have been expected if our secondary forest $^{15}N$ profiles were developing towards those found in the primary forests, this could take longer than our secondary stands studied (Hobbie and Ouimette 2009).

The subsequent significant soil $^{15}N$ depletion with stand age, which occurred most rapidly in the shallower depths most affected by burning (see trend in Fig. 5.5), would then be due to simultaneous influence of: (a) atmospheric deposition of isotopically lighter $^{14}N$ (Piccolo et al. 1994), of especial importance in this area due to the intense annual fire season (Cochrane 2011); (b) preferential leaching of soil $^{14}N$, and $^{15}N$ depleted products, during the intense annual wet season (Austin and Vitousek 1998, Myneni et al. 2007); (c) changes in plant root distribution and increased foraging depth causing changes in the utilization of soil inorganic N pools (Piccolo et al. 1994) or acting as a biological pump to the surface via litterfall (Schulze et al. 1994), of depleted $^{15}N$ - although the soil $^{15}N$ values found in deeper soils (> 30 cm) were not measured in this study; (d) possible mycorrhizal fungal activity (Hobbie and Ouimette 2009) – although such activities typically enrich soil $^{15}N$, and/or (e) mobilization of recalcitrant soil N to active pools (Davidson et al. 2007), with recalcitrant pools being depleted in $^{15}N$ if formed prior to the combustion event. Compton et al. (2007) studied soil $\delta^{15}N$ in secondary forests up to 115 years post agricultural abandonment in Rhode Island, USA and, with the exception of the organic horizon in which $\delta^{15}N$ decreased, found $^{15}N$ enrichment with stand age across all depths – although they found the same pattern of $^{15}N$ enrichment with depth in the soil as identified in our study. These differences are likely due to very different land use intensities between the two studies, with the stands studied by Compton et al. (2007) having undergone far greater land use intensity, including both mechanized agricultural and/or high intensity cattle grazing, prior to abandonment. Similar results

– to Compton et al. (2007) – obtained by Billing and Richter (2006) may be also explained through the far greater mechanized agriculture prior to abandonment.

Variation in soil $\delta^{13}C$ is generally thought to be a result of the dominant plant species composition, as decomposition related fractionation is small relative to that during carbon fixation (Nadelhoffer and Fry 1988), and is therefore driven by changes in the relative abundance of $C_3$ (i.e., most plants) to $C_4$ (i.e., corn, sugar cane, most tropical pasture grasses) plants (Schedlbauer and Kavanagh 2008). Differences in foliar carbon isotope composition between $C_3$ and $C_4$ species reflect differences in their photosynthetic pathways, with $C_3$ species have a $\delta^{13}C$ range of -32 to -20% whereas $C_4$ species range from -17% to -9% (Boutton 1991). However, soil $^{13}C$ enrichment also occurs during auto- and heterotrophic soil $C0_2$ efflux - which is $^{13}C$ depleted - from decomposition of surface litter (Schweizer et al. 1999), and during oxidation of soil organic matter and soil humification processes (Agren et al. 1996, Lin et al. 1999, Ehleringer et al. 2000), or possibly depletion from root respiration (Klumpp et al. 2004). The isotopic composition of autotrophic respiration (i.e., leaves, twigs, roots) is most likely derived from young newly fixed carbon, with the related $\delta^{13}C$ value, whereas heterotrophic respiration (i.e., decomposition) will likely have a different isotopic signature depending on the carbon turnover rate of the labile available carbon pools (Ehleringer et al. 2000, Harmon et al. 2011). Such differences have been identified in soils throughout the tropics (Schwartz 1991, Veldkamp 1994), with a $\delta^{13}C$ of -25% commonly used to represent the value of the stable pool (Bernoux et al. 1998). Profiles showing increasing $\delta^{13}C$ with depth, which occur independent of soil type (Balesdent et al. 1993), are commonly found under conditions of stable vegetation cover and low soil disturbance (i.e., tilling) (DesJardins et al. 1994) and result from reduced decomposition related isotope fractionation with depth (Agren et al. 1996) and decreases in the size of soil organic matter fractions (Feigl et al. 1995). In these situations, surface carbon is generally of young origin and labile with increasingly old and recalcitrant SOM pools with depth (Bernoux et al. 1998).

Changes in soil $\delta^{13}C$ during forest succession reflect: (a) variation in the turnover rates of soil organic matter (SOM), including decreased stability of some

previously stable – potentially $^{13}C$ enriched - C pools following burning (Bernoux et al. 1998) – including changes in relative contribution of microbial vs. plant soil organic matter (Ehleriger et al. 2000); (b) changes in vegetation, including shifts between $C_3$ and $C_4$ species, as soil $^{13}C$ composition greatly reflects that of the dominant vegetation (Nadelhoffer and Fry 1988), due to low rates of fractionation during decomposition relative to fixation (Peterson and Fry 1987) – although Billings and Richter (2006) found very slow incorporation of new plant carbon into soil horizons beyond the uppermost (< 10 cm) layers; and (c) a large flux of depleted $^{13}C$ plant lignin and root organic matter, or remnant charcoal, from combustion during the deforestation process (Skjemstad et al. 1990, Bernoux et al. 1998) – which can result in confusion as pasture carbon isotope composition could appear similar to intact forests. Decreased soil $\delta^{13}C$ in abandoned pastures and agricultural areas, as compared to forest, has been well established (Awiti et al. 2008, Schedlbauer and Davanagh 2008) with increasing historical years of cultivation of $C^4$ species having a positive (less negative) relationship with soil $\delta^{13}C$ values (forest soil $\delta^{13}C$ = -24, vs. 17 and 60 years of cultivation = -23 and -16, respectively; Awiti et al. 2008).

Although the soil $^{13}C$ depletion with stand age in our study contrasted that found by Billings and Richter (2006) whose stands were regrowing on sites subjected to intensive agriculture of cotton - a $C_3$ species, it was similar to that found by Lopez-Ulloa et al. (2005) who studied forest stands regrowing on sites opened through slash-burn and used as pasture. In our study, changes in soil $\delta^{13}C$ were unlikely dominated by a $C_4$ species signal related to the agricultural (or pasture) phase as identified in studies following more intense land use (Billings and Richter 2006). However, although subsistence agricultural species grown in our study area were primarily $C_3$, including bananas, beans, rice and yucca, the dominant crops included corn, a $C_4$ species, and rice. More likely, the decrease in soil $\delta^{13}C$ seen with increasing stand age represents a gradual return to stable primary forest values following: (a) a large signal from burning related $^{13}C$ enrichment during the slash-and-burn process (Bernoux et al. 1998), (b) a smaller $^{13}C$ enrichment signal from the corn, a $C_4$ species, cultivated during the 1-2 year no till agriculture period (Boutton 1991), (c) a transition to $C_3$

species dominated forest composition with more stable disturbance dynamics, and (d) continual input of $^{13}C$ depleted carbon during the dry season from wildfires (Finkelstein et al. 2006). Soil $\delta^{13}C$ in our study did increase with depth as expected given reduced rates of decomposition; with the development of a linear relationship between $^{13}C$ enrichment and increasing depth occurring in the primary stands as expected given their more stable forest structure and plant composition (Desjardins et al. 1994). Our primary forest soil $\delta^{13}C$ were considerably more enriched than those in our oldest secondary forest stands, possibly indicating long term $^{13}C$ enrichment via leaching.

### 5.5.3 Leaf traits

At a global scale leaf traits have been found to represent a continuous gradient of 'leaf economic spectrum' going from short-lived high photosynthetic capacity leaves to long-lived, thick, low photosynthetic capacity leaves (Wright et al. 2004). However, further analyses have revealed that the range within groups along this gradient is often larger than the differences among them (Wright et al. 2005) – in part related to broad changes in mean annual temperature and precipitation – and shifts from long-lived low nutrient leaves in low fertility soils to high nutrient content leaves on more fertile sites (Wright et al. 2001). Leaf trait variation within a primary forest (i.e., a relatively stable environment) is further constrained by phylogenetic, taxonomic or functional group differences (He et al. 2010, Powers and Tiffin 2010, Fyllas et al. 2009, Chazdon et al. 2010), growth environment (Chazdon and Field 1987, Kull and Kruijt 1999, Niinemets 2007) and propagation strategy (Swaine and Whitemore 1988), among many factors (Guariguata and Ostertag 2001). Understanding variation in leaf traits through forest succession (i.e., a highly dynamic environment) integrates across these groups as it moves though variation in inter- and intra-species competition, differences in plant growth and reproductive strategy, and plant-soil feedbacks (Binkley and Giardina 1998, Peña-Claros 2003, Toledo and Salick 2006). During succession, foliar dynamics may provide information unique

from that shown in the stand or soil properties, or largely result from overall stand changes or differences in soil properties. Understanding these factors is critical to enable the use of leaf traits, including nutrient concentrations and stable isotope ratios, to understand successional dynamics. We start by investigating, for each measured leaf trait, possible phylogenetic control over leaf trait variation, then focus on how changes in stand structure and soil properties may influence their expression. In addition, we focus on situations where leaf traits may follow different trends than those occurring belowground and thereby provide additional information.

First, we investigate whether differences in leaf traits are a result of phylogenetic control. Powers and Tifflin (2010) found that inter-specific variation accounted for 57-83% of leaf trait variance across 87 tropical dry forest tree species whereas He et al. (2010) found that 27% of leaf trait variation was due to phylogenetic differences in a grassland ecosystem. These contrast with our results, which showed phylogenetic signal only in leaf %C. This is in part explained by the dynamic nature of our study system – encompassing a large gradient of stand structure and species composition, in which the stand age or species successional status gradients outweigh differences among species. In any individual stand however it is entirely plausible that inter-species differences are of primary importance to explain leaf trait variation, although Letcher (2010) found significant over-dispersion of species - across the phylogenetic community - at stand scale during forest succession as a result of rapid transition through species 'functional' groups (i.e., along the species successional status gradient). In particular, Letcher (2010) found that no phylogenetic structure existed in the youngest stands that may be a result of the rapid rate of change in species, as indicated in Fig. 5.1 for mean stand species successional status. Fyllas et al. (2009) analyzed leaf traits from 508 species distributed across a range of soil types and precipitation regimes and found that foliar %C (as identified in our study), %N and Mg concentration were highly taxonomical constrained. However, foliar P, K, Ca and $\delta^{13}C$ were influenced by site growing conditions, with soil fertility being the most important predictor for all variables. Mean annual temperature (MAT) was negatively related to foliar N, P and K, and MAP was positively related to foliar %C and $\delta^{13}C$.

Townsend et al. (2007) used foliar N:P ratios to show that differences in growth latitude or mean annual precipitation (MAP) had a non-significant influence on foliar N:P ratios within the tropics, while large significant differences were found among species, between the dry and wet season, and with soil order. Pringle et al. (2010) found no phylogenetic signal among the leaf traits of trees growing in a seasonally dry tropical forest in Mexico, which they explained as indicating that selective pressures (i.e., functional convergence) constrained leaf traits.

In the context of forest succession, phylogenetic signal over all successional stands may be less relevant to understanding temporal dynamics than how species functional qualities change through time (Guariguata and Ostertag 2001, Chazdon et al. 2010). In particular, given successional theory, it is more likely that changes in a suite of functional characteristics are occurring through succession (Yan et al. 2006), in part due to environmental niche partitioning and strategy differentiation (Kraft et al. 2008). The importance in functional differentiation during succession was supported by the lack of phylogenetic signal across the species successional status gradient of our studied trees, although further analyses are required to unravel phylogenetic – successional status interactions during succession. Huc et al. (1994) studied differences in leaf traits among categorical divisions of species successional status in the French Guiana. Wood cellulose $\delta^{13}C$, leaf gas exchange and leaf water potential were shown to differ significantly between pioneer and late stage successional guild tree species growing in a common garden (Huc et al. 1994), and the authors highlighted the need for additional research on successional guild control over ecophysiological function (Reich et al. 1995).

Given significant changes in soil N and P pools, as expected given successional theory predicting changes from N to P limitation during forest succession (Herbert et al. 2003), we anticipated a corresponding positive shift in the foliar N:P ratio. Our results show, that in our study area, changes in foliar N:P are related to changes in species successional status (Table 5.4). Although stands younger than 10 years of age do have stand average foliar N:P value less than 14-16, the N(lower) to P (higher) limitation threshold described by Townsend et al. (2008) in a literature

review, most are above this threshold indicating that significant N limitation is not occurring in our study area. This was expected given the large N pulse seen in the soil $\delta^{15}N$ of younger stands, while N in older stands would have accumulated due to biological N fixation and atmospheric deposition. Although foliar N varied with successional status, foliar P varied only with the soil texture gradient, with foliar P tracking changes in soil P. Soil P however did not vary with stand age, indicating these changes are unrelated to successional process, but instead had a significant negative correlation with soil clay. These results are similar to those identified by Silver et al. (2000) who found that when soil clay content increased, labile P decreased while total P increased, due to P being easily complexed with exchangeable Al and Fe. Our soil P analyses (weak Bray) were designed to assess the labile P pools (Romanyà et al. 1993, Quintero et al. 2003), which would have the greatest effect on foliar P concentrations. Therefore, in this study, our results indicate that soil P represents variation in soil clay content resulting from chronosequence error rather than successional processes, which was then mirrored in the foliar P content. Changes in foliar N however resulted from, to a much lesser extent, increasing N availability during stand development, and primarily from shifts in species successional growth strategies, indicative of species growing on nutrient rich sites (Wright et al. 2001), and similar to results from Yan et al. (2006) showing increasing foliar N among three tree species increasing in successional status which was attributed to changes from conservative to resource spending in later successional species due to increases in soil fertility. Our data shows this pattern to occur across both the entire species community as well as within individual species.

While foliar $\delta^{15}N$ reflects in large part the isotopic composition of the available soil nitrogen pool (Amundson et al. 2003) – which in turn results from species composition (Martinelli et al. 1992) and N cycle openness (Robinson 2001), various sources of fractionation, including biological nitrogen fixation (Vitousek et al. 1989) which discriminates against $^{15}N$ during soil N to plant transfer decreasing foliar $\delta^{15}N$, exist which can provide additional information over soil $\delta^{15}N$ alone. During forest

succession, theory predicts decreasing N limitation and therefore greater openness of the N cycle, resulting in increased soil $^{15}N$ fractionation and therefore $^{15}N$ enrichment. Contrary to this however, simultaneous reductions in foliar and soil $\delta^{15}N$ during succession have been found in several studies. Wang et al. (2007) attributed decreases in soil and foliar $\delta^{15}N$ on an old field in northern Virginia following intensive agriculture because of increases in woody ectomycorrhizal (EM) and herbaceous vesicular-arbuscular mycorrhizal (VAM) hosted fungi causing discrimination against soil $^{15}N$ during uptake. They highlight that VAM abundance increases into early successional stands and then reduces in intermediate aged stands when EM hosted fungi (which discriminate more against $^{15}N$ than VAM) increase (Johnson et al. 1991, Hobbie et al. 2005). In addition to finding community level dynamics of decreasing foliar $\delta^{15}N$ they also identified decreasing patterns among individual species, similar to our findings. They conclude that soil $\delta^{15}N$ is the major factor driving foliar $\delta^{15}N$ due to a highly significant positive relationship ($R^2 > 0.90$). In our study, we likewise found a highly significant relationship, although the $R^2$ value of 0.25 indicated that other processes might be constraining foliar $\delta^{15}N$ dynamics, such as root development, which likely provides access to increasingly depleted N at depth (Compton et al. 2007).

Compton et al. (2007) use the divergence between foliar and soil $\delta^{15}N$ values ($\Delta\delta^{15}N_{plant\text{-}soil}$) to address drivers of foliar $\delta^{15}N$ variation, including rooting depth, as it allows for direct comparison of N fractionation during plant uptake, with increasing values indicating increased fractionation. Although we perform a similar study of divergence, we recognize that our soil analyses were limited to < 30 cm whereas rooting depths are well distributed up to 2 meters depth (Jackson et al. 1996), and sometimes extend much deeper ( > 8 meters in some primary forests in the Amazon; Nepstad et al. 1994). Divergence results, in part, from: (a) differences in the rate and abundance of EM activity; (b) changes in plant efficiency of mineral N cycling during succession, as has been found for increasing water availability (Austin and Vitousek 1998); and (c) changes in plant uptake between organic / $NH_4^+$ (cool temperate) and

$N0_3^-$ (tropical) (Amundson et al. 2003), although climatic differences would be minimal among our co-located study stands.

As woody ectomycorrhizal activity results in depletion of foliar $^{15}N$ we expected an increasing $\Delta\delta^{15}N_{plant\text{-}soil}$ divergence during forest succession. This trend would be most pronounced if soil $\delta^{15}N$ were being measured at the same depths that EM activity was greatest, and diluted if soil from shallower depths having substantial litter input and therefore soil $^{15}N$ depletion was used. During forest succession, simultaneous increases in rooting depth – as we collected leaves from top-of-canopy positions - would influence this relationship as we found soil $^{15}N$ enrichment with depth, but further detailed analysis of soil EM activity and soil $\delta^{15}N$ to depths of at least 3-5 meters would be required to interpret possible interactions. Although stand age and species successional status both exhibited the significant increases in divergence as indicative of increased EM activity, species successional status was a much stronger predictor. Although we do not have data regarding specific EM relationships among our study species, an increasing probability of EM associations occurring in later successional status species could explain this correlation – thus changes in species successional status during stand age would drive $\Delta\delta^{15}N_{plant\text{-}soil}$ divergence depletion via an iterative feedback loop., simultaneous to a general trend of $^{15}N$ depletion occurring across the species community as well as within individual species through stand age which indicates that ecological processes other than species successional status transitions are driving overall ecosystem $\delta^{15}N$ depletion patterns – as discussed in previous above – but such transitions may be accelerating ongoing $^{15}N$ depletion patterns and in particular at shallower soil depths incorporating increasingly more depleted $^{15}N$ via organic matter input.

Although patterns of decreasing $\delta^{15}N$ were found by our study, the driving factors likely differ in our study from those of Compton et al. (2007) and Wang et al. (2007). The successional chronosequence used in these studies did not undergo a burning cycle directly prior to abandonment, which significantly enriches soil $^{15}N$, rather they propose that their decreases resulted dominantly from: (a) shifts in rooting depth; (b) fractionation during plant uptake, (c) increased EM activity (although no N-

fixers were present in the Compton et al. (2007) study site), and (d) changes in soil N cycling rates. Processes dominating our study N dynamics were likely more similar to those Davidson et al. (2007). In this study, foliar N, N:P, and $\delta^{15}N$ all increased during forest succession following mechanized agriculture for sites located in the Brazilian Amazon. Likewise, we found increases in foliar N:P, driven by increases in N but no change in P, but conversely found decreasing foliar $\delta^{15}N$. We propose that although similar dynamics of N cycle recuperation (i.e., increasing leakiness and therefore N fractionation with stand development) are occurring within our study area, changes in foliar $\delta^{15}N$ are more representative of a decrease in soil $\delta^{15}N$ following high initial enrichment from combustion during the slash-and-burn process. The study plots selected by Davidson et al. (2007), although likely burned at various points, had existed long enough in an agricultural or pasture state to stabilize at more depleted $\delta^{15}N$ values prior to abandonment, with increasing time in pasture shown to result in increasingly depleted soil $\delta^{15}N$ values (Piccolo et al. 1996).

Variation in foliar $\delta^{13}C$ results primarily from differences in the ratio of internal ($c_i$) to atmospheric ($c_a$) $C0_2$ concentrations, in which a decreased internal $C0_2$ concentration relative to atmospheric (i.e., via closed stomata or rapid photosynthesis) results in decreased $^{13}C$ discrimination and enrichment (less negative) foliar $\delta^{13}C$ values (Farquhar et al. 1989). In $C_3$ plants, foliar $^{13}C$ discrimination occurs primarily during photosynthetic $C0_2$ uptake by ribulose1,5-bisphosphate ($R_uP_2$) carboxylase (Park and Epstein 1960) and during gaseous diffusion through the boundary layer and leaf stomata (Farquhar et al. 1982), and is moderated by the $C0_2$ diffusion rate into the leaf and rate of carboxylation (Farquhar et al. 1982). Therefore photosynthesis has a depleted $^{13}C$ uptake and tends to enrich the surrounding atmosphere while respiration has a depleted release and tends to deplete the atmosphere in $^{13}C$ (Yakir and Sternberg 2000). Factors affecting the $c_i$ / $c_a$ ratio include: (a) variation in the concentration of source $C0_2$ (Farquhar et al. 1989), although differences in atmospheric $C0_2$ are likely minor and not relevant in our study, and respiration derived $C0_2$, which is $^{13}C$ depleted ($\delta^{13}C$ ~ -28%, Quay et al. 1989) relative to atmospheric [although respiration itself is not a significant source of fractionation (Smith 1971)], is not significant when leaves

are sampled in locations of unimpeded air circulation (Vitousek et al. 1990) or greater than 7 m above ground in an intact primary tropical forest (Quay et al. 1989, Ometto et al. 2002); (b) $C_3$ or $C_4$ photosynthesis (Boutton 1991), which result in typical foliar $\delta^{13}C$ values of approximately -25% and -12%, respectively (Boutton 1991); (c) a wide variety of environmental stresses which may result in alter the ratio of conductance to photosynthesis (Aranibar et al. 2006), such as soil drought which influences conductance more than photosynthesis (Farquhar and Sharkey 1982, Schulze 1986), with increasing drought resulting in enriched (less negative) foliar $\delta^{13}C$ values; (d) differences in internal gas exchange in thick leaves, such as found by Vitousek et al. (1990) where enriched (less negative) foliar $\delta^{13}C$ (ranging from approximately -29.5 to -24.5 from low to higher elevations, respectively) was found within *Metrosideros polymorpha* at higher elevations as a result of increasing internal resistance to $C0_2$ diffusion to sites of carboxylation within the leaf, associated with increased leaf mass per area (LMA), as well as thicker mesophylls and increased %N (Körner and Diemer 1987); (e) differences in time-integrated water use efficiency (WUE) – assessed as the ratio of leaf assimilation rate of $C0_2$ (A) to leaf water vapor conductance (g) – with increasing WUE (i.e., decreased water vapor conductance relative to photosynthetic capacity) resulting in enriched (less negative) foliar $\delta^{13}C$ (Farquhar et al. 1989); and (f) differences in growth location, such as understory environments with decreased irradiance (low A) and higher relative humidity (open stomata) having greater $c_i / c_a$ ratio resulting in depleted (more negative) foliar $\delta^{13}C$ values (Farquhar et al. 1982).

Differences in foliar $\delta^{13}C$, resulting from combinations of the above mentioned factors, may vary in relation to: (a) species differences; (b) spatial location; and/or (c) disturbance history. Bonal et al. (2007) investigated foliar physiology of seedlings of species belonging to different successional groups, in a greenhouse experiment on seedlings, and found that although pioneer (fast growing early successional) species had higher assimilation (A) rates, reduced water use efficiency resulted in depleted (more negative) foliar $\delta^{13}C$ values than fast-growing late successional species. Interestingly, they found no linear pattern of foliar $\delta^{13}C$ change, but rather a V pattern, suggesting a transition among factors driving discrimination,

and highlighted the need to study foliar $\delta^{13}C$ dynamics along more complete successional gradients. Such non-linear variation might result from differences in seedling growth strategies, with: (a) low WUE resulting in $^{13}C$ depletion (greater discrimination) in pioneer species; (b) high A but higher WUE resulting in relative $^{13}C$ enrichment in intermediate successional species; and (c) very low A offsetting high WUE causing $^{13}C$ depletion in late successional species. Huc et al. (1994) had similar findings using $\delta^{13}C$ of cellulose in wood cores from adult trees growing in artificial stands of pioneer and late stage forest species. They found that pioneer species had the greatest $^{13}C$ discrimination, resulting from: (a) lower WUE; (b) high maximum conductance values; and (c) high specific hydraulic conductance, indicating an increased competitive ability for water and nutrient uptake in pioneer species.

Variation in foliar LMA and $\delta^{13}C$ often follow predictable spatial patterns within forests. Domingues et al. (2005) found LMA to increase and foliar $\delta^{13}C$ to become enriched (less negative) with increasing height in an Amazonia old growth forest as a result of increased A values (due to increased irradiance) resulting in reduced $c_i$ – increased $c_i$ / $c_a$ ratio. Ometto et al. (2002) had similar findings in the Brazilian Amazon, which they attributed to gradients in light and humidity – and specifically not to variation in source $C0_2$ isotope composition, which varied by only 3% throughout the full canopy profile - affecting the ratio of leaf photosynthetic capacity and stomatal conductance. However, light gradients do not necessarily result in variation in carbon isotope discrimination as A and g typically change simultaneously keeping $c_i$ / $c_a$, and therefore foliar $^{13}C$ fractionation, relatively constant (Wong et al. 1979) – at least within an individual species with low leaf plasticity, as leaves growing under increased light availability can have higher LMA values (Vitousek et al. 1990). Additional variation may also result from increasing tree height with succession, as height increases have been found to result in $^{13}C$ enrichment due to reduced conductance and increases in LMA (Koch et al. 2004) – although this pattern is non-linear and most pronounced above 30 meters which is greater than the maximum tree height in all our secondary forest stands. Although not the subject of their analyses, variation in height within a forest may occur

simultaneous with changes in species composition resulting in taxonomically constrained variation in foliar $\delta^{13}C$.

Foliar $\delta^{13}C$ variation also occurs within individual tree crowns. Waring and Silvester (1994) found that the aspect of exposure and branch length accounted for 6% of the foliar $\delta^{13}C$ variation within individual crowns of *Pinus radiata*, with shorter branches or shaded aspect of exposure being related to enriched (less negative) foliar $\delta^{13}C$ values. These differences resulted from decreased stomatal conductance on the longer branches. Differences in foliar $\delta^{13}C$ among study sites typically results from a combination of the factors identified above. For example, Ehleringer et al. (1986) found a clear decrease in foliar $\delta^{13}C$ from disturbed to undisturbed sites, indicating decreased C02 concentrations and increased water use efficiency (WUE). They explain this difference however through large changes in irradiance as altered through leaf canopy position and overstory density – likely causing changes in LMA.

We identified a highly significant decrease in foliar $\delta^{13}C$ with increasing species successional status, but not with increasing stand age. Many of the factors identified above are: (a) related to either stand structural or soil properties, which would change with stand age and therefore result in no linear pattern; or (b) were normalized for across our study stands, such as topographic differences, elevation or climatic conditions. As all our leaves were collected from top of canopy full sunlight and atmospherically well circulated positions differences in source $C0_2$ or illumination are unlikely to have had a significant impact. Increases in internal $C0_2$ diffusion resistance, as identified by Vitousek et al. (1990), are also unlikely play a major role, as early successional species (and most others as well) have, relative to high elevation *Metrosideros polymorpha*, thin leaves. In addition, internal diffuse resistance would result in reduced discrimination (enriched foliar $\delta^{13}C$) in the later successional species having greater LMA – the opposite to the positive relationship between increasing $^{13}C$ depletion with species successional status we found in our analyses.

Given this variation in foliar $\delta^{13}C$ appears to be almost entirely related to species differences in leaf physiology and growth strategy correlated to their species successional status. While we did not collect data on LMA for our study species,

Poorter et al. (2004) quantified leaf traits of < 2 m tall saplings across a successional gradient in the Bolivia Amazon and found significant decreases in specific leaf area (converse of LMA), nitrogen, water content and increases in C:N and lignin in later stage successional species. If similar patterns in LMA exist across adult individuals, as was found by Reich et al. (1995) in the Venezuelan Amazon where later stage successional species had increasingly lower rates of photosynthesis, conductance and SLA, and increased leaf life span and toughness, then decreasing conductance relative to A could result in depleted (more negative) foliar $\delta^{13}C$ values. The strong negative relationship between foliar $\delta^{13}C$ and species successional status, but not stand age, further emphasizes that this trend is occurring simultaneous to – but independent of - the negative relationship shown between soil $\delta^{13}C$ and stand age, which is in large part driven through changes in the foliar $\delta^{13}C$ input during transition through species succession status. Given the non-significant relationship between stand age and foliar $\delta^{13}C$, the significant increase in $\Delta\delta^{13}C_{\text{plant-soil}}$ we identified with increasing stand age indicates that either: (a) the incorporation of the foliar $\delta^{13}C$ into the soil slows with increasing stand age; (b) that a significant source of soil $\delta^{13}C$ enrichment develops with increasing stand age; or (c) a significant source of soil $\delta^{13}C$ diminishes with stand age. The first explanation is not likely as it is most probable that the quantity [although not necessarily the rate which undergoes a varying pattern of colonization by decomposers, exponential increase in the rate of decomposition during early stands having abundant high quality litterfall from fast growing pioneer species, followed by reduced but stable rates of decomposition of lower quality litterfall from slow growing species (Garnier et al. 2004)] of decomposition increases with stand age (Ewel 1976, ). However, increasing soil $^{13}C$ enrichment via auto- and hetero-trophic respiration and microbial fractionation during decomposition could serve to offset soil $^{13}C$ depletion [resulting from: (a) the loss of the initial large $^{13}C$ enrichment pulse following the burning; (b) incorporation of increasingly depleted $^{13}C$ organic matter into the soil; and (c) transition to all $C^3$ species] causing the increasingly negative $\Delta\delta^{13}C_{\text{plant-soil}}$ relationship.

## 5.6 Integration and conclusion

During forest succession competition among species for resources, including light, water and soil nutrients, play an important role in species composition (Huston and Smith 1987). Considering variable resources, alterations in composition during forest succession are likely partially explained through resource niche partitioning (Kobe 1999). Tree species from differing successional guilds may express different competitive capacities or nutrient use strategies during stand development (Bazzaz and Pickett 1980), including shifts in nutrient use strategies from 'conservative consumption' to 'nutrient spending' – although this is most related to shifts in plant functional type rather than community-scale dynamics (Yan et al. 2006). The interactions between these factors, including differences among taxonomic and physiological and functional diversity, has been described as being one of the least understood themes in tropical forest ecology (Clark and Clark 1992; Chazdon et al. 2010). It is difficult to separate soil and foliar processes as they develop through complex feedbacks (Binkley and Giardina 1988). For example, changing successional vegetation plays a crucial role in making nutrients from the total soil pool available to plants (Werner 1984) which feeds back to influence which species are best adapted to succeed and their spatial distribution (John et al. 2007). Processes, such as the introduction of exotic species (Matson 1990), can alter cycling processes - similar to the continuous dynamic of feedback restructuring that occurs during secondary succession. Successional dynamics and biomass accumulation following abandonment depend in large part on the dynamics of the initial disturbance (Zarin et al. 2005.

In the our study we found soil N to increase where P remained stable as expected given increasing influence of biological nitrogen fixation during succession and progressive depletion or incorporation of P into aboveground biomass. Increasing foliar %N values were shown with increasing species successional status indicating changes in growth and competitive strategy under conditions of varying N availability. Foliar P however, which did not change in soil with stand age, was found to be determined by soil texture and therefore represented chronosequence error. The

significant soil $\delta^{15}N$ depletion with stand age likely does not represent a progressive tightening of the nitrogen cycle; rather it represents the balance of other fractionation related nitrogen cycling processes in a post-fire induced $^{15}N$ enrichment context. While foliar $\delta^{15}N$ is largely determined by the soil isotope composition, increasing divergence with species successional status indicates an increase in nitrogen isotope fractionation in older stands by later succession species, possibly as result of increased EM activity and changes in root foraging depth. Soil $\delta^{13}C$ is however in large part determined by the plant composition, with few plant-soil carbon isotope feedbacks, that is again partly determined by the initial burning related soil $^{13}C$ enrichment. Foliar $\delta^{13}C$ depletion with increasing succession status, but not stand age, highlights the changes in tree growth and competition strategy during succession from thin fast growing leaves with rapid A and low WUE to slow growing species with thick well protected long lasting leaves having reduced rates of A but increased WUE. Increasing divergence between soil and foliar $\delta^{13}C$ may be a result of increases in the quantity - but less likely the rate – of carbon cycling processes, such as decomposition, as stands age. Foliar %C, however, was unrelated to stand age or species successional status but had significant phylogenetic signal, which was not found across the species successional status gradient. Phylogenetic constraints to foliar %C have been identified in other studies in less dynamic study systems, and likely other leaf traits in our study would exhibit phylogenetic signal under more stable (i.e., primary forest) conditions. The interplay among soil and foliar factors, with more specific quantification of competitive processes during forest succession, requires further investigation and will be the focus of future work.

## 5.7 Acknowledgements

We give thanks to T. Tobeck, N. Gurwick, C. Andreassi, and K. Mertes for help with laboratory analyses; M. Gilbert, J. Johnson, K. Cahill, K. Gerow and A. Storer for help with statistical analyses; A. Rominger, E. Kurten and J. Savage for help

with phylogenetic analyses; E. Soriano and the many members of our field crew from Brazil, Peru and Bolivia for help with field data collection; E. Davidson, P. Vitousek, R. Dirzo and B. Houlton for valuable comments throughout; D. Julio and the community of Molienda in Bolivia for working with us, allowing access to their properties, and for sharing their extensive knowledge of the area. This work was financially supported in part by the Department of Global Ecology of the Carnegie Institution for Science, the Department of Biology at Stanford University, a NSF doctoral dissertation improvement grant and a Global Change Education Program Graduate Research Education Fellowship (GCEP GREF) from the U.S. Department of Energy. We thank the W. Clark, N. Dickson and M. Holbrook for help during the writing and analysis process. This work was partially conducted while E. Broadbent was a doctoral fellow and A. Almeyda Zambrano was a Giorgio Ruffolo Fellow in the Sustainability Science Program at Harvard University. Support from Italy's Ministry for Environment, Land and Sea is gratefully acknowledged.

## 5.8 References

Ackerly DD (2000) Taxon sampling, correlated evolution, and independent contrasts. Evolution; international journal of organic evolution 54:1480-1492.

Agren GI, Bosatta E, Balesdent J (1996) Isotope discrimination during decomposition of organic matter: a theoretical analysis. Soil Science Society of American Journal 60:1121-1126.

Amundson R, Austin E, Schuur EA, Yoo K, Matzek V, Kendall C, Uebersax U, Brenner D, Baisden WT (2003) Global patterns of the isotopic composition of soil and plant nitrogen. Global Biogeochemical Cycles 17:1031-1042.

Andreae MO, Browell EV, Garstang M, Gregory G, Harriss R, Hill G, Jacob D, Pereira M, Sachse G, Setzer A, Silva Dias PL, Talbot RW, Torres AL, Wofsy SC (1988) Biomass-burning emissions and associated haze layers over Amazonia. Journal of Geophysical Research 93:1509-1527.

Aranibar J, Berry J, Riley WJ, Pataki DE, Law BE, Ehleringer JR (2006) Combining meteorology, eddy fluxes, isotope measurements, and modeling to understand environmental controls of carbon isotope discrimination at the canopy scale. Globa Change Biology 12:710-730.

Austin AT, Vitousek PM (1998) Nutrient dynamics on a precipitation gradient in Hawai'i. Oecologia 113:519-529.

Asner GP, Rudel TK, Aide TM, Defries R, Emerson R (2009) A contemporary assessment of change in humid tropical forests. Conservation Biology 23:1386-1395.

Balesdent J, Girardin C, Mariotti A (1993) Site-related matter in a temperate forest. Ecology 74:1713-1721.

Bazzaz FA, Pickett STA (1980) Physiological ecology of tropical succession: A comparative review. Annual Review of Ecology and Systematics 11:287-310.

Beekma J, Zonta A, Keijzer B (1996) Base ambiental para el desarrollo del departamento de Pando y la provincia Vaca Diez. La Paz, Bolivia.

Bernoux M, Cerri CC, Neill C, de Moraes JFL (1998) The use of stable carbon isotopes for estimating soil organic matter turnover rates. Geoderma 82:43-58.

Binkley D, Giardina C (1998) Why do tree species affect soils? The warp and woof of tree-soil interactions. Biogeochemistry 42:89-106.

Blomberg SP, Garland T, Ives AR (2003) Testing for phylogenetic signal in comparative data: behavioral traits are more labile. Evolution 57:717-745.

Blundell A, Peart D (2004) Density-dependent population dynamics of a dominant rain forest canopy tree. 85:704-715.

Boeckx P, Paulino L, Oyarzun C, van Cleemput O, Godoy R (2005) Soil $\delta^{15}N$ patterns in old-growth forests of southern Chile as integrator for N-cycling. Isotopes in Environmental and Health Studies 41:249-259.

Bonal D, Born C, Brechet C, Coste S, Marcon E, Roggy JC, Guehl JM (2007) The successional status of tropical rainforest tree species is associated with differences in leaf carbon isotope discrimination and functional traits. Annals of Forest Science 64:169-176.

Budowski G (1965) Distribution of tropical American rain forest species in the light of successional processes. Turrialba 15:40-42.

Boutton TW (1991) Stable carbon isotope ratios of natural materials: II. Atmospheric, terrestrial, marine and freshwater environments. In Coleman DC and Fry B (eds.), Carbon Isotope Techniques. San Diego, Academic Press: pgs. 173-185.

Canham C (1988) Growth and canopy architecture of shade-tolerant trees: Response to canopy gaps. Ecology 69:786-795

Castilho CV, Magnusson WE, Nazare R, Lima AP, Higuchi N, Luiza RC (2006) Variation in aboveground tree live biomass in a central Amazonian Forest: Effects of soil and topography. Forest Ecology and Management 234:85-96

Chao A, Chazdon RL, Colwell RK, Shen TJ (2005) A new statistical approach for assessing similarity of species composition with incidence and abundance data. Ecology Letters 8:148-159

Chave J, Andalo C, Brown S, Cairns MA, Chambers JQ, Eamus D, Fölster H, Fromard F, Higuchi N, Kira T, Lescure JP, Nelson BW, Ogawa H, Puig H, Riera B, Yamakura T (2005) Tree allometry and improved estimation of carbon stocks and balance in tropical forests. Oecologia 145:87-99.

Chazdon RL, Field CB (1987) Determinants in photosynthetic capacity in six rainforest *Piper* species. Oecologia 73:222-230.

Chazdon RL (2008) Beyond deforestation: Restoring forests and ecosystem services on degraded lands. Science 320:1458-1460.

Chazdon RL, Letcher SG, van Breugel M, Martínez-Ramos M, Bongers F, Finegan B (2007) Rates of change in tree communities of secondary Neotropical forests

following major disturbances. Philosophical transactions of the Royal Society of London 362:273-289.

Chazdon RL, Finegan B, Capers RS, Salgado-Negret B, Casanoves F, Boukili V, Norden N (2010) Composition and dynamics of functional groups of trees during tropical forest succession in northeastern Costa Rica. Biotropica 42:31-40.

Clark DA, Clark DB (1992) Life History Diversity of Canopy and Emergent Trees in a Neotropical Rain Forest. Ecological Monographs 62:315-344

Cleveland CC, Townsend AR, Schimel DS, Fisher H, Howarth RW, Hedin LO, Perakis SS, Latty EF, VonFischer JC, Else-road A, Wasson MF (1999) Global patterns of terrestrial biological nitrogen (N-2) fixation in natural ecosystems. Global Biogeochemical Cycles 13:623-645

Cochrane MA (2011) The past, present, and future importance of fire in tropical rainforests. In Bush MB, Flenley JR, Gosling WD (Eds.) Tropical rainforest responses to climate change (second edition), pp. 213-240. Springer-Verlag, New York, New York

Compton JE, Hooker TD, Perakis SS (2007) Ecosystem N distribution and $\delta^{15}N$ during a century of forest regrowth after agricultural abandonment. Ecosystems 10:1197-1208.

Cornwall WK, Cornelissen JH, Amatangelo K, Dorrepaal E, Eviner VT, Godoy O, Hobbie SE, Hoorens B, Kurokawa H, Perez-Harguindeguy N, Quested HM, Santiago LS, Wardle DA, Wright IJ, Aerts R, Allison SD, van Bodegom P, Brovkin V, Chatain A, Callaghan TV, Diaz S, Garnier E, Gurvich DE, Kazakou E, Klein JA, Read J, Reich PB, Soudzilovskaia NA, Vaieretti MV, Westoby M (2008) Plant species traits are the predominant control on litter decomposition rates within biomes worldwide. Ecology Letters 11:1065-1071.

Davidson EA, Howarth RW (2007) Nutrients in synergy. Nature 449:1000-1001

Davidson EA, Zarin DJ, Brondizio E, Vieira ICG, Sa T, Schuur EAG, Feldpausch T, Mesquita R, Moran E, Delamonica P, Ducey MJ, Hurtt GC, Salimon C, Denich M (2005) Legacy of Fire Slows Carbon Accumulation in Amazonian Forest Regrowth. Frontiers in Ecology and the Environment 3:365-369

Davidson EA, de Carvalho CJR, Figueira AM, Ishida FY, Ometto JPHB, Nardoto GB, Sabá RT, Hayashi SN, Leal EC, Vieira ICG, Martinelli LA (2007) Recuperation of nitrogen cycling in Amazonian forests following agricultural abandonment. Nature 447:995-998

Davies TJ, Kraft NJB, Salamin N, Wolkovich EM (2011) Incompletely resolved phylogenetic trees inflate estimates of phylogenetic conservatism. Ecology 93:242-247

Dawson TE, Mambelli S, Plamboeck AH, Templer PH, Tu KP (2002) Stable Isotopes in Plant Ecology. Annual Review of Ecology and Systematics 33:507-559

Desjardins T, Andreux F, Volkoff B, Cerri CC (1994) Organic carbon and $^{13}C$ contents in soils and soil size-fractions, and their changes due to deforestation and pasture installation in the eastern Amazonia. Geoderma 61:103-118

Delwiche C, Steyn P (1970) Nitrogen isotope fractionation in soils and microbial reactions. Environmental Science & Technology 11:929-935

Delwiche C, Zinke P, Johnson C, Virginia RA (1979) Nitrogen isotope distribution as a presumptive indicator of nitrogen fixation. Botanical Gazette 140:65-69

Denslow JS (1996) Functional group diversity and responses to disturbance. *Biodiversity and ecosystem processes in tropical forests*. (eds G.H. Orians, R. Dirzo & J.H. Cushman), pp. 127-151. Springer-Verlag, Berlin.

Denslow JS (1987) Tropical rainforest gaps and tree species diversity. Annual review of ecology and systematics. 30:761-766.

Denslow JS, Guzman SG (2000) Variation in stand structure, light and seedling abundance across a tropical moist forest chronosequence, Panama. Journal of Vegetation Science 11:201-212.

Domingues F, Berry JA, Martinelli LA, Ometto JP, Ehleringer JR (2005) Parameterization of canopy structure and leaf-level gas exchange for an eastern Amazonian tropical rain forest. Earth Interactions 9:1-23.

Donatti CI, Guimaraes PR, Galetti M, Auelio-Pizo M, Marquitti FM, Dirzo R (2011) Analysis of a hyper-diverse seed dispersal network: modularity and underlying mechanisms. Ecology Letters 14:773-781.

Ehleringer J, Field C, Lin Z, Kuo C (1986) Leaf carbon isotope and mineral composition in subtropical plants along an irradiance cline. Oecologia, 70:520-526.

Ehleringer J, Buchmann N, Flanagan L (2000) Carbon isotope ratios in belowground carbon cycle processes. Ecological Applications 10:412-422.

Elmore AJ, Asner GP (2006) Effects of grazing intensity on soil carbon stocks following deforestation of a Hawaiian dry tropical forest. Global Change Biology 12:1761-1772.

Ewel J (1976) Litter fall and leaf decomposition in a tropical forest succession in eastern Guatamala. Journal of Ecology 64:293-308.

Farquhar GD, Sharkey TD (1982) Stomatal conductance and photosynthesis. Annual Review of Plant Physiology 33:317-345.

Farquhar GD, O'Leary MH, Berry JA (1982) On the relationship between carbon isotope discrimination and the intercellular carbon dioxide concentration in leaves. Australian Journal of Plant Physiology 9:121-137.

Farquhar GD, Ehleringer JR, Hubick KT (1989) Carbon isotope discrimination and photosynthesis. Annual Review of Plant Physiology and Plant Biology 40:503-537.

Fearnside P (1997) Wood density for estimating forest biomass in Brazilian Amazonia. Forest Ecology and Management 90:59-87.

Fearnside PM, Guimaraes WM (1996) Carbon uptake by secondary forests in Brazilian Amazonia. Forest Ecology and Management 80:35-46

Feigl BJ, Mellilo J, Cerri CC (1995) Changes in the origen and quality of soil organic matter after pasture introduction in Rondonia (Brazil). Plant Soil 175:21-29

Feldpausch TR, Rondon MA, Fernandes EC, Riha SJ, Wandelli E (2004) Carbon and nutrient accumulation in secondary forests regenerating on pastures in central Amazonia. Ecological Applications 14:164-176.

Finegan B (1984) Forest succession. Nature 312:109-115.

Finegan B (1996) Pattern and process in neotropical secondary rain forests: the first 100 years of succession. TREE 11:793-796.

Finkelstein DB, Pratt LM, Brassell SC (2006) Can biomass burning produce a globally significant carbon-isotpe excursion in the sedimentary record? Earth and Plenetary Science Letters 250:501-510.

Fyllas NM, Patiño S, Baker TR, Bielefeld Nardoto, G, Martinelli LA, Quesada CA, Paiva R, Schwarz M, Horna V, Mercado LM, Santos A, Arroyo L, Jiménez EM, Luizão FJ, Neill DA, Silva N, Prieto A, Rudas A, Silviera M, Vieir ICG, Lopez-Gonzalez G, Malhi Y, Phillips OL, Lloyd J (2009) Basin-wide variations in foliar properties of Amazonian forest: phylogeny, soils and climate. Biogeosciences 6:2677-2708.

Garten CT Jr (1991) Nitrogen isotope composition of ammonium and nitrate and bulk precipitation and forest throughfall. International Journal of Environmental Analytical Chemistry 87:33-45.

Garnier E, Cortez J, Billès G, Navas M-L, Roumet C, Debussche M, Laurent G, Blanchard A, Aubry D, Bellmann A, Neill C, Toussaint J-P (2004) Plant functional markers capture ecosystem properties during secondary succession. Ecology 85:2630-2637.

Gehring C, Denich M, Vlek PL (2005) Resilience of secondary forest regrowth after slash-and-burn agriculture in central Amazonia. Journal of Tropical Ecology 21:519-527.

Gómez-Pompa A, Vázquez-Yanes C (1981) Successional studies of a rainforest in Mexico. In D. C. West, H. H. Shugart, and D. B. Botkin (Eds.). Forest succession, concepts and application, pp. 246– 266. Springer-Verlag, New York, New York.

Guariguata M, Ostertag R (2001) Neotropical secondary forest succession: changes in structural and functional characteristics. Forest Ecology and Management 148:185-206.

Guevara S, Purata SE, Van der Maarel E (1986) The role of remnant forest trees in tropical secondary succession. Vegetatio 66:77-84.

Gusewell S (2004) N:P ratios in terrestrial plants: variation and functional significance. New Phytologist 164:243-266.

Handley LL, Raven JA (1992) The use of natural abundance of nitrogen isotopes in plant physiology and ecology. Plant Cell and Environment 15:965-985.

He JS, Wang X, Schmid B, Flynn DFB, Li X, Reich PB, Fang J (2010) Taxonomic identity, phylogeny, climate and soil fertility as drivers of leaf traits across Chinese grassland biomes. Journal of Plant Research 123:551-561.

Hedges SB, Dudley J, Kumar S (2006) TimeTree: a public knowledge-base of divergence times among organisms. Bioinformatics 22:2971-2972.

Hedin L, Vitousek P, Matson P (2003) Nutrient losses over four million years of tropical forest development. Ecology 84:2231-2255.

Herbert D, Williams M, Rastetter E (2003) A model analysis of N and P limitation on carbon accumulation in Amazonian secondary forest after alternate land-use abandonment. Biogeochemistry 65:121-150.

Hobbie EA, Colpaert JV (2003) Nitrogen availability and colonization by mycorrhizal fungi correlate with nitrogen isotope patterns in plants. New Phytologist 157:115-126.

Hobbie EA, Jumpponen A, Trappe J (2005) Foliar and fungal 15N:14N ratios reflect development of mycorrhizae and nitrogen supply during primary succession: Testing analytical models. Oecologia 122:273-283.

Hobbie EA, Ouimette AP (2009) Controls of nitrogen isotope patterns in soil profiles. Biogeochemistry 95:355-371.

Holland EA, Dentener FJ, Braswell BH, Sulzman JM (1999) Contemporary and pre-industrial global reactive nitrogen budgets. Biogeochemistry 46:7-43.

Houghton RA, Skole D, Nobre CA, Hackler J, Lawrence K, Chomentowski WH (2000) Annual fluxes of carbon from deforestation and regrowth in the Brazilian Amazon. Nature 403:301-304.

Houlton B, Sigma DM, Hedin LO (2006) Isotopic evidence for large gaseous nitrogen losses from tropical forests. PNAS 103:8745-50.

Huc R, Ferhi A, Guehl JM (1994) Pioneer and late stage tropical rainforest tree species (French Guiana) growing under common conditions differ in leaf gas exchange regulation, carbon isotope discrimination and leaf water potential. Oecologia 99:297-305.

Huston M, Smith T (1987) Plant succession: life history and competition. American Naturalist 130:168-198.

Jackson R, Canadell J, Ehleringer JR, Mooney HA, Sala OE, Schulze ED (1996) A global analysis of root distributions for terrestrial biomes. Oecologia 108:389-411.

John R, Dalling JW, Harms KE, Yavitt JB, Stallard RF, Mirabello M, Hubbell SP, Valencia R, Navarrete H, Vallejo M, Foster RB (2007) Soil nutrients influence spatial distributions of tropical tree species. Proceedings of the National Academy of Sciences 104:864-869.

Johnson NC, Zal DR, Tilman D, Pfleger FL (1991) Dynamics of vesicular-buscular mycorrhizae during old field succession. Oecologia 86:349-358.

Kauffman JB, Cummings DL, Ward DE, Babbit R (1995) Fire in the Brazilian Amazon: 1. Biomass, nutrient pools, and losses in slashed primary forests. Oecologia 104:397-408.

Keller M, Veldkamp E, Weitz AM, Reiners WA (1993) Effect of pasture age on soil trace-gas emissions from a deforested area of Costa Rica. Nature 365:244-246.

Kembel SW, Cowan PD, Helmus MR, Cornwell WK, Morlon H, Ackerly DD, Blomberg SP, Webb CO (2010) Picante: R tools for integrating phylogenies and ecology. Bioinformatics 26:1463-1464.

Kennard DK (2002) Secondary forest succession in a tropical dry forest: patterns of development across a 50-year chronosequence in lowland Bolivia. Journal of Tropical Ecology 18:53-66.

Klumpp R, Shaufele R, Lotscher M, Lattanzi FA, Feneis W, Schnyder H (2005) C-isotope composition of C02 respired by shoots and roots: fractionation during dark respiration? Plant, Cell and Environment 28:241-250.

Kobe RK (1999) Light gradient partitioning among tropical tree species through differential seedling mortality and growth. Ecology 80:187-201.

Koch GW, Sillett SC, Jennings GM, Davis SD (2004) The limits to tree height. Nature 428:851-854.

Koerner W, Dambrine E, Dupouey JL, Benoit (1999) $\delta^{15}N$ of forest soil and understory vegetation reflect the former agricultural land use. Oecologia 121:421-425

Koerselman W, Meuleman AF (1996) The vegetation N:P ratio: a new tool to detect the nature of nutrient limitation. The Journal of Applied Ecology 33:1441-1450.

Körner CH, Diemer M (1987) In situ photosynthetic responses to light, temperature and carbon disxide in herbaceous plants from low to high altitude. Functional Ecology 1:179-194.

Kull O, Kruijt B (1999) Acclimation of photosynthesis to light: A mechanistic approach. Functional Ecology 13:24-36.

Kuo S (1996) Phosphorus. *Methods of soil analysis. Part 3: Chemical methods*. (ed D.L. Sparks), pp. 869-919. Soil Science Society of America, Madison, Wisconsin.

Kraft NJ, Valencia R, Ackerly DD (2008) Functional traits and niche-based tree community assembly in an Amazonian forest. Science 322:580-582.

Lawrence D (2005) Biomass accumulation after 10-200 years of shifting cultivation in Bornean rain forest. Ecology 86:26-33

Lin G, Enleringer JR, Rygiewicz PT, Johnson MG, Tingey DT (1999) Elevated $C0_2$ and temperature impacts on different components of soil $C0_2$ efflux in Douglas-fir terracosms. Global Change Biology 5:157-168.

Maddison DR, Moore W, Baker MD, Ellis TM, Ober KA, Cannone JJ, Gutell RR (2009) Monophyly of terrestrial adephagan beetles as indicated by three nuclear genes (Coleoptera: Carabidae and Trachypachidae). Zoologica scripta 38:43-62.

Markewitz D, Davidson E, Moutinho P, Nepstad D (2004) Nutrient loss and redistribution after forest clearing on a highly weather soil in Amazonia. Ecological Applications 14:S177-S199.

Martinelli LA, Victoria RL, Trivelin PC, Devol AH, Richey JE (1992) $^{15}N$ natural abun- dance in plants of the Amazon river floodplain and potential atmospheric $N_2$ fixation. Oecologia 90:591-596.

Martinelli LA, Piccolo MC, Townsend AR, Vitousek PM, Cuevas E, McDowell W, Robertson GP, Santos OC, Treseder K (1999) Nitrogen stable isotopic

composition of leaves and soil: Tropical versus temperate forests. Biogeochemistry 46:45-65.

Matson P (1990) Plant-soil interactions in primary succession at Hawaii Volcanoes National Park. Oecologia 85:241-246.

Moran EF, Brondizio ES, Tucker JM, Silva-Forsberg MC, McCracken S, Falesi I (2000) Effects of soil fertility and land-use on forest succession in Amazonia. Forest Ecology and Management 139:93-108.

Myneni RB, Yang W, Nemani RR, Huete AR, Dickinson RE, Knyazikhin Y, Didan K, Fu R, Negrón Juárez RI, Saatchi SS, Hashimoto H, Ichii K, Shabanov NV, Tan B, Ratana P, Privette JL, Morisette JT, Vermote EF, Roy DP, Wolfe RE, Friedl MA, Running SW, Votava P, El-Saleous N, Devadiga S, Su Y, Salomonson VV (2007) Large seasonal swings in leaf area of Amazon rainforests. Proceedings of the National Academy of Sciences 104:4820-3.

Nadelhoffer KJ, Fry B (1988) Controls on natural nitrogen-15 and carbon-13 abundance in forest soil organic matter. Soil Science Society of America 52:1633-1640.

Nepstad DC, de Carvalho CR, Davidson EA, Jipp PH, Lefebvre PA, Negreiros GH, da Silva ED, Stone TA, Trumbore SE, Vieira S (1994) The role of deep roots in the hydrological and carbon cycles of Amazonian forests and pastures. Nature 372:666-669.

Niinemets U (2007) Photosynthesis and resource distribution through plant canopies. Plant, Cell and Environment 30:1052-1071.

Nogueira E, Fearnsid P, Nelson B, Franca M (2007) Wood density in forests of Brazil's "arc of deforestation": Implications for biomass and flux of carbon from land-use change in Amazonia. Forest Ecology and Management 248:119-135.

Ometto JPH, Flanagan BLB, Martinelli LA, Moreira MZ, Higuchi N, Ehleringer JR (2002) Carbon isotope discrimination in forest and pasture ecosystems of the Amazon Basin, Brazil. Global Biogeochemical Cycles 16:1-10.

Ometto JPH, Ehleringer JR, Tomas DF, Berry JA, Ishida FY, Mazzi E, Higuchi N, Flanagan LB, Nardoto GB, Martinelli LA (2006) The stable carbon and nitrogen isotopic composition of vegetation in tropical forests of the Amazon Basin, Brazil. Biogeochemistry 79:251-274.

Ostertag R, Marín-Spiotta E, Silver WL, Schulten J (2008) Litterfall and decomposition in relation to soil carbon pools along a secondary forest chronosequence in Puerto Rico. Ecosystems 11:701-714.

Paradis E, Claude J, Strimmer K (2004) APE: Analyses of Phylogenetics and Evolution in R language. Bioinformatics 20:289-290.

Park R, Epstein S (1960) Carbon isotope fractionation during photosynthesis. Geochimica et Cosmochimica Acta 21:110-126.

Paul K, Polglase P, Nyakuengama J, Khanna P (2002) Change in soil carbon following afforestation. Forest Ecology and Management 168:241-257.

Peña-Claros M (2003) Changes in forest structure and species composition during secondary forest succession in the Bolivian Amazon. Biotropica 35:450-461.

Peterson BJ, Fry B (1987) Stable isotopes in ecosystem studies. Annual Review of Ecology and Systematics 18:293-320.

Piccolo MC, Neill C, Cerri CC (1994) Natural abundance of $^{15}N$ in soils along forest-to-pasture chronosequences in the western Brazilian Amazon Basin. Oecologia 99:1-2.

Piccolo MC, Neill C, Melillo JM (1996) $^{15}N$ natural abundance in forest and pasture soils of the Brazilian Amazon Basin. Plant Soil 182:249-258.

Pinard M, Putz F, Rumiz D, Guzmán R, Jardim A (1999) Ecological characterization of tree species for guiding forest management decisions in seasonally dry forests in Lomerio, Bolivia. Forest Ecology and Management 113:201-213.

Poorter L, van de Plassche S, Boot RG (2004) Leaf traits and herbivory rates of tropical tree species differing in successional status. Plant Biology 6:746-754.

Poorter L (2007) Are species adapted to their regeneration niche, adult niche, or both? The America Naturalist 169:433-442.

Powers JS, Tiffin P (2010) Plant functional type classifications in tropical dry forests in Costa Rica: leaf habit versus taxonomic classifications. Functional Ecology 24:927-936.

Pringle EG, Adams RI, Broadbent E, Busby PE, Donatti CI, Kurten EL, Renton K, Dirzo R (2010) Distinct leaf-trait syndromes of evergreen and deciduous trees in a seasonally dry tropical forest. Biotropica 43:299-308.

Quay P, King S, Wilbur D (1989) $^{13}C/^{12}C$ of atmospheric $C0_2$ in the Amazon basin: Forest and river sources. Journal of Geophysical Research. 94:13,327-18,336.

Quesada CA, Lloyd J, Schwarz M, Baker TR, Phillips OL, Czimczik C, Hodnett MG, Herrera R, Arneth A, Lloyd G, Santos AJ, Schmerler J, Malhi Y, Dezzeo N, Arroyo L, Silveira M, Filho NP, Jimenez EM, Paiva R, Vieira I, Neill DA, Silva N, Monteagudo A, Prieto A, Rudas A, Almeida S, Higuchi N, Lezama AT, Peacock J, Fyllas NM, Erwin T, Pitman N, Chao KJ, Honorio E, Killeen T, Terborgh J (2009) Regional and large-scale patterns in Amazon forest structure and function are mediated by variations in soil physical and chemical properties. Biogeosciences Discuss 6:3993-4057.

Quintero CE, Boschetti NG, Benevidez RA (2003) Effect of soil buffer capacity on soil test phosphorus interpretation and fertilizer requirement. Communications in soil science and plant analysis. 34:1435-1450.

Rastetter EB, Vitousek PM, Field C, Shaver GR, Herbert D, Agren GI (2001) Resource optimization and symbiotic nitrogen fixation. Ecosystems 4:369-388.

Reich P, Ellsworth D, Uhl C (1995) Leaf carbon and nutrient assimilation and conservation in species of differing successional status in an oligotrophic Amazonian forest. Functional Ecology 9:65-76.

Robinson D (2001) $\delta^{15}N$ as an integrator of the nitrogen cycle. Trends in Ecology & Evolution 16:153-162.

Romanya J, Khanna PK, Raison RJ (1994) Effects of slash burning on soil phosphorus fractions and sorption and desorption of phosphorus. Forest Ecology and Management 65:89-103.

Saldarriaga J (1985) Forest succession in the Upper Rio Negro of Columbia and Venezuela. Ph.D. dissertation, University of Tennessee, Knoxville, TN, USA.

Sanderson MJ (2002) Estimating absolute rates of molecular evolution and divergence times: a penalized likelihood approach. Molecular Biology and Evolution 19:101-109.

Schedlbauer JL, Kavanagh KL (2008) Soil carbon dynamics in a chronosequence of secondary forests in northeastern Costa Rica. Forest Ecology and Management 255:1326-1335.

Schoenholtz SH, Van Miegroet H, Burger JA (2000) A review of chemical and physical properties as indicators of forest soil quality: challenges and opportunities. Forest Ecology and Management 138:335-56.

Schulze ED (1986) Carbon dioxide and water vapor exchange in response to drought in the atmosphere and in the soil. Annual Review of Plant Physiology 37:247-274.

Schulze ED, Chapin FS III, Gebauer G (1994) Nitrogen nutrition and isotope differences among life forms at the northern treeline of Alaska. Oecologia 100:406-412.

Schuur EA, Matson PA (2001) Net primary productivity and nutrient cycling across a mesic to wet precipitation gradient in Hawaiian montane forest. Oecologia 128:431-442.

Schwartz D (1991) Interet de la mesure du $\delta^{13}C$ des sols en milieu naturel equatorial pour la connaissance des aspects pedologiques et ecologiques des relations savane-forest. Cahiers de l'Orstom, série Pédologie. 26:327-341.

Schweizer M, Fear S, Cadisch G (1999) Isotopic ((13)C) fractionation during plant residue decomposition and its implications for soil organic matter studies. Rapid Communications in Mass Spectrometry 13:1284-1290.

Skjemstad JO, Le Feuvre RP, Prebbie RE (1990) Turnover of soil organic matter under pasture as determined by $^{13}C$ abundance. Australian Journal of Soil Research 28:267-276.

Silver WL, Ostertag R, Lugo AE (2000) The potential for carbon sequestration through reforestation of abandoned tropical agricultural and pasture lands. Restoratation Ecology. 8:394-407.

Silver WL, Neff J, McGroddy M, Veldkamp E, Keller M, Cosme R (2000) Effects of soil texture on belowground carbon and nutrient storage in a lowland Amazonian forest ecosystem. Ecosystems 3:193-209.

Smith BN (1971) Carbon isotope ratios of respired $C0_2$ from castor bean, corn, peanut, pea, radish, squash, sunflower and wheat seedlings. Plant Cell Physiology. 12:451-455.

Swaine MD, Whitmore TC (1988) On the definition of ecological species groups in tropical rain forests. Plant Ecology 75:81-86.

Swenson NG, Enquist BJ (2007) Ecological and evolutionary determinants of a key plant functional trait: wood density and its community-wide variation across latitude and elevation. American Journal of Botany 94:451-459.

Tessier JT, Raynal DJ (2003) Use of nitrogen to phosphorus ratios in plant tissue as an indicator of nutrient limitation and nitrogen saturation. Journal of Applied Ecology 40:523-534.

Toledo M, Salick J (2006) Secondary succession and indigenous management in semideciduous forest fallows of the Amazon Basin. Biotropica 38:161-170.

Toledo M, Poorter L, Peña-Claros M, Alarcón A, Balcázar J, Leaño C, Licona JC, Bongers F (2011) Climate and soil drive forest structure in Bolivian lowland forests. Journal of Tropical Ecology 27:333-345.

Townsend AR, Cleveland CC, Asner GP, Bustamante MMC (2007) Controls over foliar N: P ratios in tropical rain forests. Ecology 88:107-118.

Uhl C, Buschbacher R, Serrao EAS (1988) Abandoned pastures in eastern Amazonia. I. Patterns of plant succession. Journal of Ecology 76:663-681.

Van Breugel M, Bongers F, Martínez-Ramos M (2007) Species dynamics during early secondary forest succession: recruitment, mortality and species turnover. Biotropica 35:610-619.

Veldkamp E, Weitz AM (1994) Uncertainty analysis of studies. Soil Biology and Biochemistry 26:153-160.

Vitousek PM, Reiner WA (1975) Ecosystem succession and nutrient retention: a hypothesis. BioScience 25:376-381.

Vitousek PM, Shearer G, Kohl D (1989) Foliar $^{15}N$ natural abundance in Hawaiian rainforest: patterns and possible mechanisms. Oecologia 78:383-388.

Vitousek PM, Turner DR, Kitayama K (1995) Foliar nutrients during long-term soil development in Hawaiian montane rain forest. Ecology 76:712-720.

Vitousek PM, Field C, Matson P (1990) Variation in foliar $\delta^{13}C$ in Hawaiian *Metrosideros polymorpha*: a case of internal resistance? Oecologia 84:362-370.

Wadsworth FH (1997) Forest production for tropical America. Agriculture Handbook 710. United States Department of Agriculture Forest Service, Washington, DC.

Wallander H, Morth CM, Giesler R (2009) Increasing abundance of soil fungi is a driver for $^{15}N$ enrichment in soil profiles along a chronosequence undergoing isostatic rebound in northern Sweden. Oecologia 160:87-96

Wang L, Shaner P-J, Macko S (2007) Foliar $^{15}N$ patterns along successional gradients at plant community and species levels. Geophysical Research Letters. 34:1-6.

Waring RH, Running SW (2007) Temporal changes in forest structure and function. *Forest Ecosystems: Analysis at Multiple Scales*. pp. 149-182. Elsevier, Burlington, MA.

Waring RH, Silvester WB (1994) Variation in foliar $\delta^{13}C$ values within the crowns of *Pinus radiata* trees. Tree physiology 14:1203-1213.

Webb CO, Ackerly DD, Kembel SW (2008) Phylocom: software for the analysis of phylogenetic community structure and trait evolution. Bioinformatics 24:2098-2100.

Weir J, Bermingham E, Schluter D (2009) The great American biotic interchange in birds. Proceedings of the National Academy of Sciences 106:21737-21742.

Werner P (1984) Changes in soil properties during tropical wet forest succession in Costa Rica. Biotropica 16:43-50.

Wikstrom N, Savolainen V, Chase MW (2001) Evolution of the angiosperms: calibrating the family tree. Proceedings of the Royal Society B 268:2211-2220.

Wong SC, Cowan IR, Farquahr GD (1979) Stomatal conductance correlates with photosynthetic capacity. Nature 282:424-426.

Wojciechowski MF, Lavin M, Sanderson MJ (2004) A phylogeny of legumes (Leguminosae) based on analysis of the plastic MATK gene resolves many well-supported subclades within the family. American Journal of Botany 91:1846-1862.

World Agroforestry Center. (2010) Wood Density Database.

Wright IJ, Westoby M, Reich PB (2001) Strategy shifts in leaf physiology, structure and nutrient content between species of high- and low-rainfall and high- and low-nutrient habitats. Functional Ecology 15:351-359.

Wright IJ, Reich PB, Westoby M, Ackerly DD, Baruch Z, Bongers F, Cavender-Bares J, Chapin T, Cornelissen JHC, Diemer M, Flexas J, Garnier E, Groom PK, Gulias J, Hikosaka K, Lamont BB, Lee T, Lee W, Lusk C, Midgley JJ, Navas ML, Niinemets U, Oleksyn J, Osada N, Poorter H, Poot P, Prior L, Pyankov VI, Roumet C, Thomas SC, Tjoelker MG, Veneklaas EJ, Villar R (2004) The worldwide leaf economics spectrum. Nature 428:821-827.

Wright IJ, Reich PB, Cornelissen JH, Falster DS, Garnier E, Hikosaka K, Lamont BB, Lee W, Oleksyn J, Osada N, Poorter H, Villar R, Waron DI, Westoby M (2005) Assessing the generality of global leaf trait relationships. The new phytologist 166:485-496.

Yakir D, Sternberg LD (2000) The use of stable isotopes to study ecosystem gas exchange. Oecologia 123:297-311.

Yan ER, Wang XH, Huang JJ (2006) Shifts in plant nutrient use strategies under secondary forest succession. Plant and Soil 289:187-197.

Yoneyama T, Muraoka T, Murakami T, Boonkerd N (1993) Natural abundance of 15N in tropical plants with emphasis on tree legumes. Plant and Soil 153:295-304.

Zarin DJ, Davidson EA, Brondizio E, Vieira ICG, Sa T, Feldpausch T, Schuur EAG, Mesquita R, Moran E, Dalamonica P, Ducey MJ, Hurtt GC, Salimon C, Denich M (2005) Legacy of fire slows carbon accumulation in Amazonian forest regrowth. Frontiers in Ecology 3:365-369.

Zerega NJ, Clement WL, Datwyler SL, Weiblen GD (2005) Biogeography and divergence times in the mulberry family (Moraceae). Molecular phylogenetics and evolution 37:402-416.

## 5.9 Tables

**Table 5.1:** Stand characteristics of all successional and primary (Pr) forest study sites (mean±std. dev.).

| | Stand age (years) | | | | | | | | | | | | | | | | |
|---|---|---|---|---|---|---|---|---|---|---|---|---|---|---|---|---|---|
| | 4 | 5 | 7 | 10 | 14 | 18 | 21 | 25 | 32 | 33 | 35 | 37 | 38 | 43 | 47 | Pr-1 | Pr-2 |
| Tree density (# ha-1) | 1537.5 | 1375.0 | 1637.5 | 1912.5 | 950.0 | 1450.0 | 1237.5 | 775.0 | 1350.0 | 1837.5 | 1237.5 | 1025.0 | 1375.0 | 1487.5 | 1700.0 | 1325.0 | 1387.5 |
| Dead trees (# ha-1) | 937.5 | 237.5 | 125.0 | 137.5 | 137.5 | 162.5 | 100.0 | 87.5 | 75.0 | 50.0 | 75.0 | 62.5 | 50.0 | 62.5 | 100.0 | 100.0 | 62.5 |
| Basal area (m2 ha-1) | 10.6 | 13.2 | 32.1 | 24.8 | 33.4 | 32.1 | 31.6 | 28.2 | 43.7 | 36.1 | 27.3 | 17.3 | 30.5 | 43.3 | 54.0 | 34.5 | 36.3 |
| Biomass (Mg ha-1) | 27.3 | 36.1 | 158.3 | 101.8 | 152.0 | 118.2 | 196.6 | 133.4 | 304.9 | 243.7 | 158.4 | 114.3 | 204.9 | 269.8 | 460.5 | 282.3 | 325.6 |
| CE (avg±std. dev.; 1-5) * | 4.5±0.7 | 3.5±1.5 | 2.3±1.3 | 3.2±1.4 | 3.1±1.5 | 2.9±1.4 | 2.6±1.4 | 3.6±1.4 | 2.1±1.3 | 1.9±1.2 | 2.6±1.3 | 2.8±1.6 | 2.7±1.3 | 2.5±1.3 | 2.6±1.4 | 1.9±1.2 | 1.7±1.0 |
| Tree height (avg±std. dev.; m) | 8.1±2.3 | 8.7±3.0 | 12.6±4.9 | 10.2±3.9 | 13.3±7.2 | 10.9±5.7 | 13.4±6.9 | 13.0±6.0 | 10.3±5.0 | 10.7±6.7 | 10.6±6.6 | 8.2±4.3 | 10.7±6.9 | 11.1±5.9 | 11.4±6.5 | 11.8±6.1 | 11.1±6.3 |
| Tree height (max; m) | 14 | 16 | 25 | 19 | 28 | 27 | 30 | 26 | 28 | 30 | 27 | 30 | 28 | 27 | 38 | 30 | 36 |
| DBH (avg±std. dev.; cm) ** | 8.9±3.0 | 10.3±4.0 | 13.7±7.9 | 11.7±5.3 | 17.9±11.4 | 14.0±9.3 | 15.6±9.1 | 19.2±9.8 | 15.5±13.2 | 12.5±9.8 | 13.6±9.8 | 11.6±9.0 | 13.2±10.4 | 15.3±11.8 | 14.6±13.9 | 13.5±12.3 | 13.3±12.6 |
| DBH (max; cm) ** | 17.7 | 20.0 | 59.3 | 30.0 | 69.0 | 67.0 | 45.8 | 52.0 | 78.5 | 49.5 | 55.2 | 73.0 | 50.8 | 52.8 | 102.0 | 82.0 | 78.3 |
| Lianas (avg±std. dev.; 1-4) | 2.1±1.0 | 1.5±1.1 | 1.3±0.8 | 1.6±1.0 | 1.8±1.0 | 1.8±1.2 | 1.7±1.1 | 1.5±1.0 | 1.5±0.9 | 1.7±1.1 | 1.8±1.1 | 2.5±1.3 | 1.7±1.0 | 1.3±0.7 | 1.8±1.1 | 1.4±0.6 | 1.5±0.9 |
| Mature leaves (avg±std. dev.; %) | 65.0±23.3 | 56.2±23.5 | 66.0±22.3 | 67.0±25.5 | 52.7±31.1 | 65.2±31.9 | 55.`±31.1 | 41.1±32.7 | 72.6±25.5 | 75.0±23.3 | 65.8±31.4 | 75.6±22.7 | 72.0±25.5 | 62.4±28.6 | 76.3±27.8 | 70.2±23.4 | 72.8±22.0 |
| New leaves (avg±std. dev.; %) | 5.4±9.7 | 4.1±8.7 | 3.4±9.0 | 3.7±12.6 | 4.7±18.3 | 5.7±14.3 | 5.7±12.0 | 4.4±13.4 | 5.0±17.7 | 3.4±11.4 | 6.6±17.7 | 0.9±5.7 | 2.4±7.0 | 2.4±11.6 | 2.7±11.1 | 6.7±13.8 | 4.4±10.9 |
| Senescent leaves (avg±std. dev.; %) | 13.5±10.8 | 14.0±12.1 | 7.0±8.6 | 10.3±12.9 | 10.5±11.5 | 6.2±9.1 | 7.6±9.6 | 8.6±9.1 | 6.5±10.0 | 6.7±9.8 | 6.6±9.0 | 6.2±10.3 | 7.5±9.1 | 9.7±10.1 | 5.1±8.8 | 6.0±12.7 | 4.5±7.7 |
| No leaves (avg±std. dev.; %) | 16.0±19.4 | 26.0±22.8 | 23.6±20.4 | 19.0±21.6 | 32.2±30.9 | 22.8±27.1 | 31.7±29.6 | 46.0±32.1 | 15.9±17.7 | 15.0±18.7 | 21.1±26.6 | 18.1±22.6 | 18.2±22.1 | 25.6±27.2 | 16.0±21.6 | 17.0±15.2 | 18.2±16.7 |
| Wood density (avg±std. dev.; kg m-3) | 456±112.3 | 402.7±130.4 | 496.3±124.2 | 521.3±95.2 | 459.2±128.3 | 464.8±132.9 | 485.6±107.1 | 466.9±97.9 | 611.9±91.3 | 654.0±177.3 | 526.1±91.0 | 620.8±96.9 | 578.1±88.3 | 579.2±91.1 | 601.2±83.5 | 601.3±59.2 | 606.4±83.1 |
| Richness (# sp transect-1) | 16 | 18 | 37 | 17 | 25 | 27 | 23 | 15 | 51 | 55 | 44 | 40 | 50 | 57 | 49 | 38 | 43 |
| Diversity (Shannon-Weiner) | 2.3 | 2.3 | 3.0 | 1.8 | 2.9 | 2.7 | 2.6 | 2.3 | 3.7 | 3.4 | 3.5 | 3.4 | 3.7 | 3.8 | 3.5 | 3.3 | 3.5 |
| CJ vs. primary *** | 0.99 | 0.98 | 0.87 | 0.97 | 0.94 | 0.89 | 0.93 | 0.96 | 0.75 | 0.45 | 0.68 | 0.65 | 0.65 | 0.31 | 0.31 | | |

* Crown Exposure (CE) index, ** Diameter at Breast Height (1.3 m), *** Chao-Jaccard community composition similarity versus primary forest sites.

**Table 5.2:** Soil properties for all successional and primary (Pr) forest study sites

| | Stand age (years) | | | | | | | | | | | | | | |
|---|---|---|---|---|---|---|---|---|---|---|---|---|---|---|---|
| | 5 | 7 | 10 | 14 | 18 | 21 | 25 | 32 | 35 | 37 | 38 | 43 | 47 | Pr-1 | Pr-2 |
| Carbon (C; Mg ha-1) | 25.6 | 15.1 | 18.6 | 23.4 | 20.6 | 22.9 | 23.3 | 19.4 | 34.7 | 17.8 | 28.6 | 24.4 | 27.1 | 25.7 | 20.4 |
| Nitrogen (N; kg ha-1) | 2971.6 | 1714.9 | 2222.3 | 2670.9 | 2532.5 | 2600.1 | 2189.5 | 2538.8 | 3422.9 | 2322.9 | 2883.6 | 2521.3 | 2920.4 | 3210.8 | 2365.5 |
| $\delta^{15}N$ | 9.7 | 9.8 | 10.8 | 9.2 | 9.0 | 8.0 | 7.1 | 8.3 | 7.6 | 10.0 | 8.8 | 8.9 | 9.1 | 9.2 | 9.1 |
| $\delta^{13}C$ | -27.4 | -29.3 | -27.6 | -28.1 | -28.2 | -28.1 | -27.9 | -28.2 | -28.2 | -28.0 | -28.2 | -29.2 | -28.2 | -27.1 | -27.4 |
| Phosphorus (P1; kg ha-1) * | 9.3 | 7.2 | 8.4 | 8.6 | 2.9 | 7.3 | | 7.3 | 10.1 | 1.9 | 7.8 | 11.6 | 7.9 | 9.9 | 2.8 |
| Phosphorus (P2; kg ha-1) ** | 10.7 | 10.9 | 12.0 | 11.2 | 10.9 | 10.9 | | 7.3 | 11.2 | 3.9 | 7.8 | 15.4 | 15.7 | 7.9 | 7.0 |
| Calcium (Ca; kg ha-1) | 253.0 | 138.7 | 256.4 | 305.4 | 279.5 | 348.9 | | 690.0 | 418.7 | 180.6 | 223.1 | 1465.1 | 253.4 | 269.4 | 1366.4 |
| Potassium (K; kg ha-1) | 284.6 | 93.7 | 87.6 | 148.3 | 128.4 | 235.2 | | 194.9 | 196.2 | 213.1 | 108.5 | 98.2 | 209.0 | 264.8 | 141.6 |
| Magnesium (Mg; kg ha-1) | 201.9 | 53.2 | 82.5 | 171.4 | 152.4 | 150.8 | | 254.7 | 169.4 | 121.4 | 80.9 | 196.0 | 107.9 | 134.3 | 357.2 |
| Sodium (Na; kg ha-1) | 27.8 | 23.2 | 34.3 | 34.7 | 31.1 | 53.4 | | 29.5 | 31.7 | 44.4 | 35.7 | 28.1 | 42.9 | 45.8 | 41.2 |
| Hydrogen (H; kg ha-1) | 32.3 | 21.9 | 32.2 | 26.4 | 36.5 | 40.3 | | 73.4 | 48.9 | 31.4 | 31.3 | 27.2 | 67.4 | 47.8 | 17.6 |
| CEC (kmol ha-1) *** | 69.8 | 36.4 | 55.3 | 60.8 | 67.3 | 78.1 | | 134.5 | 89.8 | 57.5 | 53.2 | 120.0 | 95.6 | 80.6 | 120.5 |
| Base saturation (%) | 54.0 | 40.3 | 42.2 | 57.0 | 46.2 | 48.9 | | 45.9 | 45.9 | 45.9 | 41.6 | 77.5 | 30.1 | 41.2 | 85.5 |
| Sand (Mg ha-1) | 1797.2 | 2478.1 | 2331.4 | 2256.3 | 1823.4 | 2338.6 | 1682.1 | 2344.1 | 1956.7 | 1261.4 | 1800.0 | 2559.8 | 2218.4 | 1358.0 | 2251.3 |
| Silt (Mg ha-1) | 1155.4 | 666.6 | 894.2 | 836.8 | 1099.8 | 668.2 | 1195.5 | 669.7 | 1060.5 | 1572.8 | 1334.5 | 863.6 | 881.0 | 1515.9 | 713.1 |
| Clay (Mg ha-1) | 613.3 | 478.2 | 766.5 | 642.5 | 694.6 | 624.6 | 597.8 | 626.1 | 716.9 | 1058.9 | 744.8 | 431.8 | 833.8 | 1073.8 | 531.4 |
| Soil mass (Mg ha-1) € | 3565.9 | 3623.0 | 3992.2 | 3735.6 | 3617.8 | 3631.4 | 3475.4 | 3639.9 | 3734.1 | 3893.1 | 3879.3 | 3855.1 | 3933.2 | 3947.8 | 3495.8 |
| Bulk density (Avg. 0-30 cm; g cm-3) | 1.233 | 1.235 | 1.357 | 1.300 | 1.235 | 1.237 | 1.180 | 1.269 | 1.303 | 1.336 | 1.323 | 1.309 | 1.338 | 1.399 | 1.183 |

* Weak Bray Extraction, ** Strong Bray Extraction, € Adjusted for mass > 2 mm, *** Cation Exchange Capacity calculated as the sum of Ca, K, Mg, Na and H (meq/100g).

**Table 5.3:** Characteristics of tree species selected for analysis of foliar properties.

| Species ID | Common name | | Scientific name | | | Wood density (kg m-3) | Successional age (years) | Total (sampled) stems ** | Foliar n α |
|---|---|---|---|---|---|---|---|---|---|
| | Portuguese | Spanish | Genus | Species | Family | | | | |
| 1 | Ambaibo | Ambaibillo | *Cecropia* | *polystachya* | Cecropiaceae | 280 | 6 | 76(14) | 28 α |
| 2 | Favera | Serebo | *Schizolobium* | *parahyba* | Fabaceae | 360 | 7 | 7(3) | 6 |
| 3 | Gameleira | Gomellera | *Ficus* | *insipida* | Moraceae | 482 | 10 | 7(2) | 4 |
| 4 | Vela blanca | | *Miconia* | sp. | Melastomataceae | 587 | 10 | 128(22) | 44 α |
| 5 | Ambaibo | Ambaibo | *Cecropia* | *sciadophylla* | Cecropiaceae | 280 | 14 | 57(9) | 18 |
| 6 | Pente de Macaco | Peine de Mono | *Apeiba* | *tibourbou* | Tiliaceae | 292 | 14 | 39(2) | 4 |
| 7 | Marupa | Chepereque | *Jacaranda* | *cuspidifolia* | Bignoniaceae | 518 | 18 | 157(28) | 56 α |
| 8 | Mutanba | Mutanba | *Guazuma* | *crinita* | Sterculiaceae | 540 | 25 | 14(5) | 10 |
| 9 | Inga | Pacai | *Inga* | sp. | Fabaceae | 603 | 32 | 86(20) | 40 α |
| 10 | Urucuseco | Urucurana | *Sloanea* | sp. | Elaeocarpaceae | 513 | 33 | 16(4) | 8 |
| 11 | Joao Mole | Joao Mole | *Neea* | sp. | Nyctaginaceae | 454 | 33 | 36(11) | 22 |
| 12 | Louro preto | Laurel | *Endlicheria* | *krukovii* | Lauraceae | 588 | 33 | 40(5) | 10 |
| 13 | Biorana | Trompillo | *Pouteria* | sp. | Sapotaceae | 769 | 35 | 21(4) | 8 |
| 14 | Pama | Nui | *Pseudolmedia* | *laevis* | Moraceae | 593 | 35 | 31(2) | 4 |
| 15 | Enviara caju | Piraquina | *Onychopetalum* | *periquino* | Annonaceae | 619 | 37 | 27(8) | 16 |
| 16 | Guayabochi | Guayabochi | *Capirona* | *decorticans* | Rubiaceae | 840 | 37 | 16(2) | 4 |
| 17 | Guariuba | Murure | *Clarisia* | *racemosa* | Moraceae | 550 | 37 | 9(2) | 4 |
| 18 | Jachi | Palo santo | *Tachigali* | *paniculata* | Fabaceae | 600 | 41 | 16(2) | 4 |
| 19 | Breu branco | | *Rollinia* | *calcarata* | Annonaceae | 520 | 43 | 16(2) | 4 |
| 20 | Balsamo | Balsamo | *Myroxylon* | *balsamum* | Fabaceae | 796 | 43 | 3(2) | 4 |

* Across all study sites, α = selected for individual species response analyses

**Table 5.4:** Best subsets models of leaf traits versus stand age, species successional status, and Principal Component Analysis (PCA) derived gradients in stand biomass and structure, and soil texture and fertility. Data represents the *t*-ratio (*F*-ratio) and *P*-value significance, with increasing * representing *P*-values of 0.1, 0.05, 0.01, and 0.001, respectively, and ϕ < 0.0001.

| Leaf traits | Stand age | Species Successional Status | PCA Axes | | | | Adj-$R^2$ | *P*-value | *N* |
|---|---|---|---|---|---|---|---|---|---|
| | | | Biomass | Structure | Texture | Fertility | | | |
| N | - | 2.54 (6.46) ** | - | - | - | - | 0.021 | 0.0116 | 265 |
| P | - | - | - | - | 2.61 (6.83) *** | - | 0.026 | 0.0096 | 222 |
| N:P | - | 4.09 (16.76) ϕ | - | - | -3.79 (14.40) ϕ | - | 0.115 | < 0.0001 | 221 |
| C % | - | - | - | - | - | - | - | - | 260 |
| N % | - | 2.40 (5.74) *** | - | - | - | - | 0.018 | 0.0173 | 262 |
| C:N | - | -2.44 (5.97) *** | - | - | - | - | 0.019 | 0.0152 | 259 |
| $\delta^{13}C$ | 3.58 (12.85) ϕ | -7.93 (62.86) ϕ | - | - | - | - | 0.202 | < 0.0001 | 258 |
| $\delta^{15}N$ | -7.54 (56.92) ϕ | - | 4.30 (18.50) ϕ | -3.17 (10.02) *** | - | - | 0.234 | < 0.0001 | 263 |

## 5.10 Figures

**Figure 5.1:** Linear relationship between stand age (years) and species successional status mean (years; left), standard error (SE; middle) and annual change (years; right). Stand values are calculated using all tree stems within each secondary forest stand.

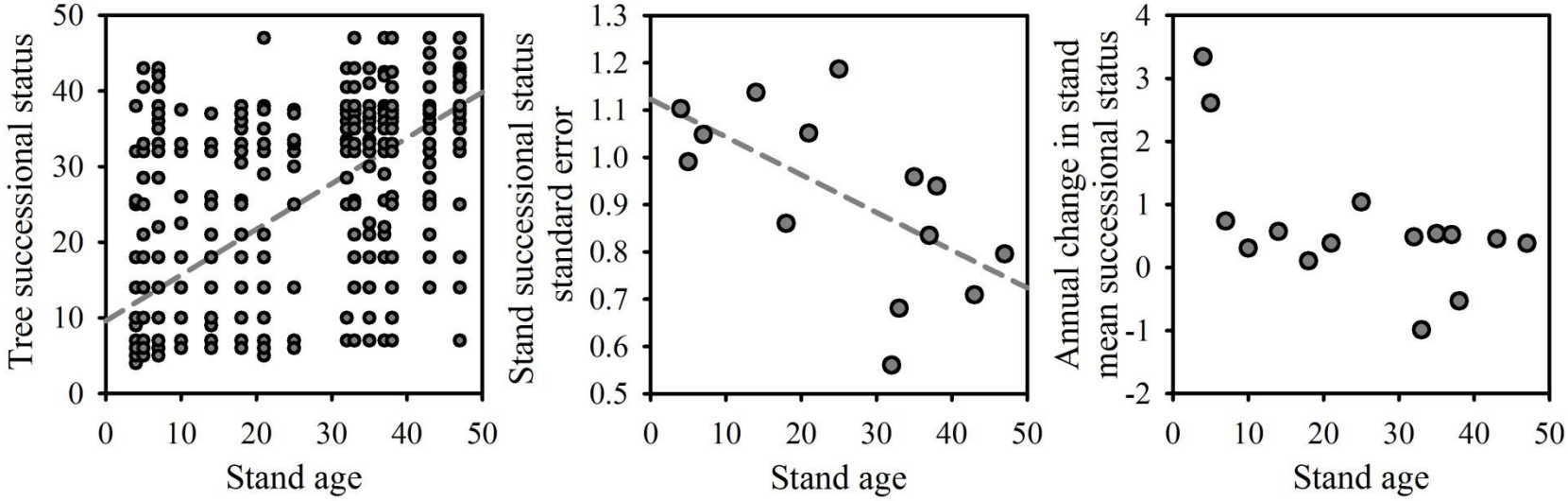

**Figure 5.2:** Percentage total living trees in understory and overstory crown exposure (CE) positions; 1-3, and 4-5, respectively. Stand development phases (top) correspond to those described by Waring & Running (2007).

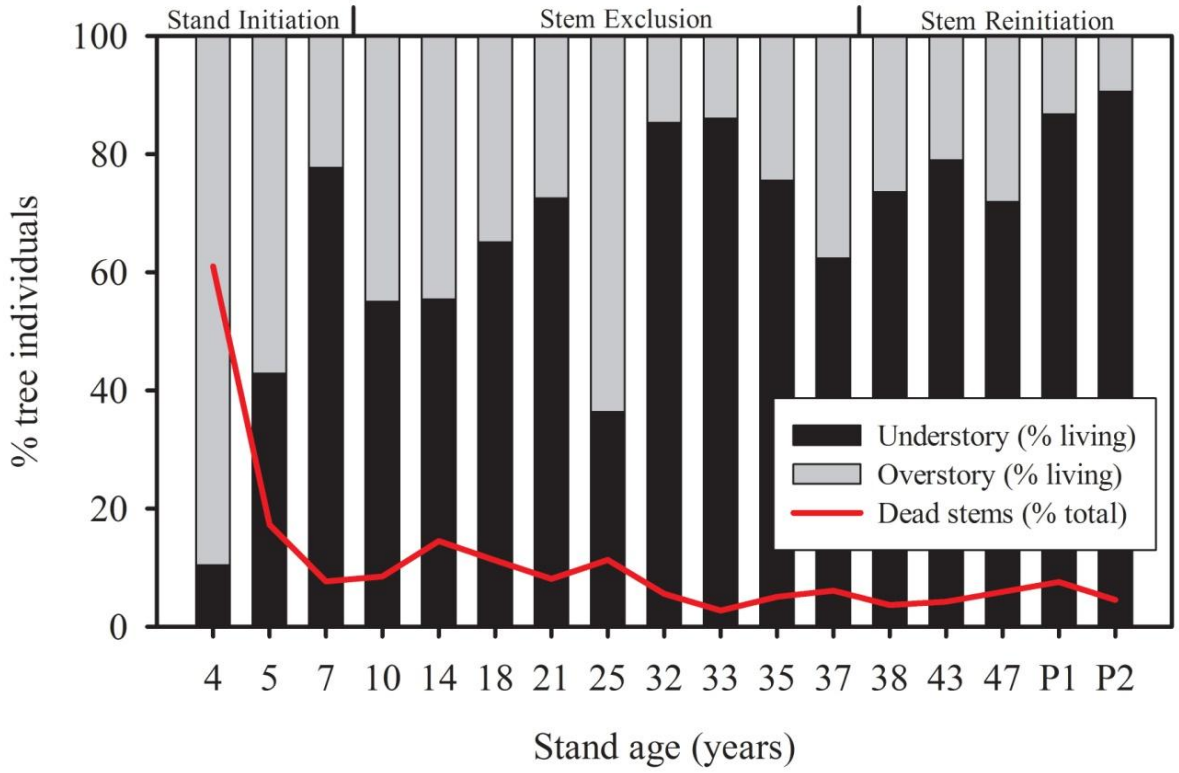

**Figure 5.3:** Stand structural and species characteristics for successional forest study sites. Species diversity is calculated using the Shannon-Weiner metric and species similarity is calculated using a Chao-Jaccard index versus primary forest composition. Michaelis-Menten relationship is shown between biomass and stand age, while quadratic are shown between tree height and diameter at breast height (DBH) and stand age.

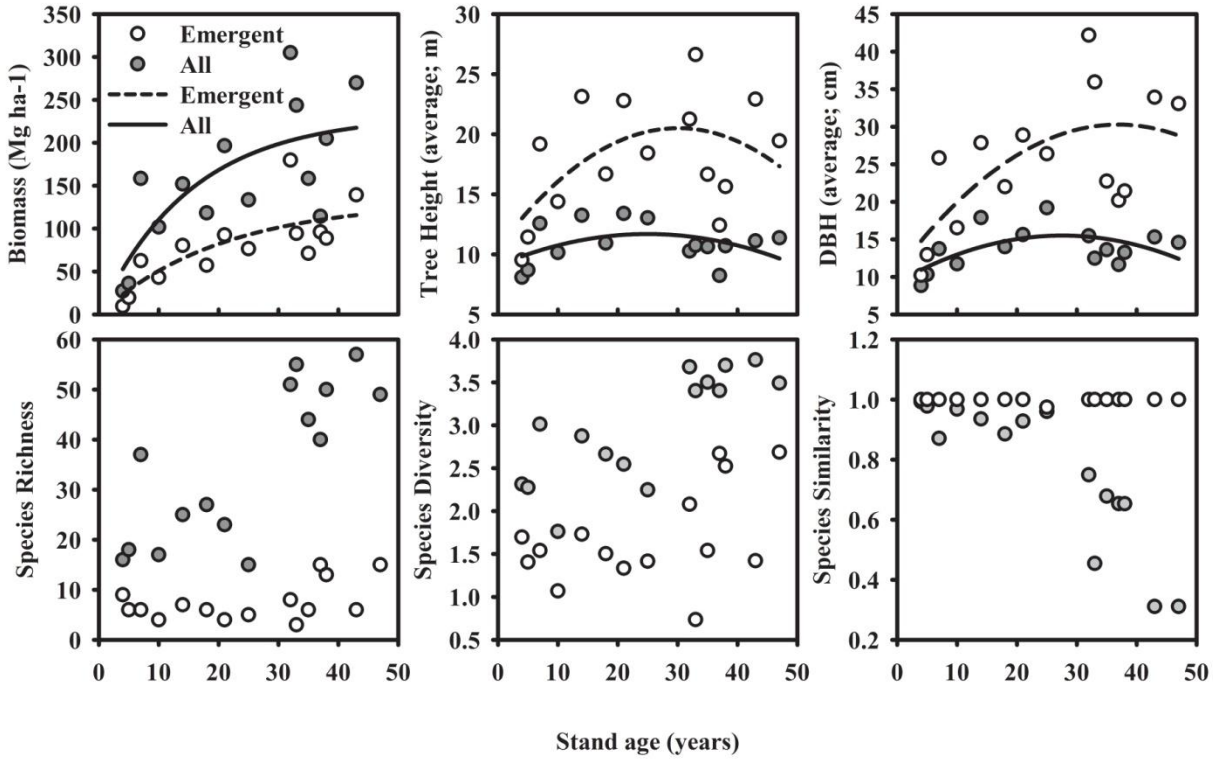

**Figure 5.4:** Selected soil properties for successional forest study sites. Significant linear regressions are shown in grey ($N$ = 13). Linear regressions for soil $\delta^{15}N$ were significant using separate depth points ($N$ = 39) and for soil $\delta^{13}C$ following exclusion of the 7 year old stand outlier ($N$ = 12).

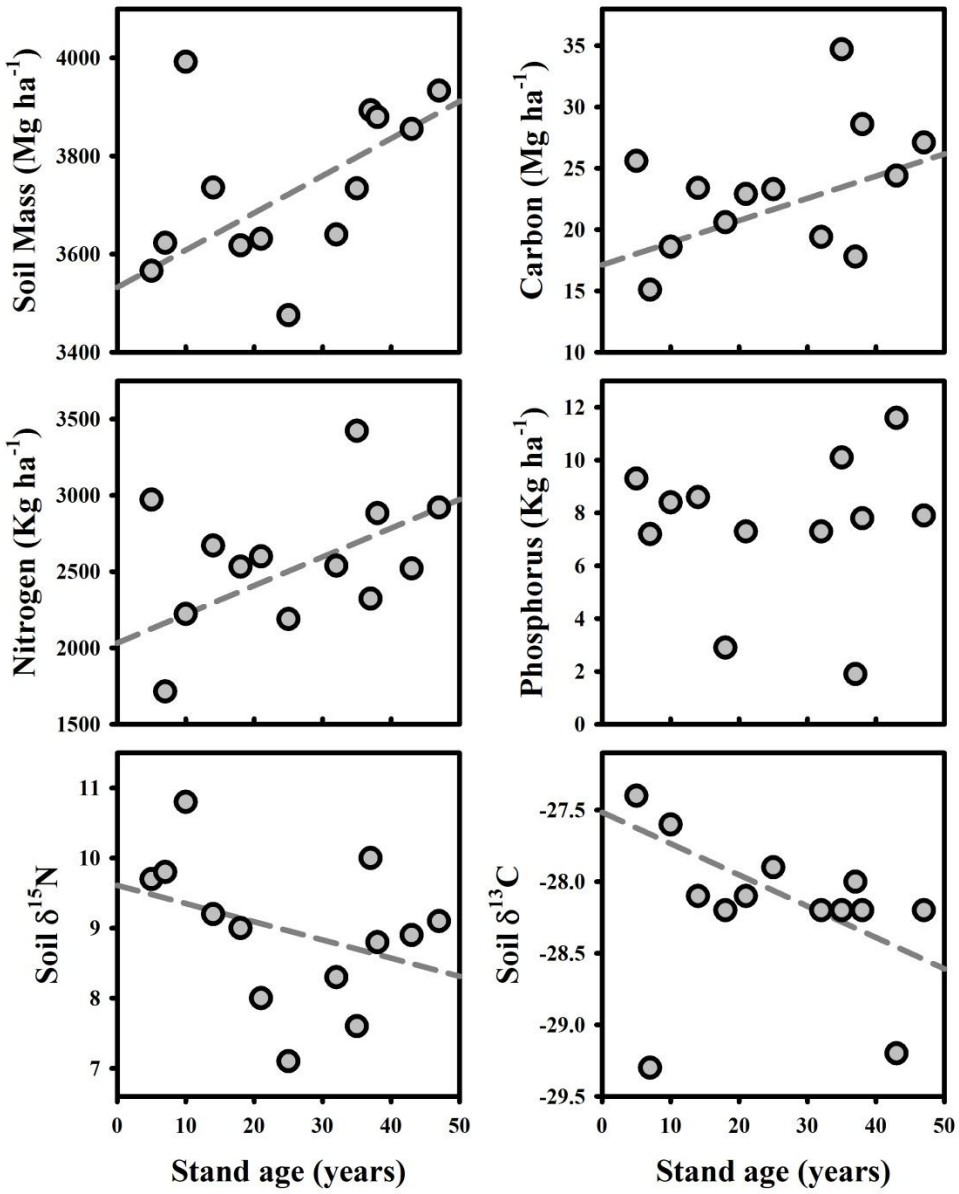

**Figure 5.5:** Soil $\delta^{15}N$ values versus stand age by soil depth. A significant relationship exists between stand age and $\delta^{15}N$ for all samples ($R^2$ = 0.26, $P$ = 0.0881, $N$ = 12) and a trend at 5 cm depth ($R^2$ = 0.26, $P$ = 0.0881, $N$ = 12).

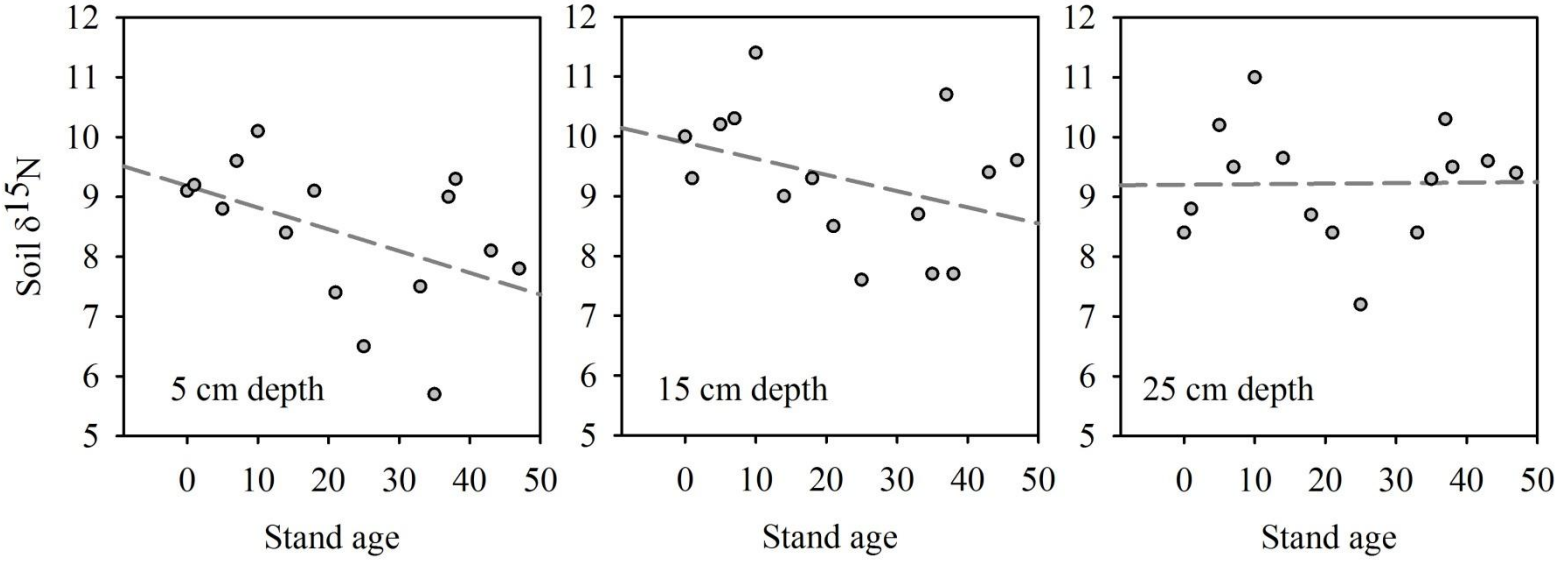

**Figure 5.6:** Foliar $\delta^{15}N$ and $\delta^{13}C$ values versus stand age and species successional status. Significant linear regressions are shown in grey.

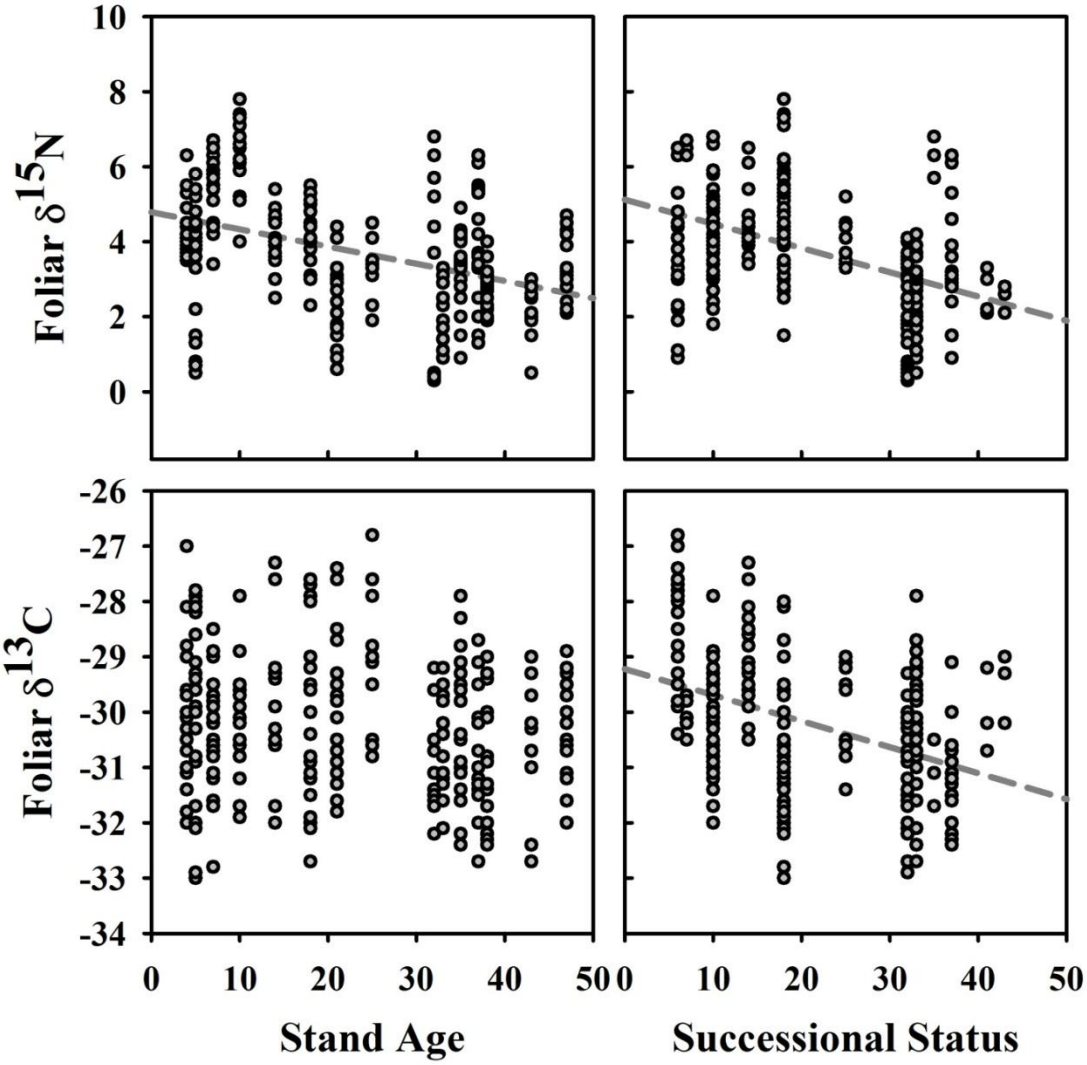

**Figure 5.7:** Foliar-minus-soil $\delta^{15}N$ and $\delta^{13}C$ values versus stand age and species successional status. Significant linear regressions are shown in grey.

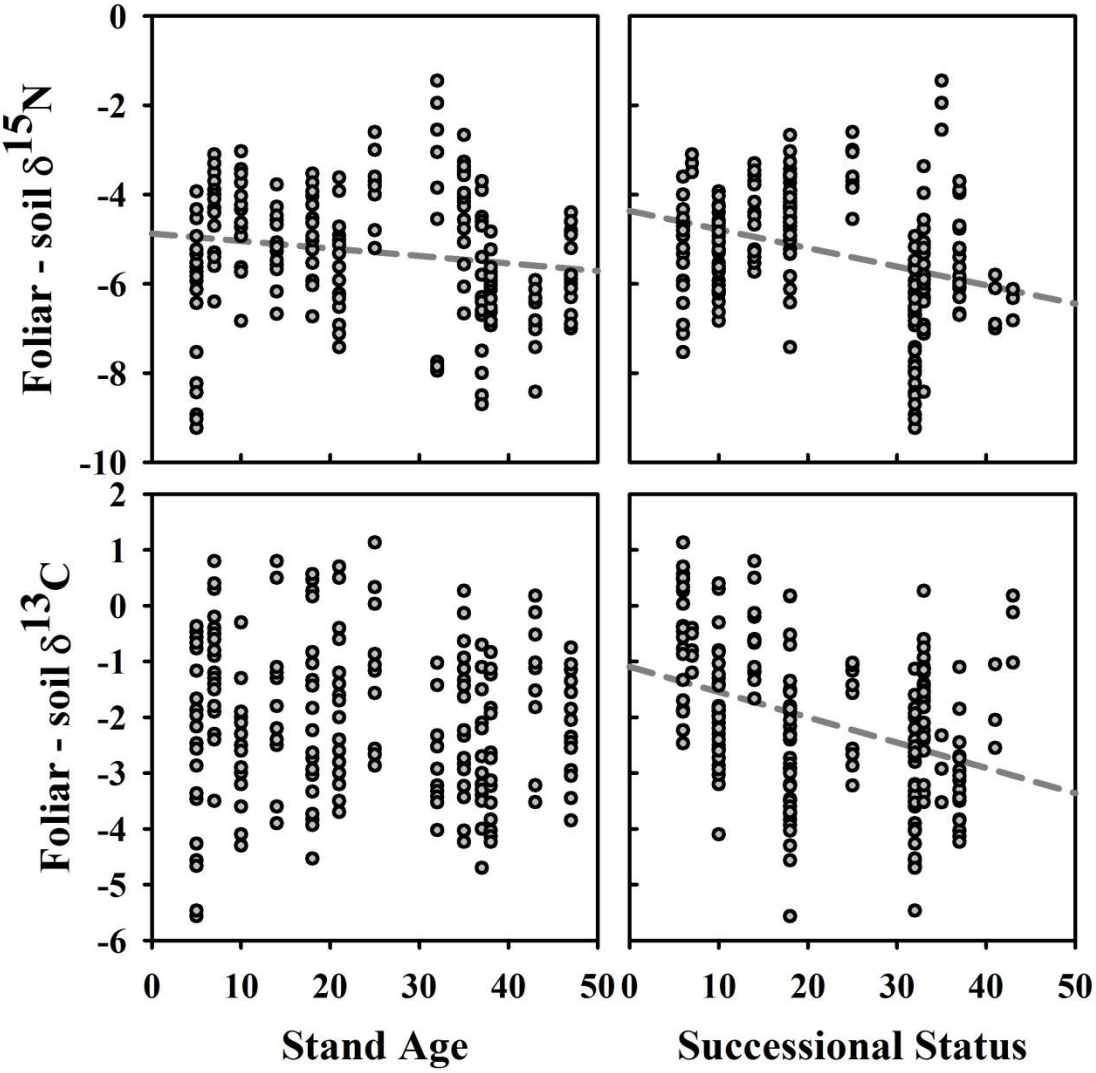

## 5.11 Supplementary material

**SM 5.1:** Ultrametric tree of species used for leaf trait phylogenetic signal analyses. Foliar %C is provided after the species name as it was the only trait identified as having significant phylogenetic signal. The scale bar (lower left corner) represents 10 million years.

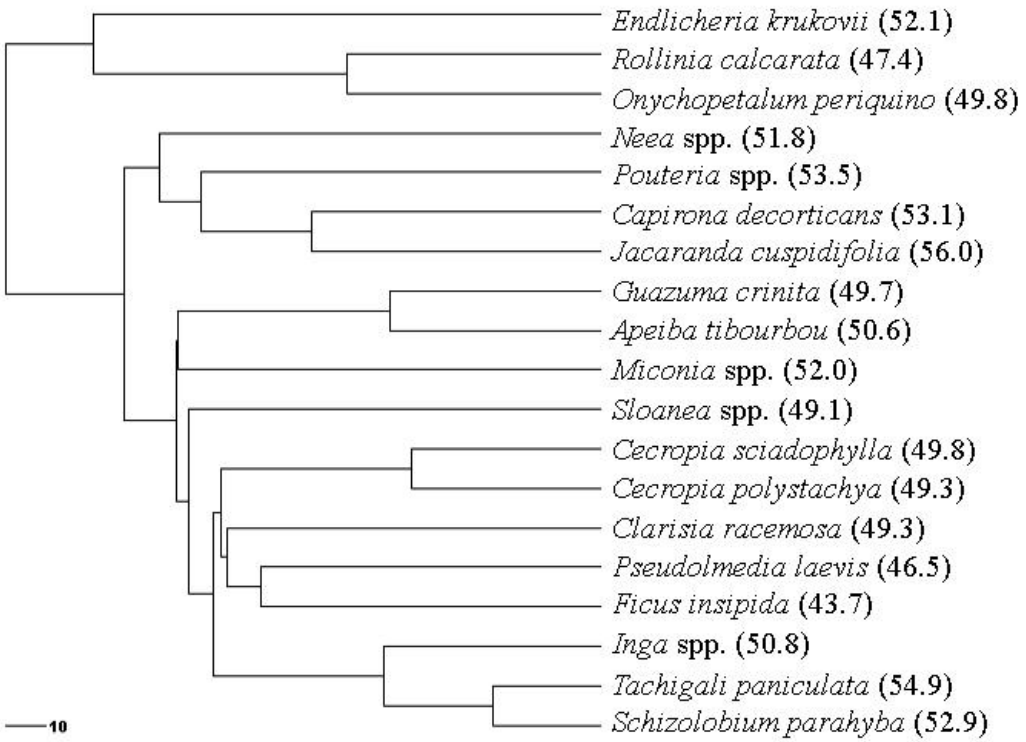

**SM 5.2:** Eigenvectors of stand and soil Principal Components Analysis (PCA) axes. Stand and soil property variables are explained and units provided in Table 5.1 and 5.2 of the main text.

| Stand biomass axis | | | Stand structure axis | | | Soil texture axis | | | Soil fertility axis | | |
|---|---|---|---|---|---|---|---|---|---|---|---|
| Stand properties | | PCA 1 | Stand properties | | PCA 2 | Soil properties | | PCA 1 | Soil properties | | PCA 2 |
| Richness | + | 0.30711 | Mean DBH | + | 0.43933 | Clay | - | 0.37631 | Nitrogen | + | 0.44133 |
| Biomass | + | 0.30329 | No leaves | + | 0.42061 | Sand | + | 0.33806 | K | + | 0.37087 |
| Max height | + | 0.2997 | Mean height | + | 0.4199 | C | + | 0.33283 | Carbon | + | 0.35208 |
| CE | - | 0.29305 | Mature leaves | - | 0.36626 | P1 | + | 0.31279 | H | + | 0.32176 |
| Diversity | + | 0.29001 | Tree density | - | 0.2818 | Silt | - | 0.30596 | $\delta^{15}N$ | - | 0.31279 |
| Chao-Jaccard | - | 0.28963 | Liana | - | 0.21519 | CEC | + | 0.2773 | Mg | + | 0.28983 |
| Wood density | + | 0.28943 | Dead trees | - | 0.2048 | P2 | + | 0.2607 | CEC | + | 0.2672 |
| Basal area | + | 0.28547 | Wood density | - | 0.17084 | Base Saturation | + | 0.25635 | $\delta^{13}C$ | + | 0.25618 |
| Senescent leaves | - | 0.28039 | Basal area | + | 0.15914 | Mg | + | 0.23177 | Na | + | 0.1867 |
| Max DBH | + | 0.27384 | New leaves | + | 0.15187 | $\delta^{13}C$ | - | 0.21944 | Sand | - | 0.18151 |
| Dead trees | - | 0.2258 | Max height | + | 0.14433 | $\delta^{15}N$ | - | 0.20182 | Clay | + | 0.17175 |
| Mature leaves | + | 0.20452 | Max DBH | + | 0.11745 | Na | - | 0.17779 | Silt | + | 0.12216 |
| New leaves | - | 0.14245 | Richness | - | 0.11551 | Soil mass | - | 0.14391 | P2 | - | 0.04887 |
| No leaves | - | 0.12287 | Chao-Jaccard | + | 0.11432 | Bulk density | - | 0.14209 | P1 | + | 0.04834 |
| Mean DBH | + | 0.10854 | Senescent leaves | - | 0.06739 | Carbon | + | 0.0838 | Soil mass | - | 0.03816 |
| Mean height | + | 0.07784 | Biomass | + | 0.06094 | H | + | 0.06165 | Bulk density | + | 0.03518 |
| Tree density | + | 0.0664 | Diversity | - | 0.05918 | K | - | 0.05983 | Base Saturation | - | 0.03317 |
| Liana | - | 0.02621 | CE | - | 0.03973 | Nitrogen | + | 0.04247 | C | + | 0.02439 |

**SM 5.3:** Pearson correlations among leaf trait variables. Data is the correlation value (N) and P-value expressed as + < 0.1, * < 0.05, ** < 0.01, and *** < 0.001.

| | P | N:P | C% | N% | C:N | $\delta^{15}N$ | $\delta^{13}C$ |
|---|---|---|---|---|---|---|---|
| N | 0.66(264)*** | 0.24(263)*** | 0.12(260)* | 0.85(262)*** | -0.85(259)*** | | |
| P | | -0.55(263)*** | -0.28(259)*** | 0.61(261)*** | -0.66(258)*** | | 0.33(258)*** |
| N:P | | | 0.49(258)*** | 0.14(260)* | | | -0.44(257)*** |
| C% | | | | 0.15(259)* | | 0.25(259)*** | -0.27(254)*** |
| N% | | | | | -0.99(259)*** | | |
| C:N | | | | | | | |
| $\delta^{15}N$ | | | | | | | 0.2(258)** |

**SM 5.4:** Pearson correlations among the predictor variables stand age (years), species successional status (status), and the PCA derived axes of stand biomass and structure and soil texture and fertility. Data is the correlation value (N) and P-value expressed as + < 0.1, * < 0.05, ** < 0.01, and *** < 0.001.

| | Status | Biomass | Structure | Texture | Fertility |
|---|---|---|---|---|---|
| Stand age | 0.63(265)*** | 0.86(265)*** | 0.1(265)+ | | 0.67(195)*** |
| Status | | 0.54(265)*** | | | 0.46(195)*** |
| Biomass | | | 0.24(265)*** | | 0.39(195)*** |
| Structure | | | | 0.64(223)*** | |
| Texture | | | | | |

**SM 5.5:** Regressions of foliar variables versus stand age (years) / species successional status (years). Statistics provided are Adj-$R^2$ (F) *df* and *P*-value. Model comparisons are conducted using the F-test in R and P values are presented as: blank < 0.1, * < 0.05, ** < 0.01, *** < 0.001, **** < 0.0001.

| Foliar variables | Combined | Stand age | Successional status |
|---|---|---|---|
| **A. Linear regression models and model comparisons** | | | |
| N:P | 0.05 (8) 260 *** | 0.01 (2) 261 NS | 0.05 (15) 261 *** |
| | | 14 *** | 1 NS |
| C:N | 0.01 (2) 256 NS | 0.00 (1) 257 NS | 0.01 (4) 257 * |
| | | 4 | 0 NS |
| $\delta^{15}N$ | 0.24 (43) 260 **** | 0.18 (57) 261 **** | 0.22 (74) 261 **** |
| | | 23 **** | 9 ** |
| $\delta^{13}C$ | 0.20 (33) 258 **** | 0.01 (3) 258 NS | 0.17 (52) 258 **** |
| | | 31.3 **** | 5.39 * |
| **B. Standardized slope values** | | | |
| N:P | -0.57 NS / 1.90 *** | NS | 0.62 |
| C:N | NS | NS | -1.65 |
| $\delta^{15}N$ | -0.33 ** / -0.52 **** | -0.66 | -0.73 |
| $\delta^{13}C$ | 0.02 **** / -0.07 **** | NS | -0.05 |

# CHAPTER 6 - APPENDIX

# THE EFFECT OF LAND USE CHANGE AND ECOTOURISM ON BIODIVERSITY: A CASE STUDY OF MANUEL ANTONIO, COSTA RICA, FROM 1985-2008

## 6.1 Abstract

Development in biodiversity rich areas is of global concern. While development may lead to socioeconomic benefits, this often comes concomitant with biodiversity loss and deforestation. Biodiversity rich areas present the opportunity for both improvements in socioeconomic conditions and conservation; however numerous challenges exist. Costa Rica's Manuel Antonio National Park presents an ideal case study to investigate the balance between alternative forms of development which have contrasting environmental impacts. The Manuel Antonio region is a highly dynamic landscape experiencing deforestation, from agriculture, cattle ranching and oil palm plantations; and also reforestation from abandonment of land holdings and nature oriented tourism. Landscape dynamics are closely intertwined with the livelihoods and perspectives on biodiversity conservation of local communities, determining ecological sustainability. We use an analysis combining multi-temporal remote sensing of land cover dynamics from 1985-2008 with questionnaire data from local families on their socioeconomic status, perspectives on conservation, and perceived changes in local wildlife populations. Our results show that, while regeneration occurred and forest fragmentation in the area decreased from 1985-2008, Manuel Antonio National Park is rapidly becoming isolated. Decreasing ecological connectivity is related to the rapid expansion of oil palm plantations adjacent to the park and throughout the lowland areas. Perceived decreases in wildlife abundance and compositional change are evident throughout the area, with local communities attributing this primarily to illegal hunting activities. Nature based tourism in the area presents an effective strategy for conservation, including reductions in hunting, through increased valuation of biodiversity and protected areas, and socioeconomic

advantages. However, without urgent efforts to limit deforestation and preserve the remaining forested corridor connecting the park to core primary forest, the ability to maintain biodiversity in the park will be reduced.

*Key words: Biological Corridor; Secondary Forests; Land Use and Land Cover Change; Sustainable Development; Remote Sensing.*

## 6.2 Introduction

Human land use activities have transformed the planet (Foley et al. 2005), resulting in unintended consequences to the natural environment (DeFries et al. 2004). Land-use related change is now considered the primary driving force of biodiversity loss worldwide (Vitousek et al. 1997), especially in tropical ecosystems (Sala et al. 2000). Costa Rica, in particular, presents some of the world's greatest challenges and opportunities for biodiversity conservation. While being one of the world's richest hotspots of biodiversity (MINAE 1992; Myers et al. 2000; Soto 1992), it also has had among the most rapid rates of deforestation (FAO 1990; Jha and Bawa 2006). Costa Rica has sought to address this through the declaration of a globally renowned network of nature reserves - encompassing more than 15% of its land area (Boza 1993).

Natural protected areas have been shown to be an effective strategy for preserving biodiversity and limiting deforestation (Bruner et al. 2001). However, adjacent forested areas are being rapidly cleared or fragmented (DeFries et al. 2005), in part as a result of population growth through migration for tourism related jobs (Wittemyer et al. 2008). Such changes are resulting in the increasing ecological isolation of parks globally (DeFries et al. 2005). Similarly, such dynamics are occurring in Costa Rica's parks, where the loss of tropical forest and ecological connectivity (Goodwin 2003) has been rapid and extensive (Sánchez-Azofeifa et al. 2001, 2003). Causes include rapid touristic development and other concomitant changes in land cover, i.e., oil palm plantations or cattle ranching, which reduce and

fragment remaining contiguous forest areas and decrease their ecological connectivity to other natural habitats (Sánchez-Azofeifa et al. 2002; Van Laake 2004). Oil palm plantations are of particular concern as they are one of the world's most rapidly increasing crops (Fitzherbert et al. 2008). Biodiversity loss also occurs through conversion of native ecosystems to plantations (Curran et al. 2004), which function as barriers to animal movement (Fitzherbert et al. 2008) and support low native biodiversity (Edwards et al. 2010). On the positive side, oil palm plantations provide employment to often-isolated communities with few other local economic opportunities (Koh and Wilcove 2007).

Costa Rica has responded to the rapid loss of connectivity through, among many activities, participation in development of a Mesoamerican Corridor - encompassing 85 Costa Rican protected areas and 14.2% of its national territory - designed to maintain viable wildlife populations (Miller et al. 2001). Although, under optimal conditions, biological corridors may augment wildlife populations of smaller natural areas (Beier and Noss 2010), corridors are easily subjected to negative anthropogenic influences due to their narrow width. In Costa Rica, with numerous smaller parks, hunting is of especial concern and its intensity has been shown to determine wildlife abundance levels within protected areas (Carrillo et al. 2000) and across the surrounding human dominated landscape (Daily et al. 2003). Hunting intensity within communities is, in some cases, controlled by poverty and improvements in income, education and healthcare have been suggested as possible methods to reduce wildlife consumption (Robinson and Bennett 2004).

Simultaneously, the Costa Rican Ministry of Tourism has sought to address the rapid, mostly tourism related, unregulated development occurring adjacent to its protected areas through establishment of the Certification for Sustainable Tourism (CST) in 1997 (Rivera 2002) - a voluntary program that certifies each tourism company according to the ecological and social sustainability of their practices (http://www.turismo-sostenible.co.cr/en/). However, a clear understanding of how certified nature oriented hotels may contribute to biodiversity conservation does not

exist (Gössling 1999), especially when considering the multitude of possible land use pressures (Alpízar 2006).

Effective conservation strategies differ between areas with touristic potential versus less accessible areas. For long-term sustainability of natural parks having high touristic potential, both ecologically and as destinations for nature tourists, biodiversity must be maintained. Although increased nature oriented tourism can promote greater conservation of natural areas (Aylward et al. 1996) and development of a conservation mentality in local communities (Almeyda Zambrano et al. 2010a), it has in some cases resulted in increased deforestation and forest fragmentation from development and unsustainable levels of visitation (Stem et al. 2003) with limited socioeconomic advantages (Campbell 1999). Changes in land cover dynamics are inter-related with changes in the social and economic dynamics of the families living and working in the region (Almeyda Zambrano et al. 2010b), and especially proximate to national parks (Andam et al. 2010), as well as with their perspectives on conservation and protected areas, which are often contentious topics in many countries (Schwartzman et al. 2000).

The main objective of this study was to evaluate how forest cover and ecological connectivity, resulting from the expansion of oil palm plantations and the development of nature based tourism, affects wildlife populations in the area surrounding Costa Rica's Manuel Antonio National Park (MANP). We investigated the interplay between these contrasting forms of development on both biodiversity conservation and socioeconomic improvement. To achieve this goal, we combined multi-temporal remote sensing analyses of land cover changes from the years 1985 through 2008 with in depth interviews with local families living in different environmental matrices, some of whom work for tourism operations in the area. The driving research question was: what is the effect of contrasting forms of development - nature oriented tourism and oil palm plantations - on wildlife populations and socioeconomic conditions in a biodiversity hotspot experiencing significant land use change? The study aims to provide a better understanding of the effects of tourism,

land conversion and forest fragmentation on the viability of small, protected areas in human dominated landscapes.

## 6.3 Methods

### 6.3.1 Study area

Our study area was located on the Pacific Coast of Costa Rica within a 30 km radius surrounding the Manuel Antonio National Park (MANP) (Fig. 1). The park was established November 15th 1972 and encompasses approximately 620 hectares of terrestrial surface, dominated by tropical wet forest, with an additional 55,000 ha of marine area. The Manuel Antonio region is considered a biodiversity hotspot (Myers et al. 2000), with the national park having more than 100 species of mammals and 180 species of birds (personal communication). A pronounced wet season extends from May to November. Costa Rica, in general, represents an ideal location to better understand the interplay between conservation and development as it is considered one world's leaders in biodiversity conservation (Sun 1988). To achieve this, Costa Rica reversed dramatic rates of historical deforestation resulting in more than 50% forest loss between 1940 and 1984 (Sader and Joyce 1988). The forest regrowth in the last two decades has occurred, among other reasons, as a result of government initiatives to promote carbon sequestration (Castro-Salazar and Arias-Murillo 1998) and conservation (Sánchez-Azofeifa et al. 2007), increased governance as shown through development of new forestry laws (Pfaff and Sánchez-Azofeifa 2004), and emigration for jobs in cities (Almeyda Zambrano et al. 2010b). Similar dynamics are occurring throughout the tropics (Chokkalingam and Jong 2001).

MANP is one of the most visited and greatest income-generating parks within Costa Rica (Sterling 1999), experiencing increasing tourism and related development, including industrial and smaller scale eco-touristic hotels. The flat low-lying areas surrounding the park are ideal for agriculture, cattle ranching and, in particular, oil palm plantation development while proximate mountainous areas exist as potential

repositories of biodiversity and reduced anthropogenic impact (Sader and Joyce 1988). The study area includes both deforestation occurring for agriculture, oil palm plantations, and forest regeneration occurring from the large-scale abandonment of previous pasture areas and nature oriented development and conservation (Sánchez-Azofeifa et al. 2001; Almeyda Zambrano et al. 2010a, 2010b). The Manuel Antonio area has great potential to simultaneously conserve biodiversity and provide economic benefits to local communities. Understanding the challenges and successes at MANP is therefore directly relevant to developing effective conservation approaches in similar biodiversity rich areas attractive to ecotourism.

### 6.3.2 Study design

Our study design used a "nested-level" approach that combined land cover change analyses using remote sensing paired with participant observation-based ground assessment, interviews and questionnaires (Almeyda Zambrano et al. 2010a). The four levels of data collection and analysis were: landscape, community, hotel-park, and household. Landscape analyses encompassed a 30 km radius surrounding the MANP for a total of 110,000 hectares (ha). Community analyses included eight communities that were within the area of influence (in both spatial and cultural contexts) of the MANP. Hotel-park analyses included the MANP, with an area of approximately 620 ha, and two hotels ranked highly by Costa Rica's Certification for Sustainable Tourism (CST): Hotel *Sí Cómo No* with five CST leaves, and Hotel *El Parador* with four CST leaves. We delineated, using a handheld GPS unit (Garmin GPSmap 60SCx), the borders of the hotel properties while the borders of the MANP were generated from existing maps. Each hotel had a private nature reserve within its property boundaries encompassing 14 ha for Hotel *Sí Cómo No* and 5 ha for Hotel *El Parador*. The *El Parador* property was located within a peninsula containing mostly intact forest area, with abundant wildlife including monkeys and sloths, but currently not under any protection status. We defined buffer zones for the park and hotels as the 1.5 km zone surrounding their borders. Community areas were defined using a 1.5 km radius around the community center. Household analyses included those directly

employed by the park and hotels and those only indirectly affected (e.g., proximate). We used these complementary scales and methods at multiple locations to enable a more thorough understanding of the varied processes affecting biodiversity conservation in the region.

### 6.3.3 Spatial analyses

We developed multi-temporal maps of the dominant land cover types - forest, mangrove forest, oil palm plantation and non-forest areas - within our study area for the years 1985, 1990, 2000 and 2008 using eighteen Landsat satellite images at a spatial resolution of 30 meters (m) acquired from the USGS (http://glovis.usgs.gov/) (Appendix 1 in Supplementary Material). All remote sensing work was conducted using the ENVI / IDL remote sensing and programming software (ITTVIS, Inc., Boulder, CO, 2000-2010) and spatial analyses were conducted using ArcGIS (V. 9.2., Environmental Systems Research Institute, Inc., Redlands, Calif.). Satellite images were georeferenced to two orthorectified Landsat images (RMSE < 15 m.) generated through a NASA directive (http://glcf.umiacs.umd.edu/portal/geocover/). Validation GPS (global positioning system) points (n=184) of primary forests, secondary forests, mangroves, oil palm plantations and non-forest areas (i.e., urban, agriculture and pasture) were acquired in July 2009. The Spectral Angle Mapper (SAM) routine in ENVI was used to classify all images as: (a) forest; (b) mangroves; (c) oil palm plantations; (d) non-forest; (e) water; (f) cloud; and (g) cloud shadow. Overall classification accuracy was 90% with a Kappa coefficient of 0.85. To reduce cloud interference and data gaps resulting from the 2003 Landsat ETM+ scan line malfunction, multiple classifications covering the same study area during the same year were merged (Appendix 1 in Supplementary Material). One study area mask was generated from the final merged classifications which included any area of cloud, cloud shadow or no data pixel. This was then applied to all classification images, resulting in classification for 88% for the total study area. Using these we calculated a detailed map of primary and secondary forests for the year 2008. Primary forests (PF) were defined as those pixels classified as forest in all 4 study years while secondary

forest (SF) pixel ages were based on last known non-forest date. The final classes were: PF (> 25 yrs. old), SF 20-25 yrs. old, SF 10-20 yrs. old, SF < 10 yrs. old.

The importance of deforestation, forest fragmentation, and topography on landscape dynamics have been previously identified in Costa Rica (Sader and Joyce 1988; Sánchez-Azofeifa et al. 2001, 2003). We investigated changes in these factors across our study area at a spatial scale of 30 x 30 meters. First, we calculated the number of spatially separated forest fragments, and their area (ha), edge length (m) and edge to area ratio (m edge m-2 area) for each study year. Fragmentation analysis was conducted over the entire study area. Second, slope was derived using 10 x 10 pixel computation cell on a digital elevation model (DEM) of the study area (http://www2.jpl.nasa.gov/srtm/) resampled to 30 m from an original resolution of 90 m. The delineation of lowland areas (0-3° slope) versus mountainous areas (> 3° slope) was conducted following visual analysis of the distribution of land cover classes in the Manuel Antonio area. Third, we generated a Euclidean distance (m) map to the park border using the Spatial Analyst extension of ArcGIS. One quarter of the spatial topography and distance data within the study area were randomly selected to avoid spatial auto-correlation issues. Linear regressions were used to identify correlations between land cover dynamics and slope, elevation and distance to park borders. We quantified ecological connectivity between communities and hotel properties and core primary forest - identified using the detailed 2008 forest age classification. Connectivity was calculated using least cost paths from the park border, the Hotel *El Parador* and Hotel *Sí Cómo No* properties, and the community center points to the core primary forest (Rouget et al. 2006; Ramos and Finegan 2006). For this purpose, we assigned relative movement costs to the main land cover classes as follows: 1 for forest, 2 for mangroves, 3 for oil palm plantation, and 4 for non-forest pixels. For this calculation the forest category included both primary and secondary forest as our methods did not permit separation of these classes prior to 2008 and our connectivity analyses extended from 1985 to 2008. Assigned cost values were based on a general review of the related literature and used for spatial and temporal

comparisons of land cover change rather than as directly biologically meaningful values.

### 6.3.4 Socioeconomic analyses

Socioeconomic data were collected to enable comparison of: (a) households working, versus not, in tourism; (b) perceptions of biodiversity conservation; and (c) linkages between these variables. Data were collected through participant observation, interviews and questionnaires during July-August 2009 (Appendix 5 in Supplementary Material). At the landscape level we interviewed MANP guides and management, hotels owners, management, staff and neighbors about the development of the study area. At the household scale, we conducted in-depth questionnaires with 121 heads of households. The random sample included employees from each hotel: Hotel *Sí Cómo No* (n=37), Hotel *El Parador* (n=41), as well as non-employee neighbors (n=43). The questionnaire, provided in Spanish (Appendix 3 in Supplementary Material), covered the general themes: household demography and economy, education, perceptions of tourism, use of natural resources, including hunting, and perceptions of wildlife abundance and composition. Non-parametric statistics were used for all analyses.

### 6.3.5 Wildlife analyses

We collected wildlife data at the household scale as part of the in-depth questionnaires with heads of households. Wildlife related questions were administered to households that had lived in the Manuel Antonio area for at least five years (n=90). Questions focused on the perception of changes in wildlife abundance and its causes and changes in the abundance of key wildlife groups. Spatial analyses were conducted by extracting the: (a) percent forest and mangrove cover (year 2008); (b) percent regrowth (year 1985-2008); and (c) ecological connectivity. These were then categorized as low, medium or high, using 33% and 66% as thresholds. We used a logistic regression to gauge the relationship between household residence time and

perceived changes in wildlife populations. We acknowledge that perceived wildlife abundance requires additional care in interpretation over that of direct measurements (i.e., camera traps), but no other method allowed for multi-temporal analysis of wildlife composition and abundance in this area. All statistics were conducted using JMP software (V.7. SAS Institute Inc., Cary, NC, 1989-2007) and a significance value of 0.05 were considered for all tests.

## 6.4 Results

### 6.4.1 Spatial analyses

At the landscape scale, forest cover and oil palm plantations increased from 44 to 58% and from 8 to 14%, respectively, between 1985 and 2008 (Appendix 2 in Supplementary Material). The rate of establishment of new oil palm plantations reduced from 1990 (469 ha $yr^{-1}$) to 2000 (216 ha $yr^{-1}$). Oil palm plantations existed only in the lowlands (from 19% in 1985 to 31% in 2008), with new areas being established on an increasing proportion of previously forested areas (9% in 1990 to 23% in 2008), resulting from decreasing availability of non-forest areas (Table 1). In 2008, palm plantations occupied most of the coastal areas of the study area, and thus directly bordered the entire North East section of park (Fig. 1). In addition, we found a 33% increase in plantation area from 1986-2008 within the park buffer as compared to 6% over the entire study area (Fig. 2). Regression analyses revealed increasing oil palm area and decreasing forest area closer to the MANP, as well as the importance of increasing elevation and slope on limiting oil palm plantation expansion. MANP showed regrowth from 1985 to 2008, with forest area increasing from 90% to 98% - the highest forest cover for any of our study sites - followed by the hotel properties (92%). The MANP and *Sí Cómo No* properties were dominated by primary forest while the *El Parador* property was half secondary forest (Fig. 3). The park had 50% more forest cover than its buffer, Hotel *Sí Cómo No* had 6% more, whereas the Hotel *El Parador* had 28% less (Appendix 2 in Supplementary Material). In 2008, the

hotels' nature reserves were connected to the MANP via intact forest and were likely important to the size of the park's contiguous forest area as well as to help mitigate ecological repercussion of adjacent development. Forest cover within our study communities decreased with increasing distance from the park boundaries (83 to 6%).

From 1985 to 2008, the number of forest fragments at the landscape level decreased while their median area increased and the percentage of all forest in the largest contiguous forest fragment increased from 82% to 89% (Table 1). Although ecological connectivity increased from 1985 to 2008 for all sites as a result of regrowth, most paths now converge through a small forested gap remaining between palm plantations to the north east of MANP (Fig. 4). A possible biological corridor (800 m wide) was identified which encompassed 1500 ha and has undergone extensive regrowth (20%). In 2008, the corridor was composed of 59% primary forest, 22% secondary forest, and 18% non-forest (Appendix 2 in Supplementary Material). A portion of the corridor integrated the *Sí Cómo No* nature reserve.

### 6.4.2 Socioeconomic analyses

Approximately half of the households interviewed - working for tourism or not - were born in the study area. Households involved in tourism were younger, had more years of education, fewer dependent children and lived significantly less time in the MANP area than those having other forms of employment (Appendix 3 in Supplementary Material). Tourism related households had significantly greater income and savings (2-3 times greater) and spent more on the "other" category after covering the basic household's needs, while spending significantly less on food and transportation resulting from hotel related benefits (Appendix 4 in Supplementary Material).

Tourism was, on average, perceived to have positive effects on biodiversity through increased values of flora and fauna and decreased hunting and deforestation. Although the two hotels were perceived to have greater positive impacts for all categories Hotel *Sí Cómo No* had significantly greater positive effects on deforestation and value of flora and fauna. Tourism was perceived to have both positive and

negative effects on socioeconomic conditions. Positive effects were increased health, education and job training opportunities. Negative effects were increased land and product prices, as well as alcoholism, drug addiction, and prostitution (Table 2) by both tourists and locals. The two hotels were perceived as having a more positive effect than tourism in general for all variables with the exception of education.

Sixty-seven percent responded that the local forest was disappearing and 100% of respondents' felt it was important to conserve the remaining forest. When asked why it was important to conserve the forest (Table 3), the respondent's top three answers were: (1) save the animals (n=36); (2) provide clean air (n=33); and (3) attract tourism (n=19). Ninety-two percent of respondents felt it was important to have natural protected areas, with the top three reasons being: (1) attract tourists (n=48); (2) protect the animals (n=46); and (3) protect the environment in general (n=20) (Table 3). Many residents reported having changed their behaviors, stopped hunting, and started working to increase regrowth as a result of feeling it could increase their economic wellbeing. Even in remote communities with little tourism, many expressed a desire to reforest areas and conserve the wildlife populations in the hope of attracting tourists to their area. A similar sentiment was expressed for mangrove conservation. There was no statistical difference in "feeling if protected areas were important" between % forest classes.

### 6.4.3 Wildlife analyses

Eighty seven species, dominated by mammals, birds and reptiles, were identified as among the top five most common at arrival or at present. Eighty percent of respondents stated that the abundance of wildlife in general, and specifically large cats and wild pigs, had declined since their arrival to the area, versus 14% and 6% for had increased and no change, respectively. The tepezcuintle (*Cuniculus paca*), macaw (*Ara spp*.) and white-tailed deer (*Odocoileus virginianus*) were identified as previously common species no longer seen. No significant relationship was detected between time of residence and perceived changes in wildlife populations across all communities or for changes in wildlife populations for communities having more

forest, greater regrowth or increased ecological connectivity. Monkeys (Ceboidea, several species), iguanas (Iguanidae, several species) and raccoons (Procyonidae, several species) were reported as among the five most abundant animals at present. The leading reported causes for the perceived decline in wildlife were: (1) hunting (36%); (2) construction (24%); and (3) deforestation (22%). We expected that wildlife populations in more forested communities would have declined for reasons different from the declines in wildlife in general. However, when asked the primary reasons for wildlife population changes, hunting was ranked number one regardless of the surrounding land cover. Our semi-structured interviews with park officials and guides highlighted that within the MANP and immediate surrounding areas, forest fragmentation and uncontrolled development of hotels were perceived as the most important factors negatively impacting wildlife populations. Hunting, including the collection of turtle eggs, was stated to occur primarily outside the MANP boundaries. The increasing isolation of the park, however, was evidenced by the lack of large mammals which indicated that the current extent and connectivity of existing natural habitats are insufficient (Chiarello 1999; Newmark 1996).

## 6.5 Discussion

Conservation strategies based on parks and nature-based tourism requires consideration of accessibility, biodiversity, and political stability. They must include a legally delineated system of natural areas with adequate governance, effective employment of local populations, and be an economically competitive alternative to other land use practices (Defries et al. 2007; Fitzherbert et al. 2008; Yaap et al. 2010). Biodiversity conservation becomes more complex when multiple viable land uses exist and trade-offs become necessary. In biodiversity rich and tourist friendly areas, such as the Manuel Antonio area, conservation can best occur using an approach combining public and private protected areas, including national parks, ecotourism ventures, and private properties. Regrowth in abandoned agricultural fields or pastures due to increased land values or migration to cities may reduce forest

fragmentation (Moran et al. 1996) – sometimes at the expense of the wellbeing of local communities. Further study of the interactions, feedbacks and trade-offs between household social and economic factors and conservation is crucial to simultaneously address livelihood and conservation needs.

Although parks can present an effective conservation strategy (Bruner et al. 2001), many parks globally have shown encroachment and the park system in Costa Rica has been described as "inadequately funded, minimally policed, and threatened by encroachment" (Brockett and Gottfried 2002). As a result, the integrity of the MANP forest cover throughout our study period was contrary to our expectations and likely a result of both the small size, and therefore easier policing, of the park, as well as apparently effective park policies towards protection against encroachment, as has been found in other parks globally (Hayes 2006). Additional threats to parks however exist and include fragmentation and ecological isolation from other intact forest areas.

One important source of fragmentation and ecological isolation at present is oil palm plantations. Oil palm plantations are one of the most rapidly expanding forms of agriculture in tropical regions today (Tilman et al. 2001, Fitzherbert et al. 2008). Although oil palm plantations do present employment opportunities, often in self-contained communities with schools, health care and infrastructure (Koh and Wilcove 2007), their rapid growth throughout the tropics is problematic. Recent studies have shown that palm plantations are very low in diversity, with abandoned pastures supporting higher species richness (Fitzherbert et al. 2008), and act as barriers to animal movement (Edwards et al. 2010). Like findings in Southeast Asia by Koh et al. (2011), we found palm plantation establishment occurred increasingly on previously forested lands as the availability of easily converted non-forested lowland areas declined. This is contrary to many oil palm producers' arguments that palm plantations do not represent a threat to biodiversity as they are established on disturbed forests or old croplands (Koh and Wilcove 2007). Similar dynamics were identified by Koh (2008) who found that ameliorating the negative impacts of oil palm plantations directly was not viable and suggested that the focus should instead by on

maintaining remaining natural forests and creating buffer zones around oil palm estates.

Given the negative ecological repercussions of forest conversion a 'win-win' scenario would have local communities employed in ecological sustainable enterprises, especially in areas of high biodiversity. Nature tourism represents one possible solution. To be effective it should: (a) have minimal environmental impact, (b) promote conservation, and (c) improve local livelihoods (Ceballos-Lascurrain 1987; Scheyvens 1999; Christ et al. 2003). Similar to previous studies (Almeyda Zambrano 2010 a, b) we found this 'win-win' scenario could exist as households employed by nature oriented tourism often have socio-economic advantages over those with non-tourism related employment, including at oil palm plantations. In addition, nature oriented hotels - as found in our study - sometimes have private nature reserves resulting in the maintenance, or regeneration, of forest cover. However, while nature oriented tourism was perceived to have mostly positive socio-economic effects, versus tourism in general, negative effects, such as the increase of land and product prices, remained. Complicating matters, improvements in household economy do not necessarily correlate to increased conservation or valuation of biodiversity - conversely, they sometimes lead to increased environmental degradation (Rock 1996).

The perceptions of biodiversity held by local communities play a key role in determining whether conservation efforts succeed or fail (Abbot and Thomas 2001). To maximize conservation we recommend a two pronged approach to environmental education, that: (a) emphasizes the unique cultural and environmental value of biodiversity to the local communities; and (b) highlights the economic importance that biodiversity plays in the local areas. Tourism can play a critical role in local residents' perception of the value of fauna, flora and conservation. However, in our study area, the perceived biodiversity benefits of nature oriented tourism and the high importance of forests and natural protected areas being developed within local communities had yet to translate to an increase in wildlife abundance or change in hunting behavior. This ongoing hunting pressure has been demonstrated for other national parks in Costa

Rica where reductions in hunting vigilance resulted in immediate increases in hunting activities and concomitant declines in wildlife populations (Carrillo et al. 2010). This disjunction may be a result of ongoing poverty requiring subsistence activities. Alternatively, hunting may be seen as part of the local culture and not contradict their valuation of biodiversity and protected areas - although the majority of interviewed households perceived hunting as a negative impact.

In this context, the viability of an ecological corridor approach faces two main challenges: (a) is it feasible to establish an ecological corridor of sufficient size across this landscape where other land uses are potentially more economically rewarding? And (b) if feasible can an isolated reserve of insufficient size to support large animal species benefit from increased connectivity? In our study area an ecological corridor is likely more feasible than in more remote-less touristic locations due to the high income (the greatest of any Costa Rican protected area; Sterling 1999) of the MANP relative to its size. In addition, income from ecotourism and the interest of even remote communities to participate in ecotourism activities provide added leverage to offset other land use possibilities. Given the extensive areas already occupied by oil palm plantations and their desire to appear green (Koh and Wilcove 2007), opportunity may exist to include such companies in the effort to increase ecological connectivity of the MANP. If such a corridor becomes feasible, will it be useful? Studies addressing this topic have showed that corridor utility differs by species group, with few benefits identified for boreal bird species (Hannon and Schmiegelow 2002), but found to be the most efficient approach for mammal conservation in Eastern North America (Gurd et al. 2001). Simberloss et al. (2012) highlight this issue and present the argument that corridors and other landscape conservation approaches are not mutually exclusive. The value of an approach simultaneously integrating protected areas, conservation corridors and landscape permeability is highlighted by Kostyack et al. (2011). Such an effort would necessarily include the MANP, ecotourism and private nature reserves, community based initiatives for reforestation and biodiversity conservation and cooperation - or involvement - of Oil Palm producers.

The methods used in this study have several caveats: (a) our remote sensing approach did not allow identification of secondary forest age prior to 2008. While for immediate conservation purposes this is sufficient, improvements to this method would be required to better understand the temporal dynamics of wildlife populations in our area; (b) while secondary forests are clearly superior to pasture or oil palm plantations for supporting fauna, their value has not been well defined (Bowen et al. 2007). A more detailed literature review coupled with field studies is required to enable better allocation of pixel costs for quantification of ecological connectivity; and (c) our study did not directly address linkages between the spatial configuration of remaining habitat and fauna dynamics (McAlpine et al. 2006).

## 6.6 Conclusions

Although we found net regrowth in the study area over the interval 1985-2000, we also found that MANP is becoming increasingly isolated from core primary forest areas in the nearby mountainous regions. Areas immediately to the North West of the park have undergone more consistent regrowth, due in part to nature-based ecotourism with private protected areas. Ecotourism activities resulted in additional economic and educational gains by households directly employed as well as by those in surrounding areas. In spite of regrowth, wildlife populations are widely perceived to be in decline throughout both the area surrounding the park and in outlying communities. This decline is attributed primarily to ongoing hunting activities among local communities, habitat fragmentation and continued deforestation. Efforts to maintain viable wildlife populations within the park and to maintain connectivity between the park and core primary forest areas in the mountains will be impeded until better regulation of hunting takes place. In addition, regardless of hunting activities, oil palm plantations pose an increasing threat to the park, given their encirclement directly adjacent to the MANP border. Further oil palm expansion could soon isolate the park geographically, as the last remaining forested corridor connecting the park to core primary forest areas is cut off. Similar dynamics of fragmentation and isolation,

in particular from the expansion of palm plantations, are likely occurring throughout the many low lying park areas in Central America and will be the focus of future research.

Based on the results of this study we recommend the following be conducted for conservation areas undergoing similar land use pressures: (a) calculation of standardized movement costs for connectivity analyses; (b) development of regulations to limit hunting and uncontrolled expansion of oil palm plantations; (c) remote sensing analyses of changes in land cover and ecological connectivity; (d) estimation of the viability of alternate land uses, including nature oriented tourism; (e) development, implementation and monitoring of conservation and management approaches incorporating both socio-economic considerations and biodiversity; and (f) conservation of forested properties adjacent to parks and within potential biological corridors. Further research on the complex and contrasting effects of land cover change and sustainable development in areas of high biodiversity is warranted.

## 6.7 Acknowledgments

We thank the many households in the Manuel Antonio area communities who invited us into their lives. We thank the *Sí Cómo No* and *El Parador* hotels for allowing us to conduct our investigation on their premises and allowing us time with their workers during their busy schedules. We thank the Woods Institute for the Environment at Stanford University for providing the majority of field work funding support. We thank the Departments of Biology and Anthropology at Stanford University who provided E. Broadbent and A. Almeyda Zambrano with the time to conduct this field work and a Department of Energy (DOE GCEP) fellowship to ENB for financial support. We thank E. Vargas for help with logistics in Costa Rica. We thank M. Honey for ongoing support and insights to this research. We thank the W. Clark, N. Dickson and M. Holbrook for help during the writing process. This work was partially conducted while the E. Broadbent was a doctoral fellow and A. Almeyda Zambrano was a Giorgio Ruffolo Fellow in the Sustainability Science Program at

Harvard University. Support from Italy's Ministry for Environment, Land and Sea is gratefully acknowledged. We thank the anonymous reviewers for their many excellent comments throughout the revision process.

## 6.8 Tables

**Table 6.1:** Forest fragmentation and land cover from 1985 to 2008.

| Study area | Study year | | | |
|---|---|---|---|---|
| | 1985 | 1990 | 2000 | 2008 |
| Fragments (< 1 ha) | 6228 | 5066 | 4364 | 2998 |
| Fragments (> 1 ha) | 1140 | 824 | 652 | 509 |
| Median patch size ($m^2$) * | 24300 | 26100 | 24368 | 26100 |
| Median edge (m) * | 1080 | 1080 | 1026 | 1080 |
| Edge / area ratio | 0.0429 | 0.0415 | 0.0424 | 0.0413 |
| Total area in largest fragment (%) | 81.7 | 83.3 | 86.4 | 88.7 |
| Lowland forest (%) | 13 | 19 | 26 | 23 |
| Lowland palm (%) ** | 19 | 23 | 27 | 31 |
| Lowland non-forest (%) | 60 | 49 | 37 | 37 |
| Mountainous forest (%) | 57 | 69 | 79 | 77 |
| Mountainous palm (%) ** | 0 | 0 | 0 | 0 |
| Mountainous non-forest (%) | 43 | 31 | 20 | 22 |

* Includes only fragments > 1 ha in area. ** palm refers to oil palm plantations.

**Table 6.2:** Perceived impacts of the Sí Cómo No (SCN) and El Parador (EP) hotels versus tourism in general (T). Ranks range from 1-5; values > 3 indicate a negative impact and < 3 a positive impact. The matched pairs statistical analysis was used for mean comparisons.

| Category | Mean ± Std. Dev. (N) | | | *P*-value | |
|---|---|---|---|---|---|
| | SCN | EP | T | SCN | EP |
| Health | 1.6 ± 0.9 (33) | 2.0 ± 0.9 (32) | 2.5 ± 0.8 (104) | < 0.0001 | 0.0766 |
| Education | 1.8 ± 0.8 (32) | 2.0 ± 1.0 (33) | 1.9 ± 0.9 (104) | 1 | 0.1865 |
| Job training | 1.7 ± 0.9 (31) | 1.5 ± 0.8 (29) | 1.9 ± 1.0 (96) | 0.0699 | 0.2064 |
| Hunting | 1.8 ± 0.7 (32) | 1.9 ± 1.0 (32) | 2.1 ± 0.9 (95) | 0.4743 | 0.8312 |
| Deforestation | 1.7 ± 0.7 (31) | 2.3 ± 1.1 (33) | 2.7 ± 1.4 (100) | < 0.0001 | 0.2089 |
| Value of flora and fauna | 1.2 ± 0.6 (33) | 1.5 ± 0.7 (35) | 1.6 ± 0.9 (107) | 0.0006 | 0.5206 |
| Land price | 3.2 ± 1.1 (33) | 3.0 ± 0.9 (32) | 3.3 ± 0.8 (104) | 0.3441 | 0.5608 |
| Products price | 3.2 ± 0.9 (33) | 3.1 ± 0.9 (35) | 3.6 ± 1.1 (103) | 0.0368 | 0.1022 |
| Alcoholism | 2.7 ± 0.5 (32) | 2.8 ± 0.7 (33) | 3.4 ± 0.8 (101) | < 0.0001 | 0.0002 |
| Drug addiction | 2.8 ± 0.6 (31) | 2.8 ± 0.8 (34) | 3.7 ± 0.9 (104) | < 0.0001 | < 0.0001 |
| Prostitution | 2.7 ± 0.8 (30) | 2.5 ± 0.9 (32) | 4.0 ± 1.0 (94) | < 0.0001 | < 0.0001 |

**Table 6.3:** Ranked household perceptions of most important reasons to protect forest and for having natural protected areas.

| Category | Most important reasons N (rank)* | |
|---|---|---|
| | To protect forests | To have natural protected areas |
| So the animals can live | 36 (1) | 0 |
| Pure air | 33 (2) | 9 |
| Attractive to tourists | 19 (3) | 48 (1) |
| Clean water | 16 | 11 |
| So our children can see it / Plants and animals | 13 | 5 |
| Conservation / Protection of the environment | 11 | 20 (3) |
| Conservation of plants and animals | 10 | 20 (3) |
| The source of life | 9 | 0 |
| Prevent global warming | 8 | 0 |
| Nature is beautiful | 6 | 0 |
| Protect the plants | 0 | 10 |
| Recreation | 0 | 10 |
| To protect the animals, there is no hunting | 0 | 46 (2) |
| To stop humans from destroying it | 0 | 14 |

## 6.9 Figures

**Figure 6.1:** Detailed forest classification map of the study area in the year 2008. Insets show: (A) a close up of the park (MANP) and hotel nature preserves; and (B) the general location of study area in Costa Rica. The scale bar applies to the overview map only.

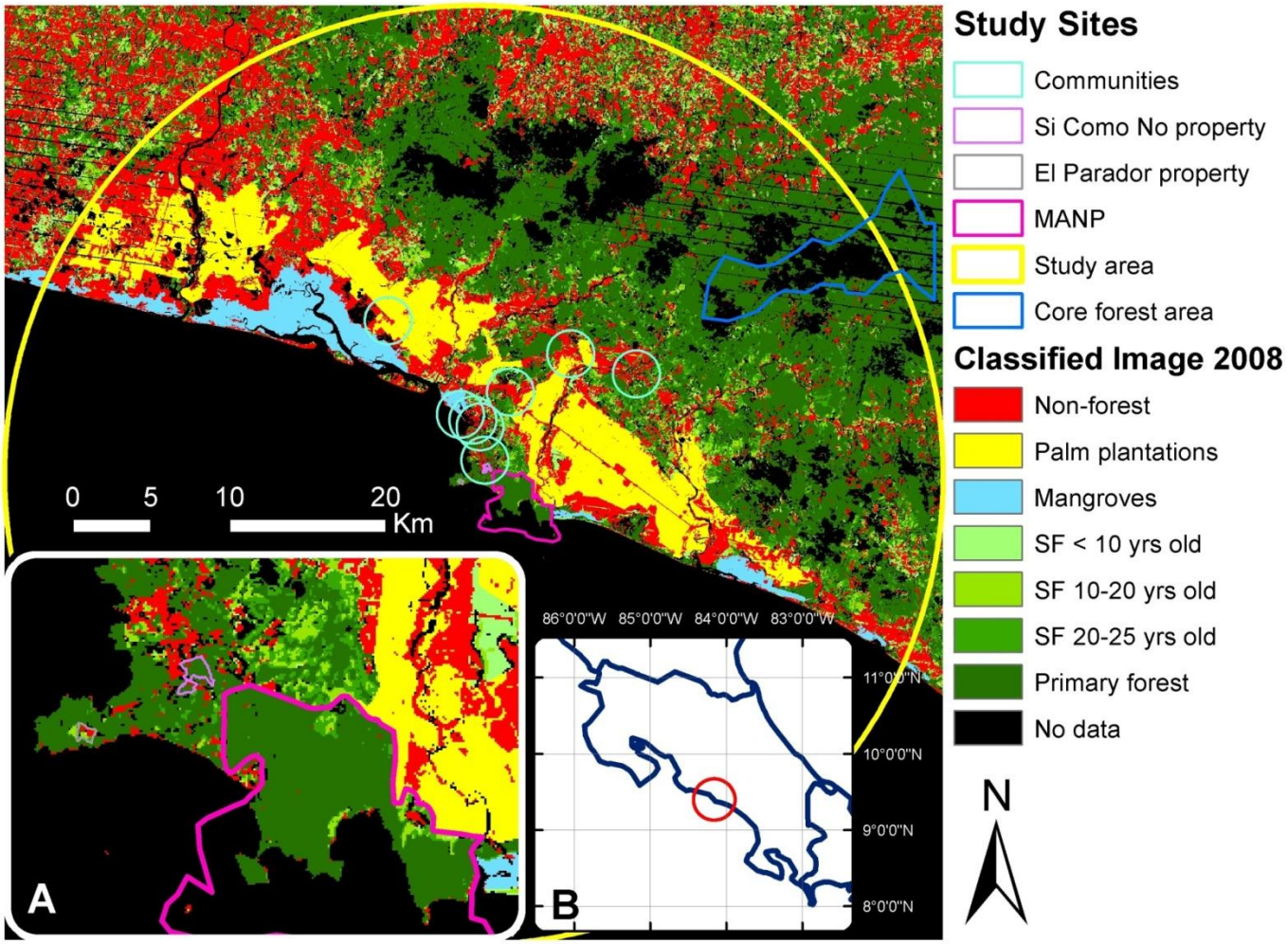


.

**Figure 6.2:** Land cover change (% area) from 1985 through 2008 within the Manuel Antonio National Park (MANP), its buffer (1.5 km), and across the entire study area..

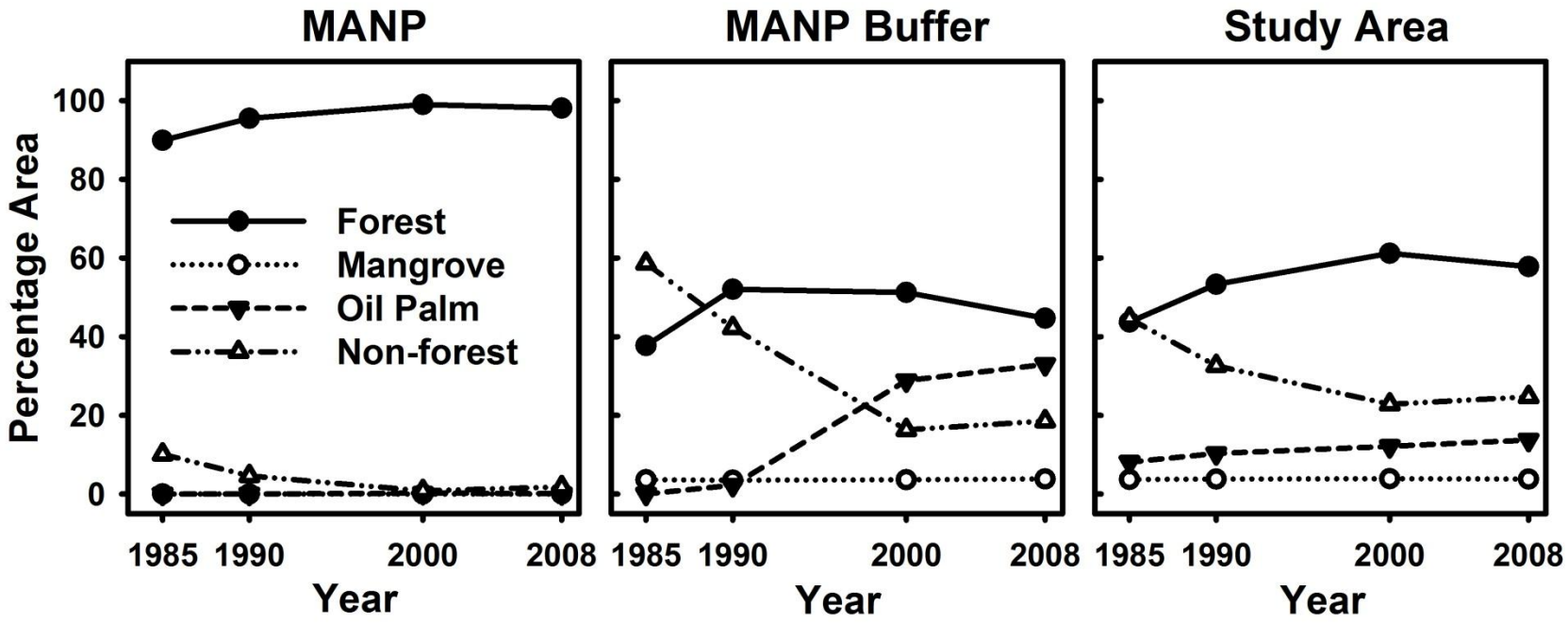

**Figure 6.3:** Land cover classes (% area) in the year 2008 within selected study sites, including the Manuel Antonio National Park (MA), and their adjacent buffer areas (1.5 km).

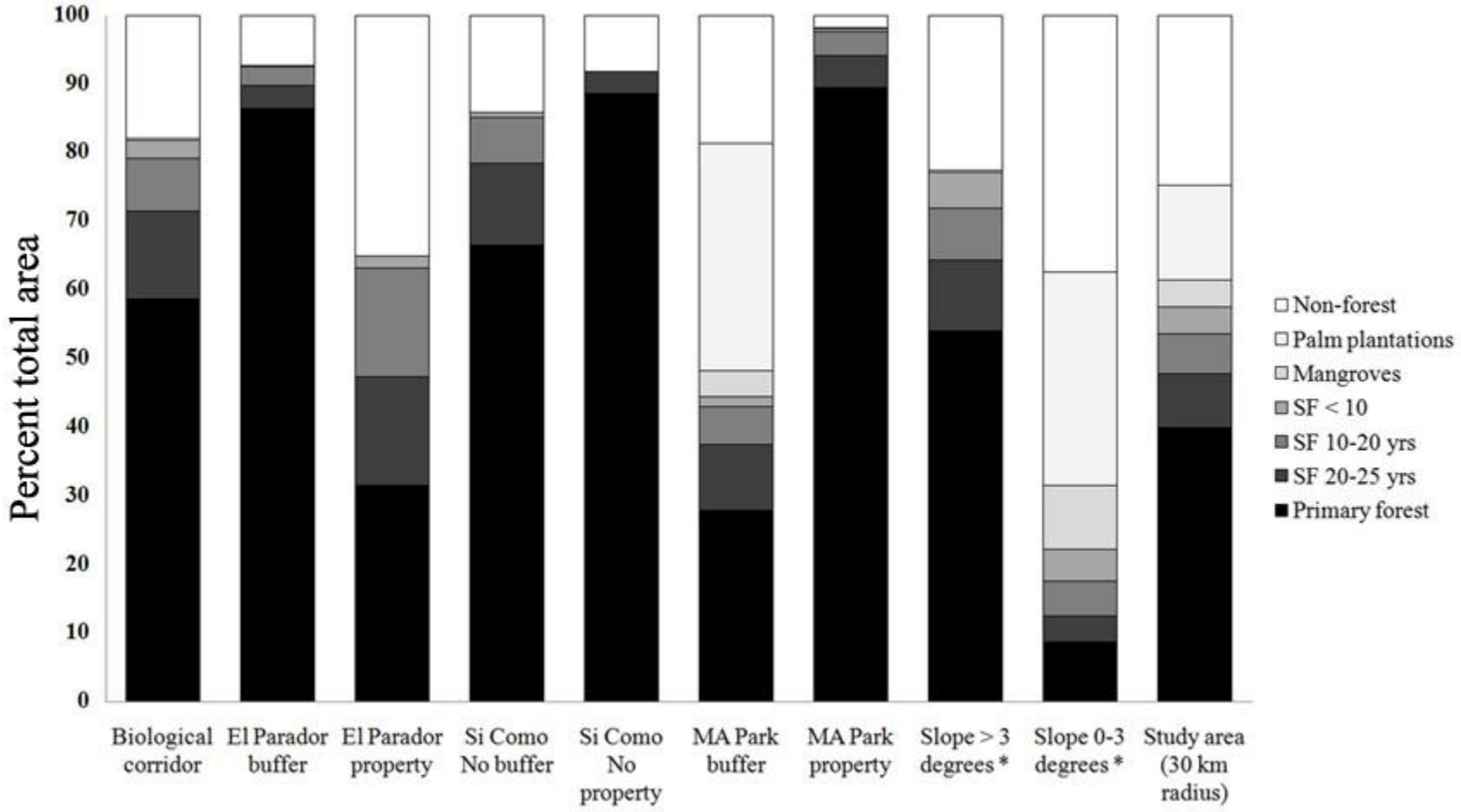

**Figure 6.4:** Least cost paths between all study sites (SS), including the Manuel Antonio National Park (MA) and core primary forest (CPF). The proposed biological corridor (800 m width) location is provided in the right inset.

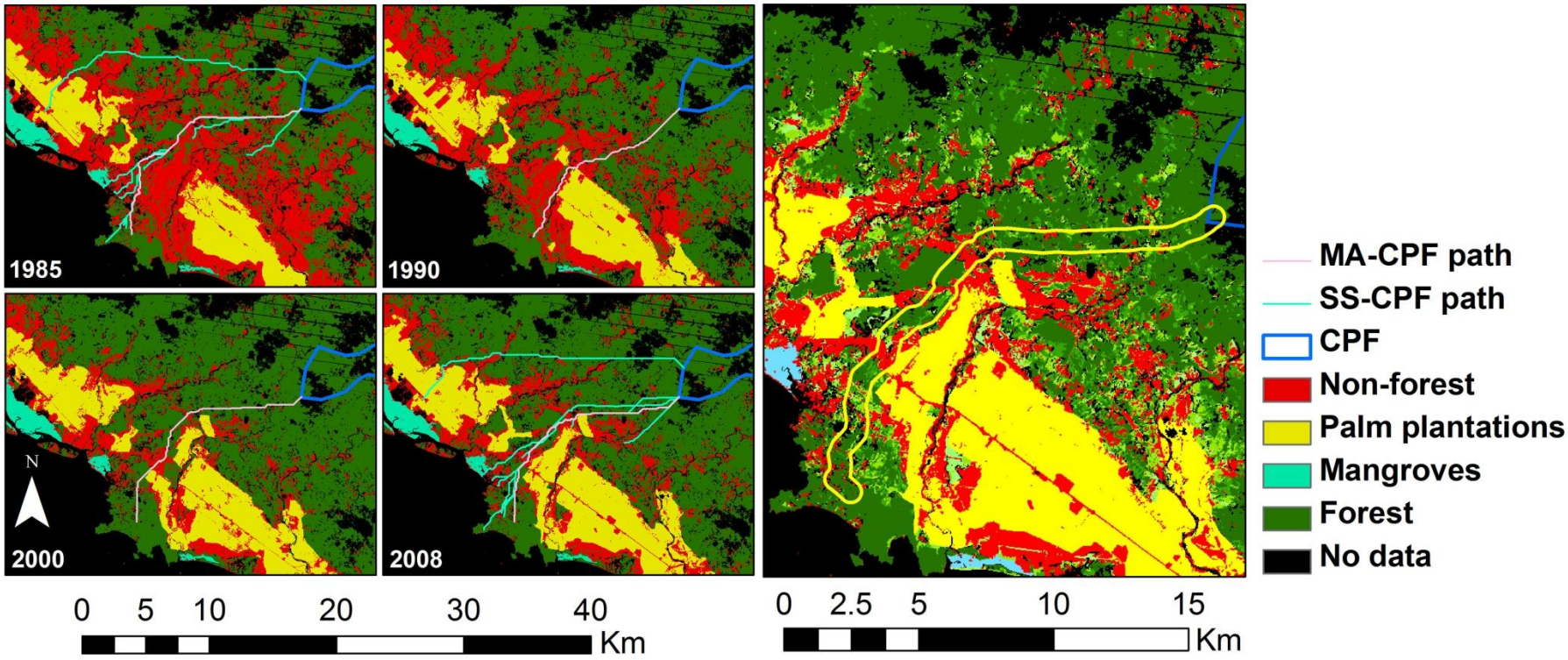

## 6.10 References


Abbot DH, Joanne IO, Neba SE, Khen MW (2001) Understanding the links between conservation and development in the Bamenda Highlands, Cameroon. World Dev 29:1115-1136

Almeyda Zambrano AM, Broadbent EN, Durham WH (2010a) Social and environmental effects of ecotourism in the Osa Peninsula of Costa Rica: the Lapa Rios case. J of Ecotourism 9:62-83

Almeyda Zambrano AM, Broadbent EN, Wyman MS, Durham WH (2010b) Ecotourism impacts in the Nicoya Peninsula, Costa Rica. Int J of Tourism Res 12:803-819

Alpízar, F (2006) The pricing of protected areas in nature-based tourism: a local perspective. Ecol Econ 56:294-307

Andam KS, Ferraro PJ, Sims KR, Healy A, Holland MB (2010) Protected areas reduced poverty in Costa Rica and Thailand. Proc Natl Acad Sci 107:9996-10001

Aylward B, Allen K, Echeverría J, Tosi J (1996) Sustainable ecotourism in Costa Rica: the Monteverde Cloud Forest Preserve. Biodivers Conserv 5:315-343

Beier P, Noss RF (2010) Do habitat corridors provide connectivity? Conserv Biol 12:1241-1252

Bowen ME, McAlpine CA, House, APN, Smith GC (2007) Regrowth forests on abandoned agricultural land: A review of their habitat values for recovering forest fauna. Biol Conserv 140:273-296

Boza M (1993) Conservation in action: past, present, and future of the National Park System of Costa Rica. Conserv Biol 7:239-247

Brockett CD, Gottfried RR (2002) State policies and the preservation of forest cover: lessons from contrasting public-policy regimes in Costa Rica. Lat Am Res Rev 37:7-40

Bruner A, Gullison R, Rice R, da Fonseca G (2001) Effectiveness of parks in protecting tropical biodiversity. Science 291:125-128

Campbell L (1999) Ecotourism in rural developing communities. Ann of Tourism Res 26:534-553

Carrillo E, Wong G, Cuarón AD (2000) Monitoring mammal populations in Costa Rican protected areas under different hunting restrictions. Conserv Biol 14:1580-1591

Castro-Salazar R, Arias-Murillo G (1998) Costa Rica: toward the sustainability of its forest resources. FONAFIFO, San Jose, Costa Rica

Ceballos-Lascurrain H (1987) The future of ecotourism. Mexico Journal January: 13-14

Chiarello AG (1999) Effects of fragmentation of the Atlantic forest on mammal communities in south-eastern Brazil. Biol Conserv 89:71-82

Chokkalingam U, de Jong, W (2001) Secondary forest: a working definition and typology. Int For Rev 3:19-26

Christ C, Hillel O, Matus S, Sweeting J (2003) Tourism and biodiversity: Mapping tourism's global footprint. United Nations Environment Program and Conservation International: Washington, DC

Curran LM, Trigg SN, McDonald AK, Astiani D, Hardiono YM, Siregar P, Caniago I, Kasischke E (2004) Lowland forest loss in protected areas of Indonesian Borneo. Science 303:1000-1003

Daily GC, Ceballos G, Pacheco J, Suzán G, Sánchez-Azofeifa A (2003) Countryside biogeography of Neotropical mammals: conservation opportunities in agricultural landscapes of Costa Rica. Conserv Biol 17:1814-1826

Defries RS, Foley JA, Asner GP (2004) Land-use choices: balancing human needs and ecosystem function. Front Ecol Environ 2:249-257

DeFries R, Hansen A, Newton AC, Hansen MC (2005) Increasing isolation of protected areas in tropical forests over the past twenty years. Ecol Appl 15:19-26

DeFries R, Hansen A, Turner BL, Reid R, Liu J (2007) Land use change around protected areas: management to balance human needs and ecological function. Ecol Appl 17:1031-1038

Edwards DP, Hodgson JA, Hamer KC, Mitchell SL, Ahmad AH, Cornell SJ, Wilcove DS (2010) Wildlife-friendly oil palm plantations fail to protect biodiversity effectively. Conservation Letters 3:236-242

FAO (1990) Forest resources assessment 1990: Tropical countries. FAO Forestry Paper 112. Rome, Italy

Fitzherbert EB, Struebig MJ, Morel A, Danielsen F, Brühl CA, Donald PF, Phalan B (2008) How will oil palm expansion affect biodiversity? Trends Ecol Evol 23:538-45

Foley JA, Defries R, Asner GP, Barford C, Bonan G, Carpenter SR, Chapin FS, Coe MT, Daily GC, Gibbs HK, Helkowski JH, Holloway T, Howard EA, Kucharik CJ, Monfreda C, Patz JA, Prentice IC, Ramankutty N, Snyder PK (2005) Global consequences of land use. Science 309:570-574

Goodwin BJ (2003) Is landscape connectivity a dependent or independent variable? Landscape Ecol 18:687-699

Gössling S (1999) Ecotourism: a means to safeguard biodiversity and ecosystem functions? Ecol Econ 29:303-320

Gurd D, Nudds T, Rivard D (2001) Conservation of mammals in eastern North America wildlife reserves: how small is too small? Conserv Biol 15:1355-1363

Hannon SJ, Schmiegelow, FK (2002) Corridors may not improve the conservation value of small reserves for most boreal birds. Ecol App 12:1457-1468

Hayes TM (2006) Parks, people, and forest protection: an institutional assessment of the effectiveness of protected areas. World Dev 34:2064–2075

Jha S, Bawa KS (2006) Population growth, human development, and deforestation in biodiversity hotspots. Conserv Biol 20:906-912

Koh LP, Wilcove DS (2007) Cashing in palm oil for conservation. Nature 448:993-994

Koh LP (2008) Can oil palm plantations be made more hospitable for forest butterflies and birds? J Appl Ecol 45:1002–1009

Koh LP, Miettinen J, Liew SC, Ghazoul J (2011) Remotely sensed evidence of tropical peat forest conversion to oil palm. PNAS 108: 5127-5132

Kostyack J, Lawler JJ, Goble DD, Olden JD, Scott M (2011) Beyond reserves and corridors: policy solutions to facilitate the movement of plants and animals in a changing climate. BioScience 61:713-719

McAlpine CA, Rhodes JR, Callaghan JG, Bowen ME, Lunney D, Mitchell DL, Pullar DV, Possingham HP (2006) The importance of forest area and configuration relative to local habitat factors for conserving forest mammals: A case study of koalas in Queensland, Australia. Biol Cons 132:153-165

Miller K, Chang E, Johnson N (2001) Defining common ground for the Mesoamerican Biological Corridor. World Resources Institute, Washington DC

MINAE (1992) Estudio nacional de biodiversidad. MINAE, San Jose, Costa Rica

Moran EF, Packer A, Brondizio E, Tucker J (1996) Restoration of vegetation cover in the eastern Amazon. Ecol Econ 18:41-54

Myers N, Mittermeier RA, Mittermeier CG, da Fonseca GA, Kent J (2000) Biodiversity hotspots for conservation priorities. Nature 403:853-858

Newmark WD (1996) Insularization of Tanzanian Parks and the local extinction of large mammals. Conserv Biol 10:1549-1556

Pfaff A, Sánchez-Azofeifa, AG (2004) Deforestation pressure and biological reserve planning: a conceptual approach and an illustrative application for Costa Rica. Resour Energy Econ 26:237-254

Rivera J (2002) Assessing a voluntary environmental initiative in the developing world: the Costa Rican Certification for Sustainable Tourism. Policy Sci 35:333-360

Robinson J, Bennett E (2004) Having your wildlife and eating it too: an analysis of hunting sustainability across tropical ecosystems. Ani Cons 7:397-408

Rock MT (1996) The stork, the plow, rural social structure and tropical deforestation in poor countries? Ecol Econ 18: 113-131

Sader SA, Joyce AT (1988) Deforestation rates and trends in Costa Rica, 1940 to 1983. Biotropica 20:11-19

Sala OE, Chapin III FS, Armest JJ, Berlow E, Bloomfield J, Dirzo R, Huber-Sanwald E, Huenneke LF, Jackson RB, Kinzig A, Leemans R, Lodge DM, Mooney HA,

Oesterheld M, LeRoy Poff N, Sykes MT, Walker BH, Walker M, Wall DH (2000) Global biodiversity scenarios for the year 2100. Science 287:1770-1774

Sánchez-Azofeifa AG, Daily GC, Pfaff ASP, Busch C (2003) Integrity and isolation of Costa Rica's national parks and biological reserves: examining the dynamics of land-cover change. Biol Conserv 109:123-135

Sánchez-Azofeifa AG, Pfaff A, Robalino JA, Boomhower JP (2007) Costa Rica's payment for environmental services program: intention, implementation, and impact. Conserv Biol 21:1165-1173.

Sánchez-Azofeifa AG, Rivard B, Calvo J, Moorthy I (2002) Dynamics of tropical deforestation around national parks: remote sensing of forest change on the Osa peninsula of Costa Rica. Mt Res Dev 22:352-358

Sánchez-Azofeifa AG, Harriss RC, Skole DL (2001) Deforestation in Costa Rica: a quantitative analysis using remote sensing imagery. Biotropica 33:378-384

Schwartzman S, Nepstad D, Moreira A (2000) Arguing tropical forest conservation: people versus parks. Conserv Biol 14:1370-1374

Scheyvens R (1999) Ecotourism and the empowerment of local communities. Tourism Management 20: 245-249

Soto R (1992) Evaluación ecológica rápida de la península de Osa, Costa Rica. Fundación Neotrópica, San Jose, Costa Rica

Stem C, Lassoie J, Lee D, Deshler D (2003) How "Eco" is ecotourism? A comparative case study of ecotourism in Costa Rica. J Sustain Tour 11:322-347

Sterling E (1999) The Green Republic: A conservation history of Costa Rica. University of Texas Press, Austin

Sun M (1988) Costa Rica's campaign for conservation. Science 239:1366-1369

Tilman D, Fargione J, Wolff B, D'Antonio C, Dobson A, Howarth R, Schindler D, Schlesinger WH, Simberloff D, Swackhamer D (2001) Forecasting agriculturally driven global environmental change. Science 292:281-284

Van Laake P (2004) Focus on deforestation: zooming in on hot spots in highly fragmented ecosystems in Costa Rica. Agr Ecosyst Environ 102:3-15

Vitousek P, Mooney H, Lubchenco J, Melillo JM (1997) Human domination of Earth's ecosystems. Science 277:494-499

Wittemyer G, Elsen P, Bean WT, Burton ACO, Brashares JS (2008) Accelerated human population growth at protected area edges. Science 321:123-126.

Yaap B, Struebig MJ, Paoli G, Koh LP (2010) Mitigating the biodiversity impacts of oil palm development. CAB Rev 5:1-11

## 6.11 Supplementary material

**SM 6.1:** Landsat satellite imagery.

| Date | Path | Row | Satellite | Sensor | Merged |
|---|---|---|---|---|---|
| 1985-02-19 | 15 | 53 | Landsat 5 | MSS | A |
| 1985-03-07 | 15 | 53 | Landsat 5 | MSS | A |
| 1985-02-03 | 15 | 54 | Landsat 5 | MSS | A |
| 1985-03-07 | 15 | 54 | Landsat 5 | MSS | A |
| 1990-02-09 | 15 | 53 | Landsat 4 | TM | B |
| 1991-03-24 | 15 | 53 | Landsat 5 | TM | B |
| 1990-02-25 | 15 | 54 | Landsat 4 | TM | B |
| 1990-03-05 | 15 | 54 | Landsat 5 | TM | B |
| 2000-02-13 | 15 | 53 | Landsat 5 | TM | C |
| 2000-12-21 | 15 | 53 | Landsat 7 | ETM+ | C |
| 2000-06-12 | 15 | 54 | Landsat 7 | ETM+ | C |
| 2000-01-12 | 15 | 54 | Landsat 5 | TM | C |
| 2007-02-08 | 15 | 53 | Landsat 7 | ETM + | D |
| 2007-02-24 | 15 | 53 | Landsat 7 | ETM + | D |
| 2008-01-26 | 15 | 53 | Landsat 7 | ETM + | D |
| 2008-01-26 | 15 | 54 | Landsat 7 | ETM + | D |
| 2008-03-14 | 15 | 54 | Landsat 7 | ETM + | D |
| 2009-03-01 | 15 | 54 | Landsat 7 | ETM + | D |
| 2000-12-21 | 15 | 54 | Landsat 7 | ETM+ | Ortho. * |
| 2001-06-15 | 15 | 53 | Landsat 7 | ETM+ | Ortho. * |

* Ortho-rectified.

**SM 6.2:** Land cover change from 1985 to 2008.

| Place | Percentage change per land cover type [a] | | | | Connectivity [b] | |
|---|---|---|---|---|---|---|
| | Forest | Mangroves | Palm Plantations | Non-forest | 1985 | 2008 |
| Biological corridor | 19.97 | 0 | 0.22 | -20.19 | | |
| Community Cocal de Quepos | 10.82 | 1.52 | 0.00 | -12.35 | 1076 | 1021 |
| Community Damas | 0.69 | 0.75 | 1.39 | -2.83 | 1400 | 1187 |
| Community INVU | 18.99 | 0.08 | 0.00 | -19.07 | 986 | 895 |
| Community La Inmaculada | 16.77 | 0.00 | 12.31 | -29.08 | 761 | 760 |
| Community Londres | 18.18 | 0.00 | 0.00 | -18.18 | 302 | 288 |
| Community Manuel Antonio | 11.51 | 0.00 | 0.00 | -11.51 | 1017 | 952 |
| Community Naranjito | -1.79 | 0.00 | 34.85 | -33.06 | 506 | 435 |
| Community Quepos Centro | 17.01 | 0.17 | 0.00 | -17.18 | 1030 | 940 |
| Hotel Parador buffer | 1.28 | 0.00 | 0.00 | -1.28 | | |
| Hotel Parador property | 8.62 | 0.00 | 0.00 | -8.62 | 1126 | 1046 |
| Hotel *Sí Cómo No* buffer | 13.99 | 0.00 | 0.00 | -13.99 | | |
| Hotel *Sí Cómo No* property | -2.53 | 0.00 | 0.00 | 2.53 | 1011 | 934 |
| MANP buffer [c] | 6.97 | 0.18 | 32.92 | -40.07 | | |
| MANP [c] | 8.23 | 0.00 | 0.13 | -8.36 | 1041 | 922 |
| Mountainous areas [d] | 20.50 | 0.00 | 0.24 | -20.73 | | |
| Lowland areas [e] | 9.97 | 0.34 | 12.51 | -22.82 | | |
| Study area (30 km buffer) | 14.08 | 0.13 | 5.62 | -19.83 | | |

[a] Calculated as 2008 minus 1985, [b] calculated as travel cost. Buffers are 1.5 km surrounding the property boundary, [c] MANP = Manuel Antonio National Park, [d] slope > 3°, [e] slope <= 3°.

**SM 6.3:** Comparison between Sí Cómo No (SCN) and El Parador (EP) hotels employees and their neighbors (C) on average values of background variables.

| Socio-demographic Variables | Mean (Std. dev.) | | | N | | | | P-value |
|---|---|---|---|---|---|---|---|---|
| | SCN | EP | C | SCN | EP | C | Test | |
| Ratio females/males interviewed | 0.64 | 0.63 | 1.05 | 36 | 39 | 43 | | |
| Female head of household | | | | | | | | |
| % born in area of influence | 50% | 56% | 57% | 24 | 25 | 30 | cp | 0.871 |
| Years living in current community | 17.0 (13.6) | 15.5 (13.8) | 22.1 (14.9) | 24 | 25 | 32 | w | 0.135 |
| Years of education | 09.9 (03.8) AB | 11.6 (03.7) A | 07.8 (03.4) B | 24 | 29 | 32 | w,t | < 0.001 |
| Age | 34.8 (09.3) AB | 30.0 (09.1) A | 38.7 (09.4) B | 25 | 29 | 34 | w,t | 0.002 |
| Male head of household | | | | | | | | |
| % born in area of influence | 50% | 48% | 63% | 30 | 29 | 41 | cp | 0.367 |
| Years living in current community | 16.6 (15.5) B | 15.4 (12.4) B | 27.2 (18.5) A | 26 | 31 | 39 | w,t | 0.009 |
| Years of education | 08.3 (03.7) AB | 09.9 (03.9) A | 07.7 (03.7) B | 32 | 32 | 39 | w,t | 0.034 |
| Age | 34.1 (11.5) B | 31.0 (10.1) B | 42.4 (11.7) A | 32 | 32 | 40 | w,t | < 0.001 |
| Number of dependent children | 01.0 (01.3) B | 00.8 (01.1) B | 01.5 (01.3) A | 36 | 39 | 43 | w,t | < 0.001 |

cp: contingency table and Pearson coefficients were used for both comparisons; w: Wilcoxon/Kruskal-Wallis Tests (Rank Sums) was used. Post-hoc analyses were conducted using the Tukey-Kramer HSD test.

**SM 6.4:** Comparison between Sí Cómo No (SCN) and El Parador (EP) hotels employees and their neighbors (NE) on average monthly household expenditures (US $) for the month of June, 2009.

| Variables | Means | | | N | | | P-value |
|---|---|---|---|---|---|---|---|
| | SCN | EP | NE | SCN | EP | NE | |
| Amount ** | | | | | | | |
| Food | 191.9 (113.1) A | 117.5 (79.1) B | 211.7 (130.9) A | 34 | 38 | 41 | < 0.001 |
| Housing | 35.9 (58.0) A | 58.0 (72.4) A | 32.8 (88.0) A | 34 | 39 | 41 | 0.0265 |
| Utilities | 54.3 (37.4) | 39.4 (27.0) | 55.3 (33.8) | 34 | 38 | 41 | 0.1430 |
| Transportation | 25.2 (38.1) A | 40.2 (38.1) A | 40.6 (82.8) A | 34 | 38 | 41 | 0.0208 |
| Education | 29.8 (44.5) | 41.6 (95.9) | 39.6 (64.7) | 34 | 38 | 41 | 0.3700 |
| Recreation | 45.2 (72.0) | 47.3 (92.8) | 19.5 (35.8) | 34 | 38 | 41 | 0.2771 |
| Savings | 36.8 (82.2) A | 68.6 (138.7) A | 17.7 (42.7) A | 34 | 38 | 41 | 0.0039 |
| Investment | 97.3 (174.7) | 69.0 (170.9) | 28.8 (71.7) | 34 | 38 | 41 | 0.1070 |
| Medical | 22.2 (90.0) | 34.1 (92.8) | 15.0 (43.4) | 34 | 38 | 41 | 0.1885 |
| Other | 57.2 (69.6) A | 49.1 (74.6) AB | 22.1 (43.0) B | 34 | 38 | 41 | 0.0388 |
| Total US $ | 594 | 565 | 484 | | | | |

* The Wilcoxon/Kruskal-Wallis Tests (Rank Sums) was used for all comparisons. Post-hoc analyses were conducted using the Tukey-Kramer HSD test. ** Amount is in US $ monthly.